Investigating the role of eyes absent homolog 1 (EYA1) in aspirin-induced gastric ulceration

Thesis submitted in accordance with the requirements of the University of Liverpool for the degree of Doctor in Philosophy

by

Alexander James Penrose

June 2019

Declaration

This thesis is the result of my own work. The material contained within this thesis has not been presented, nor is currently being presented, either wholly or in part for any other degree or qualification.

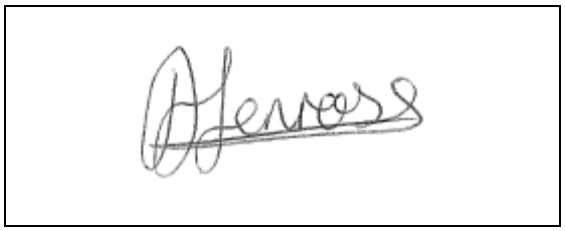

Alexander James Penrose

This research was carried out in the Department of Molecular and Clinical Pharmacology, in the Institute of Translational Medicine, at the University of Liverpool.

Acknowledgements

Thanks to Dan, Sudeep and Munir and the rest of my Wolfson family for all your guidance and support for the past 5 years! I feel I have grown a lot as a person and a scientist, since I arrived as a fresh-faced MRes and I owe that all to you. I hope you will miss me as much as my cakes.

Special thanks to Shankar, Gerry and team for welcoming me into their lab group, teaching me so many new techniques and showing me how to be more efficient in the lab! But more importantly, for making me feel like part of the group and taking me outdoors.

Thanks to Dr. Roz Jenkins for your help getting all the mass spec data and Nick for the many things you helped me with and taught me throughout my PhD.

I would also like to thank the Medical Research Council (MRC) for funding me on this research project and the University as a whole for providing me with so many amazing experiences. This includes all of the people and memories from my three courses and my time as a residential adviser. Especially thanks to Ruari and Ché for keeping my head screwed on throughout!

Thanks to Gurpreet for working your computer wizardry whenever I need tech support and showing me how to level up my Microsoft Office skill branch. Thanks to Sammie for letting me nick your Graphpad account and all your support.

Extra special thanks to my parents and grandparents for all their help funding throughout my 8-9 year university stint and all my family and friends their support too!

Contents

Publications and communications

Published papers

Carr D.F., Ayehunie S., Davies A., Duckworth C.A., French S., Hall N., Hussain S., Mellor H.R., Norris A., Park B.K., **Penrose A.**, Pritchard D.M., Probert C.S., Ramaiah S., Sadler C., Schmitt M., Shaw A., Sidaway J.E., Vries R.G., Wagoner M., Pirmohamed M. (2017). TOWARDS BETTER MODELS AND MECHANISTIC BIOMARKERS FOR DRUG-INDUCED GASTROINTESTINAL INJURY. Pharmacol Ther., 172:181-194.

Abstract

Non-selective NSAIDs are some of the mostly commonly used drugs worldwide; over 60 million US citizens regularly take NSAIDs while 30% of the general population use low-dose aspirin for cardiovascular disease prevention. NSAID use increases the risk of GI complications by 3-5 times compared to non-use. Estimates of NSAID-related mortality rates are between 3,200-16,500 in the USA and 400-1,000 in the UK, with the economic burden estimated to be over 3 billion USD a year in the USA alone.

Whilst the majority of the adverse GI effects caused by NSAIDs are presumed to be dependent on the inhibition of COX-1-mediated prostaglandin synthesis, prostaglandin-independent mechanisms are also important in ulcer pathogenesis. Various genetic risk factors have been identified for NSAID-induced gastric injury. Uncovering the role of these polymorphisms has provided a better understanding of the mechanism through which NSAIDs cause gastric ulceration and bleeding.

A genome-wide association study recently identified a novel association between a polymorphism in the Eyes Absent Homolog 1 (*EYA1*) gene and gastric ulceration. EYA1 is a transcriptional cofactor that plays an important role in organogenesis and has more recently shown to play a role in promoting DNA repair following genotoxic stress. The main aim of the thesis was to determine the role of EYA1 in aspirin-induced gastric epithelial cell death using AGS cells, a gastric epithelial cell line.

Aspirin induced time- and dose-dependent gastric epithelial cell death via the apoptotic pathway. EYA1 protein expression was barely detectable in AGS cells and several other cell lines. In view of the low expression, AGS cells were stably transfected with GFP-tagged human EYA1 via chemical co-transfection with a transposase plasmid, and isolated from puromycin selection to obtain the AGS-EYA1 cell line. EYA1-GFP localised to the nucleus of AGS cells, which is interesting considering most reports in rodent models require co-transfection of a *SIX* gene to translocate EYA1 from the cytosol to the nucleus.

Using the native AGS cells as a control, aspirin-induced apoptosis was abolished in the AGS-EYA1 cell line. The protection provided by EYA1 overexpression occurred upstream of caspase-9 cleavage. BAX and MCL-1S protein expression was significantly reduced in AGS-EYA1 cells, which may suggest a mechanism for the protection against aspirin toxicity. Alternatively, EYA1 may reverse the apoptotic stimulus at the source, e.g. repair of damaged DNA; however, this hypothesis was not tested in this study.

By analysing gene and protein expression data available from open source databases, EYA1 was found to have very low RNA expression in healthy stomach tissue. There were also no reports of EYA1 protein expression in stomach tissue. Moving forward it will be imperative to characterise the expression of EYA1 in healthy and ulcerative stomach tissue and the effects of genetic polymorphisms on EYA1 expression.

In summary, the results presented in this thesis suggest that human EYA1 localises to the nucleus of gastric epithelial cells where it can provide protection against aspirin-induced cytotoxicity. The mechanism of this protective effect may be due to EYA1-mediated downregulation of pro-apoptotic proteins or by the induction of genotoxic repair pathways. Validation of this association in non-tumorigenic tissues could provide novel strategies to prevent NSAID-induced gastropathy.

Abbreviations

Acronyms	Name
15R-HETE	15R-hydroxyeicosatetraenoic acid
2,3-DHBA	2,3-dihydroxybenzoic acid
AA	Arachidonic acid
aa	Amino acid
ACEI	Angiotensin converting enzyme inhibitors
Ach	Acetylcholine
ACN	Acetonitrile
ADR	Adverse drug reaction
AGT	Angiotensin
AIF	Apoptosis-inducing factor
ALT	Alanine aminotransferase
ANOVA	Analysis of variance
ANP	Atrial natriuretic peptide
ANS	Autonomic nervous system
Apg	Autophagy proteins
ARB	Angiotensin receptor blocker
AS	Ankylosing spondylitis
ASA	Aspirin
ATP	Adenosine triphosphate
AV	Annexin V
BCA	Bicinchoninic acid
BFA	Brefeldin A
bFGF	Basic fibroblast growth factor
BiP/GRP-78	binding immunoglobulin protein/78 kDa glucose-regulated protein
BOR	Branchio-Oto-Renal
BSA	Bovine Serum Albumin
CA	Coronary artery
CAD	Caspase-mediated DNase
CAGE	Cap Analysis of Gene Expression
cAMP	Cyclic adenosine monophosphate
CAT	Catalase
CBS	Cystathionine B-synthase
CCK2	Cholecystokinin-2
CGRP	Calcitonin gene-related peptide
CHOP	C/EBP homologous protein
CI	Confidence interval
CINOD	COX-inhibiting nitric oxide donor
cNOS	Constitutively expressed NOS

CNS	Central nervous system
COPD	Chronic obstructive pulmonary disorder
COX	Cyclooxygenase-1
CRF	Corticotropin-releasing factor
CSE	Cystathionine-γ-lyase
CV	Cardiovascular
CVD	Cardiovascular disease
CYP	Cytochrome P450
DACH	Dachshund family transcription factor
DAPI	4′,6-diamidino-2-phenylindole
DDD	Defined daily doses
DMEM	Dulbecco's Modified Eagle Medium
DMF	Dimethylformamide
DMSO	Dimethyl sulphoxide
dNTP	Deoxynucleotide
EC	Enterochromaffin
ECL	Enterochromaffin-like
ECL reagent	Enhanced Chemiluminescence reagent
ECM	Extracellular matrix
ED	EYA domain
EGD	Oesophagogastroduodenoscopy
EGF	Epidermal growth factor
EGFR	Epidermal growth factor receptor
EHR/EMR	Electronic health/medical record
eIF2α	Eukaryotic initiation factor 2α
ENCODE	Encyclopedia of DNA Elements
eNOS	Endothelial NOS
ENS	Enteric nervous system
EP	Prostaglandin E2 receptors
eQTL	expression quantitative trait loci
ER	Endoplasmic reticulum
ESCEO	The European Society for Clinical and Economic Aspects of Osteoporosis and Osteoarthritis
ET-1	Endothelin-1
EYA	Eyes Absent
FA	Formic acid
FACS	Fluorescence-activated cell sorting
FANTOM	Functional ANnoTation Of Mammalian Genome
FBS	Foetal bovine serum
FDA	U.S. Food and Drug Administration
FDR	False discovery rates
FPKM	Fragments Per Kilobase of exon per Million reads
GAPDH	Glyceraldehyde 3-phosphate dehydrogenase

GDC	Genomic Data Commons
GFP	Green fluorescent protein
GI	Gastrointestinal
GMBF	Gastric mucosal blood filtration
GPMdb	Global Proteome Machine Database
GRP	Gastrin-releasing peptide (Chapter 1)
GRP	Glucose-regulated protein (Chapter 4)
GSH	Glutathione
GSH-Px	Glutathione peroxidase
GTEx	Genotype-Tissue Expression
GWAS	Genome-wide association study
H&M	Headache and migraine
H_2S	Hydrogen sulphide
HBDR	Human Developmental Biology Resource
HBSS	Hanks' Balanced Salt Solution
HCl	Hydrochloric acid
HDC	Histidine deacetylase
HEK	Human Embryonic Kidney
HGC-27	Human gastric carcinoma subclone-27
HLA	Human leukocyte antigen
HPA	Human Protein Atlas
HPM	Human Proteome Map
HRP	Horseradish peroxidase
IAP	Inhibitor of apoptosis
ICAM-1	Intercellular adhesion molecules
ICF	Immunocytofluorescence
IF	Immunofluorescent
IGF-1	Insulin-like growth factor-1
IL	Interleukin
iNOS	Inducible NOS
IP	Prostacyclin receptors
IP_3	Inositol triphosphate
IRE1	Inositol requiring 1
JNK	c-Jun N-Terminal kinase
LC3b	Light chain 3b
LC-MS/MS	Liquid chromatography–mass spectrometry
LD	Linkage disequilibrium
LDA	Low-dose aspirin
LFA	Lipofectamine
LOX	Lipoxygenase
MDC1	Mediator of DNA damage checkpoint 1
MHC	Major histocompatibility complex
MMP	Matrix metalloprotease

MOMP	Membrane permeabilization
MRN	MRE11/RAD50/NBS1
MS	Musculoskeletal
MTT	3-(4,5-Dimethylthiazol-2-yl)-2,5-Diphenyltetrazolium Bromide
$NAD(P)H_2$	Nicotinamide adenine dinucleotide phosphate
NAT	N-acetyltransferase
NCBI	National Center for Biotechnology Information
NCI-N87	National Cancer Institute cell line N87
NEAA	Non-Essential Amino Acids
NFE2L1/Nrf1	Nuclear Factor Erythroid-2 Like-1
NHS	National Health Service
NICE	The National Institute for Health and Care Excellence
NIH	National Institute of Health
nNOS	Neuronal NOS
NO	Nitric oxide
NOS	Nitric oxide synthase
NSAID	Non-steroidal anti-inflammatory drug
OA	Osteoarthritis
OR	Odds ratio
pac	Puromycin N-acetyltransferase
PACAP	Pituitary adenylyl cyclase–activating polypeptide
PAGE	Polyacrylamide gel electrophoresis
PAI-1	Plasminogen activator inhibitor type 1
PARP	Poly (ADP-ribose) polymerase
PAX	Paired box
PBMC	Peripheral blood mononuclear cell
PBS	Phosphate Buffered Saline
PC	Phosphatidylcholine
PCR	Polymerase chain reaction
PERK	Protein kinase RNA-like ER kinase
PG	Prostaglandin
PheWAS	Phenome-wide association study
PI	Propidium iodide
PI(3)K	Phosphatidylinositol-OH kinase
PKC	Protein kinase C
PL	Phospholipid
PLA_2	Phospholipase A_2
PLC	Phospholipase C
PO	Postoperative pain
PPI	Proton pump inhibitor
PTGES/mPGES	Prostaglandin E synthase
PTGS1	Prostaglandin-endoperoxide synthase
PUD	Peptic ulcer disease

pY-P	Phosphotyrosine phosphatase
RA	Rheumatoid arthritis
RAAS	Renin-angiotensin-aldosterone system
RDGN	Retinal determination gene network
RIPA	Radioimmunoprecipitation assay
ROS	Reactive oxygen species
RPKM	Read Per Kilobase of transcript per Million
RR	Relative risk
S.O.C.	Super Optimal broth with Catabolite repression
SB	Sleeping Beauty
SDS	Sodium dodecyl sulphate
SDS	Standard deviation
Shh	Sonic Hedgehog
SIX	Sine oculis-related homeobox
SLCO1B1	Solute carrier organic anion transporter family member 1B1
SLIT1	Slit guidance ligand 1
SMAC	Second mitochondria-derived activator of caspase
SNP	Single nucleotide polymorphisms
SNV	Single nucleotide variation
SOD	Superoxide dismutase
SOX	SRY-box 2
STS	Staurosporine
SUMO1	Small ubiquitin-related modifier 1
TAD	Transactivation domain
TBS	Tris-buffered saline
TCGA-GDC	The Cancer Genome Atlas Genomic Data Commons
TEMED	Tetramethylethylenediamine
TFF	Trefoil factor
TGF-α	Transforming growth factor α
tNSAIDs	Traditional NSAID
t-PA	Tissue plasminogen activator
TPM	Transcripts Per Million
TPY	1000 person-years
TUN	Tunicamycin
TUNEL	TdT-mediated dUTP nick end labelling
TxA_2	Thromboxane A_2
UGIB	Upper gastrointestinal bleeding
UGIC	Upper gastrointestinal complications
UPR	Unfolded protein response
VEGF	Vascular endothelial growth factor
VIGOR	Vioxx Gastrointestinal Outcomes Research
VIP	Vasoactive intestinal polypeptide
XIAP	X-linked inhibitor of apoptosis protein

XIC	Extracted-ion chromatogram
z-VAD	Carbobenzoxy-valyl-alanyl-aspartyl-[O-methyl]-fluoromethylketone

Chapter 1

General Introduction

Contents

1.1 **Anatomy and physiology of the stomach**

The digestive system is a continuous complex of various glands, tissues and organs. Ingesta first enters through the oral cavity and are either broken up or directly swallowed into the pharynx. Ingesta are then pushed through various digestive organs by smooth and/or striated muscles found in the tubular tract walls (Figure 1.1).

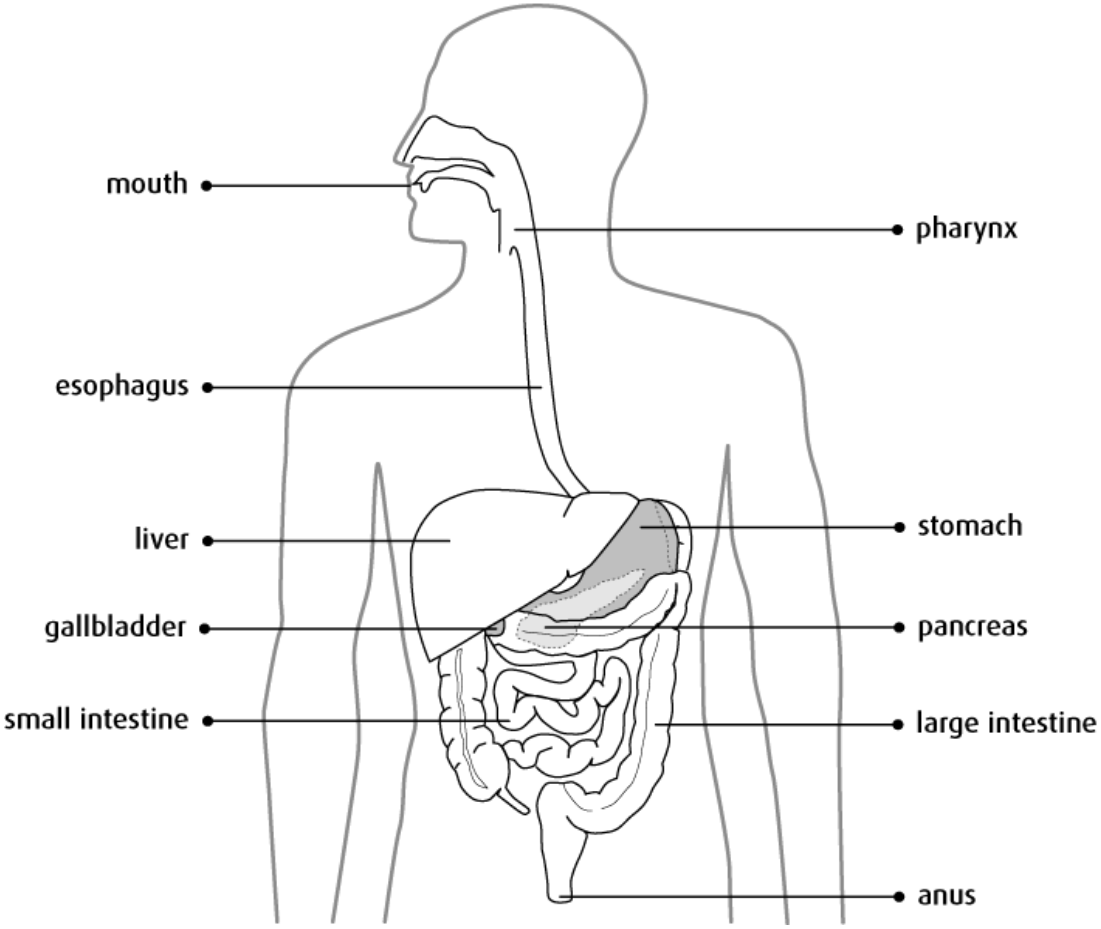

Figure 1.1 A diagram depicting the major organs involved in digestion. Ingesta enters the mouth, swallowed through the pharynx and passed down the oesophagus. Ingesta then enters the stomach, where it undergoes mechanical trituration and chemical digestion into a liquefied mixture called chyme. The acidic chyme is alkalinize in the duodenum (start of small intestine) by bicarbonate, which is secreted from the liver, pancreas and duodenum. Proteins, lipids and carbohydrates are broken down by enzymes secreted by the pancreas and liver, as well as bile secreted from the liver and held in the gallbladder. Nutrients and minerals are absorbed from chyme whilst being pushed through the small intestine. The chyme finally enters the large intestine, where remaining nutrients are absorbed with any remaining water. This process solidifies stools into faeces to be excreted by the anus. Image obtained from the Canadian Cancer Society. Anatomy and physiology of the stomach. http://www.cancer.ca/en/cancer-information/cancer-type/stomach/ stomach -cancer/the-stomach. [Date accessed, 24/08/18].

1.1.1 **Abdominal Positioning of the Stomach and its Arterial, Lymphatic and Neural Innervations**

The human stomach is a single sac-like organ found mostly in the left hypochondriac region of the abdominal peritoneum. The lower, distal section of the stomach also breaches the epigastric and upper umbilical regions. The stomach is connected proximally to the oesophagus and distally to the duodenum. Though often depicted as J-shaped, the height, weight, posture and fullness of an individual can affect the size, shape and position of the stomach. The stomach is bordered anteriorly by the liver, traverse colon and left hemidiaphragm, posteriorly by the pancreas, left kidney and adrenal gland and posterolaterally by the spleen[2]. It is held in place by gastrophrenic (diaphragm), hepatogastric (liver) gastrosplenic (spleen) and gastrocolic (traverse colon) ligamentous connections[3], as well as the greater and lesser omenta, which attach to the greater and lesser curvatures of the stomach respectively[4] (Figure 1.2).

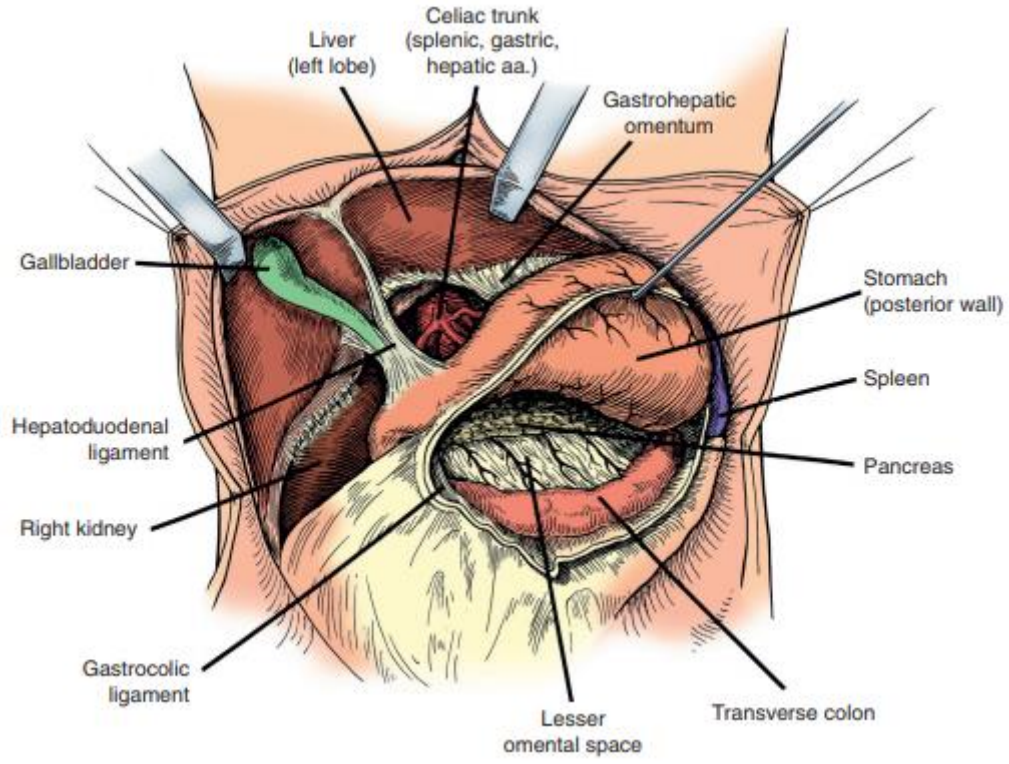

Figure 1.2 Ligamentous attachments between the stomach and surrounding organs. Image obtained from Wilson & Stevenson[3] (2019). Anatomy and Physiology of the Stomach. Shackelford's Surgery of the Alimentary Tract. Page 635.

The rich blood supply of the stomach is delivered exclusively from the coeliac trunk, which branches into three arms of anatomising vessels that provide blood to the

stomach[3] (Figure 1.3). Firstly, the left gastric artery stems directly from the coeliac artery, an offshoot of the abdominal aorta. The left gastric artery runs along the cephalad portion of the lesser curvature of the stomach and connects by anastomosis to the caudal right gastric artery, which derives from the common hepatic artery, the second arm of the coeliac artery. The arterial loop around the greater curvature of the stomach is formed by the convergence of the left and right gastroepiploic arteries. The latter also stemming from the gastroduodenal artery, while the left gastroepiploic artery arises from the splenic artery, the third arm of the coeliac artery. These features, along with several short gastric arteries from the splenic hilum that supply the fundus and distal corpus, provide most of the gastric blood supply[2,3].

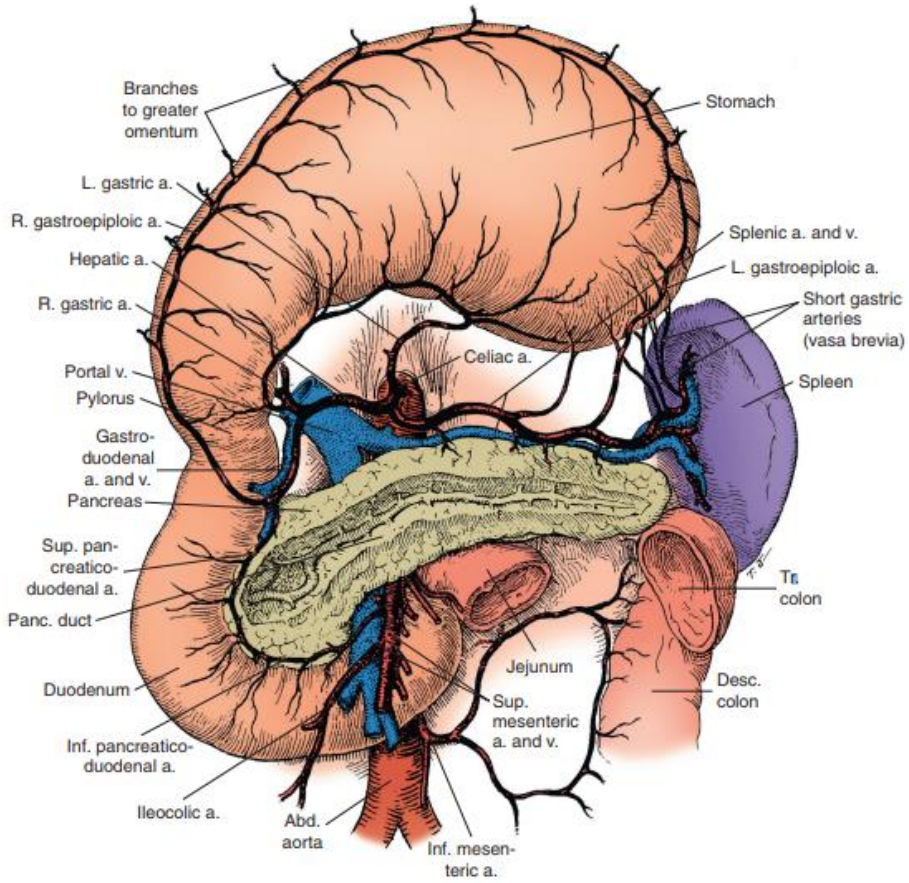

Figure 1.3 Arterial vasculature of the foregut. Blood is supplied to the stomach mostly from two arterial arcades, the left and right gastric arties merging and spanning the lesser curvature and the left and right gastroepiploic arties along the greater curvature. The anastomoses along the lesser and greater curvatures are situated between the two leaves of the lesser and greater omentum (a fold of the peritoneum that connects the stomach with other abdominal organs) respectively. Image obtained from Wilson & Stevenson[3] (2019). Anatomy and Physiology of the Stomach. Shackelford's Surgery of the Alimentary Tract. Page 638.

The major arteries around the stomach contain extramural gastric lymph nodes, which receive drainage from lymphatic vessels in the stomach wall. All gastric lymphatic drainage will be cleared into the coeliac lymph nodal basin and finally to the cisterna chyli at the lower end of the thoracic duct[2,3].

The activities of peristalsis (wave like contractions), secretions (e.g. gastrin, histamine, etc.) and several other gastric functions are regulated by the enteric nervous system (ENS) and autonomic nervous system (ANS). The ENS is a mesh of intrinsic neurones that form the interconnected submucosal and myenteric ganglia across the entire gastrointestinal (GI) tract[5]. The gastric ENS relies heavily on extrinsic signals from the ANS and is able to send sensory signals to the central nervous system (CNS) through both parasympathetic and sympathetic afferent fibers[6].

Sympathetic splanchnic nerves form the sixth to ninth thoracic vertebrae form most efferent cholinergic connections to postganglionic adrenergic neurons from the coeliac ganglia that supply to stomach. Afferent sympathetic nerves also send signals from the stomach to thoracic dorsal root ganglia[3,7]. Processing of these autonomic signals is then handled by several structures in the CNS including the solitary nucleus, hypothalamus, parabrachial complex, amygdala and the periaqueductal gray[6].

Sympathetic fibres direct to the intermural ganglia and blood vessels surrounding the stomach. Sympathetic activity includes inhibition of gastric motility, gastroesophageal and pylori sphincter constriction, and inhibition of vagal cholinergic inputs to the myenteric plexus, causing tachygastria. Other sympathetic outputs include the regulation of gastric blood flow by vasoconstriction and of gastric secretions by inhibiting submucosal secretomotor neurons and direct inhibition of parietal cells[5,8,9].

Parasympathetic innervation of the stomach originates from preganglionic motoneurons connected to the dorsal motor nucleus of the vagus. Efferent nerves to the stomach stem from divergent vagal trunks, namely the hepatic, coeliac, anterior and posterior gastric branches. Arborisation of vagal nerve fibres have been shown to envelope most myenteric plexuses in rat and guinea pig stomachs[10,11]. Afferent parasympathetic fibers, stimulated by various mechanical and chemical stimuli, send signals from the stomach back through the vagus nerve to the solitary nucleus in the brainstem[3,7].

Vagal efferent neurons synapse with myenteric ganglia within the stomach to cause smooth muscle contraction via muscarinic cholinergic excitation. Vagal smooth muscle relaxation is mostly mediated through stimulation at nicotinic synapses, evoking nitric oxide (NO) and vasoactive intestinal polypeptide release[12]. Vagal inputs also regulate gastric secretions (e.g. pepsin[13] and prostaglandins[14-16]) and parietal cell activity via postganglionic muscarinic receptor activation[17].

Several discrete central nuclei send and receive information through the vagus nerves to control gastric activity including the hypothalamus, locus coeruleus, caudal medullary raphe and the amygdala. The roles of these CNS nuclei in regulating gastric function are comprehensively reviewed in Browning & Travagli (2014)[6].

1.1.2 **Gross Anatomy and Topographical Functions of the Stomach**

The stomach is the widest and most distensible segment of the alimentary canal with a capacity of approximately 1.5 litres in adults[18]. It is commonly divided into four topographic regions: the (i) cardia, (ii) fundus, (iii) corpus (also called the body) and (iv) pylorus (pyloric antrum and pyloric canal)[4] (Figure 1.4).

Though containing no anatomical sphincter, circular muscles surrounding the gastroesophageal junction (cardiac orifice) act as a physiological sphincter that relax ahead of peristaltic waves from the oesophagus, allowing the passage of ingesta into the stomach. Tonic contractions of the gastroesophageal sphincter prevent gastric contents from travelling back up the oesophagus[18]. The role of glands in the upper cardia is primarily mucus secretion from mucous cells, while glands in the basal half of the cardia express more acid-secreting parietal cells (oxyntocardiac glands)[3].

The fundus is the dome-like cephalic region of the stomach that reaches superior to the cardiac notch. The corpus (body) of the stomach extends from the level of the cardiac orifice down to the angular incisure at the base of the lesser curvature. The fundus and corpus contain acid-secreting (oxyntic) glands and account for the majority of chemical digestion. The corpus is also easily distinguished by various irregularly folded rugae that increase the basal surface area and allow for gastric expansion following ingestion[3].

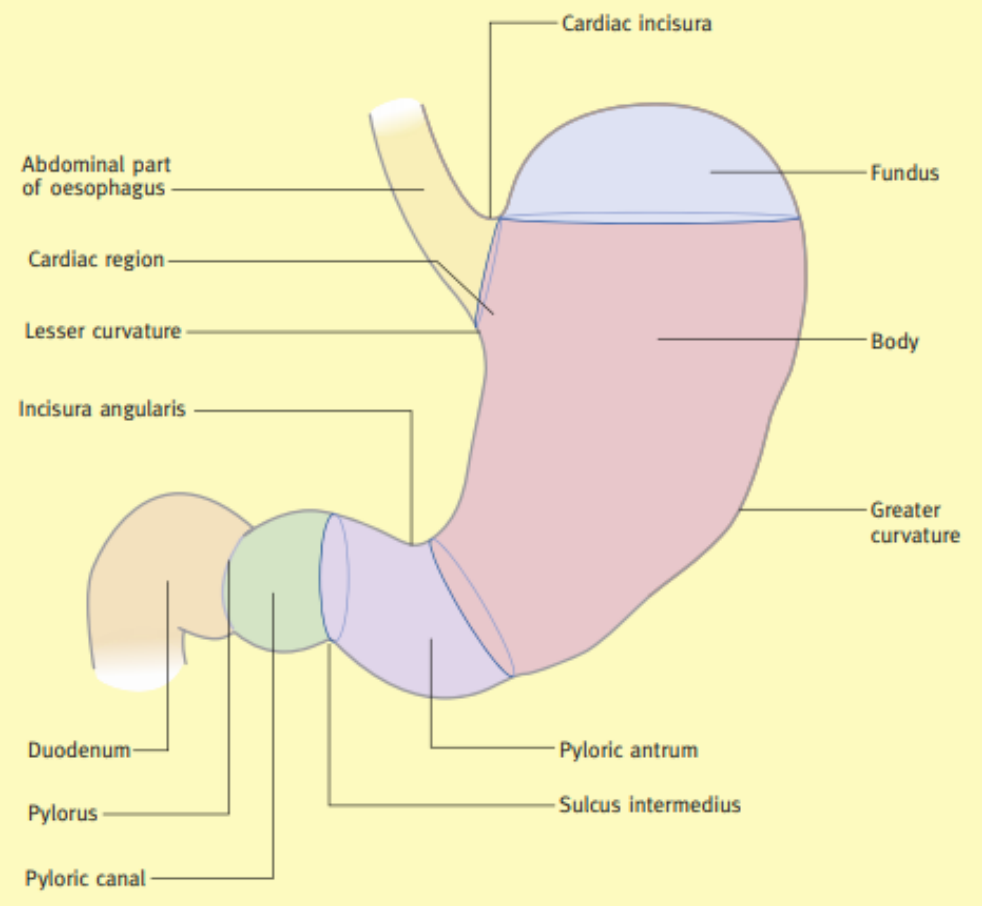

Figure 1.4 Structure and regions of the stomach. The cardiac region contains a layer of circular smooth muscle that acts physiologically as a barrier between the oesophagus and stomach. The fundus and body (corpus) of the stomach are seperated at the level of the cardiac incisura (cardiac notch) and are the main sites of gastric acid secretion. The pyloric antrum that lies distal to the body of the stomach, between the incisura angularis and sulcus intermedius, and secretes hormones that regulate gastric secretions (e.g. gastrin and somatostatin). The pyloric canal controls the outflow rate of chyme to the duodenum through the pyloric sphincter, an area containing a dense layer of circular muscle. Image obtained from Mahadeven (2014)[2].

The proximal segment of the pylorus, the pyloric antrum, is a region loosely define area between the angular incisure and the distal pyloric segment, the pyloric canal. Tonic and phasic contractions in the body and antrum of the stomach mix the gastric contents with gastric secretions, breaking down ingesta both chemically and mechanically. Antral glands also secretes mucus and hormones that regulate the cephalic (sensory stimuli, such as taste and smell) and gastric (chemical and mechanical stimuli) phases of gastric secretion[3].

The pyloric canal is the terminal tubular segment of the stomach and leads to the anatomical pyloric sphincter that forms the gastroduodenal junction. The thick coat of

circular muscle surrounding the pyloric sphincter controls gastric emptying into the duodenum. This process, like the cardiac orifice, is regulated by autonomic motor fibers. However, the pyloric sphincter also receives local inputs from hormonal stimuli and myenteric (ENS) reflexes from the stomach and/or duodenum[18].

1.1.3 **Microscopic Anatomy and Physiology of the Stomach**

Gastric wall

From the outer most layer of the stomach wall, the serosa encapsulates the stomach and is contiguous with peritoneal omenta and ligaments (Figure 1.5). The muscularis consists of three sheets of muscle, the outermost layer lying longitudinal, followed by a circular (middle) and oblique (innermost) layer around the stomach[3]. The outer layer of the ENS, the myenteric plexuses, is located between the longitudinal and circular layers of muscularis, innervated by sympathetic and parasympathetic neural fibres and serves as the central control gastric motility[5].

Underneath the muscular layers is the submucosa, which contains the arterial, venous and lymphatic vessels, as well as stretches of submucosal ganglia. The muscularis mucosae then serves as a flexible barrier between the submucosa and the innermost layer of the stomach, the mucosa.

The mucosa contains the muscularis mucosae, lamina propria (connective tissue) and the gastric pits. The long, tubular pits within the branched mucosal layer contain the gastric glands. Gastric glands are categorized as mucus-secreting cadiac glands, acid-secreting oxyntic glands (found mainly in the fundus and body), or the gastrin-secreting antral/pyloric glands (Figure 1.6).

Gastric glands

Mucous cells in the apical pit region of gastric glands (Figure 1.6) secretes an alkaline fluid containing mucin. Mucin lubricates and forms a gel coating on the interior stomach wall, shielding the mucosa from the abrasive churning of food, gastric pathogens and erosive damage from proteases and the low pH gastric fluid[19]. Mucous cells in the isthmus secrete a more acidic mucin fluid and are the progenitor cells that differentiate into all other glandular cell types. Newly formed mucous cells migrate up the neck of the gland and shed the old layer of cells into the gastric fluid. The turnover rate of surface mucous cells is between 4-7 days[3].

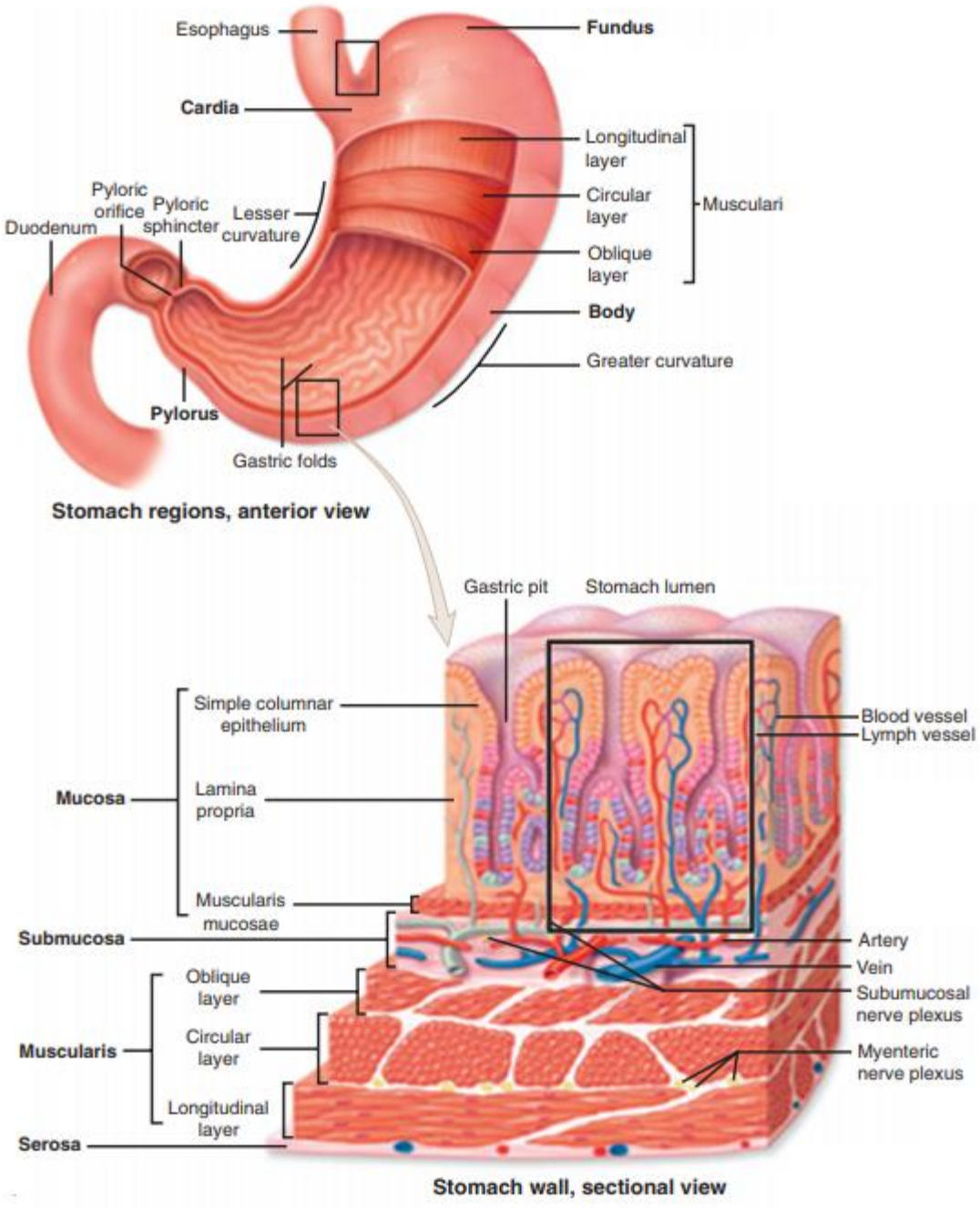

Figure 1.5 Anterior and sectional views showing the layers of the stomach wall. The stomach is surrounded by a serosal lubricant layer, which covers the longitudinal, circular and oblique layers of muscle. Myenteric ganglia lie between the longitudinal and circular muscle layers and control gastric motility. The arterial, venous and lymphatic vasculature lie within the submucosa along with submucosal nerve ganglia. The innermost layer of the gastric wall, the mucosa, contains the muscularis mucosae, lamina propria (connective tissue) and gastric glands. Image adapted from Wilson and Stevenson (2019)[3].

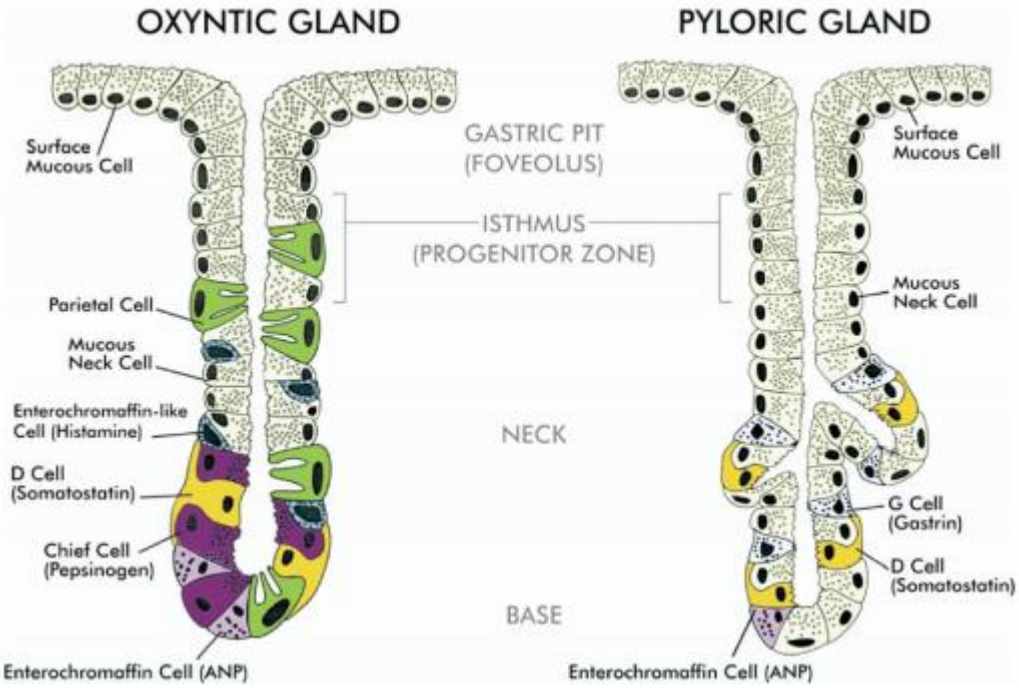

Figure 1.6 Cross-sectional view of oxyntic and pyloric (antral) gastric glands. Gastric glands are long tubular foveolae containing various epithelial cells that regulate gastric secretions. Surface mucous cells line the stomach lumen and secrete bicarbonate and mucin to form a protective layer for the gastric mucosa against gastric acid and contents. Mucous cells found within the gastric pits also secrete mucin and are able to differentiate into other types of cells within the gastric gland. Parietal and chief cells are mainly found in oxyntic glands and have the primary functions of secreting gastric acid (H^+) and pepsinogen respectively. Enteroendocrine cells are found in both types of gastric glands and provide endocrine and paracrine control of gastric activity. The hormonal secretions from these cells are heavily regulated by ENS and ANS systems. Inhibition of gastric acid secretion is mainly mediated by somatostatin release from D cells, which can be stimulated by ANP release from EC cells. Conversely, acid secretion is stimulated by histamine (oxyntic ECL cells), gastrin (antral G cells) and acetylcholine (cholinergic vagal efferent neurons). Image obtained from Schubert and Peura (2008)[17].

Parietal cells migrate to the lower neck and base of gastric glands and have the primary function of secreting hydrochloric acid (HCl; 160mM, pH 0.8)[17]. Parietal cells also secrete intrinsic factor, a glycoprotein that binds to acid-sensitive vitamin B_{12} (cobalamin) and facilitates its absorption in the terminal ileum[3]. It is estimated that 95% of parietal cells are located in the oxyntic glands (Figure 1.6), with the remaining 5% found in antral glands. However, half of all antral glands were found to contain parietal cells[20].

Chief (zymogenic) cells pre-dominate the base of oxyntic glands (Figure 1.6) and have the primary digestive function of secreting pepsinogen. This inert zymogen is secreted

into the gastric lumen from apical granules in chief cells following release of intracellular calcium stores. Chief cells are stimulated by similar stimuli to parietal cells including Ach and gastrin[3]. Pepsinogen, at gastric pH of <2, undergoes rapid activation by loss of N-terminal peptides and conformational exposure of two catalytic sites, which forms the active protease pepsin. Pepsin is one of the main digestive enzymes that hydrolyses ingested proteins with an optimal pH activity between 1.8-2.3[21].

Enteroendocrine cells are a diverse group of epithelial cells found across the entire GI tract that regulate gastric activity through paracrine and endocrine secretions (discussed further below). Enteroendocrine cells found in gastric glands include enterochromaffin (EC), enterochromaffin-like (ECL), D, G and Ghrelin cells. The activity of these cells is regulated by release of neuropeptides by efferent vagal fibers including pituitary adenylyl cyclase–activating polypeptide (PACAP), gastrin-releasing peptide (GRP), vasoactive intestinal polypeptide (VIP) and acetylcholine (Ach)[17]. Sensory afferent fibres projecting from T6-12 dorsal root ganglia innervate the stomach wall and release calcitonin gene-related peptide (CGRP). Release of CGRP from the peripheral ends of sensory neurons stimulates several reflex responses including increased gastric blood flow, release of somatostatin and inhibition of acid secretion and gastric motility[22,23] (Figure 1.7).

Gastric acid secretion

The highly acidic nature of gastric fluid serves to begin the breakdown of ingesta and activate the protease pepsin from its zymogen form pepsinogen, which is secreted by chief cells in oxyntic glands. The low pH also aids in sterilizing the stomach from pathogenic bacteria[19]. *Helicobacter pylori (H. pylori),* a common cause of gastric ulceration, has however adapted several mechanisms to thrive in the harsh gastric environment (see section 1.2.3).

Secretion of H^+ across the apical membrane of parietal cells into the gastric lumen is precisely regulated by various pathways. Neurocrine control of gastric acid secretion involves stimulatory and inhibitory stimuli from the enteric and autonomic nervous systems that act directly, via release of neuropeptides (e.g. **acetylcholine, Ach**), and/or indirectly through postganglionic enteric neuron signalling (see section 1.1.1). Gastric

acid secretion can be stimulated hormonally by release of the endocrine mediator, gastrin from antral G cells and the paracrine mediator histamine, by ECL cells.

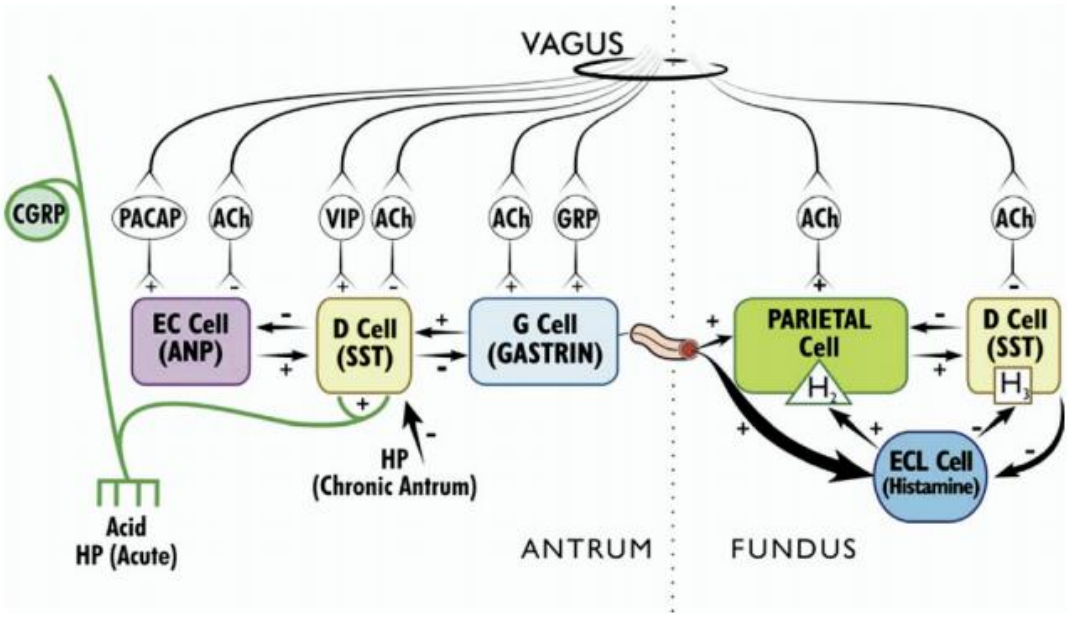

Figure 1.7 Influence of vagal and calcitonin gene-related peptide (CGRP) efferent neurons on the regulation of gastric acid secretion. Antral release of gastrin is stimulated by release of Ach and GRP from vagal efferent fibers and repressed by somatostatin release from D cells. Somatostatin acts as the main inhibitor of gastric acid secretion in antral and oxyntic glands. Its release is stimulated by low gastric pH (induced by parietal cell activity or acute H. pylori infection), CGRP sensory neurons, ANP released from EC cells, VIP vagal neurons and gastrin, and is repressed by chronic *Helicobacter pylori* (*H. pylori*) infection, vagal Ach neurons and histamine release from ECL cells. Image obtained from Schubert and Peura (2008)[17].

G cells are located in antral glands (Figure 1.6) and have the primary function of releasing **gastrin**, which is the main stimulant of acid secretion. Gastrin is post-translationally cleaved and modified into various isoforms, the main active form being gastrin-17, prior to its release in the circulatory system. Circulating gastrin is cleared mainly by the kidneys (partially by also the liver[24]) and has a short half-life (3-4 minutes) as demonstrated in porcine plasma[25].

Gastrin binds to cholecystokinin-2 (CCK_2; formerly CCK_B) receptors on parietal, enterochromaffin-like (ECL) and progenitor cells in oxyntic glands. Progenitor cells stimulated by gastrin induce proliferation of ECL and parietal cells. The ability for gastrin to stimulate parietal cells directly is much less potent than its secondary action of stimulating **histamine** release from ECL cells. Gastrin also potentiates histamine production in ECL cells by increasing histidine deacetylase (HDC) activity and gene

transcription. Gastrin is stimulated in G cells by neurocrine signalling (Ach and GRP), as well as by secretin (duodenal hormone), β2/β3-adrenergic agonists, calcitonin (thyroidal hormone), luminal amino acids, and fermented alcoholic beverages. Conversely, gastrin secretion is inhibited by somatostatin, which acts as a negative feedback of gastrin secretion and other D cell-mediated mechanisms (Figure 1.6)[3,17].

As alluded previously, histamine is produced by the HDC-mediated decarboxylation of L-histidine in ECL cells. Histamine is contained in intracellular vesicles and released upon stimulation by gastrin, PACAP, VIP and ghrelin (released by Ghrelin cells found mainly in oxyntic glands). Inhibitors of histamine include somatostatin, CGRP, prostaglandins, peptide YY and galanin. Histamine-mediated stimulation of H_2 receptors on parietal cells increases secretion of gastric acid[17]. Studies in murine stomach also show that stimulation of H_3 receptors on D cells leads to a reduced secretion of somatostatin, thereby further potentiating gastric acid secretion[26].

The main inhibitor of gastric acid secretion is **somatostatin**, which is produced by D cells in both oxyntic and antral glands[17]. Somatostatin production is stimulated by VIP, CCK, glucagon-like peptide, peptide YY, neurotensin, glucose-dependent insulinotropic polypeptide, leptin, and epidermal growth factor, CGRP, gastrin, secretin, adrenomedullin, amylin, adenosine and atrial natriuretic peptide (ANP; produced by enterochromaffm (EC) cells). Conversely, somatostatin is inhibited by Ach (released by cholinergic neurons) and interferon-γ. Somatostatin targets somatostatin receptors on ECL, G and parietal cells, inhibiting of histamine, gastrin and cyclic adenosine monophosphate (cAMP) production respectively[3,17].

Sodium/potassium-transporting ATPase, also called the proton pump, is basally contained in cytoplasmic tubulovesicles, which fuse with the apical parietal membrane upon stimulation, increasing the functional surface area between 5-10 fold. H^+/K^+ ATPase facilitates the electroneutral exchange of intracellular H^+ with luminal K^+ ions, forcing H^+ ions against a high concentration gradient and into the gastric lumen. Electroneutrality is maintained in the parietal cells by potassium and chloride channels on the apical membrane and Ae2 Cl^-/HCO_3^- exchange proteins on the basolateral membrane.

The aforementioned (bolded text above) neurohumoral stimulants act on various receptors of parietal cells to activate or inhibit two signalling pathways that lead to

activation of the proton pump, H^+/K^+ ATPase. Adenylate cyclase catalyses the conversion of adenosine triphosphate (ATP) to cAMP, which leads to the activation of protein kinase A that increase H^+/K^+ ATPase activity. Adenylate cyclase activity is stimulated by the binding of histamine binds to H_2 receptors and inhibited by somatostatin binding to somatostatin receptors on parietal cell membranes.

The other main signalling pathway involves the activation of phospholipase C (PLC) to convert phosphatidylinositol 4,5-bisphosphate, a membrane-bound phospholipid, into inositol triphosphate (IP_3). IP_3 then mobilizes Ca^{2+} release from intracellular stores, a process that causes protein kinase C-mediated H^+/K^+ ATPase activation. PLC is activated by both the binding of gastrin to CCK_B receptors and Ach to M_3 receptors on parietal cells.

1.2 **Epidemiology, Aetiology and Prophylaxis of Peptic Ulceration**

1.2.1 **Epidemiology of peptic ulcer disease (PUD) and its associated complications**

Peptic ulcers are mucosal breaches through the mucosal layer of the GI tract that are greater than 3mm (sometimes defined as >5mm) in diameter[27]. Peptic ulcers occur mostly in the stomach and proximal duodenum, but uncommonly also develop in the oesophagus and lower small intestine. Gastric ulcers are most likely to develop along the distal greater curvature but can occur in any of the four anatomical regions of the stomach. Duodenal ulcers occur mostly in the superior segment were gastric chyme first enters the small intestine. Ulcers that develop in the distal duodenal segments may indicate underlying diseases such as Crohn's, ischaemia or Zollinger-Ellison syndrome.

Since the role of *H. pylori* in peptic ulcer development was discovered in 1982 by Warren and Marshall[28], cases of *H. pylori*-infected PUD has begun to notably decline with the improving sanitary conditions and widespread use of antibiotics[29]. Despite this, the ever-looming threat of antibiotic resistance and the expanding use of non-steroidal anti-inflammatory drugs (NSAIDs) and low-dose aspirin (LDA) in an ageing population have meant that PUD and its related upper gastrointestinal complications (UGICs) are and will continue to be a major clinical challenge in terms of cost, hospital admissions, morbidity and mortality[30,31]. A retrospective study performed in a tertiary

UK hospital highlights a shift in peptic ulcer aetiology, characterized by a decrease in *H. pylori*-positive and an increase of NSAID and non-NSAID, non-*H. pylori* PUD[32].

A systematic review of the global burden of PUD estimated an annual prevalence and incidence of 0.12-1.50% and 0.10-0.19% respectively. This study however mainly focused on western populations, so does not include several developing countries that have substantially higher prevalence of H. pylori infections[33]. A recent systematic analysis by the Global Burden of Disease estimated a global PUD prevalence and incidence of approximately 75 and 10 million respectively in 2016 alone[34]. An average of 1 in 8 of the UK population will develop a peptic ulcer in their lifetime, increasing the risk of UGICs such as haemorrhage and perforation by fivefold[35].

Clinical manifestation of peptic ulcer depends on inter-individual variation, severity, location and pathogenesis of the lesion. A full list of aetiological peptic ulcer classifications is described in Table 1.1. Individuals with gastric ulceration present postprandial dyspeptic symptoms, typically including epigastric pain, gastroesophageal reflux/heartburn, bloating and nausea. In some cases, chronic ulcers, especially those that are NSAID-induced, can be asymptomatic. Individuals with self-healing asymptomatic ulcers that self-heal will likely relapse unless the causal factor is removed.

The main complications of untreated gastric ulcer are pyloric obstruction, GI bleeding and perforation. Bleeding risk is highest in people over 60 years old and typically presents as hematemesis, melena and/or anaemia. Fatality rates with gastric bleeding are between 5-10% and have a prevalence of 50-170 per 100,000[29]. Perforation, characterised by a sudden onset of constant intense upper abdominal pain, is much less common, with incidence rates of 7-10 per 100,000[29]. However, depending on age and comorbidity, perforation mortality rates can be up to 20%[36].

Though only observed rarely (<5%), fibrosis around ulcerative tissue can cause gastric outlet obstruction and is pathognomonic with postprandial vomiting. In cases of partial obstruction, pyloric oedema can usually be controlled by acid suppressing medication such as proton pump inhibitors (PPIs). Significant obstruction may however require surgical intervention including endoscopic balloon dilation, vagotomy or gastro-jejunostomy[37].

Table 1.1 Classification of peptic ulcers and examples of their associated risk factors. Table based on information from Malfertheiner *et al*.[29] and Ramakrishnan & Salinas[30].

Classification	Associated risk factors/examples
H. pylori positive	Infection most likely a consequence of direct human-to-human transmission and is acquired at early childhood[38].
Drug-induced	NSAIDs[39], bisphosphonates[40-42], clopidogrel[43], unfractionated heparin[44], intra-arterial infusion chemotherapy[45] and crack cocaine[46]
H. pylori and NSAID positive	See above
Acid hypersecretory state	Zollinger-Ellison syndrome[47] and systemic mastocytosis[48]
Postoperative ulcer	Subtotal gastrectomy, pancreatic resection and Roux-en-Y gastric bypass surgery[49,50]
Other rare diseases	Crohn's disease of stomach of duodenum[51], eosinophilic gastroduodenitis[52], radiation damage[53], viral infections[54] and gastric colonisation of *Helicobacter heilmannii*[55]
Cameron ulcer	Gastric ulcer caused by hiatus hernia passing through the diaphragmatic hiatus[56]
Stress ulcer	After acute illness, multi-organ failure, ventilator support, extensive burns (Curling's ulcer), or head injury (Cushing's ulcer)[57]
Idiopathic ulcer	No positive marker for any of the above classifications[58]

Due to the generally non-specific nature of the symptoms, diagnosis of gastric ulcer must be confirmed by endoscopy if the patient is over 55 and/or presents other concerning symptoms (e.g. signs of bleeding, perforation, obstruction or malignancy). Patients under 55 years of age with no other perturbing symptoms are tested for *H. pylori* infection and advised to discontinue the consumption of gastric irritants including NSAIDs, smoking and alcohol[30].

1.2.2 **Gastric defence: protective factors**

To understand how peptic ulcers arise, it is first important to understand the numerous redundant gastric defence and repair mechanisms that must be overcome by

ulcerogenic agents and pathogens. The following section aims to give a succinct description of the key pre-epithelial, epithelial and subepithelial processes that work together to repel aggressive luminal factors.

Mucus-bicarbonate barrier

The frontline defence against gastric aggressors is a gel-like layer constituting of mostly water (approx. 95%), but also mucin glycoproteins, bicarbonate anions and surfactant phospholipids, all of which are secreted by surface epithelial cells (Figure 1.8). The luminal surface of the mucus gel has a hydrophobic layer of surface-active phospholipids, making the mucus gel mostly immiscible with the luminal gastric fluid[59].

Over 20 mucin proteins have been described from the MUC gene family and they either are secreted (gel forming or non-gel forming) or membrane-associated proteins. The gel forming mucins (MUC2, MUC5AC, MUC5B, MUC6 and MUC19) are differentially expressed throughout the gastrointestinal tract[60] and are released from surface epithelial cells along with trefoil factor peptides (TFF1-3). TFFs promote restitution (epithelial cell migration), regeneration (proliferation and differentiation of epithelia) and stability of the mucus barrier at gastric lesion sites by interacting with mucin proteins[61].

Restitution of the surface epithelium following gastric injury has shown to take only a few minutes in animal models[62,63]. MUC6 produced by neck and gland cells and MUC5AC synthesized by surface epithelial and pit cells polymerize to form long mucin chains that provide the structural support of gastric mucus[64]. Glycan structures on MUC5AC and MUC6 have also shown to have protective effects against *H. pylori*[65,66]. Gastric mucus secretion is regulated by gastrin and secretin hormones, as well as prostaglandins and acetylcholine[67].

Bicarbonate is released through Cl^-/HCO_3^- anion exchangers from the apical membrane of surface epithelium. Bicarbonate secretion is stimulated by binding of E-type prostaglandins (e.g. PGE_2) to prostaglandin E_2 receptors (EP receptors 1-4), increased luminal acid and several hormonal regulators (reviewed in [68]).

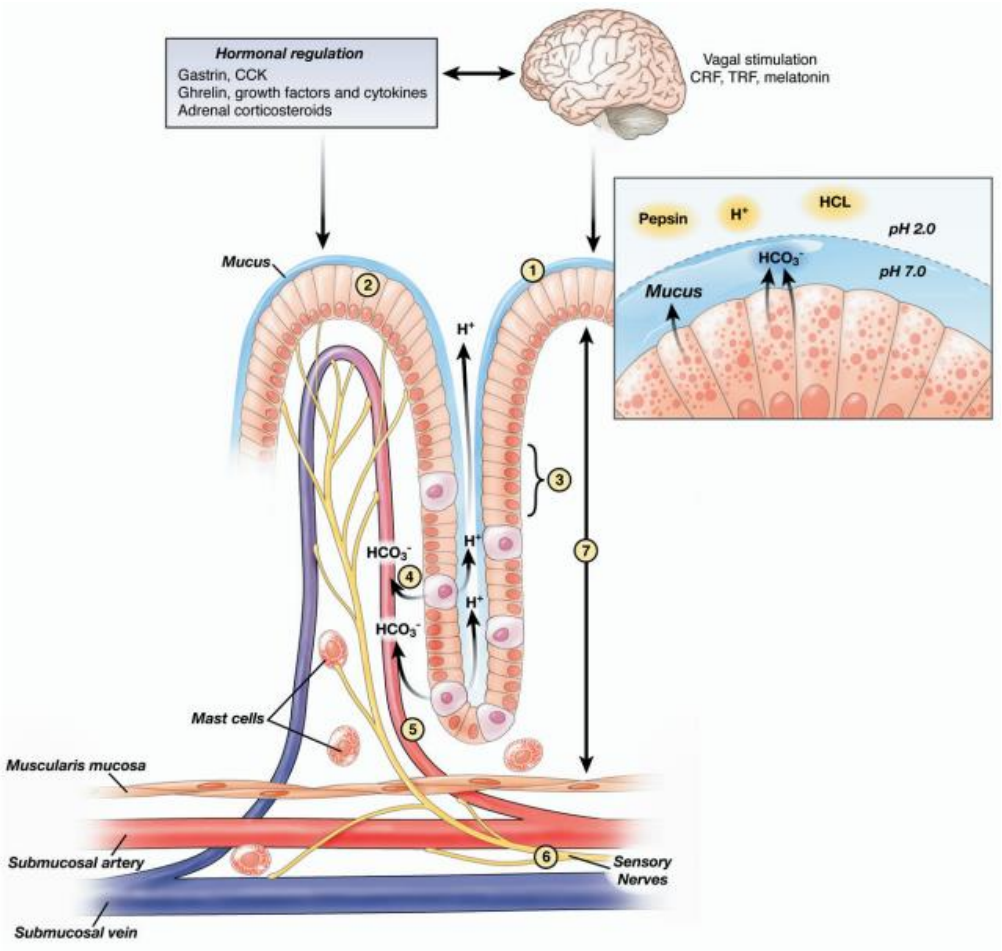

Figure 1.8 The mechanisms of endogenous gastric mucosal defence. (1) The mucus barrier is comprised of mucin polymers and bicarbonate ions and acts as a physical barrier between gastric acid/pepsin and the mucosal tissue. (2) Surface epithelial cells are connected by tight junctions, secrete mucus and bicarbonate ions, generate mediators of mucosal repair (prostaglandins, trefoil factors, heat shock proteins, etc.) and produce the antibacterial peptides cathelicidin and β defensin. (3) Surface epithelial cells are constantly replaced by progenitor cells stimulated by TGFα and IGF-1 growth factors. (4) HCO_3^- anions are secreted from the basolateral membrane of parietal cells into the interstitium near capillary blood vessels. Bicarbonate ions then migrate toward surface epithelial cells for the maintenance of the mucus barrier and the neutralization of gastric acid in the duodenum. (5) Prostaglandins, nitric oxide and hydrogen sulphide cause vasodilation of mucosal capillaries, which supply essential nutrients and remove noxious agents, and prevent adhesion/aggregation of leukocytes/platelets. (6) Sensory afferent nerves that permeate through the lamina propria detect chemical stress and release calcitonin gene-related peptide and substance P, which ultimately stimulates vasodilation of submucosal blood vessels. (7) Prostaglandins stimulate/facilitate almost all mucosal defence mechanisms. Figure adapted from the following reviews ([69-71]).

Epithelial defensive mechanisms

When the mucus barrier is breached, gastric protection then relies on secondary defence mechanisms. The next line of gastric defence is the epithelial barrier, which is continuously renewed from mucosal progenitor cells and can be completely replaced in 3-7 days[70] (Figure 1.8). Proliferation of progenitor cells is regulated by the binding of transforming growth factor α (TGF-α) and insulin-like growth factor 1 (IGF-1) to epidermal growth factor receptors (EGFRs)[72]. PGE_2 and gastrin can also stimulate epithelial proliferation by causing EGFR transactivation and mitogen-activated protein kinase pathway activation[73]. Surface epithelial cells form tight junctions to prevent back diffusion of acid and pepsin[67]. Surface epithelial cells have a hydrophobic phospholipid exterior that repels luminal fluid containing acid and pepsin[59]. Intracellular heat shock proteins activate following cellular stress (e.g. heat, oxidation, chemical, etc.) to prevent/repair protein denaturation[68]. Cationic peptides cathelicidin and β defensins, produced in gastric epithelial cells, prevent bacterial colonisation by disrupting bacterial membranes[74] and promote ulcer healing through TGFα-dependent transactivation of EGFR[75].

Role of mucosal blood flow in gastric defence

Arteries within the submucosa branch into capillaries that permeate through the lamina propria, removing toxic metabolites and supplying mucosal cells with oxygen and essential nutrients (Figure 1.8). Mucosal stress, detected by sensory afferent neurons, leads to vasodilation of mucosal blood vessels by the release of prostaglandin I_2 (PGI_2) and NO from vascular endothelial cells[76]. This causes an increase in mucosal blood flow to allow for a rapid removal of noxious agents and dilution of back-diffused acid. NO and hydrogen sulphide (H_2S) are endogenously generated gaseous mediators that have anti-apoptotic/anti-necrotic[77,78] and proangiogenic[79,80] properties. NO, PGI_2 and H_2S inhibit leukocyte adhesion to vascular endothelium, preventing ischemic damage during gastric mucosal damage[70,81].

Neurohormonal regulation of gastric defence

As described in 1.1.1, gastric functions are heavily regulated by the CNS and ENS. Central and peripheral corticotropin-releasing factor (CRF) release, following acute stress, causes inhibition of gastric motility and emptying and type 2 CRF receptor-

mediated anti-apoptotic effects in gastric epithelial cells[82]. Several other hormonal peptides stimulated by sensory afferent nerves, CGRP or NO provide gastroprotection by increasing PGE_2 levels (thyrotropin-releasing hormone[83]), gastric mucosal blood flow (gastrin[84,85], CCK-8[86,87], bombesin[88], epidermal growth factor[89], peptide YY[90], NK_2 receptor agonists[91] and ghrelin[92]) and reduced gastric acid secretion (transforming growth factor alpha and epidermal growth factor[93]). Endogenous glucocorticoid hormones release following stress activates the hypothalamo-pituitary-adrenocortical axis and provides potent gastroprotection against gastric injury[94,95]. The gastroprotective effects of glucocorticoids are similar to that of prostaglandins in that they increase mucosal blood flow and mucus production, as well as reduce gastric motility and microvascular permeability[96].

Overarching gastroprotective role of COX-mediated prostanoid generation

As mentioned above, prostaglandins (mainly PGE_2 and PGI_2) reduce acid secretion and leukocyte/platelet adhesion and increase mucosal blood flow, HCO_3^- and mucus secretion. However, prostaglandins play a role in almost all gastric defence pathways (Figure 1.8). As well as the mechanisms already mentioned, prostaglandins also reduce epithelial permeability[97] (acid back-diffusion) and gastric hypermotility[98], inhibit release of inflammatory mediators[99] and TNFα overexpression[100], and stimulate angiogenesis through the release of vascular endothelial growth factor (VEGF) from gastric fibroblasts[99,101].

Inflammation is a natural defence mechanism that prevents entry of microbes into systemic circulation and removes damaged tissue to aid in tissue repair. However, in some cases, inflammation can amplify damage at wound sites by the local release of apoptotic/necrotic mediators or by causing vasoconstriction and oedema, restricting arterial oxygen and nutrient supplies to ulcer sites[102]. PGE_2 strongly inhibits release of leukotriene B_4 and interleukin-8 (IL-8) from neutrophils[103-105], platelet-activating factor, tumour necrosis factor-α (TNF-α) and histamine from mast cells[106], and TNF-α and IL-1 from macrophages[107,108].

The constitutively expressed cyclooxygenase-1 (COX-1) and inducible COX-2 isozymes catalyse the conversion of arachidonic acid to prostaglandin H_2, the rate-limiting step in the generation of prostanoids, a subclass of eicosanoids consisting of the thromboxanes, prostacyclins and prostaglandins[1].

COX-1 is expressed in nearly all tissues and performs homeostatic functions including, gastric cytoprotection, platelet aggregation and renal blood flow autoregulation[109,110]. COX-2 is expressed at low levels in stomach tissue, but can be rapidly upregulated in inflammatory cells during pathological states including inflammation and tumorigenesis[109,111].

Selective COX-1 and COX-2 inhibitors decrease gastric mucosal blood flow and increase leukocyte adherence respectively, in a rat model, suggesting discrete functions for these isozymes in gastroprotection[112]. Inhibition or knockdown of COX enzymes only causes gastric lesions when both isoforms are depleted, but increased ulceration can occur with depletion of one isoform under acid challenge, NO suppression and afferent nerve ablation[113,114]. COX-1 and COX-2 are upregulated in tissue surrounding ulcer sites and cause inhibition or knockdown. COX-2 or combined COX-1/COX-2 inhibition/knockdown impairs ulcer healing[115,116].

1.2.3 **Gastric defence: aggressive factors**

Aggressive factors differ in the lumen of the stomach and small intestine. The main aggressors in the stomach are the gastric acid, proteases (most notably pepsin), bile salts, ingesta (e.g. alcohol and NSAIDs) and pathogenic infections (e.g. *H. Pylori*)[117]. Whereas, aggressive factors in the small intestine include bile acid, hydrolases/proteases, pancreatic secretions and intestinal bacteria[118]. As described above, pro-inflammatory responses caused by NSAIDs, H. pylori and other gastric stressors are another key aggressive factor in ulcer pathogenesis and recurrence[119].

Though there are several causes of peptic ulceration (Table 1.1), the following sections will focus on the two major factors of clinically diagnosed peptic ulcers: *H. pylori* infection and NSAID use, plus the role of environmental and psychological risk factors. NSAID-induced gastric ulceration is covered in more detail in section 1.3.

Helicobacter Pylori (H. Pylori)

A recently performed meta-analysis including 183 studies estimated the global prevalence of *H. pylori* infection to be 44.3%. The study also identified a significantly higher infection rate in developing countries compared to developed countries, 50.8% and 34.7% respectively[120]. Whilst almost half of the world's population carry gastric colonies of *H. pylori*, there is a 5-10% risk for those infected to develop peptic ulcer

disease[29] and a 1% risk of developing distal gastric cancer. The occurrence and type of ulceration depends on various infection factors such as pattern of gastritis, changes to hormone and acid secretions, gastric/duodenal metaplasia, mucosal penetrance, host immunity, ulcerogenic strains of *H. pylori* and host genetic factors[29].

Pan-gastritis, due to an evenly distributed gastric *H. pylori* infection, is commonly associated with intestinal metaplasia and reduced acid secretion. Acid hyposecretion is secondary to a loss of parietal cells from oxyntic glands during atrophic gastritis. Conversely, antral-predominant gastritis is accompanied by gastric metaplasia, decreased somatostatin release and increased gastrin and acid secretion. Antral-predominant gastritis and pan-gastritis are associated with increased risks for development of duodenal and gastric ulcers respectively[121].

Other risk factors

While *H. pylori* infection and NSAIDs are the most important factors for the development of PUD, various other risk factors have been identified that significantly affect its occurrence, recurrence and morbidity (Table 1.2).

Several epidemiological studies have identified a higher rate of peptic ulcer in males[35,122-125]. This phenomenon may be due to either genetic or lifestyle differences between genders. Alcoholism is higher in men[126-128], a risk factor discussed further below. A mechanistic study in male and female rats found that ethanol-induced gastritis caused higher epithelial proliferation and PGE_2 production in female rats[129]. A protective role has also been shown for oestrogen, in that it reduces gastric acid secretion[130] and protects against ulcer formation[129].

Increasing age is strongly associated with PUD and PUD-related disease and mortality, most likely because of the increased prevalence of comorbidities (including *H. pylori* infection[131]), NSAID, anticoagulant and steroid use. Impaired gastric defence[132] and immunosenescence[133] that accompany old age may also contribute to these factors. A UK study that analysed data between 1997-2005 found the incidence rate for gastric ulcer raged from 0.17 per 1000 person-years (TPY) in the 40–54 age group to 0.63 per TPY in the 75–85 age group, and 0.23 per TPY to 0.49 per TPY respectively for duodenal ulcers[35]. A meta-analysis performed by Hernández-Díaz and Rodríguez highlights the increasing incidence rates of serious UGIC with age[134]. A

systematic review by Lau, *et al*. also found that the most important risk factor for mortality in PUD was age, with relative risk greatly increasing from the age of 60[135].

Table 1.2 Risk factors associated with peptic ulcer disease. Table adapted from Lau, *et al*., 2011[135]. Relative risk and odds ratios were not included because there was significant variance across and within studies. This is likely due to discrepancies between studies, as well as demographic and ethnic differences. t-PA, tissue plasminogen activator; PAI-1, plasminogen activator inhibitor type 1; NSAID, non-steroidal anti-inflammatory drug.

Risk factor	Occurrence	Recurrence	Mortality
Male sex	✓		
Increasing age	✓	✓	✓
Serious comorbidity	✓	✓	✓
t-PA, I/D or D/D genotypes	✓		
PAI-1 4G/4G genotype		✓	
Socioeconomic status	✓		
High alcohol consumption	✓		
Smoking	✓		
NSAID/aspirin use	✓	✓	
Anticoagulant use		✓	
Immunosuppressant use		✓	
Corticosteroid use		✓	✓
Shock		✓	✓
Low haemoglobin levels at initial presentation		✓	✓
Low blood pressure		✓	✓
Treatment delay			✓
H. pylori infection	✓	✓	
History of peptic ulcer	✓		
No history of peptic ulcer			✓
Large ulcer size (>1cm)	✓	✓	
Forrest class I-II		✓	✓
Recurrence of complication			✓

Various comorbidities are associated with a higher risk of PUD and PUD-related disease occurrence and recurrence, with multiple and more severe comorbidities further increasing risk[136,137]. Large retrospective and expert consensus studies have identified the following comorbidities as risk factors: liver cirrhosis, arthritis, bronchitis, chronic obstructive pulmonary disease, heart disease, renal insufficiency, diabetes mellitus, cerebrovascular disease, malignancy and connective tissue disease[136,138-140].

Tissue plasminogen activator (t-PA) and plasminogen activator inhibitor type 1 (PAI-1) are key regulators of fibrinolysis (the breakdown of fibrin in blood clots). A study in Korea highlighted a potential association between polymorphisms in these genes, increased occurrence of duodenal ulcer (t-PA I/D or D/D genotypes) and recurrence of peptic ulcer rebleeding (PAI-1 4G/4G genotype)[141].

Other genetic risk factors suggested to play a role in PUD pathophysiology include polymorphisms in inflammatory cytokines TNF-α[142] and interleukins-1B, -1RN[143], 2, -4, -6 and -8[144-146]. The O blood group has been associated with a higher risk of developing peptic ulcers[147,148], but earlier studies contradict this association[149,150].

Low socioeconomic status, defined as low levels of income, occupational status and/or educational achievement, is associated with many health issues[151] including peptic ulceration[152,153]. The link between social class and PUD may be explained by an increased risk of *H. pylori* infection found in crowded living conditions with poor hygiene standards[154,155], as well as increase rates of psychological stress, strenuous physical labour, substance abuse and analgesic use[140,153].

Alcohol and other constituents of certain alcoholic beverages increase gastric acid secretion and gastrin levels, with low and high doses increasing and reducing gastric emptying respectively[156]. Ethanol concentrations greater than 5% disrupt the mucosal barrier, causing focal areas of hyperaemia, oedema, epithelial necrosis and haemorrhage. Alcohol misuse was also found to reduce gastric mucosal PGE_2 synthesis[157]. Though direct relationships between alcohol, PUD, peptic ulcer bleeding and ulcer healing have shown inconsistent results[135,158], alcohol cessation is commonly advised for suspected cases of PUD[30].

The harmful effects of cigarette smoking are much more apparent than alcohol consumption. A large population-based study reported the prevalence of PUD to be 1.5-2 times higher in former/current smokers compared to those that have never smoked[136]. Smoking is also linked to delays in ulcer healing, which is likely related to the direct effects of smoking on gastrointestinal mucosa. The adverse effects of smoking on GI mucosa include: reactive oxygen species (ROS)-mediated epithelial cell death; impaired epithelial cell renewal; increased gastric acid production; reduced gastric and pancreatic bicarbonate production; pyloric incompetence/duodenogastric

reflux; increased risk of *H. pylori* infection and higher circulating levels of free radicals[159].

Non-NSAID iatrogenic ulcers have been reported with the use of clopidogrel (antiplatelet), bisphosphonates (anti-osteoporotic), unfractionated heparin (anticoagulant) and 5-fluorouracil (anti-cancer)[44]. Clopidogrel[160], corticosteroids[161] and anticoagulants[162] have been demonstrated to exacerbate risk of PUD and PUD-related complications with concomitant NSAID use.

Prophylaxis and management of peptic ulcer disease

Treatment of peptic ulceration consists of treating complications, identifying and eliminating the underlying cause of disease, relieving symptoms and healing ulcers. Oesophagogastroduodenoscopy (EGD) is indicated in cases of suspected PUD if patient is over 55, shows evidence of bleeding, weight loss, persistent vomiting or symptoms that do not subside with medication. For cases where EGD is unsuitable, such as suspected gastric outlet obstruction, barium or Gastrografin contrast radiography can be used[30].

Testing for *H. pylori* infection can be performed using various methods (reviewed in Ramakrishnan, 2007[30]). In patients that test positive for *H. pylori* infection, first-line treatment involves the administration of a PPI (detailed in NICE guidelines CG17[163]), and a 7-day course of two antibiotics including amoxicillin (except with penicillin allergies) and clarithromycin, metronidazole or tetracycline[163].

NSAID use should be avoided where possible but COX-2 selective NSAIDs can be used for patients at high risk, such as patients with history of previous ulcer for whom continuation of NSAID therapy is necessary. Regardless of cause, full-dose PPI or H_2 receptor antagonist therapy should be given for 4-8 weeks for all diagnosed peptic ulcers. Another useful agent in the protection against NSAID-induced peptic ulcer is the PGE_1 analogue, misoprostol[164,165].

Despite advancements in PUD management, peptic ulcer complications still have a substantial impact on morbidity, mortality and healthcare cost, most likely due to the widespread use of aspirin and other NSAIDs in an ageing population. The total cost for the management of PUD was estimated to be over 3 billion USD per annum in studies performed over the years 1998[166] and 2004[167]. PUD-related complications are

likely to account for a substantial proportion of the economic burden, based on a study that estimated the cost of bleeding, perforation, or both combined to be 12,000, 19,000, and 26,000 EUR per person respectively[168].

Refractory ulcers (defined as not having healed after 8-12 weeks of medical treatment or persistent complications despite medical treatment) and recurrent ulcers (recurrence after ulcer has healed) require long-term acid-suppression therapy. However, long-term PPI therapy has been associated with increased risk of gastric cancer, pneumonia, enteric infection and vitamin B12 deficiency[169,170].

1.3 **NSAIDs and their associated adverse drug reactions**

1.3.1 **Adverse drug reactions**

An adverse drug reaction (ADR) is defined as "A response to a drug which is noxious and unintended, and which occurs at doses normally used in man for the prophylaxis, diagnosis, or therapy of disease, or for the modifications of physiological function" by the World Health Organisation[171].

Adverse effects can either be related (i.e. on-target or type A reactions) or unrelated (i.e. off-target or type B reactions) to the known pharmacological actions of a drug. Several patient, drug and disease-related factors play a role in the development of ADRs (reviewed in Alomar, 2013[172]). On-target ADRs, such as haemorrhage with anti-coagulant use and sedation with anxiolytic use, are mostly reversible and subside by the lowering dosage or drug withdrawal.

Off-target ADRs can arise from overdose (paracetamol-induced hepatotoxicity) or factors such as pregnancy (thalidomide-induced teratogenicity) and predisposing disorders (prednisone-induced hypertension in congestive heart failure). Off-target reactions can also be idiosyncratic in nature, occurring only in a very small percent of the population. Many of these rare reactions are life threatening and usually go undetected during drug toxicity testing[173]. An idiosyncratic reaction can be caused by the direct action of a drug/metabolite or immune-mediated (referred as hypersensitivity reactions), such as carbamazepine-induced hypersensitivity[174].

ADRs present a heavy burden on both health care resources and finances. A prospective study performed across two UK hospitals found that ADRs account for 6.5% of all hospital admissions and 4% of hospital bed capacity, which is estimated

to cost £466 million per annum[31]. In the same study, mortality rates amongst ADR-related admission were 0.15%, suggesting an average of 5700 deaths per year in England alone[31]. Likewise, hospital admission estimates in the USA and Canada are 4.2-30% and 5.7%-18.8% in Australia, with the economic burden costing up to 30.1 billion USD (approx. £23.1 billion) every year[175].

ADRs are responsible for approximately 30% of drug attrition cases in pre-clinical and clinical stages of drug discovery[176]. Rarer genotypes, unforeseen drug-drug interactions and *in vitro*/*in vivo* model limitations are common causes of undetected ADRs reaching post-production and causing the drug withdrawal[177]. An analysis of the most common organs/tissues responsible for drug attrition in two pharmaceutical companies between 1993-2006, found that cardiovascular (CV) and liver toxicity accounted for 42.1% and gastrointestinal/pancreatic for 3.4% of all cases[178]. More updated estimates suggest clinical attrition due to GI adverse reactions is as high as 11% and that around 14-23% of drugs cause GI-related toxicity during clinical screening[179].

1.3.2 **Non-Steroidal Anti-Inflammatory Drugs and Coxibs**

COX inhibitors encompass the 'traditional' NSAIDs (tNSAIDs), which inhibit both COX-1 and COX-2 with no strong preference, and the coxibs, which have a strong selectivity to the COX-2 isoform. The COX-2 selective NSAIDs were designed in an attempt to retain the anti-inflammatory/analgesic properties but lessen the adverse gastrointestinal effects of non-selective NSAIDs.

Together there are now over 50 NSAIDs sold globally, with some commonly used examples described in Table 1.3. NSAIDs are used across most branches of medicine due to the widespread occurrence of inflammation and pain symptoms both outside and within the clinic. Several NSAIDs also possess anti-pyretic activity, making them useful for the treatment of fevers.

The analgesic effects of NSAIDs are used to relief postoperative, dental, menstrual and chronic joint pain, as well as headache and migraine symptoms. Anti-inflammatory effects are used to treat acute (e.g. sprains, fractures, etc.) and chronic (e.g. osteoarthritis, rheumatoid arthritis ankylosing spondylitis, etc.) swelling (Table 1.3).

Table 1.3 Indications for commonly used COX inhibitors in clinical practice. AS, ankylosing spondylitis; CV, cardiovascular; D, dysmenorrhoea; G, acute gout; H&M, headache and migraine; MS, musculoskeletal injuries and pain; OA, osteoarthritis; PO, postoperative pain; RA, rheumatoid arthritis. *NSAIDs also available as over-the-counter proprietary medications. Table adapted from Rang, *et al*. (2016)[110] and information from the NICE guidelines for NSAIDs[180].

Drug	Type	Indication	Comments
Ibuprofen*	Propionate	RA, OA, MS, PO, D, H&M	Fewer side effects but less potent anti-inflammatory effects. Can be given to children.
Naproxen*	Propionate	RA, OA, G, MS, PO, D	Good efficacy and low incidence of side effects
Diclofenac salts	Phenylacetate	RA, OA, G, MS, PO, H&M	Similar potency to naproxen.
Indometacin	Indole	RA, OA, G, MS, PO, D	High incidence of side-effects but can be used in moderate to severe disease
Aspirin*	Salicylate	Mostly CV usage but also for short term mild to moderate pain and pyrexia relief	Anti-platelet effect at low doses, potential use in cancer, Alzheimer's disease and radiation-induced diarrhoea
Mefenamic acid	Fenamate	RA, OA, PO, D	Occasionally associated with diarrhoea and haemolytic anaemia
Celecoxib	Coxib	RA, OA, AS	Reduced risk of serious upper GI events
Etoricoxib	Coxib	RA, OA, G, AS	Same as benefit as celecoxib

COX-mediated prostanoid biosynthesis and NSAIDs

COX-1 and COX-2 exist as membrane-bound homodimers and are inactive as monomeric species (Figure 1.9). Though there are mixed reports, several studies have shown differential localisation of COX-1 and COX-2 to the ER and nucleus respectively. One COX monomer stabilises the other monomer, allowing arachidonic acid (AA) to dock in the hydrophobic pocket of the adjacent enzyme[110].

Hydrolysis of cell membrane glycerophospholipids by phospholipase A_2 (PLA_2) during inflammation generates AA[181]. COX enzymes contain a hydrophobic channel through which AA enters to undergo two sequential catalytic reactions. First, a cyclooxygenase reaction links two O_2 molecules with AA at the C11 and C15 positions, generating the highly unstable PGG_2. A peroxidase reaction then converts PGG_2 to PGH_2 by reducing the molecule to produce a hydroxyl group at C15. PGH_2 is converted to the various prostaglandins and thromboxane A_2 (TxA_2) by tissue-specific isomerases[110,182] (Figure 1.9). Prostanoids act autocrine and juxtacrine modulators of various physiological systems, such as the CNS, gastrointestinal, respiratory, immune, endocrine, genito-urinary and CV system[183].

As well as the cytoprotective and anti-inflammatory actions in the stomach (Section 1.2.2), prostaglandins also serve as important mediators of pain signalling and early to late stages of inflammation. IL-1 released as part of the inflammatory response during infection causes the release of prostaglandins in the CNS, which disrupt the thermostatic control in the hypothalamus and causing a fever[110]. Prostaglandins also sensitise peripheral nociceptor endings by activating ion channels through protein kinase A and C (PKC) signalling pathways and consequentially potentiating pain signalling[184].

Inhibition of prostaglandin synthesis by use of NSAIDs can therefore prevent fever and pain signalling by resetting hypothalamic thermoregulation and inhibiting hyperalgesia. Inhibition of prostaglandin synthesis also reduces vasodilation at the cerebral vasculature, which may help alleviate headaches and migraines[110].

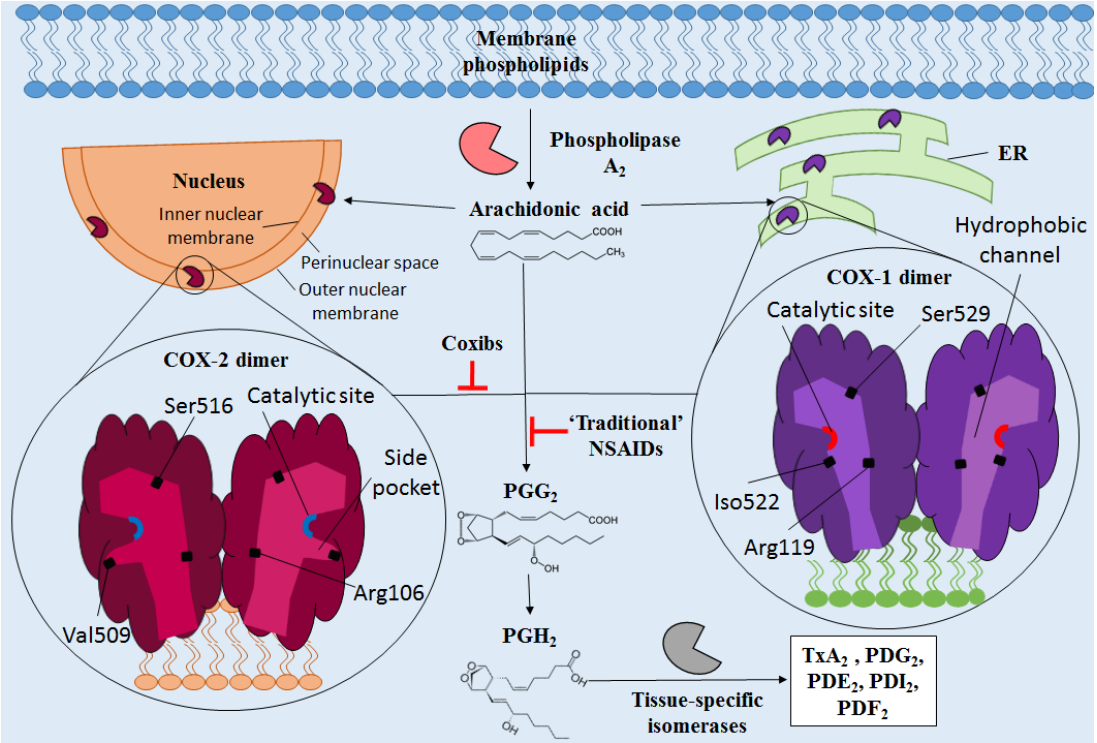

Figure 1.9 COX-mediated prostanoid synthesis. Cytokines, lysophospholipids, endotoxic lipopolysaccharides and other stress stimuli cause the kinase-mediated activation of PLA_2 during inflammation. PLA_2 hydrolyse the fatty acyl group on membranous glycerophospholipids, generating the free fatty acid, arachidonic acid. COX-1 and COX-2 enzymes localise to the endoplasmic reticulum (ER) and perinuclear space. COX enzymes first oxidize arachidonic acid to form PGG_2 and then reduce PGG_2 to form PGH_2. PGH_2 is then converted by tissue specific isomerases to the various prostanoids (TxA_2, PGD_2, PDE_2, PDI_2 and PDF_2). An isoleucine to valine change at position 522 on COX-1 (NP_000953.2) and 509 on COX-2 (NP_000954.1) reveals a side pocket in COX-2. This side pocket confers the selectivity of coxibs by allowing room for their bulky sulphur-containing groups[110,182].

COX-2 is responsible for the majority of prostaglandins synthesized in inflammatory cells and inflamed tissues following induction by inflammatory stimuli, hormones and growth factors. Examples of prostaglandin-induced pro-inflammatory effects include increased vasodilation, permeabilization of microvasculature, immune cell proliferation and activity, and inflammatory hyperalgesia[183].

The opposing roles of prostaglandins on inflammation are dependent on several factors surrounding their receptor subtypes. These include the type of cell/tissue expressing the receptors, subtype expression profiles, ligand affinity, and differential coupling to signal transduction pathways[183,185]. NSAIDs may also inhibit the anti-

inflammatory role of COX enzymes, which could explain the hypotheses that suggest long-term NSAID use may accelerate the progression of arthritic disease[186,187].

Vane and Piper first described the inhibitory effects of NSAIDs on COX-mediated prostanoid biosynthesis in 1971[188]. The non-selective NSAIDs are a diverse set of carboxylic acids (Figure 1.10) that inhibit all COX isoforms. These drugs act as competitive inhibitors by forming hydrogen bonds with the arginine residues at position 119 on COX-1 and 106 on COX-2, thus precluding entry of AA to the COX catalytic domain (Figure 1.9).

The exchange of a valine, at position 509 in COX-2, for an isoleucine, at the equivalent position in COX-1 (aa522), reveals a side pocket near the COX-2 active site (Figure 1.9). This COX-2 only side pocket enables access for bulkier, sulphur-containing coxib NSAIDs, which is restricted in the COX-1 hydrophobic channel. Other amino acid changes between the two isoenzymes have also been suggested to increase the accessibility of this COX-2 only side pocket, namely a COX-1 to COX-2 512His>513Arg and 433Ile>420Val[182].

NSAID-related ADRs

The most common side effects associated with long-term NSAID use are GI, CV and renal. GI-related toxicity will be covered in detail in section 1.4. Short-term use of NSAIDs for the management of pain and inflammation is generally well tolerated[189]. However, risk of ADRs increases with age, the presence of co-morbidities, long-term exposure and high doses of NSAIDs, factors that are common in the management of chronic conditions such as arthritis. Safety profiles vary considerably between individual NSAIDs, meaning that the selection of NSAID must therefore be tailored to best accommodate the safety of the patient.

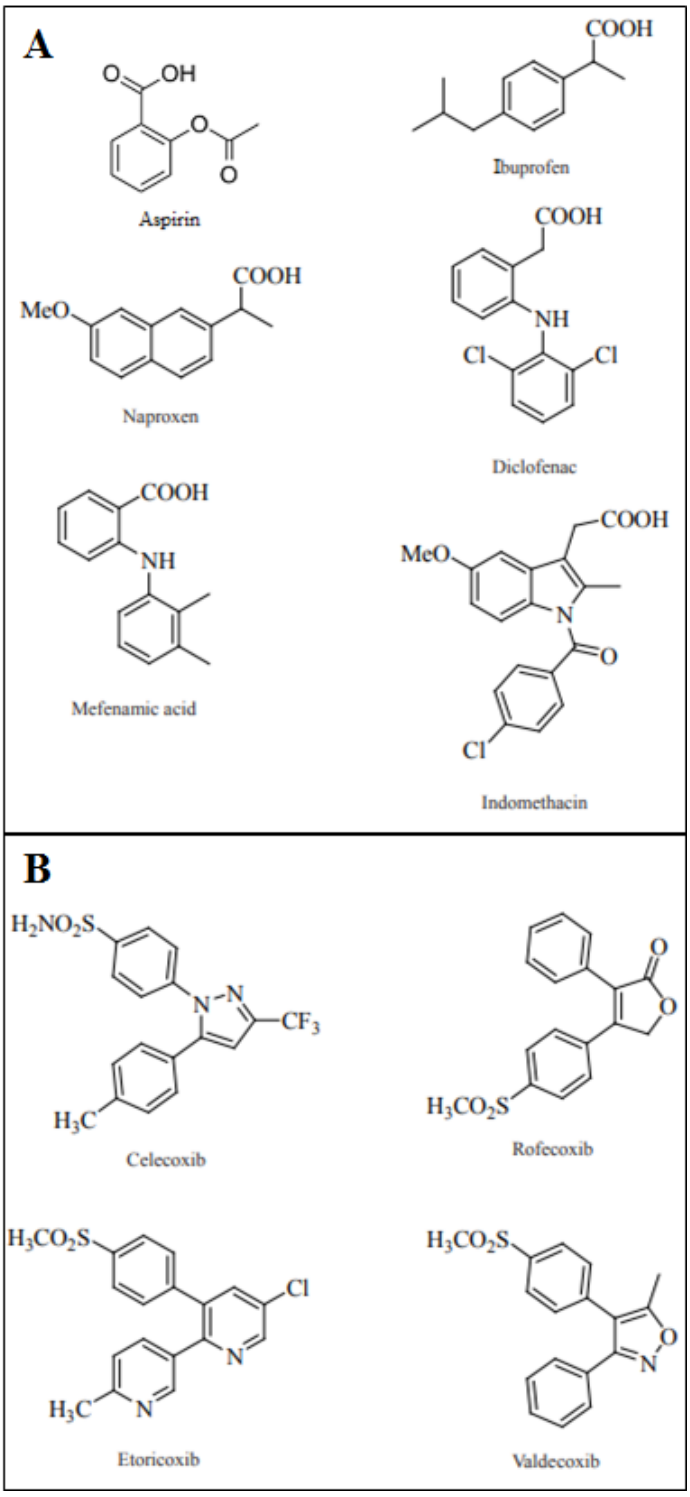

Figure 1.10 Chemical structures of commonly used non-specific and COX-2 selective 'Coxib' NSAIDs. Non-selective NSAIDs (A) are mostly carboxylic acids, whereas coxibs (B) are larger molecules often containing sulphonamide or sulphone groups. The large sulphur-containing groups in coxib NSAIDs are thought to confer selectivity for the COX-2 isoenzyme.

The European Society for Clinical and Economic Aspects of Osteoporosis and Osteoarthritis (ESCEO) recommend the following guidelines for oral NSAID use for

the management of persistent symptoms in patients with osteoarthritis[190]. For those at no apparent risk, either non-selective NSAID and PPI or COX-2 selective NSAID can be used. For those at increased GI risk only, e.g. history of peptic ulcer, COX-2 selective NSAID and PPI are recommended. For those at increased CV risk, e.g. hypertension, naproxen is recommended and COX-2 selective NSAIDs, high doses of diclofenac, ibuprofen and other non-selective NSAIDs should be avoided. Finally, in patients with glomerular filtration rates below 30cc/min, NSAID use should be avoided all together and otherwise used with caution.

Nephrotoxicity

COX-derived prostanoids control various renal functions including, salt and water excretion, glomerular filtration rate and renal blood flow. NSAID-mediated COX inhibition thereby prevents renal haemodynamics and function but also causes tubular obstruction through crystal deposition and direct cellular cytotoxicity[191].

The overall incidence of observable nephrotoxicity is approximately 1-5% in patients taking NSAIDs. While uncommon in young healthy individual, NSAID-induced nephrotoxicity is a significant concern for those at increased risk, with incidence rising to 20% in those with predisposing conditions[192]. Neonates, elderly and those with co-morbidities (liver, kidney and heart failure) are the most susceptible to developing acute kidney injury with NSAID therapy. Chronic and inappropriate consumption of NSAIDs can cause analgesic nephropathy, which is characterised by chronic nephritis, cortical atrophy, capillary sclerosis and papillary necrosis[193].

Cardiovascular toxicity

In an attempt to circumvent gastrointestinal adverse effects of non-selective NSAIDs, which are largely mediated by COX-1 inhibition, COX-2 selective NSAIDs were designed at the end of the 20th century. Several large clinical trials that were performed to compare the GI tolerability of this new class of NSAIDs against tNSAIDs found cardiovascular ADRs were higher with COX-2 selective therapy compared to tNSAIDs[194-197].

One study performed by the Vioxx Gastrointestinal Outcomes Research (VIGOR) group found that the COX-2 selective NSAID, rofecoxib (50mg), produced equivalent clinical efficacy and significantly reduced the risk of clinically important and

complicated GI events (relative risk, 0.5; 95% confidence interval, 0.3-0.6; P<0.001) compared to non-selective NSAID naproxen (1g). Unfortunately, incidence of myocardial infarction was 4 times higher in the rofecoxib group compared to the naproxen group (0.4% vs. 0.1%, RR, 0.2; 95% CI, 0.1-0.7), with risk increasing in a time- and dose-dependent manner[194]. Consequentially, Vioxx was voluntarily withdrawn from the market in September 2004, followed by valdecoxib (Bextra) and lumiracoxib (Prexige) in 2005 and 2007 respectively[198].

Though the study lacked an untreated group to determine whether the difference was due to a protective effect of naproxen or an exacerbated toxic effect of rofecoxib, this finding sparked major concern over the CV safety of non-aspirin NSAIDs and COX-2 selective NSAIDs. Meta-analysis of later studies have confirmed an increased risk of developing CV events with both classes of NSAIDs but the magnitudes of the different types of CV events vary considerably between individual NSAIDs (see tables 3-5 in Varga, *et al.*)[199].

CV risk seems to be associated more with extent and duration of COX-2 inhibition, rather than extent of COX-2 selectivity[200]. COX-2 is an important mediator of systemic and renal PGI_2 biosynthesis, which acts as a vasodilator and reduces vascular tone, blood pressure and thrombogenic/atherosclerotic events. COX-2 selective NSAIDs simultaneously reduce COX-2-generated PGI_2, whilst maintaining levels of COX-1 generated TxA_2, which is a vasoconstricting and thrombogenic prostanoid. Inhibition of PGI_2 generation, combined with the nephrotoxic effects of NSAIDs described above (e.g. retention of salts and water), are the most likely causes for the increased CV risk with NSAID therapy[199].

CV risk with NSAID therapy is significantly increased in those with prior diagnosis of hypertension. An important class of antihypertensive drugs, the angiotensin converting enzyme (ACE) inhibitors, act by inhibiting the renin-angiotensin-aldosterone system (RAAS), causing a decrease in water retention and therefore blood pressure. COX-2 generated prostanoids in macula densa cells of the renal cortex regulate the release of renin and water retention. Inhibition of this system normally acts as a counter measure for the increase in water retention caused by NSAIDs, but this protective measure is partially lost in those taking therapeutic inhibitors of RAAS for hypertension[199].

Hypersensitivity reactions

NSAIDs have been reported to exhibit adverse effects to other bodily processes, albeit much less commonly than those mentioned above. Approximately 5% of asthmatic patients experience bronchospasm exacerbations whilst taking non-competitive NSAIDs, especially those with NSAID allergies. The mechanism for this effect is supposedly related to abnormal cysteinyl-leukotriene production and sensitivity[110,201].

Rashes are common idiosyncratic reactions observed with NSAIDs such as mefenamic acid (10-15% occurrence) and sulindac (5-10% occurrence). Symptoms can vary from mild erythema/urticaria to exceedingly rare but potentially fatal diseases such as Steven-Johnson syndrome[110].

CNS toxicity

NSAIDs have been shown in several studies to prevent neurodegenerative diseases such as Alzheimer's disease and Parkinson's disease. However, various adverse CNS reactions have also been reported with NSAID use. These include aseptic meningitis possibly through hypersensitivity mechanisms, increased risk of stroke following reduced endothelial prostacyclin production and increase blood pressure secondary to renal effects (salt/water retention), medication overuse headaches, seizures at both therapeutic doses and overdoses, ataxia and dizziness[202].

NSAIDs suppress proliferation and induce cytotoxic damage to bone marrow mesenchymal stem cells and osteoblasts[203]. These effects have shown to suppress bone repair, formation and remodelling[203] and may be another factor in the exacerbation of arthritic diseases[187].

Hepatotoxicity

Hepatotoxicity is another uncommon (approx. 0.001-0.01% of prescriptions) ADR associated with NSAID use and can present as asymptomatic elevations in serum alanine aminotransferase (ALT) levels, hepatitis presenting with jaundice and even fatal liver failure[204]. The mechanism is not fully understood with reports of both dose-dependent and –independent associations with different NSAIDs[205] and cellular injury caused by drugs/metabolites forming adducts to proteins[206]. Examples of these include the increased risk of drug-induced liver injury associated with diclofenac and sulindac[207].

Severe hepatic failure has led to the post-marketing withdrawal of several NSAIDs including, bromfenac, ibufenac, benoxaprofen and lumiracoxib[208,209]. A genome-wide association study (GWAS) identified an association between human leukocyte antigen (HLA) alleles and lumiracoxib-related liver injury, suggesting that this type of toxicity may also be immune-mediated[209].

1.3.3 **Aspirin: It's Clinical Relevance and Pharmacokinetics**

Aspirin was first synthesized and marketed in the mid-late 19th century by acetylating the ortho-hydroxyl group of salicylic acid (Figure 1.10). However, the use of salicin containing remedies, such as willow leaf extracts, have been documented to as early as 4000BC for analgesic and antipyretic purposes[210].

Since the discovery of the mechanism of action of 'aspirin-like' drugs by Piper and Vane[188,211], the use of high-dose aspirin as an anti-inflammatory agent has diminished due to the development of better-tolerated NSAIDs, but can still be found as a component of various over the counter preparations for short-term pain relief[110].

Unlike other NSAIDs that only reversibly inhibit COX, aspirin can also permanently inactivates COX enzymes by acetylating the serine at position 529 on COX-1 and 516 on COX-2 (Figure 1.9). Irreversible inhibition of platelet COX-1 derived TxA_2 is the underlining mechanism for the prolonged antiplatelet property of aspirin. Platelets are anucleated and can therefore not synthesize new COX-1 protein. The lifetime of human platelets is approx. 8-10 days with around 10-12% of platelets renewed every day[212].

Though aspirin-acetylated COX-2 can no longer produce PGG_2, arachidonic acid is instead converted to 15R-hydroxyeicosatetraenoic acid (15R-HETE). 15R-HETE is a precursor for the production of lipoxins, which have anti-inflammatory properties. This alternative catalytic product of COX may play a role in the therapeutic actions of aspirin[213].

The inability to produce new COX enzymes and slow turnover mean that only small daily doses of aspirin is required for its antiplatelet activity. Patients with a history of cardiovascular disease (CVD) have a significantly increased risk of experiencing another CV event. Antiplatelet doses of aspirin are now standard therapy in the

secondary prevention of myocardial infarction and other occlusive vascular diseases[214].

The Antithrombotic Trialists' Collaboration conducted meta-analyses of studies attempting to measure the protective potential of anti-platelet drugs, including aspirin, against serious vascular events. An analysis of the use of aspirin in the primary prevention of CV events in people with no signs of increased risk, determined that there was no clear net value given the increased risk of GI and extracranial bleeding[215].

As well as serving a crucial role in the management of pain, inflammation and CV disease, the anti-inflammatory properties of aspirin may also prove useful in the treatment of neurodegenerative disease (e.g. Alzheimer's Disease), cancer (e.g. colorectal cancer) and radiation-induced inflammatory processes (e.g. radiation-induced proctosigmoiditis)[110]. The use of NSAIDs in the prevention and management of cancers[216] and Alzheimer's disease[217] have had conflicting findings and the exact relationships remain uncertain.

Pharmacokinetics of aspirin

Pharmacokinetics is a field of research that describes the absorption, distribution, metabolism and excretion of drugs within an organism. Aspirin is rapidly absorbed in the stomach and upper small intestine with peak plasma levels of the drug obtained after 30-40 minutes for uncoated aspirin[218] and 4-5 hours for enteric-coated formulations[219]. Aspirin is rapidly hydrolysed in the gut and liver by esterases to salicylic acid and acetic acid[218]. The biological half-lives of aspirin and salicylic acid are approximately 20 minutes and 4-6h in systemic circulation respectively[220].

Salicylic acid has very weak inhibitory effects on COX enzymes. The anti-inflammatory properties of salicylic acid are possibly due to its ability to inhibit NF-κB activity (also possible with aspirin)[221], leukocyte function[222] and suppress COX-2 gene expression both *in vitro* and *in vivo*[223].

Aspirin, as with other NSAIDs, can come in various formulations, including tablets, soluble powder and topical gels. Dosage and length of aspirin treatment varies depending on medical indication however is usually taken orally at 75-325mg daily for use as an anti-thrombotic agent or 300-900mg every 4-6 hours (up to 4g/day) for analgesic/anti-inflammatory use[224].

Plasma salicylate concentrations required to achieve an adequate anti-inflammatory response are considered greater than 0.15mg/mL (1.1mM) and lower than 0.3mg/mL (2.2mM) to avoid adverse systemic reactions such as tinnitus, hyperventilation, and hyperpyrexia[225]. Hypersensitivity reactions are possible at much lower concentrations of aspirin (2.9-33.3μM) & salicylate (18.1-245μM)[226].

A small study (n=8) conducted by Yamashita *et al*. administered salicylic acid in 150mL water and measured gastric juice volumes and salicylate concentrations[227]. Steady-state volume of gastric fluid was found to be 42mL (4-133mL) and salicylate concentrations were 60% and 1% of the initial dose after 5 and 60 minutes respectively. The minimum recommended aspirin dose for CV disease and pain management is 75mg and 300mg respectively. Aspirin concentrations in stomach fluid can therefore theoretically fall between 0.03-104.1mM and 0.1-416.3mM for CVD and analgesia respectively, as described in Table 1.4. Due to limitations in solubility, concentrations used fell within the range of 1-50mM aspirin.

Table 1.4 Theoretical concentrations aspirin in gastric fluid. Concentrations in gastric fluid using the lower (4mL), upper (133mL) and steady state (42mL) gastric volumes of gastric fluid and following the ingestion of aspirin used in the management of cardiovascular disease (75mg) and analgesia (300mg). Concentrations were also measured when considering the absorption rates after 5 minutes (60% of initial dose) and 60 minutes (1% of initial dose).

		Aspirin Concentration (mM)		
		Low range vol. (4ml)	**Average vol. (42ml)**	**High Range vol. (133ml)**
75mg Aspirin	**Initial**	104.1	9.9	3.1
	5 mins (60%)	62.4	5.9	1.9
	60 mins (1%)	1.0	0.1	0.03
300mg Aspirin	**Initial**	416.3	39.6	12.5
	5 mins (60%)	249.8	23.8	7.5
	60 mins (1%)	4.2	0.4	0.1

The burden of aspirin-related gastrointestinal ADRs

Aspirin was the most common drug reported in a prospective study of ADRs leading to hospitalisation, and accounted for 18% of all admissions. The majority of these patients were taking low-dose aspirin therapy (74%) and the most common reported ADR was GI bleeding (72%)[31].

The side effects of aspirin encompass many of those seen with other NSAIDs (see section 1.3.2) but also include specific ADRs such as Reye's syndrome, salicylism (tinnitus, nausea and vomiting) and acute salicylic poisoning (respiratory acidosis, hyperthermia, coma and bleeding)[110].

As well as fatal GI and intracranial bleeding, aspirin is also associated with several GI toxicities ranging from dyspepsia to gastric and duodenal ulceration. Endoscopic surveys identified gastroduodenal ulcers or erosions in 47.8% of asymptomatic patients taking aspirin between 100-325mg/day[228]. Asymptomatic erosions and ulcerations greatly increases the risk of patients developing perforation and bleeding before seeking medical attention. Given the frequency and seriousness of the adverse reactions caused by aspirin therapy, a vigilant benefit-to-risk analysis must constantly be employed throughout treatment of those at increased risk of developing GI injury. Such close monitoring is especially important in the management/prevention of CVD cases with reports of previous GI bleeding, where cessation of aspirin treatment decreases risk of bleeding however increases overall survival[229].

A survey published on Upper Gastrointestinal Symptoms Related to Low-Dose Aspirin (UGLA) found the prevalence of any upper GI symptom was 15% in patients on low-dose aspirin therapy[230]. The more common, less severe symptoms of low-dose aspirin therapy are also a major concern due to causing reduced adherence. A meta-analysis of 32 studies containing 144,800 patients found poor compliance to low-dose aspirin therapy ranged from 10% to over 50% and up to 30% of patients discontinuing their treatment[231].

The risks associated with not adhering or discontinuing low-dose aspirin therapy was assessed in a meta-analysis of six studies. Aspirin non-adherence or discontinuation in patients with coronary artery (CA) disease, CA bypass graft and CA stents was

associated with three-fold higher risk of developing a severe CVD event overall, with risk estimates as high as 90-fold in the CA stent population alone[232].

1.4 NSAID-induced gastrointestinal pathologies

1.4.1 Epidemiology of NSAID-induced gastrointestinal ADRs

The most common side effects of NSAIDs occur in the gastrointestinal tract. Minor, moderate and severe ADRs caused by topical and systemic effects of NSAIDs occur in both the upper and distal parts of the GI tract. Mild symptoms, such as dyspepsia, nausea vomiting, heartburn and abdominal pain can occur in 40% of NSAID users. Unfortunately, these symptoms do not always pre-empt the more severe reactions such as gastric/duodenal ulceration (most commonly localised to the gastric antrum) or its accompanying complications (bleeding, perforation and obstruction)[233].

In fact, 50-60% of patients are asymptomatic prior to developing GI complications caused by NSAIDs and up to 50% of patients with dyspepsia present healthy gastric mucosa. Studies have estimated that of the 30-50% of NSAIDs users who develop gastric erosions, the adaptive gastric defence system usually repairs the damage before symptoms arise[233]. However, approximately 25% of long-term NSAID users will develop gastrointestinal ulcers, with the risk of gastric ulcers (15%) being slightly higher than duodenal ulcers (10%)[234].

Unlike upper GI damage, lower GI injuries caused by NSAIDs remain poorly characterised and are associated with higher mortality rates, longer hospital occupation and a greater economic burden[235]. A population-based study in Spain reported an increase in hospitalisation due to lower GI events and a simultaneous decrease in upper GI events. The decrease to upper GI events is likely due to lower *H. pylori* infection rate and improved applications in ulcer prevention, whereas increasing lower GI events may reflect the ageing population or lack of measures for the prevention of these distal effects[235]. Lower GI events include increased gut permeability, inflammation, blood loss/anaemia, malabsorption, mucosal ulceration and uncomplicated/complicated diverticular disease[236].

The risk of developing peptic ulcer complications (e.g. bleeding, perforation and pyloric obstruction) within the first year of tNSAID use is 1-2%, which is an increase of 3-5 times compared to non-users[236]. A meta-analysis of randomised control trails

comparing the upper GI risk caused by COX-2 selective and non-selective NSAIDs found the occurrence of ulcers (RR, 0.26; 95% CI, 0.23– 0.30) and ulcer complications (RR, 0.39; 95% CI, 0.31– 0.50) to be lower with COX-2 inhibitors[237]. A separate meta-analysis of 28 observational studies assessed the pooled relative risk of upper gastrointestinal complications with individual NSAIDs. The ranking was as follows: celecoxib (1.5), ibuprofen (1.8), rofecoxib (2.3), sulindac (2.9), diclofenac (3.3), ketoprofen (3.0), naproxen (4.1) and indometacin (4.1) in order from lowest to highest relative risk (RR)[238].

The main risk factors associated with NSAID-induced gastrointestinal ADRs are similar to those mentioned in Table 1.2. The risk of ulcer occurrence following NSAID therapy is highest within the first 3 months with one study quoting odds ratios of 8.00, 3.31 and 1.92 for 0-1, 1-3 and 3+ month(s) respectively[239]. *H. pylori* infection also has a synergistic effect on GI risk, with a meta-analysis of 16 studies showing a combined odds ratio of 61.1 (95% CI, 9.98 to 373) in *H. pylori*-positive NSAID users[240].

NSAIDs are regular medications for more than 60 million USA citizens[241]. The most commonly quoted estimates for NSAID-related mortality is 16,500 annual deaths per year in the US, though they are reports that estimate as low as 3,200[241]. In the UK, approximately 10 million people aged 60 and over take NSAIDs. In this group, NSAIDs are causally associated with around 3500 hospitalisations and 400-1000 deaths[242]. Together these statistics show that NSAID-induced GI events are a common cause of global morbidity and mortality, especially in those aged 60 and over.

1.4.2 **Mechanisms of NSAID-induced peptic ulceration**

There are currently two accepted branches to the pathogenesis of NSAID-induced peptic ulceration: a) topical mechanisms, which constitute the direct damage to the gastroduodenal mucosa and b) systemic effects, which occur after the drug reaches the circulatory system.

Historically, COX inhibition was thought to be the prevailing cause of NSAID-mediated GI injury. Without downplaying the importance of obstructed PG synthesis in ulcer pathogenesis, studies have shown that mucosal PG generation could be inhibited (via parenteral NSAID administration) by 95-98% without causing mucosal damage in mice[243,244].

Recent publications have since highlighted the importance of the topical and systemic effects of NSAIDs that are prostaglandin-independent in ulcer pathogenesis[1,245]. It is important to remember that a large proportion of people consume NSAIDs without suffering GI damage, which is a testament to the adaptive defence of the GI tract. The multifactorial process of ulcer pathogenesis therefore depends on the cumulative effects of NSAIDs, as well as accompanying risk factors (Table 1.2) that ultimately overcome the adaptive GI defences.

NSAID-induced topical damage of GI mucosa

Orally ingested NSAIDs cause luminal disturbances to the mucus and epithelial layers of the stomach even before prostaglandin-mediated systemic effects. These damaging topical effects to the GI mucosa are attributable to the physiochemical properties of NSAIDs. NSAIDs are lipid-soluble weak acids with pKa values of around 3-5[245]. As described in section 1.2.2, the mucus lining of the stomach is the first line of defence against gastric aggressors (acid, pepsin, etc.). The mucus gel layer is lined with a hydrophobic layer of zwitterionic phospholipids. NSAIDs, like these phospholipids, are amphiphilic molecules with a hydrophobic monocarboxylic head and a hydrophilic tail region. These chemical properties allow NSAIDs to interact with the luminal mucosa, decreasing its hydrophobicity and weakening its integrity[246] (Figure 1.11).

Mitochondrial toxicity

Prior to the hypothesis that the anti-inflammatory effects of NSAIDs were a result of prostaglandin synthesis inhibition, the ability for conventional NSAIDs to cause mitochondrial uncoupling was mistakenly used as the measure of their efficacy. Indeed, they were even marketed on that basis[245].

Mitochondria are double-membraned-bound organelles that, among a host of functions, facilitate the synthesis of ATP, an essential source of chemical energy in most cells, and regulate programmed cell death (apoptosis). At a low gastric pH (1.5-3.5), weakly acid NSAIDs remain mostly unionised (50-99.9%), entering exposed epithelial cells at a rate that depends on the specific lipid solubility (log P) of the drug. Once the drug enters the neutral pH environment of the cytosol (6.5-7.0) the drug rapidly ionises (99.9-99.99%), becomes less lipid soluble and trapped inside the epithelial cell, a process called ‘ion trapping’. The drug accumulates to high

intracellular concentrations that are able to uncouple the electron transport chain and cause mitochondrial dysfunction[245] (Figure 1.11).

NSAID-induced mitochondrial disturbances can lead to several cytotoxic events including depletion of intracellular ATP levels, activation of apoptotic pathways and generation of ROS[247]. As ATP reserves run low, the tight junctions between gastric epithelial cells weaken, increasing mucosal permeability and levels of acid back diffusion[248]. Dysfunctional mitochondria are liable to rupture or leak apoptotic factors following mitochondrial outer membrane permeabilization such as cytochrome C[249], second mitochondria-derived activator of caspase (SMAC)[249] and apoptosis-inducing factor (AIF)[250].

ROS produced during mitochondrial stress may also activate apoptotic signalling pathways or cause direct cellular damage by oxidising proteins, lipid membranes and nucleic acids[251]. Analgesic/anti-inflammatory drugs that have a safer GI profile, such as nabumetone (anonacidic NSAID pro-drug), acetaminophen (nonacidic analgesic), and esterified nonacidic pro-NSAIDs (e.g. flubiprofen), do not uncouple oxidative phosphorylation *in vitro*[252]. COX-2-selective NSAIDs also cause mitochondrial uncoupling but have a lesser effect since they do not accumulate in GI epithelia[253].

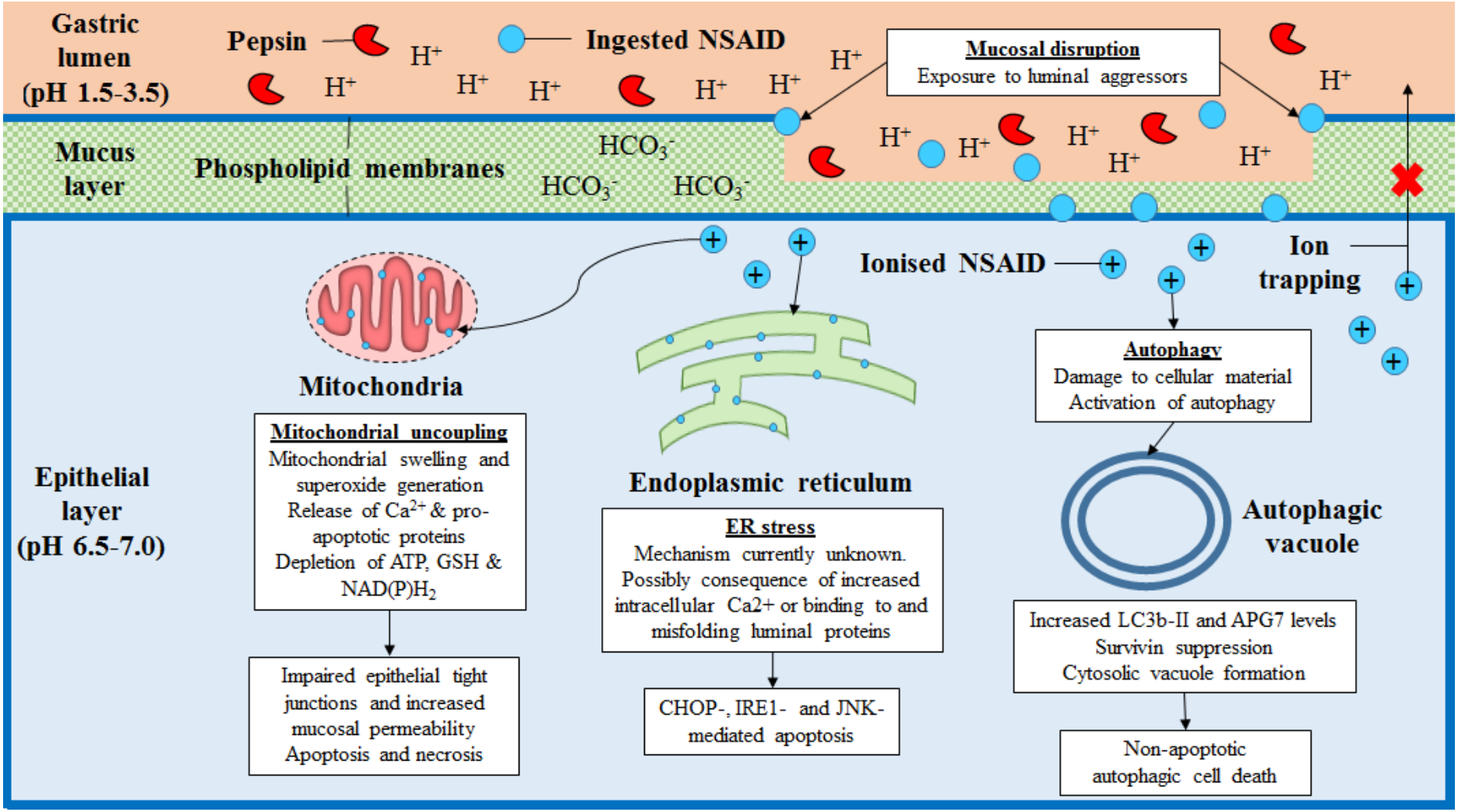
Gastric lumen (pH 1.5-3.5)
Pepsin
H+
Ingested NSAID
Mucosal disruption
Exposure to luminal aggressors
Mucus layer
Phospholipid membranes
HCO3-
Ionised NSAID
Ion trapping
Mitochondria
Mitochondrial uncoupling
Mitochondrial swelling and superoxide generation
Release of Ca2+ & pro-apoptotic proteins
Depletion of ATP, GSH & NAD(P)H2
Impaired epithelial tight junctions and increased mucosal permeability
Apoptosis and necrosis
Endoplasmic reticulum
ER stress
Mechanism currently unknown. Possibly consequence of increased intracellular Ca2+ or binding to and misfolding luminal proteins
CHOP-, IRE1- and JNK-mediated apoptosis
Autophagy
Damage to cellular material
Activation of autophagy
Autophagic vacuole
Increased LC3b-II and APG7 levels
Survivin suppression
Cytosolic vacuole formation
Non-apoptotic autophagic cell death
Epithelial layer (pH 6.5-7.0)

Figure 1.11 The topical damage caused by weak acid NSAIDs to gastric epithelial cells. Orally administered NSAIDs, which remain mostly unionised at low gastric pH, compromise the mucosal erosions and pass into exposed epithelial cells. NSAIDs become ionised in the neutral pH environment of the epithelial cytosol and become trapped, as the hydrophilic moieties prevent it from diffusing back through the hydrophobic cell membrane, a process called 'ion trapping'. Accumulation of ionised NSAIDs within the epithelium causes uncoupling of the electron transport chain. This in turn leads to mitochondrial dysfunction, characterised by release of free radicals, proangiogenic factors and depletion of ATP, ultimately leading to impaired tight junctions, increased mucosal permeability and apoptosis. NSAIDs also activate several ER stress response pathways. If ER homeostasis cannot be restored by unfolded protein response mechanisms, apoptotic pathways will be activated through C/EBP homologous protein (CHOP) and inositol requiring 1 (IRE1). Finally, autophagy is a protective mechanism to degrade unwanted cellular material in autophagosomes, which are constructed from the cleavage of microtubule-associated light chain 3b (LC3b) and autophagy proteins (Apg). Certain NSAIDs have been shown to induce excessive autophagy, which leads to a non-apoptotic cell death. GSH, glutathione; JNK, c-Jun N-Terminal kinase; $NAD(P)H_2$, nicotinamide adenine dinucleotide phosphate. Adapted from Bjarnason, *et al*.[245]

ER toxicity

Disturbances to ER homeostasis such as viral infection, hypoglycaemia, hypoxia, Ca^{2+} and iatrogenic (e.g. NSAIDs) toxicity can result in a build-up of unfolded proteins in the ER (Figure 1.11). ER stress activates the unfolded protein response (UPR), a pathway that aims firstly to restore ER function by upregulating expression of chaperones (binding immunoglobulin protein, BiP, also known as 78 kDa glucose-regulated protein, GRP-78), foldases and genes in the endoplasmic-reticulum-associated protein degradation pathway. These downstream effects are controlled by three distinct membrane-bound proteins, namely inositol requiring enzyme 1 (IRE1), activating transcription factor 6 and protein kinase RNA-like ER kinase (PERK). If the damage to the cell is irreparable, prolonged ER stress can activate mitochondrial apoptosis. While ER Ca^{2+} release and ER caspases (caspase-4 and 12) are implicated in ER-mediated apoptosis, the widely accepted mechanism is that C/EBP homologous protein (CHOP) inhibits anti-apoptotic protein BCL-2, relieving the pro-apoptotic factors BAX and BAX[254].

The exact mechanism by which NSAIDs elicit ER stress is not yet known, but it is likely related to increased intracellular Ca^{2+} and NSAID-mediated protein misfolding[255]. However, a review by Mügge and Silva shows that over the past 15 years there have been reports that many of the commonly used NSAIDs activate early

and late markers of ER stress. Commonly indicated are the PERK and ATF6 pathways with increased CHOP and GRP78 expression. Meanwhile the activation of the IRE1-XBP1 (X-box binding protein 1) pathway seems to be caused by a select few NSAIDs (e.g. indomethacin, acetaminophen, ibuprofen and celecoxib)[254].

NSIAD-induced autophagy

A more recent review highlights reports that NSAIDs aspirin, indomethacin, sulindac and celecoxib can also induce autophagy[256]. Autophagy is a protective mechanism that encapsulates damaged/unwanted cellular components (e.g. organelles, proteins and macromolecules) within a double-membrane vacuole called an autophagosome. However, excessive autophagy can cause a non-apoptotic cell death called "type II programmed cell death". This pathway has been suggested as another topical mechanism of NSAID-induced gastric injury[257] (Figure 1.11).

The autophagosome fuses with lysosomes, which degrade and sometimes recycles its contents. Microtubule-associated protein light chain 3b (LC3b) is converted into a lipid moiety and incorporated into the autophagosome membrane following enzymatic conversion from various autophagic proteins (Apg-4, -3 and -7, and the Apg12–Apg 5–Apg16 protein complex)[257]. Survivin, a member of the inhibitor of apoptosis (IAP) family, can prevent autophagy-mediated cell death but has been shown to be downregulated by NSAIDs *in vitro* and *in vivo*[258].

Systemic effects of NSAIDs on the GI mucosa

As discussed in section 1.2.2, gastric defence and repair heavily relies on the constitutive generation and activity of COX-derived prostanoids. Though inhibition of PG synthesis alone is not always associated with gastric injury[259,260], the most important systemic activity of NSAIDs in ulcer development is actually a secondary effect of their primary therapeutic target, COX inhibition (Figure 1.12). Immunoneutralized PGs[261] and parenterally administered NSAIDs[262-265] have been shown to sensitise and induce adverse gastroduodenal events, emphasizing the importance of these nontopical effects. This is also supported by the fact that selective inhibition or double knockdown of COX-1 and COX-2 induces gastric ulcer (section 1.2.2).

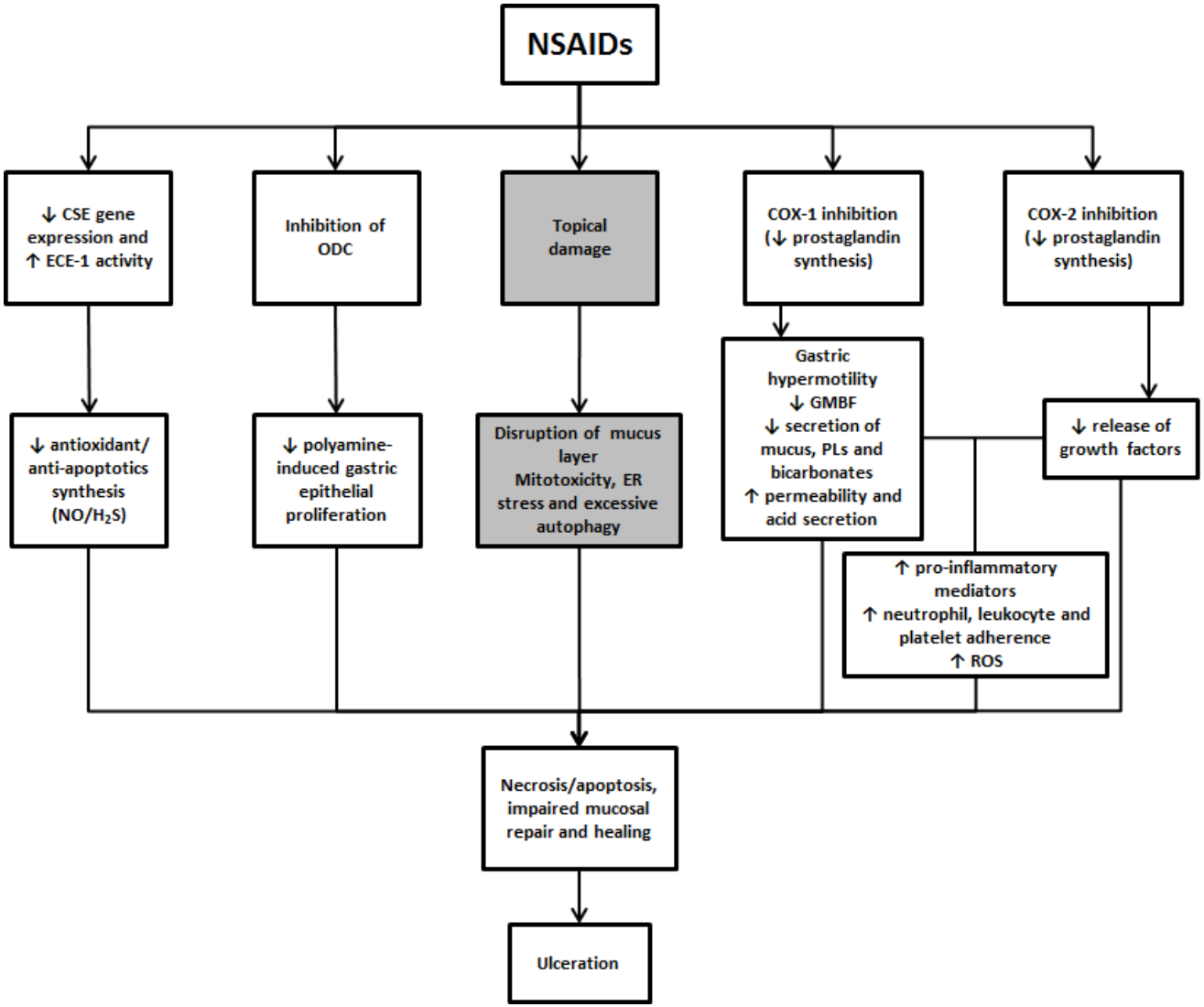

Figure 1.12 Mechanisms of NSAID-induced peptic ulcer. Topical (gray) effects of NSAIDs include disruption of the phospholipid lining of the mucus layer, uncoupling of mitochondrial oxidative phosphorylation, induction of ER stress and excessive autophagy. Systemic (white) effects include the inhibition of nitric oxide (NO), hydrogen sulphide (H_2S) and polyamine synthesis. Inhibition of prostaglandin synthesis impairs various pathways of the gastric defence system, including increased gastric motility, permeability, acid secretion and pro-inflammatory responses, and decreased gastric mucosal blood filtration (GMBF), growth factor release, mucus, phospholipid (PL) and bicarbonate secretion. All of these direct and indirect effects culminate with epithelial cell death, impaired mucosal repair and ultimately ulceration. Image adapted from Musumba, *et al*. (2009)[1].

Gastric hypermotility

One of the earlier events following NSAID administration is gastric hypermotility, which causes microvascular disturbances at mucosal foldings, leading to neutrophil-endothelial interaction, oxyradical production, lipid peroxidation, vascular permeability and subsequent cellular damage. The proposed mechanism for NSAID-induced gastric hypermotility may been associated with vagal-cholinergic and glycoprivic receptor signalling[266]. Lesion-free hypermotility was induced by a selective COX-1 inhibitor (SC-560) in rat intestine, along with a simultaneous rise in COX-2 expression. COX-2 upregulation may be a compensatory mechanism that restores depleted gastric PGE_2 and mucosal integrity[267].

Acid secretion

As previously described, gastric acid is a major luminal aggressor that can turn superficial erosions into mucosal breaches/ulcers and delay restitution/regeneration of gastric lesions. Acid secretion is regulated by various signalling pathways, including suppression by COX-1-derived prostaglandins acting on local[268-270] (parietal cells) and central[271] (hypothalamus, raphe nuclei, etc.) EP_3 and prostacyclin receptors (IP).

The effect of prostacyclins on acid secretion seems to be context dependent. COX inhibition with intraperitoneal indomethacin increases basal and pentagastrin-stimulated acid secretion during gastric inflammation in rats[268], but only increases basal acid secretion in healthy humans[272].

Alternatively, naproxen has shown to increase gastric acidity by reducing the volume of the basal acid output in healthy subjects[273]. The action of EP_4 agonists on ECL cells stimulates histamine secretion, which suggests a dual action of PGs on acid secretion[268].

Mucosal blood flow and the inflammatory response

Damage to the lamina propria activates sympathetic sensory afferent neurons that causes a CGRP-induced increase (Figure 1.7) in PGI_2 production in vascular endothelial cells. PGI_2, as well as CGRP-induced NO production, leads to prompt hyperaemia to the gastric mucosa[274,275]. In a study comparing the occurrence of gastric ulceration and gastric mucosal blood flow (GMBF), ibuprofen treated subjects displayed significantly decreased GMBF and increased ulcer occurrence. The second

group were co-administered rebamipide, a gastroprotective agent that increases PG biosynthesis. The ibuprofen and rebamipide group displayed no decrease in GMBF and no endoscopic signs of gastric ulcers[276].

Ulcer healing, initiated by CGRP and PG-induced VEGF upregulation (section 1.2.2), is impaired during NSAID therapy[277]. Platelets are important mediators of ulcer healing, releasing growth factors that promote angiogenesis and epithelial cell growth, and facilitating haemostasis. Thromboxane, synthesised primarily by COX-1, is released during the clotting process to aggregate platelets and acts as a potent vasoconstrictor. NSAID-mediated COX inhibition therefore suppresses thromboxane synthesis/ulcer healing and increases bleeding risk[99]. This effect is exacerbated with concomitant use of anti-platelet drugs, such as clopidogrel[160].

NSAIDs cause various pro-inflammatory events including increased vascular adhesion molecules (leukotriene B4; macrophage-1 antigen, CD11b/CD18; and intercellular adhesion molecules, ICAM-1) and leukocyte activity. Leukocytes (primarily neutrophils) adhere to vascular endothelial cells, restricting gastric microcirculation, and release pro-inflammatory cytokines such as TNF-α, that directly propagate gastric injury and impair healing[99]. Pre-treatment with PGE_2 has shown to significantly reduce gastric injury and abolish elevated TNF-α levels[278].

Gastric mucosal restitution

As well as the VEGF, basic fibroblast growth factor (bFGF), platelet-derived growth factor, epidermal growth factor (EGF), TFFs, hepatocyte growth factor and TGF-α also contribute to gastric restitution and regeneration following gastric injury. This includes the proliferation, morphogenesis and migration of epithelial, fibroblast and vascular endothelial cells[279,280].

The aforementioned growth factors are upregulated at ulcer margins and stimulated by PGE_2 and increased plasma gastrin levels[279], therefore the inhibition of PGE_2-mediated growth factor stimulation likely contributes to the impaired ulcer healing observed with NSAID therapy. However, indomethacin has been shown to impair EGF-mediated proliferation both in both *in vitro* and *in vivo* models[281]. This suggests that NSAIDs can inhibit both the expression and activity of growth factors.

Polyamines such as putrescine, spermidine and spermine are also involved in the growth, migration and proliferation stages of gastric restitution following injury from NSAIDs[282]. NSAIDs post-transcriptionally inhibit one of the key regulators of polyamine biosynthesis, ornithine decarboxylase, reducing intracellular polyamine levels by up to 50%[283]. Using a rat model, indomethacin-induced gastric injury was attenuated by spermine pre-treatment. The reduced gastric injury observed with spermine pre-treatment was associated with increased mucin production and normalisation of elevated gastric acidity, myeloperoxidase and serum NO levels[284].

Remodelling of the extracellular matrix (ECM) at gastric ulcer margins is an essential part of ulcer healing and is regulated mainly by matrix metalloproteases (MMPs)[285,286]. MMPs are a family of zinc-dependent endopeptidases that degrade and remodel various ECM components of the gastric mucosa, such as collagen, gelatin, stromelysin and matrilysin. MMP gene expression and activity are heavily regulated. MMPs exist as zymogens that are activated by other MMPs and serine proteases. Tissue inhibitor of metalloproteinases 1-4 also reversibly bind to and inhibit MMPs.

NSAIDs cause a transient decrease to MMP-2 activity, a constitutively expressed isoform involved in ECM turnover. MMP-9 is induced by inflammatory cytokines and produced mostly by macrophage-like cells at NSAID-induced gastric ulcer borders, suggesting that MMP-9 is important in ulcer healing[286]. The protective effects of MMP-9 are supported by the findings that NSAID-induced PG inhibition causes reduced MMP-9 expression and activity[287,288]. However, other studies have shown that downregulation of MMP-9 activity accelerates ulcer healing and protects against ulcer development and that NSAIDs-induced MMP-9 and -3 in gastric ulcer tissue is associated with inflammation and disruption of the gastric mucosa[289,290].

Inorganic gaseous mediators

As previously mentioned (section 1.2.2), NO and H_2S, like prostanoids, exert various effects to maintain the integrity of the gastric mucosa. NO is synthesized by three different isoforms of nitric oxide synthase (NOS), namely neuronal NOS (nNOS), endothelial NOS (eNOS) and inducible NOS (iNOS).

The Ca2+/calmodulin dependent constitutive enzymes (cNOS), nNOS and eNOS, produce low levels NO, which promotes mucosal repair and ulcer healing through

vasodilation (increasing GMBF) and VEGF stimulation (angiogenesis)[291]. A study demonstrated that indomethacin increases endothelin-converting enzyme-1 activity, a metallopeptidase that cleaves endothelin-1 (ET-1) into its active form. ET-1 is a highly potent vasoconstrictor that suppresses cNOS activity and causes gastric mucosal injury in NSAID-treated rats[292].

Conversely, iNOS has shown to cause paradoxical effects of gastric ulcers. One study shows that upregulation of iNOS acts as a compensatory mechanism in ulcer repair following COX deficiency or inhibition by increasing vasodilation and vascular permeability[116]. However, the majority of studies suggest that the high level of NO generated by iNOS contributes to NSAID-induced ulcerogenesis[293-295]. Similarly, mice treated with a chemical iNOS inhibitor[295] or that are genetically iNOS deficient[295] presented less severe gastric lesions following treatment with indomethacin.

The main sources of endogenous H_2S in the gastric mucosa is the conversion of L-cysteine by cystathionine B-synthase (CBS) and cystathionine-γ-lyase (CSE). H_2S has a broad spectrum of signalling mechanisms including stimulation of K_{ATP} channels (vasodilation and angiogenesis), GSH synthesis (anti-oxidative response) and transient receptor potential cation channel subfamily V member 1 (gastric motility and secretion), as well as neutralising ROS and reactive nitrogen species.

Acid-induced gastric ulcers in rats caused a marked increase in the expression of H_2S, CSE and CBS[296]. Gastric CSE expression and H_2S production are inhibited by aspirin and other NSAIDs[297]. NaHS, a H_2S donor, reduces gastric mucosal injury, TNF-α, ICAM-1 and lymphocyte function-associated antigen-1 mRNA upregulation induced by NSAIDs. Without effecting prostaglandin synthesis, NaHS also restores GMBF and inhibits aspirin-induced leukocyte adherence[298].

Melatonin in gastroprotection

Melatonin is a hormone originally discovered in the pineal gland, later found to be distributed in many peripheral tissues, including the GI tract. L-tryptophan is converted to serotonin by hydrolase and decarboxylase enzymes and then from serotonin to melatonin by N-acetyltransferase (NAT) and hydroxyindolo-O-methyl-transferase enzymes. The latter two enzymes are detected in the gut and pancreas,

suggesting melatonin is produced in the GI tract and is regulated separately from pineal gland secretion[299].

Besides its role in coordinating the circadian rhythm in humans, melatonin performs a diverse set of gastroprotective effects (Table 1.5). The effects of melatonin are elicited either directly through neutralising ROS, or binding to melatonin receptors on enteric cells, and indirectly through the upregulation of other gastroprotective agents (PGs, NO and antioxidases).

Table 1.5 Gastroprotective actions of melatonin. Reactive oxygen species, ROS; superoxide dismutase, SOD; catalase, CAT; glutathione peroxidase, GSH-Px; prostaglandin, PG; nitric oxide, NO; cyclo-oxygenase, COX; inducible nitric oxide synthase, iNOS; matrix metalloproteinase, MMP.

Gastroprotective roles of melatonin	Mechanisms/evidence	Ref.
Anti-oxidant effects	Acts as a potent scavenger of ROS	300,301
	Induces anti-oxidative enzymes such as SOD, CAT and GSH-Px	302
	Prevents peroxidation of lipid membranes	303
	Reduces levels of circulating pro-inflammatory cytokines and nitrite/nitrate	304
Increased PG and NO synthesis	Gastroprotective effects of melatonin blocked by COX inhibition	305,306
	iNOS significantly upregulated in ulcerated gastric mucosa treated with melatonin	305
Dose-dependent inhibition of gastric acid and pepsin secretion	Exact mechanism unclear but may be related to central and local signalling	307
Increased gastric microcirculation	Inhibition of PG and NO synthesis attenuates increased ulcer healing and mucosal blood flow observed following melatonin administration	305
Stimulation of bicarbonate secretion	Elevated HCO_3^- and intracellular Ca^{2+} prevented by melatonin and nicotinic receptor antagonists	308
MMP regulation	Upregulation MMP-2 and attenuates MMP-9 activity	285,309

A study in aspirin-treated healthy human subjects found that co-treatment with either melatonin, its precursor L-tryptophan, significantly reduced endoscopic grading of mucosal injury. This study also found that melatonin plasma levels increase following and during aspirin therapy, an event that does not rescue the inhibition of PGE_2 synthesis[310]. Similarly, melatonin dose-dependently attenuated GI lesions in both indomethacin and piroxicam treated rats, events that were accompanied by an increase in various anti-oxidative effects[311].

1.5 **Pharmacogenetics of gastrointestinal toxicity**

Pharmacogenetics is a field of research that describes the influence of genetic variation on drug pharmacokinetics, pharmacodynamics (the study of the biochemical and physiological actions of drugs) and toxicology. Initial pharmacogenetic studies focussed on individual interactions between drugs and genes involved mostly in metabolism. Advancements in genomics such as the completion of the human genome project and the advent of large-scale GWAS have allowed for a broader interrogation of gene-disease associations. This wider approach, termed pharmacogenomics, encompasses the genomic and epigenomic interactions with drugs[312].

Single nucleotide polymorphisms (SNPs) are variations to single base pairs at a given genetic loci that have a population frequency >1%. SNPs are common genomic events, present in over 90% of human genes[313]. SNPs mostly cause indiscernible changes to non-coding (intronic) regions, but may also cause changes in regulatory and coding (exonic) regions that can effect transcription efficiency and may cause changes to miRNA/protein sequences that lead to disease. Single base substitutions in exonic regions of genes cause codon changes that may translate to altered amino acid sequences and protein structures/functions. Insertions and deletions to exonic regions of genes cause ‘frame-shifts’ during translation, which lead to misfolded and truncated proteins that will most likely be degraded by the ubiquitin proteasome system[110].

Though several associations have been identified between genetic variants and drug response, few SNPs have led to changes in prescription guidelines or dosing regimens. Tests for genetic variants increasingly used in clinical practice include those that are related to drug/metabolite pharmacokinetics (transporter and metabolising proteins),

pharmacodynamics (on and off target interactions) or a combination of both (reviewed in Rang, *et al*., 2016[110]).

1.5.1 **NSAID pharmacogenetics**

Inter-individual variability in the therapeutic and adverse effects of NSAIDs can be in part explained by genetic variation. Understanding the molecular mechanisms of how genetics can functionally influence NSAID pharmacokinetic and pharmacodynamics will allow for the administration of the most effective and safest treatment strategies.

Phase I and II drug metabolising enzymes

Metabolic inactivation and elimination of NSAIDs is mediated mainly through hepatic cytochrome P450 (CYP) oxidation, especially the CYP2C subfamily, glucuronide conjugation, via uridine-5′-diphosphate-glucuronosyltransferases, and less commonly by sulphate conjugation (sulphotransferases)[314]. CYP2C8, CYP2C9 and CYP2C19 are highly polymorphic, with 18, 60 and 35 variants reported on PharmVar database[315] (www.pharmvar.org) respectively. These variants can cause either increased/decreased expression or functionality, which has been associated with altered NSAID metabolism and clearance[316-319].

The two most common CYP2C9 variants, CYP2C9*2 and *3, display reduced enzymatic activity and both have high prevalence (14 and 8%, respectively) in European populations. Case-control studies on the effect of CYP2C9*2 and *3 genotypes on NSAID-induced upper gastrointestinal bleeding (UGIB) have shown inconsistent results. Firstly, many studies have shown no association between CYP2C9 variants and NSAID-induced UGIB[319-326]. Additionally, none of the studies that have reported associations shared concordant results (Table 1.6), which may be due to high heterogeneity between the studies. A gene-dose effect[327] and co-inheritance of other CYP2C subfamily variants[328] may be important to observe the functional effects of NSAID toxicity in patients with CYP2C9 variants.

CYP2C8 is an intermediate metaboliser of ibuprofen, diclofenac and tenoxicam NSAIDs. There are two opposing reports on the association between the CYP2C8*3 allele and NSAID-induced UGIB. One small cross-sectional study[328] supports the association when combined with the CYP2C9*2 genotype (Table 1.6), whilst a much

larger study[319] found no associations with CYP2C8*3 alleles (rs11572080 and rs10509681).

CYP2C19 probably only contributes to a small fraction of NSAID metabolism but does play a major role in PPI metabolism. CYP2C19*17 is a gain-of function variant that was associated with NSAID-induced PUD in a large Caucasian cohort (Table 1.6). However, the author concludes that this association is likely due to either other variants that are in LD with CYP2C19*17 (e.g. CYP2C9*2) or an NSAID-independent effect, i.e. altered CYP2C19-mediated arachidonic acid metabolism[319].

Other potential associations between NSAID-induced GI toxicity and polymorphisms in cytochrome P450 and UGT enzymes (e.g. UGT1A6[325]) have been identified but currently lack statistical significance[329].

Organic anion transporting polypeptide (OATP)

OATPs, also known as solute carrier organic anion transporters (e.g. SLCO1B1), transport various anionic drugs, such as statins, ACE inhibitors and angiotensin receptor blockers (ARBs), from the portal blood[330]. Two Japanese studies, by the same group, identified an association between aspirin-induced peptic ulcer and the SLCO1B1*1b haplotype[330,331] (Table 1.7). The later study expanded on the initial finding to show that in carriers of the SLCO1B1*1b haplotype, aspirin-induced peptic ulcer and PUB is associated with the use of drugs that are substrates for SLCO1B1[331]. *In vivo* studies show that the SLCO1B1*1b haplotype increases transport activity. Therefore, the SLCO1B1*1b haplotype may diminish the protective effects of ACE inhibitors and ARBs in NSAID-induced gastric injury, by lowering their blood concentrations in the stomach.

Pharmacodynamic genetic variation

COX-1 plays an important role in gastric defence and its inhibition by NSAIDs is believed to be one of the main mechanisms of NSAID-induced gastric injury, as described in sections 1.2.2 and 1.4.2. Although polymorphisms in the *PTGS2*/*COX2* gene have been shown to effect responsiveness to NSAIDs[332] and increase H. pylori positive ulcer risk[333], no association has been made with NSAID-induced GI injury.

The A842G/C50T and C-1676T polymorphisms in the prostaglandin-endoperoxide synthase 1 (*PTGS1*, also called *COX1*) gene have been associated with response to

aspirin[334] and peptic ulcer bleeding[335] respectively (Table 1.7). The c.-842A>G variant creates a putative AP2 transcription factor binding site in a promoter region upstream of the transcriptional start site, which may negatively regulate the transcription of *COX-1*. A non-synonymous c.50C>T polymorphism (Pro17Leu) was found to be in complete linkage disequilibrium with A842G[334].

A Japanese study demonstrates that subjects with the A842G/C50T haplotype showed significantly lower $PGF_{2\alpha}$ production following aspirin treatment compared to those with the wild type alleles[334]. The study did not explore the effect of this haplotype on the risk of NSAID-induced ulceration. A study performed in the Netherlands suggests that the A842G/C50T haplotype confers a reduced risk for peptic ulcer bleeding, though this association lacked statistical significance[335] (Table 1.7).

The C-1676T COX-1 polymorphism alters a putative transcription factor (GATA-1, CdxA) binding site, also found in the promoter region upstream of the *COX-1* gene[336]. Though there is no evidence of this polymorphism changing levels of PG synthesis, a Japanese group has demonstrated that the -1676T allele is a significant risk factor for NSAID-induced ulcer[336] (Table 1.7), epigastric pain syndrome and functional dyspepsia[337].

More recently, a Taiwanese study determined that the C-1676T polymorphism does not alter the risk of low-dose aspirin-induced ulcer formation[148]. These contradictory results are probably not due to a difference in populations, as a separate Japanese study also found no association between either *COX-1* variant and aspirin-induced peptic ulcer[326]. The studies that found no association only included aspirin-treated subjects, therefore the effect of the variant may be observed in non-aspirin NSAIDs.

Table 1.6 List of case-control studies that have identified statistically significant associations between cytochrome P450 CYP2C subfamily variants and NSAID-induced peptic ulcer disease (PUD) or upper gastrointestinal bleeding (UGIB). For the Figueiras study[327], the comparisons were made between the defined daily doses (DDD) for the wild type and CYP2C9*3 genotypes. Odds ratio, OR; confidence interval, CI.

Treatment	Gene	Genotype(s)	Toxicity	p-value/OR	Study and population type	Ref.
Various NSAIDs (mostly salicylates) and therapy durations	*CYP2C9*	CYP2C9*2	Bleeding events higher in patients with CYP2C9*2 genotype	P < 0.009; OR, 1.92; 95% CI, 1.14–3.25	94 bleeding patients and 124 NSAID use-matched control patients	338
<1 month treatment with NSAIDs metabolised by CYP2C9	*CYP2C9*	CYP2C9*1/*3	Higher frequency of poor metaboliser genotypes in bleeding vs. control (*1/*1) patients	P < .001; OR, 12.9; 95% CI, 2.917–57.922	26 patients with gastroduodenal bleeding lesions vs. 52 NSAID use-matched controls	339
		CYP2C9*1/*2		P = 0.036; OR, 3.8; 95% CI, 1.090 –13.190		
NSAIDs subject to extensive CYP2C8 and 2C9 metabolism	*CYP2C8* and *CYP2C9*	Joint presence of CYP2C8*3 and 2C9*2 genotypes	Higher frequency in bleeding patients vs. control	P = 0.003; OR, 3.73; 95% CI, 1.57–8.88	134 NSAID-related bleeding patients vs. 177 NSAID use-matched controls	328
DDD of NSAID 0 versus a NSAID DDD > 0.5	*CYP2C9*	CYP2C9*3	Increased risk of UGIB associated in genotypes with CYP2C9*3	*1 genotype, OR = 8.79 (4.50–17.17) vs. *3 genotype, OR = 18.07 (6.34-51.53)	103 NSAID-UGIB cases and 89 NSAID use-matched controls	327
Use of various NSAID within 3 month period before endoscopy	*CYP2C19*	CYP2C19*17	PUD distribution of CYP2C19*17: *1/*1, 64.3%; *1/*17, 71.7%; and *17/*17, 73.8%	P = 0.005; OR, 1.47; 95% CI, 1.12–1.92	835 NSAID-induced PUD cases vs. 404 healthy controls	319

Genetic variation of pro-inflammatory cytokines

Interleukins-1β is a pro-inflammatory cytokine that also inhibits gastric acid secretion. The IL-1β-511 T/T and C/T genotypes are associated with increased expression compared to wild type (C/C)[326], whereas the IL-1β -31T>C polymorphism is considered to decrease expression through disruption of the TATA box[340]. Whilst variant alleles at positions -511 (T) and -31 (C) have opposing effects on IL-1β expression, the author noted that these polymorphism were also in total linkage disequilibrium. Since carriers of IL-1b-511/-31 variant haplotype were associated with a reduced risk for *H. pylori*-positive ulceration in subjects taking low-dose aspirin[326], it is likely that the combined presence of these alleles leads to a decreased expression of the pro-inflammatory cytokine. A Korean study found that heterozygosity for two other IL-1β polymorphisms, namely -581T>C and -1061C>T, was associated with increased risk of low-dose aspirin-induced peptic ulcer. Unfortunately, the authors did not discern the effects of these SNPs on IL-1β expression or activity[341].

IL-17A is a pro-inflammatory cytokine that bridges the adaptive and innate immune systems. The IL-17A G-197A genotype was recently associated with increased risk for peptic ulcer in NSAID/aspirin users[342]. The study that identified this association observed no effect of the variant allele on IL-17A expression or activity but this may be because the experimental design did not sufficiently model the inflammatory conditions observed with *H. pylori* infection[342]. In fact, an unrelated study did find that the number of variant 'A' alleles positively correlated with IL-17A levels[343].

Polymorphisms related to GMBF

NO is a double-edged sword in PUD as it can either promote ulcer healing through increasing GMBF and angiogenesis, or causing oxidative damage and inhibiting/disrupting platelet aggregation, thereby increasing bleeding risk. Carriers of the eNOS 'a' allele displayed a significantly lower risk for UGIB among users of low-dose aspirin[344] (Table 1.7). The 'a' allele of the *eNOS* gene is a set of 4 intronic tandem repeats of a 27-bp sequence in intron 4, whilst those with the wild type 'b' allele have 5 tandem repeats. The effect of the variant 'a' allele on the plasma levels of NO metabolites has yielded conflicting results[345-348], making it difficult to understand the functional significance of this association.

Table 1.7 Other confirmed associations between genetic variation and NSAID-induced PUD and upper gastrointestinal bleeding. Cyclooxygenase, COX; aspirin, ASA; prostaglandin $F_{2\alpha}$, $PGF_{2\alpha}$; interleukin, IL; odds ratio, OR; confidence interval, CI.

Treatment	Gene	Genotype(s)	Effect on toxicity	p-value/OR	Study and population type	Ref.
30 minutes of incubation with 30μM ASA or 0.26M ethanol	*COX-1*	A-842G/C50T haplotype	Inhibition of $PGF_{2\alpha}$ formation in patients with variant haplotype	P = 0.01	8 subjects heterozygous for A-842G/C50T vs. 29 wild-type subjects	334
NSAIDs and length of treatments undefined	*COX-1*	A-842G/C50T haplotype	A-842G/C50T less frequent in peptic ulcer bleeding cases	OR, 0.5; 95% CI, 0.18–1.34	106 peptic ulcer cases vs. 88 healthy control subjects	335
NSAIDs and length of treatments undefined	*COX-1*	COX-1 T-1676C	The number of -1676T alleles associated with developing gastroduodenal ulcers	OR, 5.80; 95% CI, 1.59-21.1	25 NSAID-induced ulcers vs. 22 non-ulcer controls	336
Low-dose aspirin (100mg) use, >4 weeks	*IL-1β*	IL-1β 581C/T and IL-1β 1061C/T	CT genotype of 581C/T and 1061C/T associated with ASA-induced peptic ulcers	**581C/T:** P = 0.04; OR, 4.6; 95% CI, 1.054-20.303 **1061C/T:** P = 0.04; OR, 4.6; 95% CI, 1.054-20.303,	23 peptic ulcer cases vs. 25 non-ulcer controls	341
100mg aspirin for undefined treatment lengths	*IL-1β*	IL-1β T-31C and C-511T	IL-1β -31C and -511T alleles were significantly less frequent in *H. pylori*-positive peptic ulcer cases	IL-1β T-31C: OR, 0.27; 95% CI, 0.10–0.74 IL-1β C-511T: OR, 0.27; 95% CI, 0.10–0.74	101 vs. 22 *H. pylori*-positive non-ulcer and ulcer subjects, respectively.	326
NSAIDs and treatment lengths undefined	*IL-17A*	IL-17A G-197A	"A" allele associated with an increased risk for gastro-duodenal ulcer	P = 0.0061; OR, 3.98; 95% CI, 1.48-10.7	36 NSAID-induced ulcer vs. 24 NSAID-no ulcer controls	342

Table 1.7 continued. Endothelial nitric oxide synthase, eNOS; upper gastrointestinal bleeding, UGIB; angiotensin, AGT; solute carrier organic anion transporter family member 1B1, SLCO1B1; peptic ulcer bleeding, PUB; angiotensin receptor blocker, ARB; angiotensin-converting enzyme inhibitor, ACEI.

Treatment	Gene	Genotype(s)	Effect on toxicity	p-value/OR	Study and population type	Ref.
Low-dose aspirin (<325 mg/d), >5 days per week and for at least 15 days before GI bleeding	*eNOS*	Four 27-bp direct repeats in intron 4 (wild type has 5 repeats)	Shorter repeat region associated with reduced risk of UGIB	P = 0.018; OR, 0.39; 95% CI, 0.18–0.85	88 patients with UGIB vs. 108 matched controls with no history of UGIB	344
Low-dose aspirin treatment (75-125 mg/day)	*AGT*	AGT A-20C	Homozygous CC genotype associated with increased ulcer risk	P = 0.04; OR, 9.66; 95% CI, 1.46-63.7	15 ulcer patients vs. 196 healthy controls	349
Low-dose aspirin (100 mg)	*AGT*	AGT A-20C	Homozygous CC genotype associated with increased risk for PUB	P = 0.04; OR, 4.94; 95% CI, 1.21–20.2	20 peptic ulcer bleeding cases vs. 357 non-ulcer controls	350
Low-dose aspirin (100 mg)	*SLCO1B1*	SLCO1B1*1b haplotype (A388G and 521T)	SLCO1B1 *1b haplotype associated with peptic ulcer	P < 0.001; OR, 3.64; 95% CI, 1.81–7.29	78 ulcer cases vs. 414 non-ulcer controls	330
Low-dose aspirin (100 mg)	*SLCO1B1*	SLCO1B1*1b haplotype (A388G and 521T)	SLCO1B1 *1b haplotype associated with peptic ulcer and PUB with concurrent statin, ARB or ACEI therapy	Peptic ulcer: P = 0.02 PUB: P = 0.006	68 peptic ulcer cases and 31 PUB cases vs. 363 healthy controls	331

The renin-angiotensin system plays an important role in GI homeostasis (e.g. GMBF and alimentary motility), as well as mediating various GI functions such as bicarbonate secretion, peptide digestion and the absorption of sodium, water glucose and peptides[351]. Homozygosity for the angiotensin (*AGT*) gene polymorphism A-20C has been associated with aspirin-induced peptic ulcer and peptic ulcer bleeding in Romanian study[349] but only aspirin-induced peptic ulcer bleeding (not peptic ulcers) in a Japanese cohort[350].

Studies have shown that the AGT-20 C allele increases the basal AGT promoter activity, AGT expression and plasma concentrations[352,353]. Elevated AGT levels may therefore increase NSAID-induced ulcer/bleeding risk by reducing GMBF, and therefore wound healing, in carriers of the AGT-20 C allele.

1.5.2 **EYA1 in development and disease**

The Eyes Absent (EYA) proteins were originally discovered as components of the retinal determination gene network (RDGN), which is composed of the paired box (PAX), sine oculis-related homeobox (SIX), EYA and dachshund family transcription factor (DACH) proteins. The genes involved in the RDGN are regulated by various interconnected feedback loops and their protein products form complexes that regulate the development of multiple organs, such as the eyes, muscle, ears, heart, lungs, endocrine glands, placodes, pharyngeal pouches, craniofacial skeleton, and parathyroid[354].

EYA proteins have not shown to possess DNA binding activity, so their role in transcription is likely only to act as a co-activator through its transactivation and phosphatase domains. EYA proteins have also been shown to possess tyrosine[355-358] and threonine[359] phosphatase activity. More recently, a study by Cook, *et al*. shown that EYA1- and EYA3 dephosphorylate histone H2AX following genotoxic stress, which facilitates the recruitment of DNA repair factors, namely the mediator of DNA damage checkpoint 1 (MDC1) and MRE11/RAD50/NBS1 (MRN) complex[360].

So far, the only maladies widely accepted to be caused by *EYA1* polymorphisms have been the branchio-oto-renal, branchio-otic and oto-facio-cervical syndromes[361]. However, EYA1 overexpression is being increasingly reported in a variety of human cancers and is associated with poor prognosis and tumour aggressiveness[362].

An unpublished GWAS performed by our group (Carr, DF., personal communication) identified an association between a common, intronic variant of EYA1 and aspirin-induced gastric ulceration (Figure 1.13). The most significant SNP (rs12678747) from the discovery cohort only reached genome wide significance ($p < 1x10^{-8}$) when the results were meta-analysed with the results of a replication cohort (p=3.12x10-11; OR=2.03; 95% CI 1.65-2.50).

Since this study will be the first to propose a role for EYA1 in PUD, there are no mechanistic explanations for this association aside from what can be postulated from the pre-determined functions of EYA1. The expression and functions of EYA1 are comprehensively reviewed in Chapters 2 and 5.

EYA1 and BOR syndrome

EYA1 was first discovered following positional cloning efforts to determine the gene responsible for Branchio-Oto-Renal (BOR) syndrome[363-365]. It is now known that the *EYA1* is the most common causative gene in BOR syndrome (around 40% of cases), with reports of *SIX1* and *SIX5* polymorphisms less commonly causing the BOR phenotype (2.8 and 5% of cases, respectively)[366].

BOR syndrome is an autosomal dominate disorder with a prevalence of 1:40,000 and is characterised by hearing loss, branchial fistulae, preauricular pits or tags, and renal abnormalities. As described in section 5.1, over 150 *EYA1* variants have been associated with BOR syndrome. Some of these BOR-causing mutations disrupt interactions of EYA1 with SIX and SRY-box 2 (SOX) proteins, but most impair the enzymatic activity of EYA1[354].

Studies have shown that mice with the $EYA1^{+/-}$ genotype presents phenotypes that resemble BOR syndrome and $EYA1^{-/-}$ mice lack ears and kidney[367,368]. In humans, the genetic heterogeneity of EYA1 mutations cause a broad spectrum of phenotypes, making the diagnosis a BOR syndrome difficult[369].

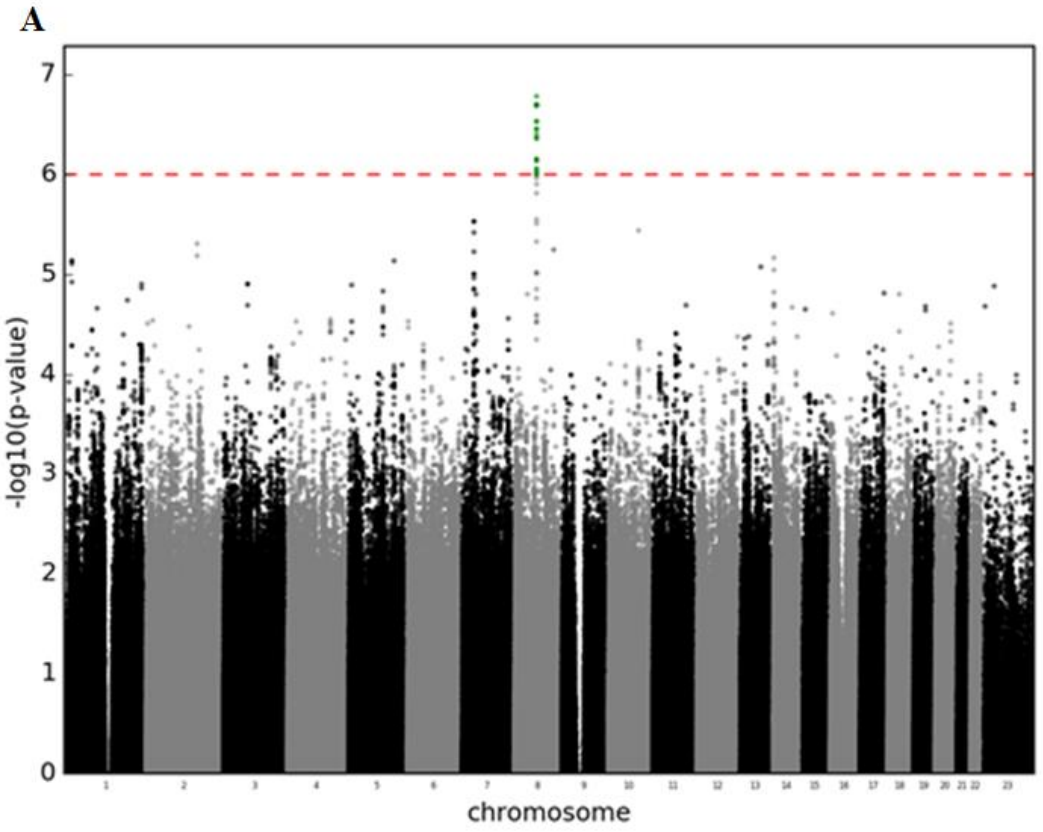
A
-log10(p-value)
chromosome

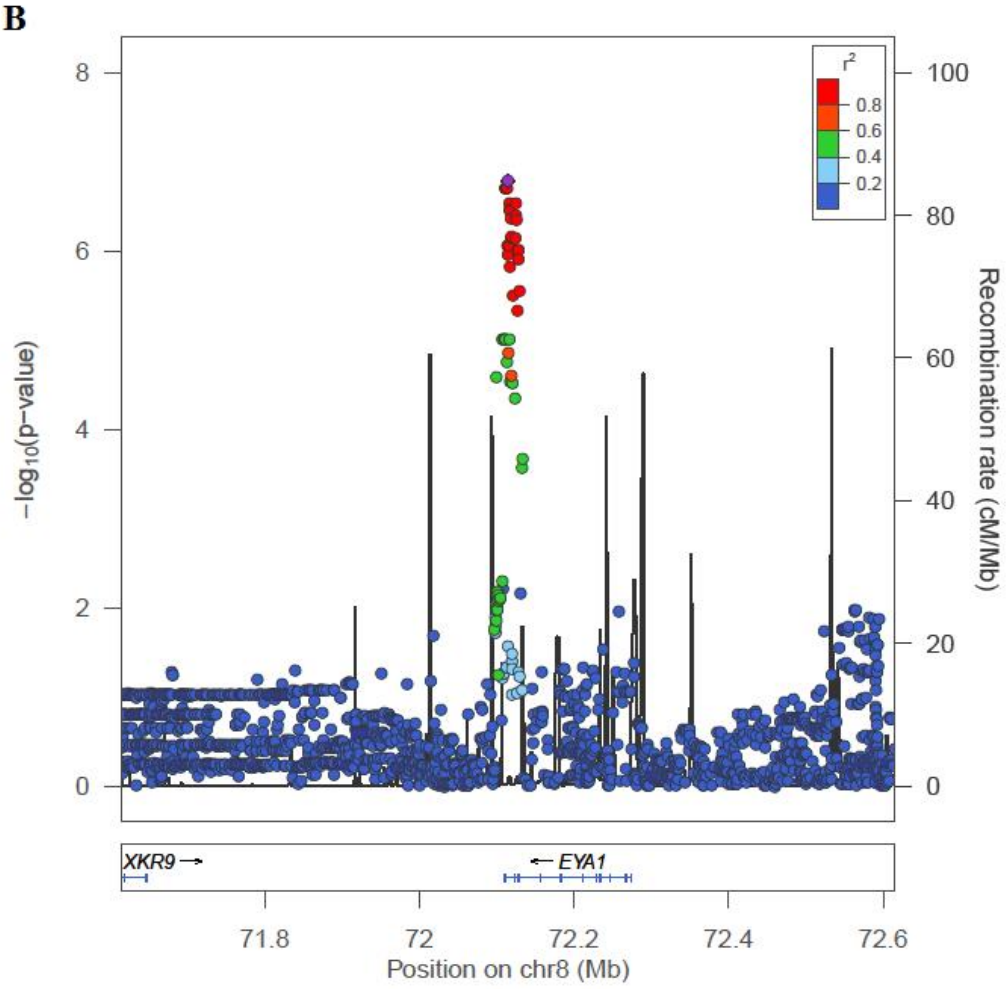
B
$-\log_{10}$(p-value)
Recombination rate (cM/Mb)
r²
0.8
0.6
0.4
0.2
XKR9
EYA1
Position on chr8 (Mb)

Figure 1.13 GWAS results showing the $-\log_{10}$ p-value associations between aspirin-induced peptic ulcer disease (y-axis) and (A) SNPs across chromosomes 1-23 (x-axis) or (B) the regional EYA1 loci on chromosome 8 (x-axis). Statistical analysis was performed using logistic regression analysis. SNPs that fall below the notional p-value of $1x10^{-6}$ are highlighted green. Information and figures provided as a personal communication with Carr, DF.

EYA1 and cancer

EYA1 overexpression has been reported in the development of various cancers (Table 1.8). This shows that regulation of *EYA1* expression plays a role in the development and functioning of various tissue types. The oncogenic effects of EYA1 are mediated through both its activity as a transcriptional cofactor and phosphatase[370]. Furthermore, there is evidence that the EYA tyrosine phosphatase promotes angiogenesis[371,372]. The C-terminal tyrosine phosphatase domain has been shown to be involved in *CCND1* gene expression and breast cancer-associated cell migration and metastasis[373].

Two studies have identified that *EYA1* silencing or downregulation is associated with gastric epithelial proliferation and metastasis[374,375]. The fact that differential *EYA1* expression influences angiogenesis, metastasis and gastric epithelial cell growth/survival provides reason to consider its relevance in gastric ulceration and ulcer healing.

Table 1.8 The pleiotropic roles of EYA1 in tumorigenesis and cancer progression.

Oncogenic process	Mechanism	Reference
Brain tumour	Eya1, Six1 and Nrp-1 and -2 regulation of Gli activators in Shh-dependent medulloblastoma.	376-379
	High EYA1 mRNA and protein expression associated with high MYCN expression in neuroblastoma (Hansen *et al*., 2016 & Albino *et al*., 2008).	380,381
	Decreased EYA1 protein expression in various grades of glioma samples.	382
Malignant peripheral nerve sheath tumor (MPNST)	Increased *EYA1* expression in MPNST cells compared to normal healthy Schwann cells.	383
Melanoma	EYA1 protein is significantly upregulated in melanoma in situ and metastases. Silencing and chemical inhibition of *EYA1*/EYA1 resulted in decreased proliferation and colony formation. A decrease in cyclin D1 and increased phosphorylated histone γH2AX was observed with EYA1 inhibition.	384
Breast cancer	Decreased miRNA-101 expression, a negative regulator of EYA1. EYA1 overexpression stimulates cell cycle progression, proliferation and survival through Notch signalling.	385
	Stabilisation of c-Myc by EYA1-mediated threonine-58 dephosphorylation. c-Myc stabilization stimulates cyclin D expression promoting cell cycle progression and tumorigenesis.	386
	PI3K/Akt-mediated Eya1 phosphorylation inhibits Eya1 SUMOylation. Phosphorylation hyperactivates EYA1 and increases breast cancer cell survival and migration.	387 388
	EYA1 phosphatase function facilitates CBP and RNA polymerase II recruitment to the cyclin D1 promoter, enhancing breast cell proliferation.	373
	EYA1 promotes migration, invasion, and transformation in breast cancer cell lines. Potentially due to Rac and Cdc42 mediated cytoskeletal re-arrangements.	389

Table 1.8 continued.

Oncogenic process	Mechanism	Reference
Wilms' tumour	Haploinsufficiency of miR-562, a negative regulator of EYA1, contributes to EYA1 overexpression in Wilms' tumour (Drake *et al*., 2009). EYA1 overexpressed in Wilms' tumour (Li *et al*., 2002 & Huang *et al*., 2006).	390-392
Intrahepatic cholangiocarcinoma (ICC)	Two missense mutations in exons 6 of *EYA1*, c.A281G and c.A371G, were significantly more common in ICC tissue compared to nontumour tissue.	393
Colorectal cancer	EYA1 is upregulated in CRC tissue, promoting tumour growth and angiogenesis. EYA1 coordinates with HIF-1α to increase VEGF-A expression via EYA1-mediated PI3K signalling activation.	372
Gastric carcinoma	*EYA1* methylated in both EBV^+ and EBV^-/high tumours. Methylation correlated with decreased gene expression.	374
	EYA1 expression significantly lower in gastric tumour tissue compared to non-tumour adjacent tissue. Negative correlation between *EYA1* expression and tumour size, lymphatic invasion and distant metastasis.	375

1.6 Aims of thesis

Given the increasing use of NSAID in the ageing population, understanding the mechanisms behind NSAID-induced GI toxicity is becoming progressively more imperative. Parenterally administered COX inhibitors only induce gastric mucosal at extremely high concentrations in the absence of concurrent luminal stimuli, with some reports stating that prostaglandin inhibition can be dissociated from NSAID-induced GI injury[243,244,259,260]. This highlights the importance of topical damage in ulcer pathogenesis.

In the past 15 years, several genetic markers of gastrointestinal risk factors have been identified for NSAID toxicity (section 1.5.1). Our group recently identified a novel

polymorphism in the *EYA1* gene that may confer risk for aspirin-induced peptic ulceration. Very little information has been published on the role of this gene in the upper GI tract[374,375] and the only work on its role in aspirin-induced gastric epithelial toxicity is preliminary studies performed by a previous member of our group[394].

It may be possible that the DNA repair and cell survival mechanisms associated with EYA1[360] play a role in gastric epithelial apoptosis caused by NSAIDs[249,395,396]. Likewise, EYA1 has been linked with cellular proliferation, migration and angiogenesis in various cancers[354]. Therefore, EYA1 may also be important in the gastric restitution and regeneration during ulcer healing.

The research in this thesis will investigate the role of EYA1 in topical gastric epithelial toxicity caused by aspirin. The aims of the study were therefore:

i. to find a suitable range of exposure times and concentrations of aspirin to use on a gastric epithelial cell line that will elicit apoptotic cell death;
ii. to determine the subcellular localisation of EYA1 in gastric epithelial cells;
iii. to elucidate how EYA1 integrates and manipulates in the apoptotic signalling pathway induced by aspirin in gastric epithelial cells;
iv. to characterise the gene and protein expression of EYA1 in human tissues by collating data available from online databases, and finally
v. to characterise the rs12678747 polymorphism identified from the NSAID-gastric ulcer GWAS, as well as other associations between ulceration and SNPs, and EYA1 polymorphisms and disease phenotypes

Chapter 2

In vitro analysis of aspirin toxicity and EYA1 expression in AGS cells

Contents

2.1 **Introduction**

As well as being an over the counter remedy for mild-moderate pain and acute inflammation, long-term low-dose aspirin therapy has become widely recommended for the prevention of cardiovascular disease, the management of myocardial infarction and transient ischaemic attacks. A meta-analysis of antiplatelet therapy for prevention of CVD in high-risk patients found that anti-platelet therapies, such as aspirin, reduced non-fatal myocardial infarction by 33%, vascular mortality by 16% and serious vascular events and non-fatal stroke by about 25%[397]. Aspirin is used less commonly for the treatment of osteoarthritis and rheumatoid arthritis given that these are conditions found primarily in the elderly, who are at an increased risk of aspirin-induced GI toxicity. Aspirin is not administered to children under the age of 16 due to the risk of Reye's syndrome; a rare but severe ADR with a mortality rate of about 40%[398].

The analgesic, anti-pyretic, anti-inflammatory and cardio-protective effects of aspirin are largely due to its ability to inhibit COX irreversibly[173,188], thereby halting TxA_2 and prostaglandin production (see section 1.3.2). The anti-platelet and anti-inflammatory effects of aspirin have shown to have compelling anti-cancer benefits including, preventing tumour progression and aggressiveness and improving cause-specific and overall survival[399]. This anti-cancer property is theoretically 5000-fold more potent when aspirin is conjugated to a nitric oxide (NO)-releasing group[400].

There are currently 234 gastric adenocarcinoma cell lines reported in the ExPASy-Cellosaurus database of cell lines used in biomedical research[131]. A list of 32 commercially available gastric adenocarcinoma cell lines are described in Table 2.1[401]. Several of these cell lines are commonly used to study NSAID-induced ulcer pathogenesis[281,402,403] and retained characteristics of gastric gland function such as the responsiveness of AGS cell to gastrin, a hormone that regulates acid secretion and epithelial cell proliferation[404]. NCI-N87 cells have also been shown to form cell-cell junctions, express MUC6 and secrete gastric lipase and pepsinogen-5[405].

Table 2.1 Specifications of commonly used gastric epithelial cell lines. Based on Table I in a study by Xu *et al*. [401]. Specifications of commonly used gastric epithelial cell lines, based on Table I in a study by Xu *et al*[401]. HGC-27: Human gastric carcinoma subclone-27. SNU: Seoul National University cell lines. NCI-N87: National Cancer Institute cell line N87. NCC: National Cancer Center cell lines. NU-GC-2: Nagoya University gastric carcinoma cell line 2. Cell lines in bold represent the gastric carcinoma cell lines used as *in vitro* models of gastric epithelial toxicity in this thesis.

Number	Cell line	Age (years)	Gender	Source of culture	Race	Differentiation	Primary culture	Refs.
1	**AGS**	54	Female	Primary tumour	American	Moderately-poorly	1979	[406]
2	**HGC-27**	-	-	Lymph node meta	Japanese	Undifferentiated	1976	[407]
3	**Hs746T**	74	Male	Left Leg	-	-	1979	[408]
4	KATO-III	55	Male	Pleural effusion	Japanese	Signet ring cell	1974	[409]
5	MKN-28	70	Female	Lymph node meta	Japanese	Moderately differentiated	1975	[409]
6	MKN-45	62	Female	Liver meta	Japanese	Poorly differentiated	1976	[409]
7	MKN-74	37	Male	Liver meta	Japanese	Moderately differentiated	1976	[409]
8	MKN-7	39	Male	Lymph node meta	Japanese	Well differentiated	1975	[409]
9	KWS-1	42	Male	Ascites	Japanese	Poorly differentiated	1982	[409]
10	OKAJIMA	38	Male	Pleural effusion	Japanese	Poorly differentiated	1976	[409]
11	SNU-1	44	Male	Primary tumour	Korean	Poorly differentiated	1984	[410]
12	SNU-5	33	Female	Ascites	Korean	Poorly differentiated	1987	[410]
13	SNU-16	33	Female	Ascites	Korean	Poorly differentiated	1987	[410]
14	NCI-N87	–	Male	Liver meta	American	Well differentiated	1976	[410]

15	SNU-719	53	Male	Primary tumour	Korean	Moderately differentiated	1991	[411]
16	SNU-216	46	Female	Lymph node meta	Korean	Moderately differentiated	1989	[411]
17	SNU-484	53	Male	Primary tumour	Korean	Poorly differentiated	1990	[411]
18	SNU-520	60	Female	Primary tumour	Korean	Poorly differentiated	1990	[411]
19	SNU-601	34	Male	Ascites	Korean	Signet ring cell	1991	[411]
20	SNU-620	59	Female	Ascites	Korean	Poorly differentiated	1991	[411]
21	SNU-638	48	Male	Ascites	Korean	Poorly differentiated	1991	[411]
22	SNU-668	63	Male	Ascites	Korean	Signet ring cell	1991	[411]
23	NCC-19	56	Male	Primary tumour	Korean	Moderately differentiated	2002	[412]
24	NCC-20	50	Female	Ascites	Korean	–	2002	[412]
25	NCC-24	49	Male	Primary tumour	Korean	Signet ring cell	2002	[412]
26	NCC-59	62	Male	Ascites	Korean	Moderately differentiated	2002	[412]
27	SNU-1750	65	Male	Primary tumour	Korean	Poorly differentiated	2001	[412]
28	SNU-1967	41	Female	Ascites	Korean	Poorly differentiated	2002	[412]
29	NU-GC-2	–	–	Lymph node meta	Japanese	Poorly differentiated	–	[413]
30	NU-GC-2	–	–	Brachial muscle meta	Japanese	Poorly differentiated	–	[413]
31	NU-GC-2	–	–	Lymph node meta	Japanese	Partial signet ring cell	–	[413]
32	NCI-N87	-	Male	Liver meta	American	Well differentiated	1990	[410]

The anti-proliferative and apoptotic effects of NSAIDs are often found to be at higher concentrations than what is required for cyclo-oxygenase inhibition[414]. In addition to this, it has been shown that COX-inhibition can be performed without inducing GI damage[243,415]. There is increasing evidence that the "topical" effects of oral NSAID therapy, as well as systemic COX-independent pathways, are also likely to be important in ulcerogenesis. Pathways of aspirin-induced cell death include activation of caspases[249,395,396,416-421], ceramide accumulation[422], inhibition of NF-κB activation[417,421,423-425], cell cycle arrest[220,426-432], inhibition of proteasome function[427,429], various forms of cellular stress and activation of stress kinases[414,433-438].

Aspirin upregulates and causes the translocation of pro-apoptotic proteins NOXA, PUMA, BID, BAX and BAX[396,418,439], whilst also down regulating anti-apoptotic proteins Survivin, MCL-1, BCL-XL and BCL-2[421,439-441] in various cell lines that originated from a diverse set of tissues.

A study by Pique *et al*. demonstrated how aspirin is able to initiate cytochrome c release before caspase-processing and loss of mitochondrial membrane potential[419]. In contrast, another study found that aspirin induced gastric mucosal death is caused by a caspase-independent pathway by increasing mitochondrial membrane permeability and causing the release of apoptosis- inducing factor (AIF)[250].

The mode of aspirin-induced cell death is therefore very complex and likely depends on cell type, aspirin concentration and exposure time. When high concentrations or long exposure times are used, aspirin has been reported to cause cell cycle arrest and necrosis[442].

2.1.1 **EYA and its chemical inhibitors**

The Eyes Absent (*EYA1-4*) genes were first described as encoding developmentally regulated transcriptional cofactors in the retinal determination gene network (RDGN) involved in metazoan organogenesis. The EYA proteins consist of a transactivation and threonine phosphatase[359] domains in a poorly conserved N-terminal region and a tyrosine phosphatase[443-445] and protein binding domain in a well-conserved C-terminal region.

EYA1 lacks a DNA-binding motif but does form a transcription complex with sine oculis homeobox 1 (SIX 1), which forms part of a complex that regulates the expression of genes involved in cell proliferation, survival and migration[387].

The tyrosine phosphatase domain has more recently been described as promoting survival and DNA repair following double-stranded DNA breaks (Figure 2.1). Cells undergoing genotoxic stress via chemicals or ionising radiation can develop double-stranded DNA breaks. This leads to the long stretches of phosphorylated serine residues on histone H2A.X, mediated by ATM/ATR phosphatidylinositol-OH kinase (PI(3)K)-family kinases. EYA1/3 proteins dephosphorylates tyrosine 142 (Y142) on histone H2A.X, allowing the recruitment of DNA repair factors, including the mediator of DNA damage checkpoint protein 1 (MDC1) and the MRN complex, to phosphoserine 139 (S139)[360,446]. In the absence of EYA1, Y142 remains phosphorylated, reducing binding of repair factors and allowing the phosphorylation of S139 by the pro-apoptotic factor, c-Jun N-terminal kinase 1 (JNK1). Phosphorylation of S139 has been shown to be a critical event in caspase-mediated DNase (CAD) facilitated DNA degradation during apoptosis[447].

EYA1 and *EYA3* knockdown (siRNA in HEK293) and *Eya1* knockout (*Eya1*$^{-/-}$ murine kidneys) experiments shown significant increase in TdT-mediated dUTP nick end labelling (TUNEL)-positive apoptotic nuclei after exposure to hypoxia-inducing reagents and ionising radiation compared to controls[360].

Given the critical roles of EYA1 in cell growth and cell fate determination, it is unsurprising that aberrant EYA1 activity is linked to various human diseases including developmental disorders and cancer[354]. In this chapter, the effect of EYA1 inhibition was studied to determine the role of this multifunctional protein in aspirin-mediated gastric epithelial toxicity.

A chemical screen conducted by Tadjuidje *et al.* identified benzbromarone and several of its metabolites as uncompetitive inhibitors of EYA phosphatase activity[371,448]. Benzbromarone was shown in this study as a potent inhibitor of EYA2 (IC50= 10.3μM) and EYA3 (IC50= 11μM) phosphatase activity. No inhibitory data was provided in the study for EYA1, but crystallographic studies suggest that benzbromarone can inhibit EYA proteins non-competitively, by binding to a hydrophobic region proximal to the highly conserved ED active site[371].

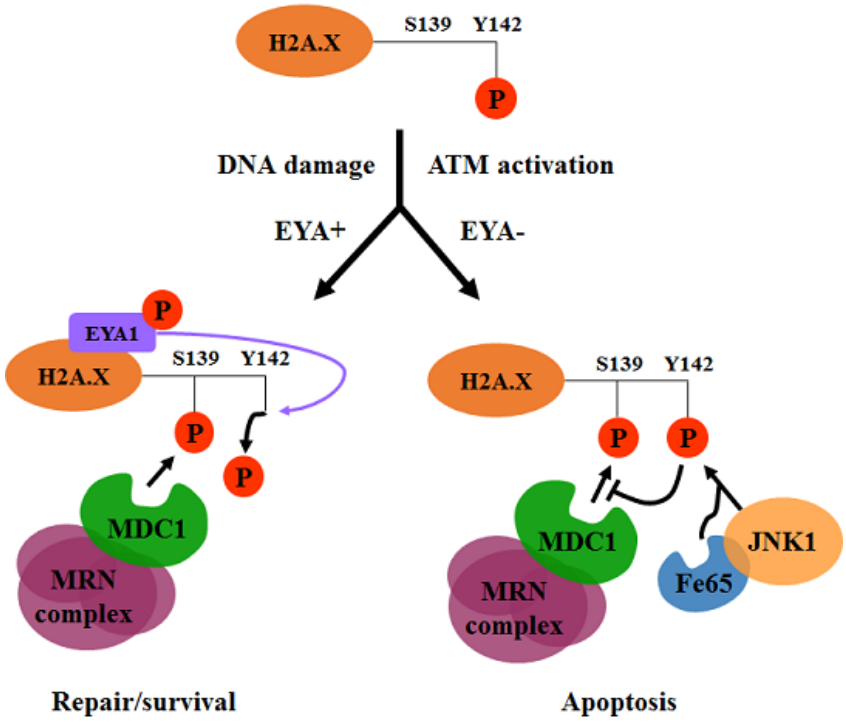

Figure 2.1 EYA1-mediated cell fate determination. The mechanism proposed by Cook *et al.* of how serine and tyrosine phosphorylation states on histone H2A.X discriminates between survival and apoptotic responses to DNA damage. DNA damage leads to ATM-mediated S139 phosphorylation. In the presence of EYA proteins, Y142 is dephosphorylated allowing the binding of repair factors (MDC1/MRN complex) which promotes cell survival. In the absence of EYA, Y142 remains phosphorylated, precluding the binding of repair factors to phosphoserine 139 and instead the recruitment of pro-apoptotic factors (JNK1).

Benzbromarone was used as a treatment for gout for 30 years before being withdrawn from several global markets due to reports of serious hepatotoxicity. The withdrawal has sparked discussion about the compound's benefit-risk ratio considering the alternative uricosuric agents, allopurinol and probenecid, can also cause life-threatening ADRs[449]. The uricosuric activity of benzbromarone is attributed to its ability to inhibit the urate transporter SLC22A12, thereby inhibiting uric acid reabsorption in the kidneys.

Benzbromarone-mediated EYA inhibition decreases endothelial cell motility and angiogenesis, which could be explained by the protective role of EYA proteins in hypoxia-mediated double-strand DNA breaks. This effect has made benzbromarone an attractive candidate for the treatment of cancer metastasis and tumour angiogenesis. Benzbromarone has shown to cause no cellular toxicity in breast epithelial cells (MCF10) up to 10μM[371] and cytotoxicity only at concentrations of 100μM in

hepatocytes (HepG2) after 48 hours exposure[450]. However, benzbromarone-induced mitochondrial toxicity could be observed at concentrations 25μM and above.

2.1.2 **Aims and Objectives**

The aim of this chapter was to conduct experiments to determine a suitable dose and time course in which aspirin can cause apoptotic cell death of AGS gastric epithelial cell line. A study using colon cells has shown that histone γ-H2AX is phosphorylated at S139 when treated with 10mM aspirin for 8h[430], suggesting that γ-H2AX phosphorylation plays a role in aspirin-mediated apoptosis. Given the recently discovered association between EYA proteins and γ-H2AX in attenuating apoptosis by promoting DNA repair following genotoxic stress[360], we hypothesised that inhibition of endogenous EYA1 by benzbromarone could exacerbate aspirin-mediated gastric epithelial toxicity. Experiments were also conducted to study the mode of aspirin-mediated AGS cell death and measure endogenous EYA1 expression in AGS cells.

2.2 **Materials and Methods**

2.2.1 **Materials**

Unless otherwise specified, all reagents were purchased from Sigma-Aldrich Co., Dorset, UK. Dimethyl sulphoxide (DMSO), Tris Base, Pierce BCA Protein Assay Kit, Foetal bovine serum (FBS), Phosphate Buffered Saline (PBS), trypan blue, glycine, methanol, sodium chloride, potassium chloride, Pierce™ BCA Protein Assay Kit, Sodium and Potassium Chloride, Trizma Base, Tween-20, tissue culture flasks and plates were purchased from Fisher Scientific, Loughborough, UK. Ultimate security Cryogenic Vials were purchased from Alpha Laboratories Ltd., Eastleigh, UK. Acrylamide Solution was purchased from Geneflow Ltd., Elmhurst, UK. Sterile 30mL Universal tubes were purchased from Greiner Bio-One, Stonehouse, UK. Precision Plus Protein Kaleidoscope and Clarity ECL Substrate were purchased from Bio-Rad, Hertfordshire, UK. Rabbit Anti-EYA1 primary and Goat Anti-Rabbit Ig HRP secondary antibodies were purchased from Abcam, Cambridge, UK. Rabbit Anti-EYA1 primary antibodies were also purchased from Sigma-Aldrich Co. and Insight Bioscience, Wembley, UK. Rabbit Anti-caspase-3, -cleaved caspase-3, -caspase-9, -

PARP and -GAPDH primary antibodies were purchased from Cell Signaling Technology, Hitchin, UK.

2.2.2 **Cell lines and culture conditions**

The human gastric adenocarcinoma cell line, AGS cells, were provided by Prof. Andrea Varro (Cellular and Molecular Physiology, University of Liverpool, UK) and the Human Embryonic Kidney (HEK) cells were provided by Andrea Davies (Molecular and Clinical Pharmacology, University of Liverpool, UK). AGS and HEK cells were cultured in Dulbecco's Modified Eagle Medium (DMEM; 4500 mg/L glucose, +L-glutamine, +sodium bicarbonate) containing 10% FBS. The human gastric adenocarcinoma, HGC-27 cell line, was purchased from Sigma-Aldrich and cultured in EMEM (EBSS) supplemented with 2mM Glutamine, 1% Non-Essential Amino Acids (NEAA) and 10% FBS.

All cells were frozen at a density of $2x10^6$ cells per mL in 1.8mL cryogenic vials in their respective growth media and 5% DMSO. Cells were thawed at 37°C, placed into 10mL complete media and pelleted by centrifugation at 168g for 5min. Cell were resuspended in 1mL complete media, placed in a flask with 20mL pre-warmed medium and incubated in a humidified atmosphere of 5% CO_2/95% air at 37°C.

Cells were passaged after reaching <80% confluence. Passage was performed by discarding growth media and washing the cells gently with HBSS. Cells were covered in 5mL of 0.05% trypsin with 0.68mM EDTA until they detached from the culture flask. The trypsin was inactivated by adding the suspended cells to 10mL of serum-containing growth media in a 30mL tube and cells were centrifuged at 168g for 5min. The supernatant was discarded and the cell pellet was re-suspended in DMEM (10% FBS). An aliquot of suspended cells were counted using 0.4% trypan blue exclusion and a Countess Automated Cell Counter (Fisher Scientific). Cells were seeded into T75/T175 tissue culture flasks or 6, 12, 24 or 96 well plates.

2.2.3 **Preparing drug solutions**

The aspirin concentrations used were chosen to represent the high concentrations that would be found in the stomach of patients that develop gastrointestinal complications after taking the drug[227].

Aspirin and benzbromarone stock solutions were made in DMSO, 138.8 and 2000 times greater than each final concentration used, respectively. All final drug-containing media solutions were sonicated for 5min in an Ultrasonic Cleaner (VWR, Radnor, Pennsylvania) to dissolve the drugs in solution.

Drug-treated media were prepared by diluting 7.2µL of the aspirin stock solutions with 0.5µL benzbromarone per 1mL complete DMEM, giving all final drug solutions contained 0.77% DMSO.

2.2.4 **3-(4,5-Dimethylthiazol-2-yl)-2,5-Diphenyltetrazolium Bromide (MTT) assays**

AGS cells were seeded at 15,000 cells/well in 96-well plates with 100µL/well DMEM (10% FBS) and incubated for 24h or until wells reached 70-80% confluence.

Cells were treated with a range of aspirin concentrations (1-50mM) in the presence and absence of 1, 2.5 and 10µM benzbromarone for 24h and 10µM benzbromarone for 48 and 72h. At the end of the drug exposure, 20µL of 12mM MTT was added to each well and plates were incubated in the dark for 3h. Each well received 100µL of 20% w/v sodium dodecyl sulphate lysis buffer (20g SDS in 100mL of a 50% DMF solution) and plates were re-incubated overnight.

The absorbance in each well was measured at 595nm using a DR X 880 Multimode Detector and Detection Software (Beckman Coulter Inc., California, USA). Quadruplicate technical repeats were averaged and average background absorbance caused by the media was subtracted from all values. The average values for each treatmentwere expressed as percent viabilityby comparing to the vehicle control either with or without benzbromarone. Three biological replicates were obtained for each treatment and time point. Data from the viability assays were also analysed to assess the toxicity caused by 10µM benzbromarone at 48 and 72h time points (Appendix 2.1).

2.2.5 **Flow Cytometry (Annexin-V/PI)**

AGS cells were seeded at 150,000 cells per well in 12-well plates with 1mL per well DMEM and incubated for 24h or until wells reached 70-80% confluence. Cells were treated with a range of aspirin concentrations (1-30mM) for 24 and 48h. Three biological replicates were obtained for each treatment of aspirin at each time point.

At the end of the treatment, supernatant from each well was placed in 1.5mL microcentrifuge tubes and cells were washed with 500µL PBS. The wash from each well was placed in the respective tubes and cells were covered in 500µL trypsin-EDTA solution for 10min. Supernatant/wash solutions were centrifuged at 500g for 5 min and supernatant was discarded. The detached cells in each well were placed in the corresponding tubes and spun again at 500g for 5min. Supernatant was removed, cells were resuspended in 500µL 1x Annexin Binding solution containing 0.005% annexin V-fluorescein isothiocyanate (and tubes were incubated for 8min at room temperature. Finally, 5µL propidium iodide (PI; 1mg/mL) was added to each tube and mixed gently. Percentage unstained cells (live), FITC (apoptotic), PI (necrotic) or FITC&PI (necroptotic) stained cells were determined using fluorescence-activated cell sorting (FACS). Representative images of forward and side scatter gating are provided for both control and aspirin treated cells (Appendix 2.2)

2.2.6 **Western blots**

AGS, HEK, and HGC-27 cells were plated at 500,000 cells/well on a 6 well plate, incubated at 37°C/5% CO_2, until reaching 70% confluence and lysed using 120µL/well RIPA buffer with 1% protease inhibitor. MDA-MB-231, MCF-7 and Jurkat protein lysates were provided by Dr. S. Varadarajan (Molecular and Clinical Cancer Medicine, University of Liverpool, UK). SH-SY5Y protein lysate was provided by Dr. G Sills (Molecular and Clinical Pharmacology, University of Liverpool, UK).

Protein concentrations of all lysates were determined using a BCA assay cocktail. The BCA assay was performed by loading 9µL/well of a range of albumin concentrations (0-18µg) in duplicates as standards and 1, 3 and 5µL of each sample. Next 200µL of BCA reagent (49:1 of BCA reagent A: reagent B) was added to all wells and the plate was incubated for 30min at 37°C in the dark. The plate was cooled for 1 minute before reading the absorbance in each well at 595nm using a spectrophotometer. The average sample concentrations were determined by removing the background absorbance from all values and using a linear trend line of the known standard concentrations and their absorbances to convert the sample absorbances to protein concentrations.

Before performing the western blot, 10% acrylamide gels were cast using the reagents outlined in Table 2.2. LDS reducing buffer was made by mixing LDS sample buffer

and sample reducing agent at a 7:3 ratio and adding 5µL of the mix to eppendorfs containing 20µg of each sample as determined by the BCA assay. The reduced samples were denatured at 95°C for 5min, spun down in a microcentrifuge and placed on ice for 5min.

Table 2.2 Reagents used to make polyacrylamide gels for western blotting. X= Y/12*30; Y= ((desired % gel)/30)*12; Z=9-Y.

Reagents	**Volume per gel**	
	4% Stacking gel	**X% Resolving gel**
Stacking gel buffer (0.5M Tris/HCl pH6.8/1% SDS)	1.25 mL	-
Resolving gel buffer (1.5M Tris/HCl pH8.8/1% SDS)	-	3mL
ProtoGel Acrylamide Solution (30% Solution at 37.5:1 Ratio)	666.6 µL	YmL
ddH_2O	3.05 mL	ZmL
Ammonium Persulphate (10% solution)	25 µL	40µL
Tetramethylethylenediamine (TEMED)	5µL	8µL
Total volume	5mL	12mL

Acrylamide gels were loaded into a gel tank and topped up with SDS running buffer (192mM glycine, 25mM Trizma Base, 3.47mM SDS in water). Next, 10µL of protein ladder was added to each gel and reduced samples were loaded. The gels were run for 90 mins at 130V.

Gels were removed and placed in separate transfer cassettes, each containing 2 sponges, 2 filter papers, a nitrocellulose membrane and the gel. Cassettes were filled with transfer buffer (192mM glycine and 250mM Tris Base in an 80:20 ddH_20/methanol solution) and ran at 100V for 1h. Once the transfer had finished, the membranes were stained with Ponceau Red solution to confirm successful transfer and

blocked in a 5% skimmed milk-TBS-T (150mM NaCl, 2mM KCl, 25mM Trizma base, pH 7.4) solution for 30min at room temperature.

Membranes were washed with TBS solution containing 0.1% Tween 20 and the incubated with a Rabbit Anti-caspase-3, cleaved caspase-3, caspase-9, PARP and GAPDH overnight at 4°C. Three rabbit anti-EYA1 primary antibodies targeting the middle (Abcam) and the C-terminal (Sigma and Insight Biotechnology) regions were also added to separate membranes overnight at 4°C. Membranes were washed five times for 5min per wash and incubated with Goat Anti-Rabbit Ig HRP secondary antibody for 1h at room temperature. Membranes were washed a further five times and covered in ECL reagent (1:1 luminol substrate to peroxide solution mix) for 5min in the dark at room temperature. Membranes were dried with tissue paper and bands were detected using a Bio-Rad ChemiDoc Imaging System.

2.2.7 **Statistical analysis**

All statistical analyses were performed using Prism version 7.00 for Windows, GraphPad Software, La Jolla California USA (www.graphpad.com). A P value of <0.05 was considered statistically significant for each statistical method used. Specific statistical methods used for each experiment are detailed in the results section.

2.3 **Results**

2.3.1 **EYA inhibition exacerbates aspirin-induced AGS cytotoxicity**

The effect of EYA chemical inhibition on aspirin-induced AGS cytotoxicity was measured by MTT following co-treatment of various concentrations of aspirin and benzbromarone for various time points. A clear dose response was observed across each time point for increasing aspirin concentrations, as well as a time-dependent effect at 10-20mM across the 3 time-points (Figure 2.2 and Figure 2.3).

No statistically significant change was observed at 1 and 2.5μM benzbromarone with all tested aspirin concentrations at 24h. There were however noticeable differences in viability at 30 and 40mM aspirin between 0 and 10μM benzbromarone, $P = 0.0071$ and 0.0001 respectively (Figure 2.2). This concentration of benzbromarone was then tested with lower aspirin concentrations for longer exposure times.

An exacerbation in toxicity was also observed with co-treatment of 10μM benzbromarone and 5 and 10mM aspirin ($P < 0.0001$) at 48h (Figure 2.3A). No differences were observed between control and benzbromarone co-treatment for any of the aspirin concentrations tested at 72h (Figure 2.3B).

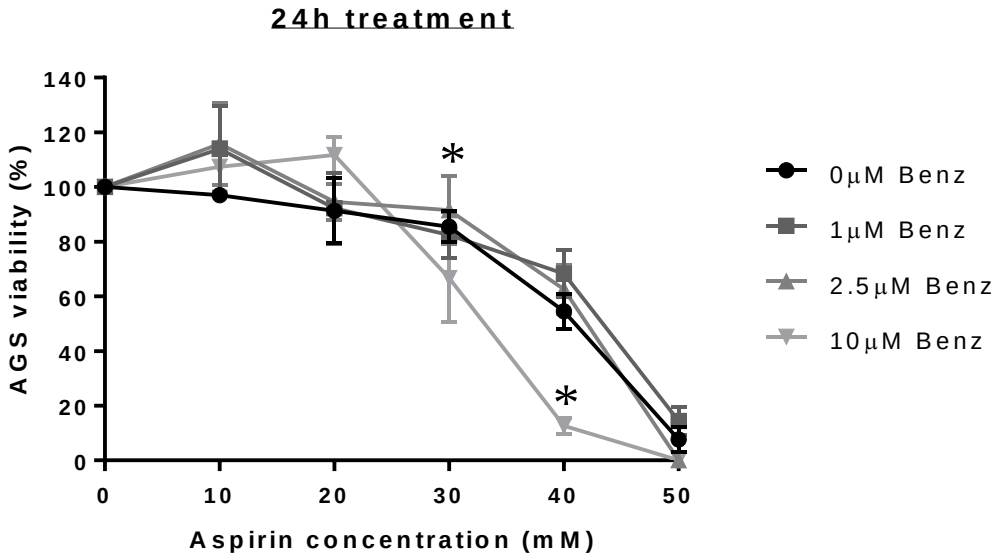

Figure 2.2 Effect of benzbromarone on aspirin-induced AGS cytotoxicity. AGS cells were treated with aspirin (10-50mM) for 24 hours. Each aspirin concentration was co-incubated with 1, 2.5 and 10μM of an EYA inhibitor, benzbromarone, for 24 hours. MTT assays were performed to assess cytotoxicity as described in section 2.2.4 and values expressed as percentage viability of vehicle control (0.77% DMSO). Data are shown as the mean value ± SD (n=3). Two-way ANOVA analysis with Dunnett's correction was used to compare differences between benzbromarone treatments for each aspirin concentration. * denotes $p < 0.05$.

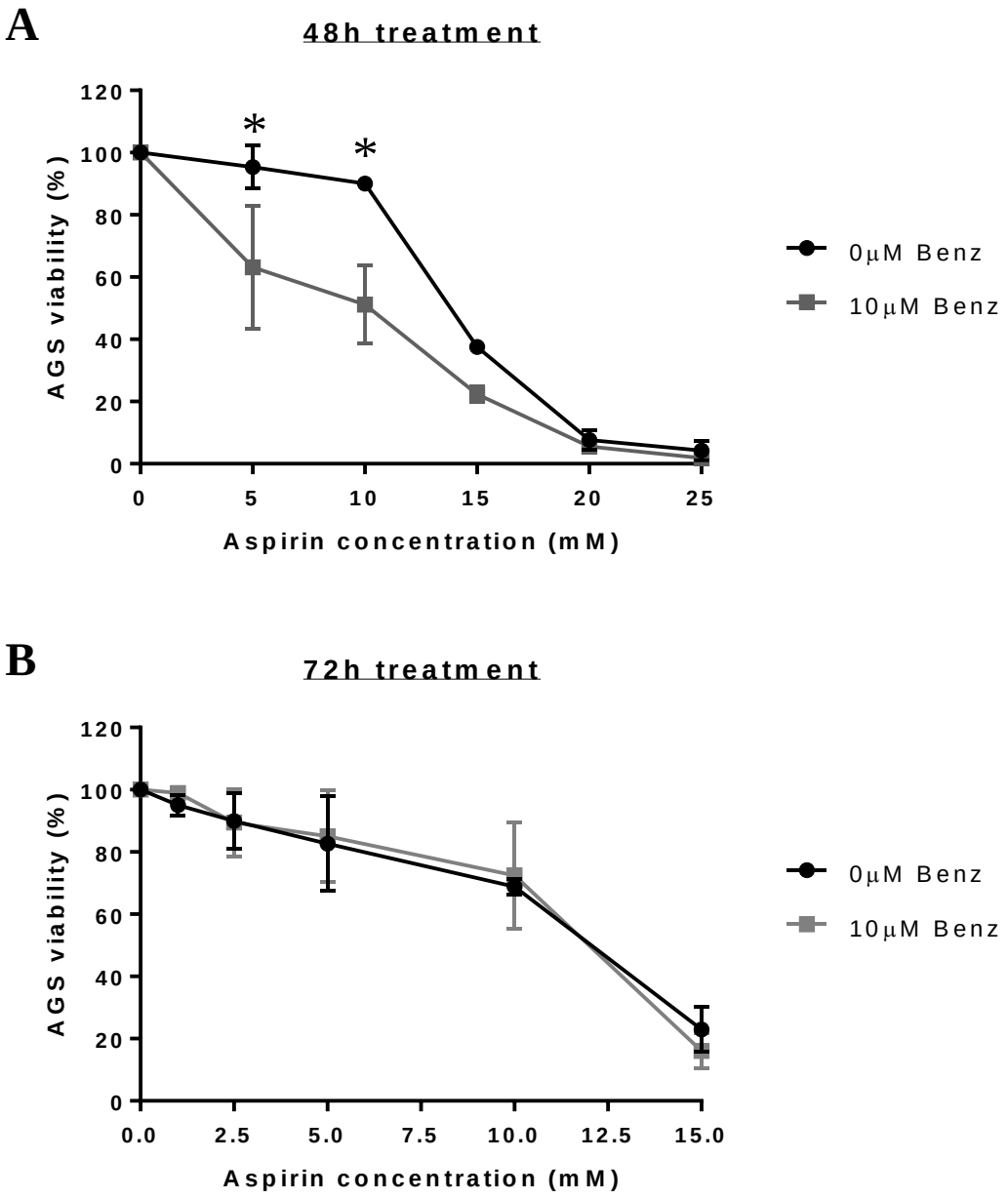

Figure 2.3 Effect of EYA inhibition on aspirin-induced AGS cytotoxicity. AGS cells were treated with 5-25mM aspirin for 48 hours (A) and 1-15mM aspirin for 72 hours (B). Each aspirin concentration was also co-incubated with 10μM benzbromarone for the respective times. MTT assays were performed to assess and values expressed as percentage viability of vehicle control (0.77% DMSO). Results are expressed as the mean percentages that have been normalised to the relevant vehicle control ± SD (n=3). Two-way ANOVA analysis with Sidak's correction was used to compare differences between benzbromarone treatments for each aspirin concentration for each time point. * denotes $p < 0.05$.

At 48h, 10μM benzbromarone had not significant effect of AGS viability (Appendix 2.1). However, after 72h viability was significantly reduced by 30% (Appendix 2.1).

This effect was controlled for by comparing co-treated cells to cells treated with 10μM benzbromarone only.

2.3.2 **Aspirin-induced apoptosis is concentration and time dependent**

Western blot analysis of AGS cells treated over several time points with 25mM aspirin revealed that the procaspase-3 is cleaved to the active p12 and p17 fragments as early as 16h after aspirin exposure (Figure 2.4). Total caspase-3 processing was observed by 48h. It is important to note that this time-based experiment was only performed once and will therefore need to be repeated to ensure the validity of these results.

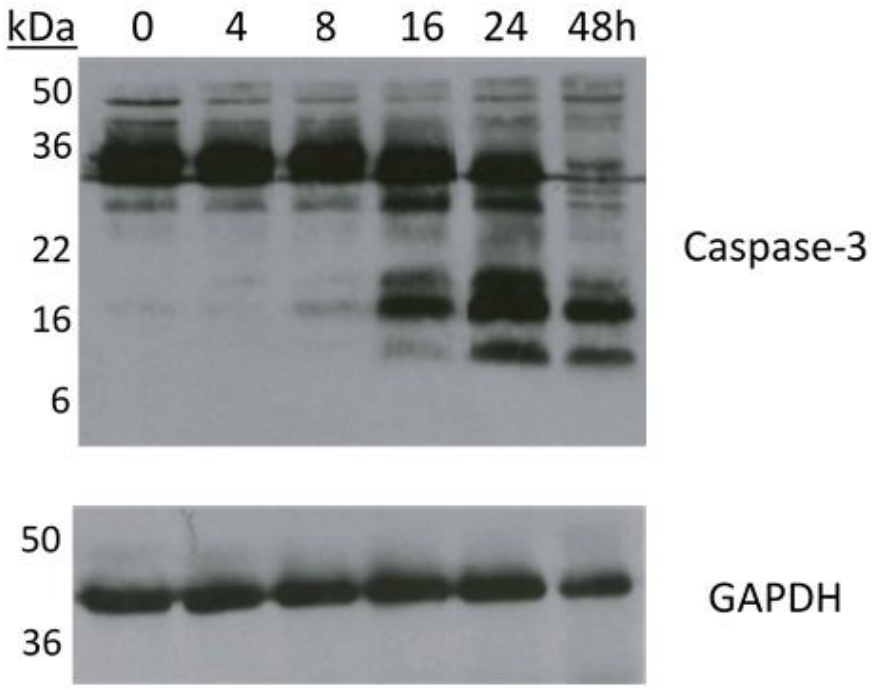

Figure 2.4 Time-dependent caspase-3 cleavage in AGS cells treated with aspirin. AGS cells were treated with 25mM aspirin for the times indicated and 20μg of protein from whole cell lysates were used to analyse pro-caspase-3 cleavage to the active p17 and p12 fragments by western blot. Glyceraldehyde 3-phosphate dehydrogenase (GAPDH) was used as a loading control (n=1).

To better characterise the ratio of apoptotic and necrotic death caused by aspirin, Annexin-PI staining was performed on AGS cells treated with a range of aspirin concentrations for 24 and 48h (Figure 2.5), and examined by flow cytometry.

AGS cells exposed to increasing concentrations of aspirin for 24h showed signs of cytotoxicity at concentrations starting from 10mM, with a significant drop in viable cells (AV-/PI-) at 30mM, 45.0% ± 24.2%, compared to control, 85.8% ± 2.9%, P = 0.002 (Figure 2.5A). The mode of death at 30mM aspirin at 24h treatment was a

mixture between apoptotic (AV+/PI-; 17.4% ± 29.8%), necrotic (AV-/PI+; 25.4% ± 19.7%) and late apoptotic/necrotic (AV+/PI+; 12.2% ± 14%).

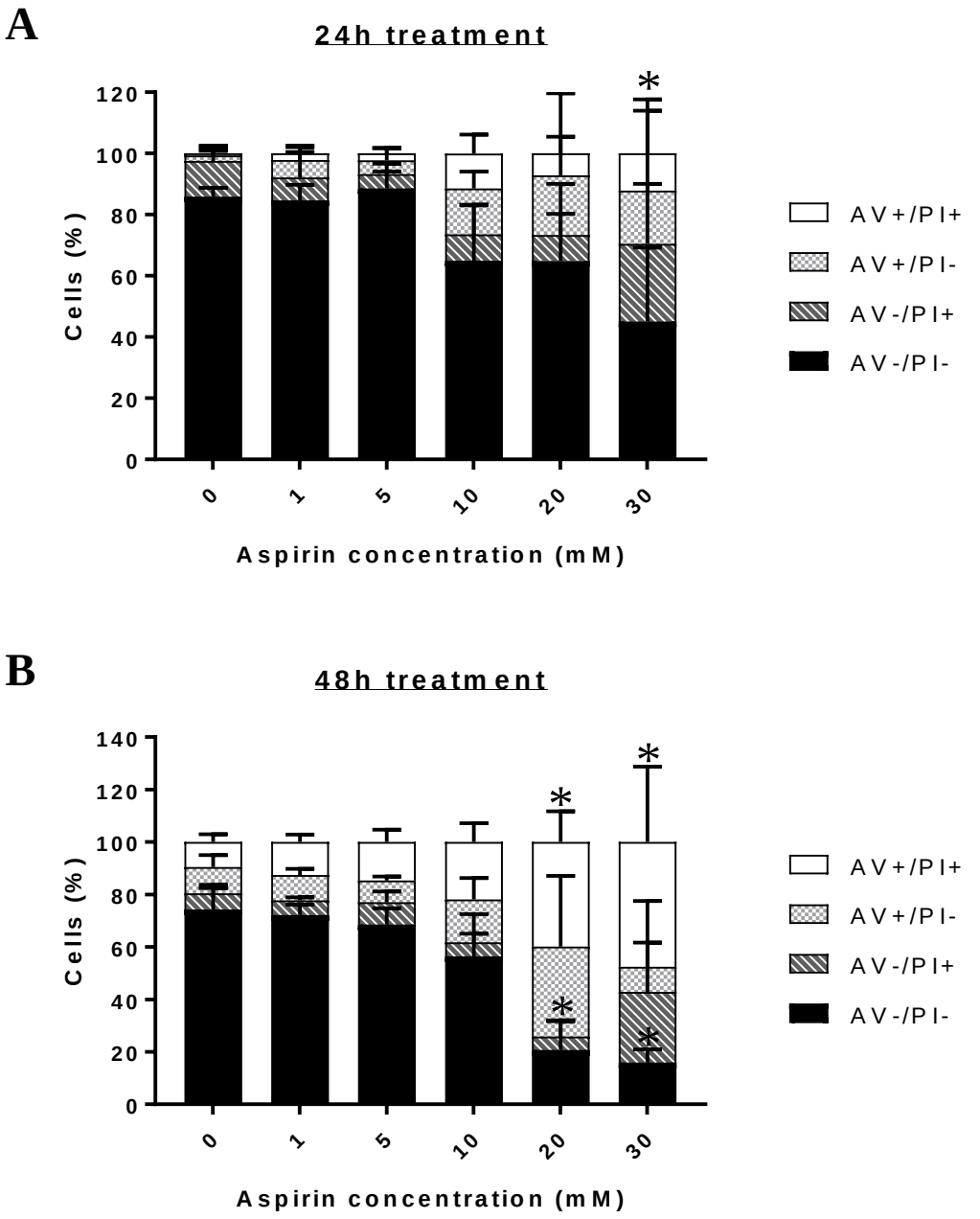

Figure 2.5 Apoptosis/necrosis profile in aspirin-mediated AGS cytotoxicity measured by flow cytometry. AGS cells were treated with aspirin (1-30mM) for 24 (A) and 48h (B) and resuspended in binding buffer containing FITC-conjugated Annexin V and propidium iodide. FACS analysis was used to measure percentage unstained (AV-/PI-), necrotic (AV-/PI+), apoptotic (AV+/PI-) and late apoptotic/necrotic cells (AV+/PI+). Data shown are mean values ± SD (n=3). Statistical analysis was conducted using two-way ANOVA followed by Dunnett's post hoc correction. * denotes $p < 0.05$.

At 48h significant reductions in viable cells can be observed with both 20 and 30mM aspirin, 20.7 ± 11.0% and 16.0% ± 5.0% respectively, compared to control, 74.2% ± 8.2%, $P = 0.0001$ (Figure 2.5B). After 48h exposure to 20mM aspirin, the majority of cell death was caused by apoptotic, 34.3 ± 27.0% vs. 10.1 ± 4.5% (control), and late apoptotic/necrotic death, 39.9% ± 11.8 vs. 9.5% ± 3.0 (control), $P = 0.02$. At the same exposure time, 30mM aspirin caused cell death mainly by necrosis, 27.0 ± 34.6% vs. 6.2% ± 3.3% (control), and late apoptosis/necrosis, 47.6% ± 28.7% vs. 9.5% ± 3.0% (control), $P = 0.0024$. The time point and aspirin concentration that shown the greatest amount of apoptosis was 20mM aspirin at 48h, 34.3% ± 27.0%.

Western blotting was performed to determine whether aspirin treatment lead to apoptotic cell death. AGS cells treated for 48 with aspirin >20mM resulted in Apaf-1 and cytochrome c mediated cleavage of procaspase-9 (47kDa) to the active p37 fragment. As expected processing of procaspase-3 and poly (ADP-ribose) polymerase (PARP) was also observed at aspirin concentrations >20mM (Figure 2.6). This experiment was also only performed once, however the results are consistent with experiments performed in chapter 4 (see Figure 4.3).

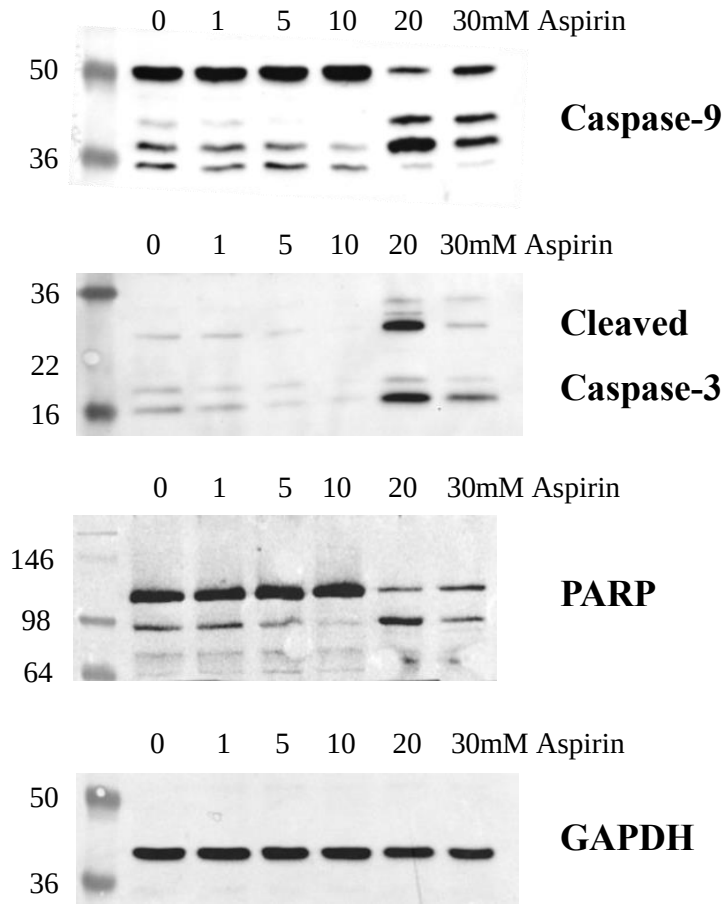

Figure 2.6 AGS cell death induced by aspirin exhibits characteristic hallmarks of apoptosis. AGS cells were treated with aspirin (1-30mM) for 48h and 20μg of protein from whole cell lysates were used to perform western blot analysis of PARP, caspase-3 and -9 cleavage. Aspirin concentrations >20mM induced the processing of caspase-9 to the p35 form, caspase-3 to the p17 form and PARP to the p89 form. GAPDH was used as a loading control (n=1).

2.3.3 **Endogenous EYA1 protein shows low/no expression in 7 cell lines**

Following difficulty to detect endogenous EYA1 protein in AGS cells using western blotting, a selection of 7 cell lines were used to determine whether endogenous expression could be detected using the same technique, with lysates from either another gastric epithelial cell line or cell lines from a different tissue types.

As can be seen in Figure 2.7A-C, endogenous EYA1, which has a predicted molecular weight of 64kDa, could not be detect using antibodies that target two separate immunogens in seven different cell lines: AGS (gastric), HGC (gastric), MDA-MB-231 (breast), MCF7 (breast), Jurkat (blood), HEK (kidney) and SH-SY5Y (neuronal).

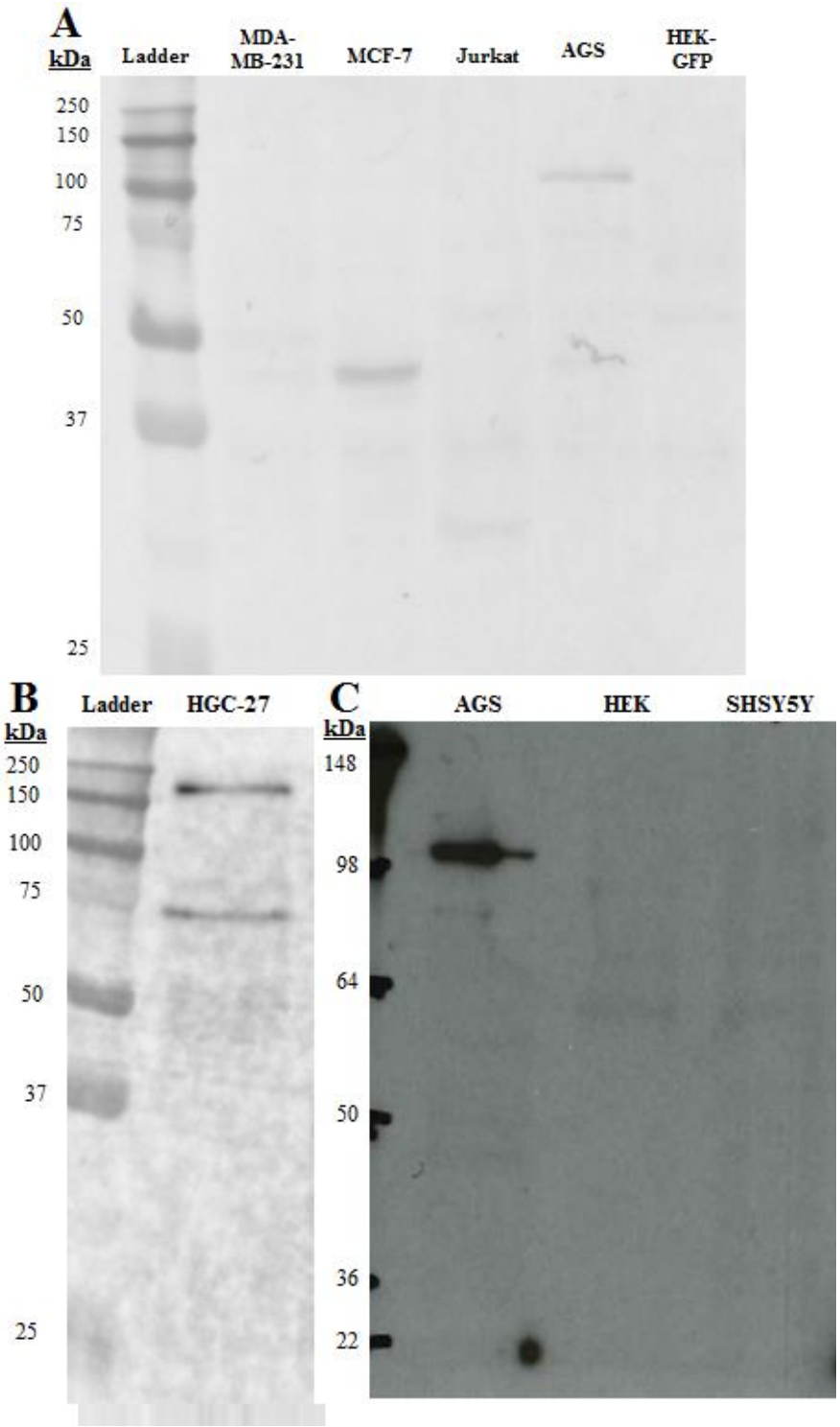

Figure 2.7 Endogenous EYA1 protein expression in seven morphologically independent cell lines. Western blot analysis of endogenous EYA1 protein expression was performed in whole cell lysates (20µg) of (A) MDA-MB-231, MCF7, Jurkat, AGS, HEK-GFP, (B) HGC and (C) HEK and SH-SY5Y cell lines. Western blots were performed with three rabbit anti-EYA1 antibodies, the images shown are representative images using the Abcam primary antibody. EYA1 has a predicted molecular weight of 64kDa. No band could be detected for EYA1 at this size in all seven cell lines (n=1).

A band at 100kDa was observed consistently in the AGS protein samples (Figure 2.7A&C and Figure 2.8). Since there have been no reports of EYA1 dimerising, it is likely that this band is a result of non-specific binding of the primary antibody.

In an attempt to see if a band could be detected at the right size, 50 and 100µg of whole AGS and SH-SY5Y protein lysates were also loaded for western blot analysis (Figure 2.8). A weak band can be observed at ~65kDa for both cell lines at both amounts of protein loaded. These EYA1 western blotting experiments were only performed once and will therefore need to be repeated to ensure the validity of these results.

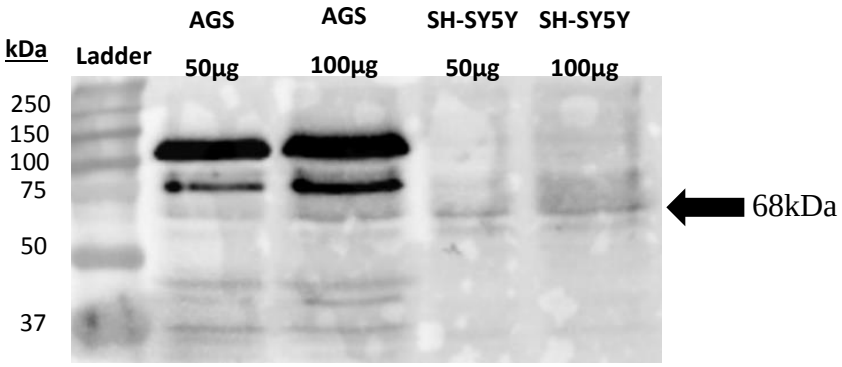

Figure 2.8 Endogenous EYA1 protein expression in AGS and SH-SY5Y cell lines. Both 50 and 100µg of whole protein lysates from AGS and SH-SY5Y cells were loaded for western blot analysis to try to detect endogenous EYA1 protein expression (n=1).

2.4 **Discussion**

Analysis of aspirin-induced apoptosis and necrosis/secondary necrosis using annexin-V/PI FACS showed that 20mM aspirin treatment over 48h to AGS cells provided the greatest proportion of apoptosis (Figure 2.5B). This finding is reflected in the caspase-3 cleavage western blots where pro-caspase-3 had been completely processed using 25mM aspirin (Figure 2.4) and caspase-9 and PARP cleavage was detected from aspirin concentrations >20mM (Figure 2.6) after 48h exposure. Previous reports using AGS cells have also shown that PARP, caspase-3 and -9 cleavage occur at aspirin exposures >12h[395,396].

The FACS experiment also suggests a shift in the mode of death from mostly apoptotic to mostly late-apoptotic/necrotic above 20mM aspirin at 48h exposure (Figure 2.5B). This could be because at such high concentrations of aspirin, the cell is damaged more

by the external damage caused by the increasingly acidic growth conditions rather than intracellular injury.

As can be seen from the MTT (Figure 2.2 and Figure 2.3), western blot (Figure 2.4 and Figure 2.6) and FACS (Figure 2.5) experiments, aspirin causes time- and dose-dependent cytotoxicity in AGS cells. This is in accordance with previous findings with several cell lines including lymphocytes[416,439], colon[451,452], endometrial[440], breast[453] and gastric epithelial cells[249,395]. Aspirin has, however, also been shown to have a cytoprotective effect on neuronal cells by inhibiting NF-κB-mediated inflammatory pathway[417].

Benzbromarone exacerbated AGS cell death when co-incubated with 40mM aspirin at 24h and 5-10mM aspirin over 48h. This finding could be explained by the hypothesis that in the event of DNA damage, if EYA1 does not dephosphorylate γ-H2AX, an adaptor protein Fe65 binds to Y142 and recruits pro-apoptotic factors such as c-Jun N-terminal kinase 1 (JNK1)[360]. These findings could therefore be supported by determining the role of JNK1 in AGS cells co-treated with aspirin and benzbromarone.

Interestingly, JNK-activation is associated with indomethacin-induced ER stress and gastric mucosal cell death[437]. Aspirin has also shown to cause JNK activation, but JNK inhibitors did not rescue aspirin-induced apoptosis in lymphocytes[439]. In the B16 and SK-26 human melanoma cell lines, aspirin-induced JNK activation suppressed proliferation[454].

The MTT assay is a fast, high-throughput method for assessing cell viability by measuring mitochondrial productivity. Decreased mitochondrial output however, does not unequivocally indicate impaired viability and can instead be due to either cell cycle arrest or inhibited mitochondrial respiration[455]. It is important to note when interpreting these results that high aspirin concentrations have been known since the late 1930s to cause uncoupling of oxidative phosphorylation[456-458]. It has also been long established that benzbromarone induces mitochondrial uncoupling, decreased ATP turnover and maximal respiration in rodent mitochondria[459,460]. This finding was later replicated in the human liver cell line, HepG2 cells[450].

There are a plethora of assays to measure cell death, each with advantages and disadvantages. For a rapid and simple method of obtaining quantitative data on drug-

induced cell death such as the MTT assay, flow cytometry methods can be used to detect PS externalisation and caspase activation[455].

Another consideration is that benzbromarone has only been reported to inhibit EYA2 and EYA3 homologs[371,448]. It would first be necessary to confirm that benzbromarone inhibits EYA1-mediated dephosphylation of γ-H2AX phosphotyrosine (Y142) before suggesting an association between EYA1-function and aspirin-induced AGS toxicity.

It was therefore necessary to ascertain the basal level of EYA1 protein expression. However, after using three human polyclonal EYA1 antibodies each with unique immunogens on seven different cell lines (five distinct cell types), no endogenous EYA1 could be detected by immunoblotting (Figure 2.7). A weak band was visible at 64kDa after loading 2.5 and 5 times the amount of protein from AGS and SH-SY5Y cell lysates (Figure 2.8), however several non-specific bands were also detected. Given that multiple EYA1 antibodies with distinct immunogens were used and two other reports of successful EYA1 protein detect have been reported using the Abcam antibody (ab85009)[372,373], it is likely that the lack of detection of EYA1 in these cell lines is due to low basal expression. Though there have been no reports of EYA1 protein expression in SH-SY5Y cells, RNA-seq data available from the Human Protein Atlas database[461] suggests that SH-SY5Y cells have a relatively high RNA expression of *EYA1* (see Chapter 5, Figure 5.1D).

A study by Nikpour *et. al*. revealed that EYA1 gene expression is significantly decreased in human gastric tumour tissue[375]. This could explain the low expression of EYA1 in the AGS and HGC-27 cell lines (Figure 2.7A&B), given that they are both derived from gastric adenocarcinomas. There are conflicting reports of endogenous EYA1 protein expression in HEK293 cells; one group was unable to detect expression in HEK293 cells[462], whereas there are reports of endogenous expression in HEK293[387] and HEK293TN[463] cells. Endogenous human EYA1 protein expression has also been reported in the colon cancer cell lines, HCT116[388], LoVo, HT29, SW620, SW480 and CaCO2[372] and breast cancer cell lines BT549[387], MDA-MB-231[373], BT-474[373] and SKBR3[385].

Phosphorylation and dephosphorylation of proteins by kinase and phosphate enzymes regulate various cellular processes including metabolism, proliferation, apoptosis, subcellular trafficking and inflammation[464]. Reversible protein phosphorylation

usually occurs at serine, threonine and tyrosine residues in eukaryotic cells, causing a switch in activity[465,466] or subcellular localisation[467,468]. Phosphorylation can also promote or prevent the addition/removal of other post-translational modifications[469,470]. Small ubiquitin-related modifier 1 (SUMO1) mediates the hyper-SUMOylation of EYA1[471]. PI3K/Akt signalling, which is commonly hyper-activated in cancer, enhances phosphorylation of EYA1 residue S298, increasing the transcriptional activity[387] and decreasing the proteasomal degradation[388] of EYA1 by inhibiting its SUMOylation. The inhibition of proteasomal degradation and analysis of EYA1 phosphorylation and ubiquination states may reveal why endogenous expression is low in these cell lines.

The outcomes of this chapter are that optimal times and concentrations have been identified to induce gastric epithelial cell apoptosis with aspirin. It was also determined that endogenous EYA1 protein is expressed at a low abundance in AGS cells. Overexpression of EYA1, rather than chemical inhibition, would therefore provide a better model to study its effect on aspirin-mediated gastric epithelial apoptosis.

Chapter 3

Transient and stable expression of EYA1

CONTENTS

3.1 **Introduction**

Transfection is a commonly used method of studying gene function, their regulation and the functions of their products and represents a powerful analytical tool in understanding disease. Chemical transfection is the most widely used method in contemporary research and generally involves positively charged chemicals (e.g. lipofectamine) forming complexes with negatively charged nucleic acids[472].

Various studies have used lipofectamine to perform transient and stable transfections in AGS cells[473,474]. Puromycin is a potent antibiotic, allowing for a fast selection process that can allow puromycin-resistant colonies to form within a week[475]. Puromycin has been shown to be effective against AGS cells at concentrations of 1-5μg/mL following 2-5 days of selection[476-480].

Studies on murine *Eya1* transfection in HEK293[462] (human) and COS-7[367,481] (monkey) cells have shown that Eya1 protein localises entirely in cytoplasm but can be translocated to the nucleus by co-transfecting with *Six1/2*. It has also been demonstrated that Six proteins interact with Eya1 via the Eya domain and that certain mutations, including those that cause BOR syndrome, prevent Six-Eya1 interaction and nuclear translocation[367]. Six proteins not only facilitate nuclear translocation of Eya1 but also prevent proteasomal degradation, an event regulated by the APC/C-Cdh1- mediated ubiquitin-proteasome pathway[482].

A study including a transfection with human EYA1 cDNA in HEK293TN cells showed that expression of the human EYA1 protein was present in both the cytoplasm and nucleus but was exclusively nuclear upon co-expression with SIX1[463].

The aims of this chapter were first to (i) determine the transfection efficiency of AGS cells using chemical (lipofectamine) transfection; to (ii) produce an AGS cell line that could stably express EYA1-GFP; and to (iii) confirm that full-length EYA1 protein was still present in the stable cell line after several passages. Mass spectrometry was used as a highly sensitive method to try to detect endogenous EYA1 in the native AGS cells line.

3.2 **Materials and methods**

3.2.1 **Materials**

Unless stated otherwise, reagents were purchased from Sigma-Aldrich Co., Dorset, UK. EYA1 and pCMV6-XL5 vectors were purchased from Origene, Rockville, USA. pCMV(CAT)T7-SB100 (Addgene plasmid # 34879; submitted by Zsuzsanna Izsvak[483]) was purchased from Addgene, Teddington, UK. One Shot® TOP10 Chemically Competent E. coli, LB Agar, UltraPure Agarose, GeneJET Plasmid Maxiprep Kit, 1 Kb Plus DNA Ladder, Lipofectamine 2000 and LTX Transfection Reagents, PLUS Reagent, PBS, TRIzol Reagent, High-Capacity cDNA Reverse Transcription Kit, Tween-20, Alexa Fluor 488 goat anti-rabbit secondary antibody, Alexa Fluor 568 Phalloidin, Prolong Gold Antifade Mountant, 10X BlueJuice Gel Loading Buffer, Midori Green Advance DNA stain, 1 Kb Plus DNA Ladder, MAX Efficiency™ DH5α™ Competent Cells, PureLink Genomic DNA Kit, EF-1α forward primer, Pierce BCA Protein Assay Kit were purchased from Thermo Fisher Scientific. Normal Rabbit and Mouse Serum (Sterile), Anti-EYA1 antibody (ab85009), Anti-beta Actin Antibody (ab8227) and Goat Anti-Rabbit IgG H&L (HRP) (ab97051) were purchased from Abcam. Clarity™ Western ECL Substrate was purchased from Bio-Rad, Hertfordshire, UK. Wizard® SV Gel and PCR Clean-Up System was purchased from Promega UK, Southampton, UK. KpnI and XhoI restriction enzymes, NEBuffer 2.1, T4 DNA Ligase, Q5 High-Fidelity DNA Polymerase, Deoxynucleotide (dNTP) Solution Mix and OneTaq DNA polymerase were purchased from New England BioLabs, Ipswich, UK. QIAprep Spin Miniprep Kit, RNeasy Mini Kit, QIAshredder were purchased from Qiagen, CA, USA.

3.2.2 **Cell lines and culture conditions**

Since EYA1 protein showed very low expression (see section 2.3.3) in AGS cells, two further gastric epithelial cell lines (Hs 746T (ATCC® HTB135™)[408] and HGC-27[407]) were purchased on the basis of being the two human gastric cell lines with the highest *EYA1* gene expression, according to the web-based systems biology software NextBio[484] (http://nextbio.com).

AGS, HGC-27 and HEK

AGS, HGC-27 and HEK cell were cultured as described in section 2.2.2.

Hs746T

The Hs746T (ATCC® HTB135™) cell line was purchased from ATCC and cultured in Dulbecco's Modified Eagle Medium (DMEM; 4500 mg/L glucose, +L-glutamine, +sodium bicarbonate) containing 10% foetal bovine serum under standard conditions. Cells were cryogenically preserved as described in section 2.2.2.

3.2.3 **Transient transfection with EYA1-pCMV6-XL5**

Plasmid transformation and extraction

The (untagged)-Human eyes absent homolog 1 (EYA1; transcript variant 3, NM_000503.3) and the pCMV6-XL5 cloning vectors were reconstituted in 100µL dH_20 to 100µg/mL.

Separate One Shot E. coli vials were transformed with 100ng of each vector, incubated on ice for 30 min and heat-shocked at 42°C for 30 seconds. The vials were placed on ice for 2 min before adding 350µL S.O.C. (Super Optimal broth with Catabolite repression) medium to each vial. The vials were shaken horizontally at 37°C for 1h at 225rpm. After the incubation, 20, 50, 100 and 200µL of the transformed bacteria were spread onto pre-warmed agar plates containing 100µg/mL ampicillin and incubated inverted at 37°C overnight. One well isolated colony from both the EYA1 and pCMV6-XL5 transformed plates were cultured in 10mL selective LB Broth containing 100µg/mL ampicillin and left on a shaker at 300rpm, 37°C for 8hr. The starter culture was diluted 1mL culture in 500mL selective LB Broth and grown for a further 12-16h (at 300rpm & 37°C) until reaching an optical density between 2-3 at 600nm.

Cultures were separated in 50mL tubes and centrifuged at 4500g for 10 min to obtain pellets for plasmid extraction using a GeneJET plasmid Maxiprep extraction kit. Supernatant was discarded, and cells were resuspended in 6mL resuspension solution (containing 4% RNase A solution) divided amongst the tubes used to spin down the culture. The separate resuspended EYA1/pCMV6-XL5 transformed cells were collected in a single falcon tube each. Next, 6mL of lysis solution was added per tube, inverted 6 times and incubated for 3 min at room temperature. After the incubation, 6mL of neutralization solution was added to each tube and inverted 8 times, followed by the addition of 0.8mL/tube of endotoxin binding reagent. The tubes were inverted eight more times, left at room temperature for a further 5 min and 6mL of 96% ethanol

was added per tube. Tubes were inverted 6 times and centrifuged for 40 min at 4500g to pellet cell debris and chromosomal DNA. Supernatants were transferred to a new 50mL tube, a further 6mL of 96% ethanol was added to each tube and tubes were inverted 6 times. The lysates were placed in spin columns and centrifuged for 3 min and 3000g to capture the DNA in the silica membrane. The flow-through was discarded between each spin until all the samples had passed through the purification columns. The membrane was washed with 8mL wash solution I, centrifuged at 3000g for 2 min and the flow-through was discarded. The membrane was washed twice with 8mL of wash solution II, centrifuged at 3000g for 2 min and the flow-through was discarded. Both tubes were centrifuged for a further 5 min at 3000g to removed residual wash solution. The columns were placed in new 50mL tubes, 0.7mL of elution buffer was added to each tube and incubated for 2 minutes at room temperature. The plasmids were collected in 1.5mL microcentrifuge tubes and the elution step was repeated with an extra 0.5mL elution buffer to increase the plasmid yield by 20-30%.

To confirm successful transformation and isolation of the plasmid, samples (and elution buffer blank) were diluted to 100ng/µL in nuclease-free water and ran through a 1% agarose gel (1g of agarose in 100mL 1x Tris/Borate/EDTA buffer) containing 0.06% ethidium bromide at 100V for 1.5h. The images were collected using the Digigenius gel documentation system (Syngene, Cambridge, UK). Supercoiled pCMV6-XL5 and EYA1 plasmids were identified at around 4500 and 6500bp, respectively, when compared against a 1kb DNA ladder.

Polymerase Chain Reaction

Optimal transfection conditions were determined by both end-point polymerase chain reaction (PCR) and ICF. AGS cells were plated at 100,000 cells/well on a 24 well plate, left overnight at 37°C/5%CO_2 and transfected over 24h with 500ng EYA1/pCMV6-XL5 plasmid and 1, 1.5, 2 or 2.5µL lipofectamine 2000 per well. Cells were lysed using 250µL/well TRIzol reagent for gene expression analysis. RNA was isolated from the TRIzol lysates by phase separation in chloroform, alcohol precipitation and wash in IPA and 75% ethanol, and finally, rehydration in ddH_2O. Samples were reverse transcribed (25°C 10 min, 37°C 120 min & 85°C 5 min) in semi-skirted 96-well PCR plates using the High-Capacity cDNA Reverse Transcription Kit as shown in Table 3.1.

Component	Volume/ Reaction (µL)
10X Reverse Transcription (RT) Buffer	2
25X dNTP Mix (100mM)	0.8
10X RT Random Primers	2
MultiScribe™ Reverse Transcriptase	1
Nuclease-free H_2O	9.2
RNA Sample	5
Total per Reaction	**20**

Table 3.1 Reagents used to reverse transcribe RNA collected from AGS cells transfected with EYA1-pCMV6-XL5 with a range of Lipofectamine 2000 concentrations over 24, 48 and 72h.

All cDNA samples were normalised to 100ng/µL in ddH_2O. Samples were amplified by PCR to measure EYA1 gene expression using the reagents shown in Table 3.2.

Forward and reverse primers were designed using Primer-BLAST[485] for the EYA1 accession number NM_000503[486] (F: 5'-AGGTTCAG-CAATTGGGAGCA-3' and R: 5'-GGGTATGGTCTGTTGGAAGGG-3'). Amplified cDNA samples were analysed by running through 4% agrose gel (containing 0.06% ethidium bromide) alongside a 100bp ladder and PCR master mix blank for 2.5h. EYA1 transcripts were identified at roughly 90bp.

Immunofluorescent and western blot detection of EYA1

For immunofluorescence analysis of transfection, glass slides were placed in each well of a 12 well plate and coated for 30 min with 500µL/well of a 0.5% gelatine solution. Excess gelatine was aspirated and each well was washed with 1mL PBS. AGS cells were plated at 150,000 cells/well, left overnight and transfected over 24hr with 1µg EYA1/pCMV6-XL5 plasmid and 2, 3, 4 or 5µL lipofectamine 2000 per well.

Cells were washed with PBS and fixed in 500µL of 2% formaldehyde for 15 min at room temperature. From this point on, cells were washed twice with 500µL PBS between each step. Cells were quenched in 500µL of 50mM ammonium chloride for 10 min to reduce autofluorescence caused by aldehyde fixation.

Cells were permeabilised in 1mL of PBS containing 0.2% Triton X-100 for 10 min at room temper-ature and covered with a block solution containing 0.1% Tween-20, 1% Bovine Serum Albumin (BSA) and 5% rabbit serum in PBS at 500µL/well for 1h.

Component	Volume/Reaction (µL)
ddH_2O	9.5
PCR Buffer	3
$MgCl_2$	1.5
dNTP	0.5
Forward Primers	1µL of EYA1 or pCMV6-XL5 primers
Reverse Primers	1µL of EYA1 or pCMV6-XL5 primers
Taq Polymerase	0.5
cDNA Sample	1
Total per Reaction	**20**

Table 3.2 Reagents used to amplify EYA1 cDNA collected from AGS cells transfected with EYA1-pCMV6-XL5 with a range of Lipofectamine 2000 concentrations over 24, 48 and 72h.

From this point on, all solutions were added at 200µL/well. Rabbit anti-EYA1 primary antibody solution (1 in 140 dilution into blocking solution) was added to each well for 30 min. Blocking solution containing both Alexa Fluor 488 goat anti-rabbit secondary antibody (1 in 1000) and Alexa Fluor 568 Phalloidin (1 in 40) was added for 30 min in the dark. Finally, Hoechst solution (1 in 5000 into blocking solution) was added to each well for 10 min in the dark and cover slips were mounted onto glass slides using mounting medium. All cover slips were analysed using a Zeiss Axio Observer Z.1 microscope (Zeiss, Oberkochen, Germany) with a 40 times oil immersion lens and 349, 488 and 568nm filters.

For western blot analysis of transfection, AGS cells were plated at 450,000 cells/well on a 6 well plate, incubated overnight and transfected over 24h with 2500ng EYA1/pCMV6-XL5 plasmid and 10µL lipofectamine 2000 per well. At the end of the 24h time point, cells were lysed using 120µL/well RIPA buffer with 1% protease inhibitor cocktail and protein concentrations were determined using a BCA assay. Next, 20µg of each sample was reduced, heat shocked at 85°C, cooled on ice and run through 10% polyacrylamide gels. Following gel electrophoresis, the proteins were transferred from the gels to nitrocellulose membranes and blocked in a 10% skimmed milk solution for 30 min at 4°C. Membranes were washed with TBS-T and incubated with either Rabbit Anti-EYA1 primary antibody overnight or Rabbit Anti-β-Actin primary antibody for 1h at 4°C (EYA1: 1 in 500 and β-Actin: 1 in 5000, both in 2% milk solution). Membranes were washed and incubated with Goat anti-Rabbit IgG HRP secondary antibody for 1h at 4°C. Membranes were washed again and covered

in ECL reagent for 5 min. Protein bands were detected using a ChemiDoc Imaging System (Bio-Rad).

3.2.4 **Subcloning/Cloning and sequencing EYA1 plasmids**

Subcloning EYA1 from pCMV6-XL5 vector to pEGFP-C1 vector

The *EYA1* insert from the pCMV6-XL5 vector was subcloned into a pre-cut pEGFP-C1 vector using the following method. Initially, a PCR (1x [2 min 94°C], 35x [30sec 94°C, 30sec 58°C & 90sec 72°C], 1x [2 min 72°C]) was performed to amplify the *EYA1* insert from the pCMV6-XL5 plasmid (Table 3.3). The XhoI-forward, 5'-CTCCTCCTCGAGCTATGGAAATGAGGATCTAACCAG-3', and KpnI-reverse, 5'-GGTGGTGGTACCTTACAGGTACTCCAGTTCCAAGG-3' primers were designed to have a melting temperature (T_m) between 66-68°C and extra nucleotides added before the start codon to: include the restriction site, keep the ORF in frame and a 5'-overhang to facilitate restriction enzyme binding.

The amplified *EYA1* insert was purified from the reaction mix by adding 5µL of BlueJuice Gel Loading Buffer (10X) to the samples and running the samples through a 1% agrose gel (containing 0.005% Midori green) alongside a 1kb DNA ladder. The amplified band was highlighted and cut out of the gel using a UV tray and the *EYA1* insert was eluted from the gel using a DNA-gel extraction kit.

The cut gel was weighed in a 1.5mL microcentrifuge tube, 10µL of membrane binding solution was added per 10mg of gel and heated at 70°C until fully dissolved. The gel solution was placed in a Minicolumn assembly, left at room temperature for 1 minute and centrifuged at 16,000g for 1 min. The flowthrough was discarded and the membrane was washed twice with 700 and then 500µL of Membrane Wash Solution by centrifuging at 16,000g for 1 min and 5 min, respectively. To remove excess wash solution, the assembly was centrifuged a further 1 min and the filter column was placed into a new collection tube.

The *EYA1* insert was eluted by adding 30µL nuclease free water to the Minicolumn, incubated at room temperature for 1 min and centrifuged at 16,000g for 1 min. The concentration and purity of the eluted sample was determined using a Nanodrop 8000 spectro-photometer (Thermo Fisher).

Component	Volume/ Reaction (µL)
ddH_2O	32.75
5x Q5 Reaction Buffer	10
Deoxynucleotide (dNTP) Solution Mix	1.25
XhoI-forward primer	2.5
KpnI-reverse primer	2.5
Q5 High-Fidelity DNA Polymerase	0.5
EYA1-pCMV6-XL5 plasmid	0.5
Total per Reaction	**50**

Table 3.3 Reagents used to amplify EYA1 insert from EYA1-pCMV6-XL5 plasmid to obtain full length EYA1 DNA.

The restriction sites of the eluted KpnI/XhoI EYA1 sample were cut by adding 30µL of sample with 1.5µL of both KpnI and XhoI restriction enzymes in 4µL 10X NEBuffer 2.1 and 3µL nuclease-free water and incubating at 37°C overnight. The digested DNA insert was gel purified as previously described and ligated into a pre-cut pEGFP-C1 vector and a ligase control (Table 3.4) over 30 min at room temperature.

Component	Volume/Reaction (µL)	
Pre-cut vector	1	1
Digested EYA1 insert	-	7.5
Ligase enzyme	1.5	1.5
NEBuffer 2.1	10	10
Nuclease free water	7.5	-
Total per Reaction	**20**	**20**

Table 3.4 Reagents used to ligate full-length EYA1 insert into pEGFP-C1 plasmid.

Chemically competent DH5α E. Coli were transformed with 5µL and 10µL of the EYA1-pEGFP-C1 plasmid and grown on kanamycin agar plates made with agar containing 50µg/mL kanamycin. Colonies were grown in LB Broth starter culture containing 50µg/mL kanamycin over 8 hours. Successfully transformed cultures were identified by extracting plasmid from 2mL of each starter culture using a DNA Miniprep Kit and amplifying the full length EYA1 insert using end point PCR (15 cycles; 1x [2 min 94°C], 15x [30 sec 94°C, 30 sec 58°C & 2 min 72°C], 1x [3 min 72°C]).

The starter culture was diluted 1 in 500 into 400mL kanamycin-containing LB Broth and left to grow overnight (16h). A glycerol stock was also made from the same starter culture chosen to make the overnight culture by adding 500µL of the culture to 500µL

of 30% glycerol and freezing the cells at -20°C. The EYA1-pEGFP-C1 plasmid was extracted from the overnight culture by maxi prep and the concentration and purity of the sample was determined by Nanodrop.

Cloning of EYA1 cDNA from AGS cells into pEGFP-C1

AGS cells were seeded at 150,000 cells/well in 12-well plates with 1mL of DMEM per well and incubated until 70% confluent. RNA from the cells was collected using the QIAshredder lysis and RNeasy RNA purification kits.

Media was aspirated from the wells and cells were lysed by adding 350µL RLT buffer to each well. Lysates were homogenised by centrifuging each sample through QIAshredder spin column assemblies at 16,000g for 2 min. An equal volume of 70% ethanol was added to each sample and mixed thoroughly by pipetting. Samples were added to RNeasy spin column assemblies and centrifuged for 30s at 8000g. The flow-through was discarded; 700µL Buffer RW1 was added to each spin column and samples centrifuged for a further 30s at 8000g. Two more washes were performed (30s and 2 min) using 500µL Buffer RPE, discarding the flow-through between each wash. Spin columns were placed in new 2mL collection tubes and centrifuged at 16,000g for 1 min. Spin columns were placed in 1.5mL microcentrifuge tubes; 40µL RNase-free water was added to each spin column and centrifuged at 8000g for 1 min to elute the RNA. RNA concentrations and purities were determined using Nanodrop.

Eluted RNA from AGS cells was reverse-transcribed to cDNA. In a PCR tube, 2µg RNA was mix with 10µL RT buffer, 1µL 20X reverse transcriptase and made up to 20µL with water. The tube was sealed and placed in a thermocycler under the following settings: 37°C for 60 min, 95°C for 5 min and stored at 4°C until ready to use. The cDNA concentrations were determined by Nanodrop and samples were diluted 1 in 20. A PCR (1x [2 min 94°C], 35x [30 sec 94°C, 30 sec 58°C & 2 min 72°C], 1x [3 min 72°C]) was performed to amplify the EYA1 cDNA using the reagents outlined in Table 3.5 and the XhoI-forward and KpnI-reverse primers used previously.

Component	Volume/Reaction (µL)
ddH_2O	29.25
5x Q5 Reaction Buffer	10
dNTP Solution Mix	1.25
Forward Primers	2.5
Reverse Primers	2.5
Q5 High-Fidelity DNA Polymerase	0.5
EYA1 cDNA	4
Total per Reaction	50

Table 3.5 Reagents used to amplify full-length EYA1 cDNA from AGS cDNA.

The amplified EYA1 cDNA was extracted from the PCR reaction mix by gel purification. The restriction sites of the eluted EYA1 cDNA were digested with KpnI and XhoI restriction enzymes overnight using the same reaction as shown previously. The reaction was gel purified once more and the cut EYA1 cDNA was ligated into a pre-cut pEGFP-C1 empty vector. DH5α E. Coli were transformed with 5µL and 10µL of the new EYA1-AGS-pEGFP-C1 plasmid and grown on kanamycin agar plates. Selective colonies were grown in kanamycin-LB broth, successfully transformed cultures were confirmed by end-point PCR and glycerol stocks were made. A large culture was grown overnight to harvest the EYA1-AGS-pEGFP-C1 plasmid by Maxiprep and the concentration of the eluted plasmid was determined by Nanodrop.

Correcting the EYA1-GFP plasmid sequence using overlapping PCR

To insert a single cytosine base into the EYA1 clone, the two PCR reactions were performed simultaneously using the original EYA1-pEGFP-C1 plasmid (Figure 3.1). One reaction using the XhoI EYA1 forward primer and the following reverse primer, 5'-GGCGGTTCTTGAAGCTGGTAAGTGGCATTGGTG-3' and a separate reaction using the KpnI reverse primer and the following forward primer, 5'-CACCAATGCCACTTACCAGCTTCAAGAACCGCC-3'. Samples were run through a 1% agarose gel and the 785bp upstream and 1027bp downstream fragments were gel purified.

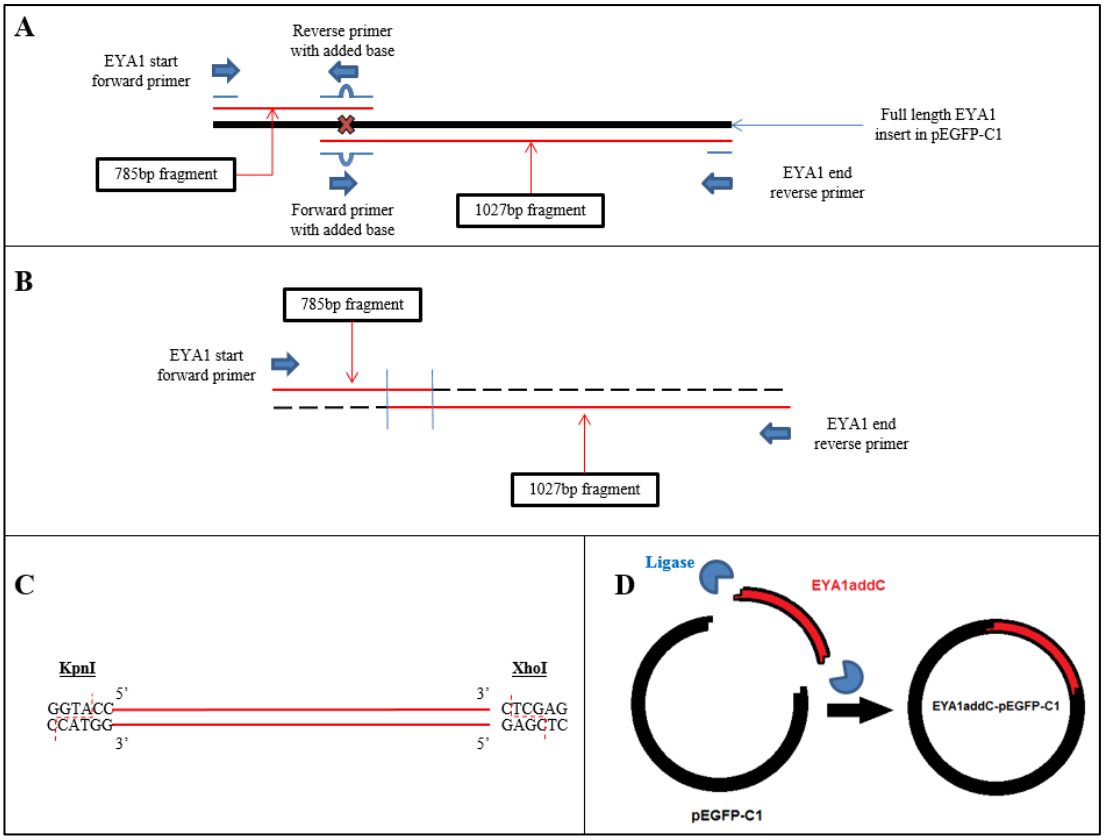

Figure 3.1 Introducing the missing cytosine into EYA1 cDNA using overlapping PCR and cloning of EYA1(addC) into pEGFP-C1. EYA1 cDNA used as a template for two separate PCR reactions. Reaction 1 contained a KpnI-EYA1 forward primer and a reverse primer, which bound over the site of the deletion that contained the missing cytosine. Reaction 2 contained a forward primer also containing the missing cytosine and an XhoI-EYA1 reverse primer (A). The second PCR combined the 785 and 1027bp fragments produced in the first set of PCR reactions. The overlapping region on each fragment acted as a 'primer' to extend each fragment into full-length EYA1 cDNA, containing the missing cytosine (B). The full-length EYA1 cDNA was restriction digested (C) and ligated into KpnI/XhoI cut pEGFP-C1 plasmid (D).

The upstream and downstream fragments were mixed 3:2 respectively and PCR with only 5 cycles was performed without adding primers; 1.25µL dNTP, 5µL of the fragment mixture, 10µL of Q5 reaction buffer, 0.5µL Q5 polymerase and 28.25µL nuclease-free water. The overlapping sequences on each fragment were used as a 'primers' to extend each fragment to full length EYA1.

A last PCR was performed by taking 45µL of the previous reaction, adding 2.5µL of the XhoI EYA1 forward primer and KpnI reverse primer and 0.5µL Q5 polymerase and running another 30 cycles. The amplified EYA1 insert was gel purified and digested overnight with XhoI and KpnI. The digested insert was gel purified, ligated into a pre-cut empty pEGFP-C1 and transformed into DH5α E. Coli to the point where

the new plasmid, EYA1(addC)-pEGFP-C1, could be extracted by Maxiprep. Glycerol stocks of the EYA1(addC)-pEGFP-C1 transformed bacteria were made as previously described.

Subcloning EYA1(addC)-GFP from pEGFP-C1 vector into pSBi-puro vector

The EYA1(addC)-GFP insert was amplified from the pEGFP-C1 plasmid using the reagents/thermocycler settings as outlined in Table 3.3, except for using the following primers: NcoI-forward, 5'-ACCGGTACCGGTACCATGGTGAGCAAGGGCGA-3' and XbaI-reverse, 5'-TGCTCTAGATTACAGGTACTCCAGTTCCAAGGCAT-G-3'. The amplified insert was gel purified and an overnight digestion reaction was performed at 37°C using the reagents described in Table 3.6.

Component	Reaction 1	Reaction 2
pSBi-puro vector	1µg	-
EYA1(addC)-GPF insert	-	500ng
NcoI restriction enzyme	1.5µL	1.5µL
XbaI restriction enzyme	1.5µL	1.5µL
10X CutSmart buffer	8µL	8µL
Nuclease free water	60.66µL	41µL
Total per Reaction	**80µL**	**80µL**

Table 3.6 Reagents used to digest EYA1(addC)-GFP insert and pSBi-puro vector using restriction enzymes NcoI and XbaI.

Samples were gel purified to remove reactants from the digestion reaction. The digested EYA1-(addC)-GFP insert and pSBi-puro vector were ligated together, as well as pSBi-puro alone, over 30 min at room temperature using the reagents outlined in Table 3.7.

One Shot E. Coli were transformed with 5µL of each reaction mix, as described in section 3.2.3, plated on agar plates containing 100µg/µL ampicillin and incubated overnight.

To ensure successful transformation, samples from isolated colonies were added to tubes containing 5µL OneTaq DNA polymerase, 1µL EF-1α forward (5'- TCAAGC-CTCAGACAGTGGTTC-3') and EYA1 reverse (5'-CTGCTGTGGGATCTGTAA-CTGC-3') primers and 4µL distilled water.

Table 3.7 Reagents used to ligate NcoI and XbaI cut EYA1(addC)-GFP insert into pSBi-puro vector

Component	Reaction 1	Reaction 2	Reaction 3	Reaction 4
Cut pSBi-puro vector	50ng	50ng	50ng	50ng
Cut EYA1(addC)-GFP insert	-	50ng	100ng	150ng
Ligase enzyme	1.5µL	1.5µL	1.5µL	1.5µL
10X CutSmart buffer	2µL	2µL	2µL	2µL
Nuclease free water	15.5µL	10.5µL	5.5µL	0.5µL
Total per Reaction	**20µL**	**20µL**	**20µL**	**20µL**

Samples were ran through a 35-cycle PCR reaction (1x [2 min 94°C], 35x [30sec 94°C, 30sec 58°C & 1 min 72°C], 1x [3 min 72°C]) and run through a 1.5% agarose gel with a 100bp ladder to detect which samples contained the 1648bp EYA1-GFP amplicon.

Successfully transformed colonies were grown, glycerol stocks were made and pSBi-puro and EYA1(addC)-GFP-pSBi-puro plasmids were extracted from bacterial cultures using a plasmid Maxiprep extraction kit (see section 3.2.3. for method).

Plasmid sequencing

All DNA sequencing was performed commercially by Sanger Sequencing (Source Bioscience, Rochdale, UK) and data was analysed using Chromas trace viewer 2.6 (Technelysium Pty Ltd, South Brisbane, Australia).

The EYA1-pCMV6-XL5, EYA1-pEGFP-C1, EYA1-AGS-pEGFP-C1 and EYA1(addC)-pEGFP-C1 plasmids were diluted to 100ng/µL and sent for sequencing using the following primers: pCMV forward primer- 5'-GAGCTCGTTTAGT-GAACCGTC-3', pCMV reverse primer- 5'-CAAGGCCAGGAGAGGCACTG-3', pEGFP-C forward primer- 5'-CATGGTCCTGCTGGAGTTCGTG -3' and pEGFP-C reverse primer- 5'-GTTCAGGGGGAGGTGTG-3'.

The full EYA1(addC)-GFP-pSBi-puro plasmid sequence was determined using the following forward; 5'-CCAGTCCGCCCTGAGCAAAG-3', 5'-CTCAGCTATGGC-ACAAGCTTC-3', 5'-GTGACCAAGTCCATATAGATGATG-3' and reverse; 5'-CGGTCACGAACTCCAGCAGG-3' primers.

HEK, HGC-27 and SH-SY5Y RNA lysates were collected, converted to cDNA and diluted to 10ng/µL. EYA1 cDNA was amplified from all samples, gel purified and sent for sequencing using the following primer, 5'-TGGATTGTCACAGTCTCA-3'. All cDNA sequencing reactions were compared against the EYA1 reference sequence NM_000503.3.

3.2.5 **Transient EYA1 expression (EYA1-pEGFP-C1, EYA1-AGS-pEGFP-C1, EYA1-pCMV6, pEGFP and EYA1(addC)-pEGFP-C1)**

To compare the levels and localisation of overexpressed EYA1/EYA1-GFP in cells transfected with the pCMV/pEGFP plasmids compared to the new EYA1(addC) plasmid, both western blot and ICF experiments were carried out.

Western blots

HEK cells were plated at 350,000 cells/well on a 6-well plate, left overnight and transfected over 48h with 2µg of either: EYA1-pEGFP-C1, EYA1-AGS-pEGFP-C1, EYA1-pCMV6, pEGFP or EYA1(addC)-pEGFP plasmid, 2µL PLUS reagent and 6µL lipofectamine LTX per well. Cells were lysed using 120µL/well RIPA buffer with 1% protease inhibitor cocktail and protein concentrations were determined using a BCA assay. Next, 20µg of each sample was run through three separate 7% polyacrylamide gels (2.8mL 30% polyacrylamide per 12mL mixture). The reason 7% gels were made, was because the N-terminal GFP attached to the EYA protein added an extra 27kDa to the protein size to make the total size around 91kDa. Protein in the gels were transferred to nitrocellulose membranes and blocked in skimmed milk.

Membranes were incubated for 1h at 4°C and each membrane was covered in a Rabbit Anti-EYA1 primary antibody from one of the following three different suppliers:

- Abcam, internal epitope- PYSYQMQGSSFTTSSGIYTGNNSLTNSSGFNS-SQQDYPSYPSFGQGQYAQ;
- Insight Bioscience and Sigma, C-terminal Epitope- ERIIQRFGRKVVYVVI-GDGVEEEQGAKKHAMPWRISSHSDLMALHHALE).

Abcam and Insight EYA1 antibodies were diluted 1 in 500 and Sigma antibody 1 in 1000 in 2% milk solutions and incubated on membranes overnight. Membranes were washed and incubated for 1h with Goat anti Rabbit Ig HRP secondary antibody at 4°C.

Membranes were covered in ECL reagent (Bio-Rad) for 5 min in the dark and protein bands detected using a ChemiDoc Imaging System.

ICF

HEK cells were seeded at 300,000 cells/well on gelatine-coated coverslips in a 12 well plate, transiently transfected with 1µg/well of pEGFP, EYA1-pEGFP or EYA1(addC)-pEGFP and 3µL/well Lipofectamine 2000 for 24h. Cells were fixed in 4% formaldehyde for 10 min, blocked in 2% BSA solution (1g in 50mL PBS) for 10 min and stained with Hoechst solution (diluted 1 in 5000 in PBS) for 5 min.

Coverslips were mounted on glass slides using 10µL Prolong Gold solution and analysed used a Zeiss microscope with a 40 times oil immersion lens and 349, 488 and 568nm filters. The Zen software was used to take representative photo-micrographic images of the coverslips. One image was taken for the pEGFP and EYA1-pEGFP transfected HEK293 cells and 4 images were taken of the EYA1(addC)-pEGFP transfected cells.

AGS, HGC-27 and Hs 746T cells were plated in duplicate at 150,000 cells/well on gelatine coated coverslips in a 12 well plate and transfected with 1µg of blank vector/EYA1(addC)-pEGFP, 1µL PLUS and 3µL Lipofectamine LTX. Cells were fixed 24h post-transfection in 2% formaldehyde, quenched in 50mM ammonium chloride and permeabilised in 0.2% Triton X-100. Cells were covered in block solution (PBS containing 0.1% Tween-20 and 1% BSA and 5% mouse serum) and incubated with mouse anti-EYA1 primary antibody solution (1 in 120 dilution into blocking solution). Alexa Fluor 568 goat anti-mouse secondary antibody solution and Hoechst were added to each well and cover slips were mounted onto glass slides using Prolong Gold Antifade Mountant. One representative image was taken of both the vector and EYA1(addC)-pEGFP transfected cells for each cell line, using a Zeiss Axio Observer Z.1 microscope with a 40 times oil immersion lens and 349, 488 and 568nm filters.

3.2.6 **Transient and stable EYA1(addC)-GFP-pSBi-puro transfections**

AGS cell were plated at 350,000 cells/well across a six-well plate and incubated overnight. To optimise the co-transfection, AGS cells were transfected with 2500ng/well of either pSBi-puro or EYA1(addC)-GFP-pSBi-puro, and increasing amounts of pCMV(CAT)T7-SB100[483] (0.25, 0.5 ad 1µg/per well) using the

lipofectamine LTX PLUS protocol. The pCMV(CAT)T7-SB100 (pCMV-SB100) plasmid is a mammalian vector containing a *Sleeping Beauty* (SB) transposon cassette. Transposons facilitate the cutting of inverted terminal repeats (ITRs) that flank the gene of interest (in this case EYA1(addC)-GFP) and transposition into the host (AGS) genome, thereby enhancing the integration of the gene of interest when trying to perform stable transfection[487]. Fluorescence images and protein lysates were taken 24h post transfection.

AGS cells were plated across another six-well plate and co-transfected with either pSBi-puro or EYA1(addC)-GFP-pSBi-puro and 0.25µg pCMV-SB100. After 48h, the untransfected, pSBi-puro and one well of the EYA1(addC)-GFP-pSBi-puro transfected AGS cells were treated with 0.25µg/mL puromycin. The remaining wells containing EYA1(addC)-GFP-pSBi-puro transfected AGS cells were treated with 25ng/mL, 0.5µg/mL and 1µg/mL puromycin. Puromycin selective media was replaced at the same concentrations every 24h, until only puromycin resistant AGS colonies were growing in the plates. Plates were checked using a fluorescence microscope to ensure only transfected cells were growing. Once cells had reached 70% confluence in the wells, the cells where trypsinized and grown in T25 and then T75 culture flasks. Transfected cells were kept in puromycin selective media for 2 weeks to ensure stable expression. AGS cells with stable EYA1 expression (termed AGS-EYA1) were cryopreserved as described in section 2.2.2.

3.2.7 Proteomic analysis of endogenous and ectopically expressed EYA1 protein in AGS and AGS-EYA1 cells

Whilst subculturing AGS and AGS-EYA1 cells, 500,000 cells were placed in 1.5mL eppendorf tubes, centrifuged at 500g for 5 min, washed with HBSS, re-spun and lysed in 120µL RIPA buffer containing 1% protease inhibitor cocktail. Sample concentrations were determined using a BCA assay.

Samples were electrophoresed on a 12% SDS-PAGE gel and the protein bands were visualised by staining with Coomassie Blue. A series of bands across the entire mass range were excised from the gel, de-stained and dried[488]. The samples were rehydrated in 10 ng/µl trypsin solution and incubated at 37°C overnight. The peptides were extracted[489] and dried in a SpeedVac, followed by resuspension in 5-10µl 0.1% formic acid (FA) for liquid chromatography–mass spectrometry (LC-MS/MS) analysis.

Samples were delivered into a Triple TOF 6600 mass spectrometer (SCIEX, Warrington, UK) by automated in-line reversed phase liquid chromatography (LC), using an Eksigent NanoLC 415 System equipped with trap (nanoACQUITY Symmetry C18 trap column, 100Å, 5 µm, 180 µm x 20 mm; Waters, Elstree, UK) and analytical column (nanoACQUITY BEH C18 column, 300Å, 1.7 µm, 75 µm X 250 mm; Waters). A NanoSpray III source was fitted with a 10µm inner diameter PicoTip emitter (New Objective, Basingstoke, UK). Samples were loaded in 0.1% formic acid onto the trap, which was washed with 2% acetonitrile (ACN)/0.1% FA for 10 mins at 2µL/min before switching in-line with the analytical column. A gradient of 2-50 % (v/v) ACN, 0.1 % (v/v) FA over 90 min was applied to the column at a flow rate of 300nL/min. Spectra were acquired automatically in positive ion mode using information-dependent acquisition powered by Analyst TF 1.7 software (SCIEX), using mass ranges of 400-2000 atomic mass units (amu) in MS and 100-1800 amu in MS/MS. Up to 25 MS/MS spectra were acquired per cycle (approx. 10Hz) using a threshold of 100 counts per second, with dynamic exclusion for 12sec and rolling collision energy.

Proteins were identified using ProteinPilot software v5.0 (SCIEX) using the ParagonTM algorithm[490] and the SwissProt database (release 2017_03, 20201 human entries) with biological modifications allowed. The data were also searched against the reversed database and only proteins which fell within a 5% global false discovery rate[491] were considered as true positives. PeakView software (SCIEX) was used to extract parent ions of the appropriate m/z (extracted ion count, XIC) and the area under the curve of each XIC peak was determined. In this way, the approximate relative quantification of individual EYA1 peptides was assessed across the samples.

3.3 **Results**

3.3.1 **Assessment of EYA1 overexpression in AGS cells transiently transfected with EYA1-pCMV6-XL5 plasmid**

Chemically competent E. Coli were transformed with both the pCMV6-XL5 and EYA1-pCMV6-XL5 plasmids. Both plasmids were isolated from cultures and run on 1% agarose gels to ensure the plasmids are the correct size (Figure 3.2). AGS cells were transiently transfected with pCMV6-XL5 and EYA1-pCMV6-XL5 and transfection was analysed by PCR, immunofluorescence and western blotting. As can

be seen by Figure 3.3A, *EYA1* mRNA expression was greatly increased in EYA1-pCMV6-XL5 transfected AGS cells with all lipofectamine concentrations used, compared to the endogenous EYA1 expression seen in the vector transfected cells.

In contrast, no noticeable change in EYA1 protein expression could be detected by western blotting (Figure 3.3B) and the band seemed to be at a lower molecular weight (55kDa) than expected (expected size of EYA1= 64kDa). It was possible to detect a slight increase in EYA1 protein in the EYA1-pCMV6-XL5 transfected cells compared to the pCMV6-XL5 transfected and untransfected cells using immunofluorescence (Figure 3.4), but expression was still lower than expected and diffused throughout the cell.

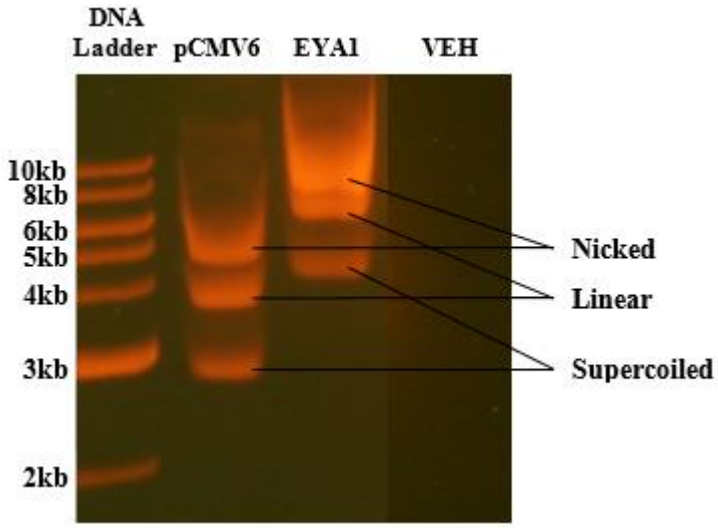

Figure 3.2 Supercoiled, linear and nicked EYA1-pCMV6-XL5 (~6.5kb) and pCMV6-XL5 (~4.5kb) plasmids extracts run on a 1% agarose gel alongside a 1kb DNA ladder and a vehicle control (VEH; elution buffer).

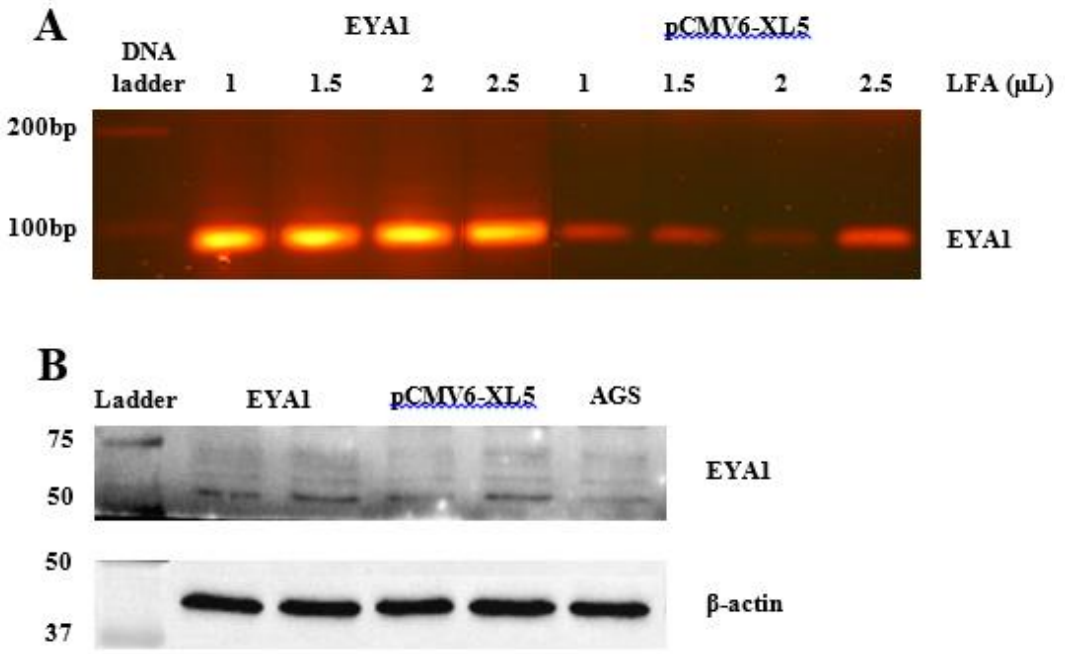

Figure 3.3 Analysis of EYA1 transient transfection in AGS cells. PCR analysis (A) of EYA1 gene expression in EYA1-pCMV6-XL5 and pCMV6-XL5 transfected AGS cells (n=2). To find the optimal transfection conditions, cells were transfected with 1, 1.5, 2 and 2.5µL lipofectamine (LFA) 2000/well. Western blot analysis of EYA1 protein expression (B) was measured in EYA1-pCMV6-XL5 and pCMV6-XL5 transfected AGS cells, as well as untransfected cells (n=2). β-actin was used as a loading control.

3.3.2 Assessment of EYA1 overexpression in HEK293 and three gastric cell lines transiently transfected with EYA1 plasmids

In order to visualize transfected EYA1 protein more easily, the EYA1 construct was sub-cloned from the pCMV6-XL5 plasmid to a plasmid with an N-terminal GFP tag, the pEGFP-C1 plasmid. This plasmid was sent for sequencing to ensure no errors were incorporated during the sub-cloning process.

The sequencing results (Figure 3.5) were compared against the EYA1 isoform 1 reference sequence NM_000503.3; this revealed a deletion of a single cytosine at position 769 (769delC) as well as a single base substitution at position 813 (813A>G). The same deletion was also found when sequencing the original EYA1-pCMV6-XL5 plasmid (data not shown). The deletion causes a frameshift and a premature stop codon, leading to a truncated protein, which would be lacking the entire EYA domain (Table 3.8).

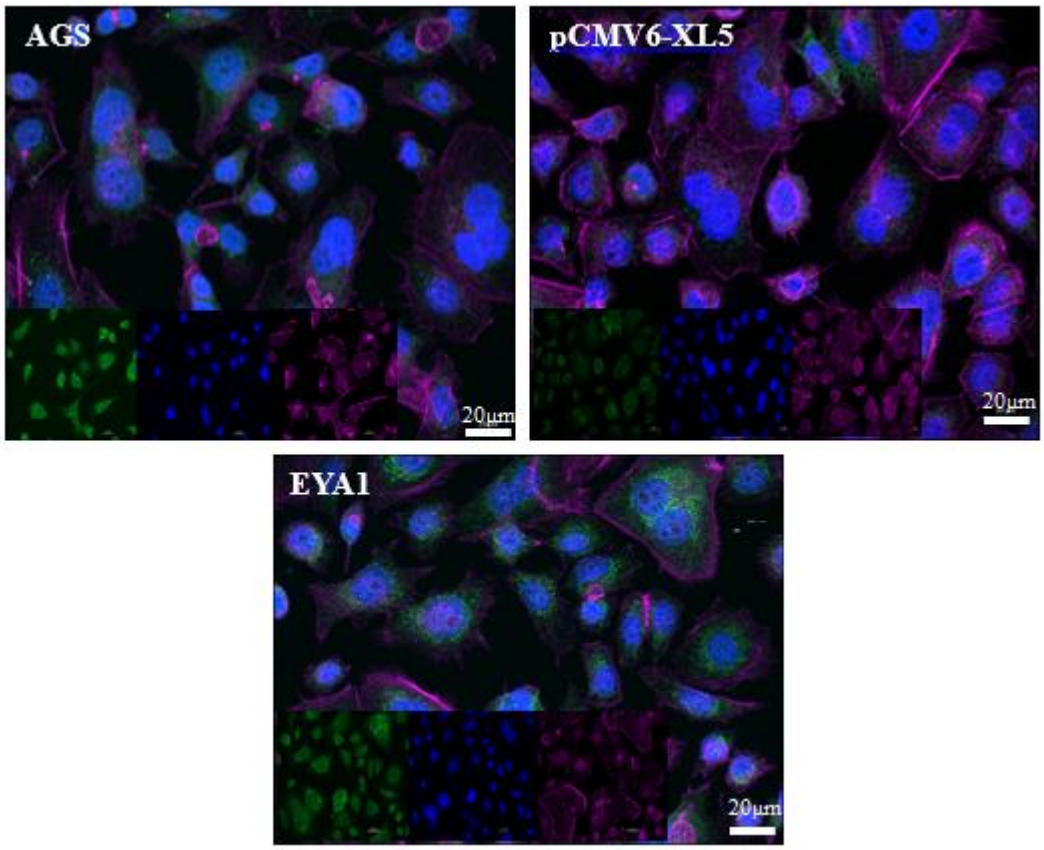

Figure 3.4 Immunofluorescent staining in EYA1-pCMV6-XL5 transfected AGS cells. AGS cells transfected after 24h were fixed and stained with EYA1 (green) antibody, Phalloidin (violet; F-Actin) and Hoechst (blue; nucleus). Three images were acquired for each treatment using a Zeiss fluorescence microscope (40X magnification).

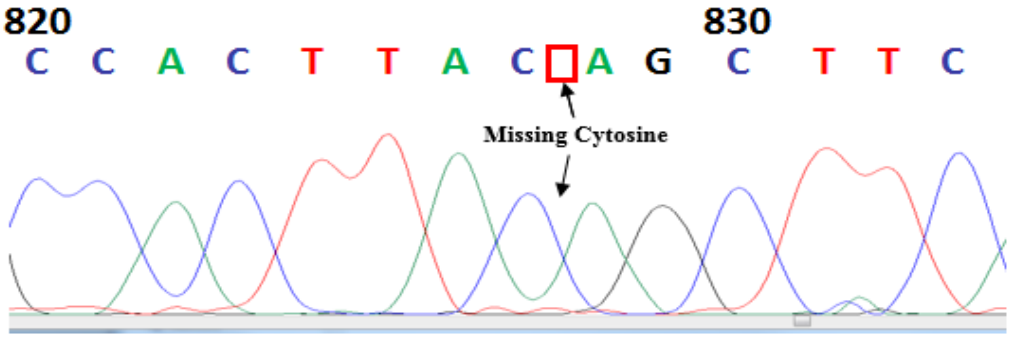

Figure 3.5 Chromatogram of the EYA1-pEGFP-C1 sequencing reaction. The EYA1-pEGFP-C1 plasmid was sequenced by Sanger Sequencing (Source Bioscience) and the following image was taken using Chromas trace viewer 2.6 (Technelsyium Pty Ltd). The trace starts from 761C of the EYA1 reference sequence: NM_000503.3.

Table 3.8 Comparison of EYA1 reference protein sequence and predicted protein sequence of the del769C containing EYA1-pCMV6-XL5 plasmid. The deletion-causing change to the amino acid sequence is highlight in red and the altered amino acid sequence is denoted by underlined text.

Reference EYA1 protein sequence	**EYA1 protein sequence with del769C**
MEMQDLTSPHSRLSGSSESPSGPKLGNSHI NSNSMTPNGTEVKTEPMSSSETASTTADG SLNNFSGSAIGSSSFSPRPTHQFSPPQIYPS NRPYPHILPTPSSQTMAAYGQTQFTTGMQ QATAYATYPQPGQPYGISSYGALWAGIKT EGGLSQSQSPGQTGFLSYGTSFSTPQPGQ APYSYQMQGSSFTTSSGIYTGNNSLTNSS GFNSSQQDYPSYPSFGQGQYAQYYNSSPY PAHYMTSSNTSPTTPSTNATY<u>QLQEPPSGI TSQAVTDPTAEYSTIHSPSTPIKDSDSDRL RRGSDGKSRGRGRRNNNPSPPPDSDLERV FIWDLDETIIVFHSLLTGSYANRYGRDPPT SVSLGLRMEEMIFNLADTHLFFNDLEECD QVHIDDVSSDDNGQDLSTYNFGTDGFPA AATSANLCLATGVRGGVDWMRKLAFRY RRVKEIYNTYKNNVGGLLGPAKREAWLQ LRAEIEALTDSWLTLALKALSLIHSRTNCV NILVTTTQLIPALAKVLLYGLGIVFPIENIY SATKIGKESCFERIIQRFGRKVVYVVIGDG VEEEQGAKKHAMPFWRISSHSDLMALHH ALELEYL</u>	MEMQDLTSPHSRLSGSSESPSGPKLGNSHI NSNSMTPNGTEVKTEPMSSSETASTTADG SLNNFSGSAIGSSSFSPRPTHQFSPPQIYPS NRPYPHILPTPSSQTMAAYGQTQFTTGMQ QATAYATYPQPGQPYGISSYGALWAGIKT EGGLSQSQSPGQTGFLSYGTSFSTPQPGQ APYSYQMQGSSFTTSSGIYTGNNSLTNSS GFNSSQQDYPSYPSFGQGQYAQYYNSSPY PAHYMTSSNTSPTTPSTNATY<u>**SFKNRHLA SPAKQLRIPQQSTAQSTAHQHPLKIQILI DCVEVQMGNHVDGAEETIILHLPQILIL RECSSGTWMRQSLFSTPCLLGPTTPTD MGGIHPLQFPLDCEWKK-Stop**</u>

Two approaches were used to obtain a plasmid with the reference sequence. Firstly, RNA from the AGS cell line was used to perform a RT-PCR amplification of endogenous *EYA1* cDNA, which was cloned into the pEGFP-C1 plasmid (Figure 3.6). The other approach was to use an overlapping PCR reaction, whereby both forward and reverse primers contained the missing cytosine (Figure 3.7).

These new plasmids were sent for sequencing (Figure 3.8) and all EYA1 plasmids were used to transiently transfect HEK293 cells over 48h. Overexpression was detected by western blotting using three anti-EYA1 antibodies. Immunofluorescence analysis was also performed with HEK cells transiently transfected with GFP-tagged EYA1 plasmids.

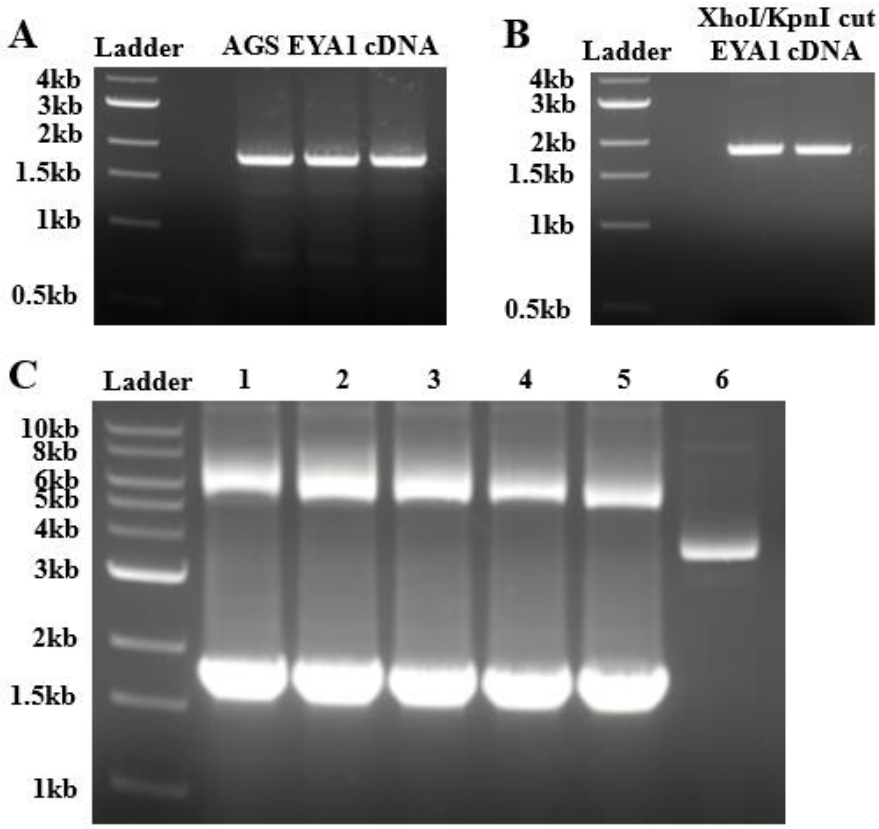

Figure 3.6 Cloning of endogenous EYA1 cDNA from AGS cells into the pEGFP-C1 plasmid. Images show the gel purification of amplified EYA1 cDNA (A) and XhoI and KpnI digested EYA1 cDNA (B). Digested EYA1 cDNA was ligated into pre-cut pEGFP-C1 plasmid, transformed into DH5α E. Coli and grown on kanamycin-containing agar plates. Six colonies were screened (C) and correctly transformed colonies where cultured further.

The sequencing results of the EYA1-AGS-GFP plasmid showed that the same deletion (769C) was present in the EYA1 cDNA from AGS cells as the original plasmid. EYA1 cDNA from HEK293, SH-SY5Y and HGC-27 cell lines were sequenced to investigate further the presence of the recurring single base deletion.

Interestingly, all cell line EYA1 cDNA sequences contained the missing cytosine at amino acid position 769 (Figure 3.8). Sequencing of the EYA1(addC)-GFP plasmid confirmed that the overlapping PCR reaction successfully corrected the EYA1 cDNA insert sequence (Figure 3.8).

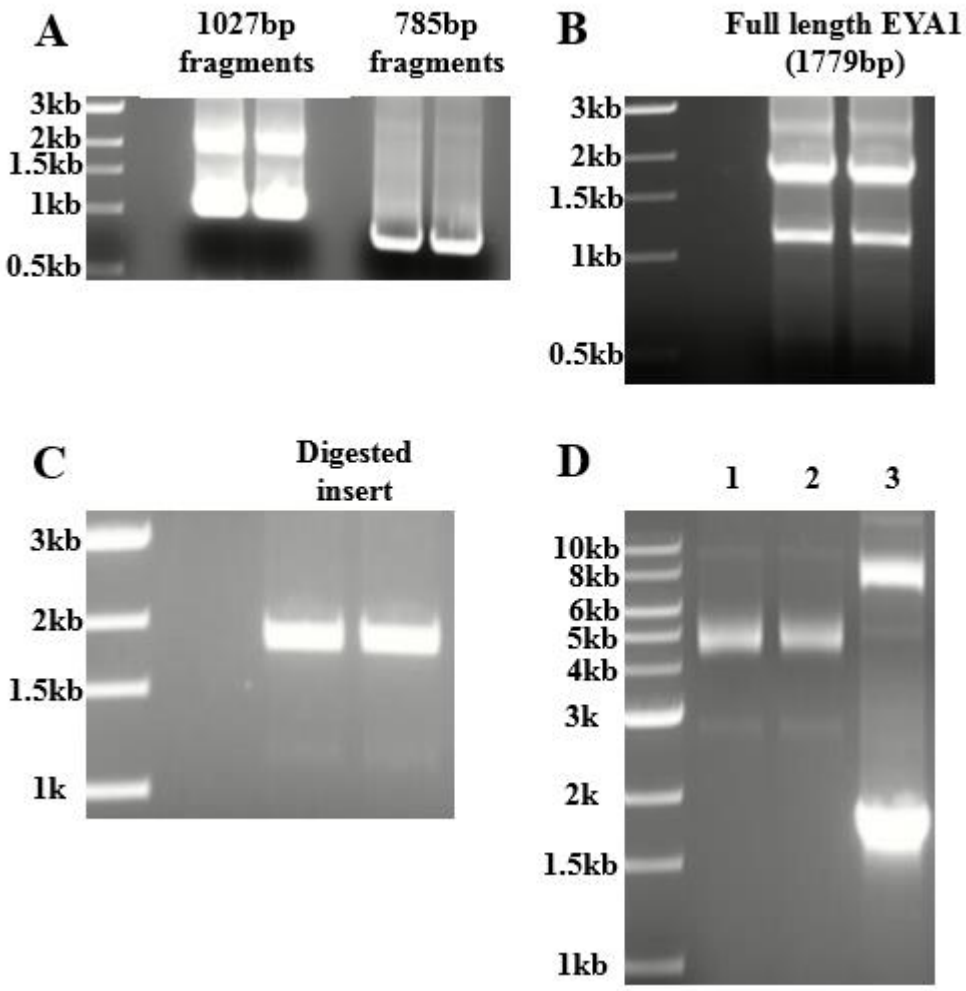

Figure 3.7 Producing a pEGFP-C1 plasmid containing a full-length EYA1 cDNA insert. Two PCR reactions were performed using EYA1-pEGFP-C1 plasmid using forward and reverse primers containing the extra cytosine (A). A second PCR reaction was performed using each fragment as "primers" to produce full-length EYA1(addC) insert (B). The insert was digested using XhoI and KpnI restriction enzymes (C) and ligated into pre-cut pEGFP-C1 plasmid. The ligation mix was used to transform D5Hα E. Coli and colonies were screened by running a PCR to identify bacteria successfully transformed with full length EYA1 (D).

As can been seen in Figure 3.9A-C, overexpressed EYA1 could only be detected in HEK cells transfected with EYA1(addC)-GFP-C1 plasmid. A weak band was again detected at 55kDa using the Abcam Anti-EYA1 antibody (Figure 3.9A) but, assuming this is endogenous EYA1, expression still remained constant between control, EYA1-AGS-GFP and EYA1-pCMV-XL5 transfected cells. This experiment lacked a loading control. However, the results are consistent across the three antibodies used and with previous western blot/immunofluorescent experiments that show no/low EYA1

expression following transfection with the EYA1-pCMV6-XL5 (Figure 3.3B) and EYA1-pEGFP-C1 plasmids (data not shown).

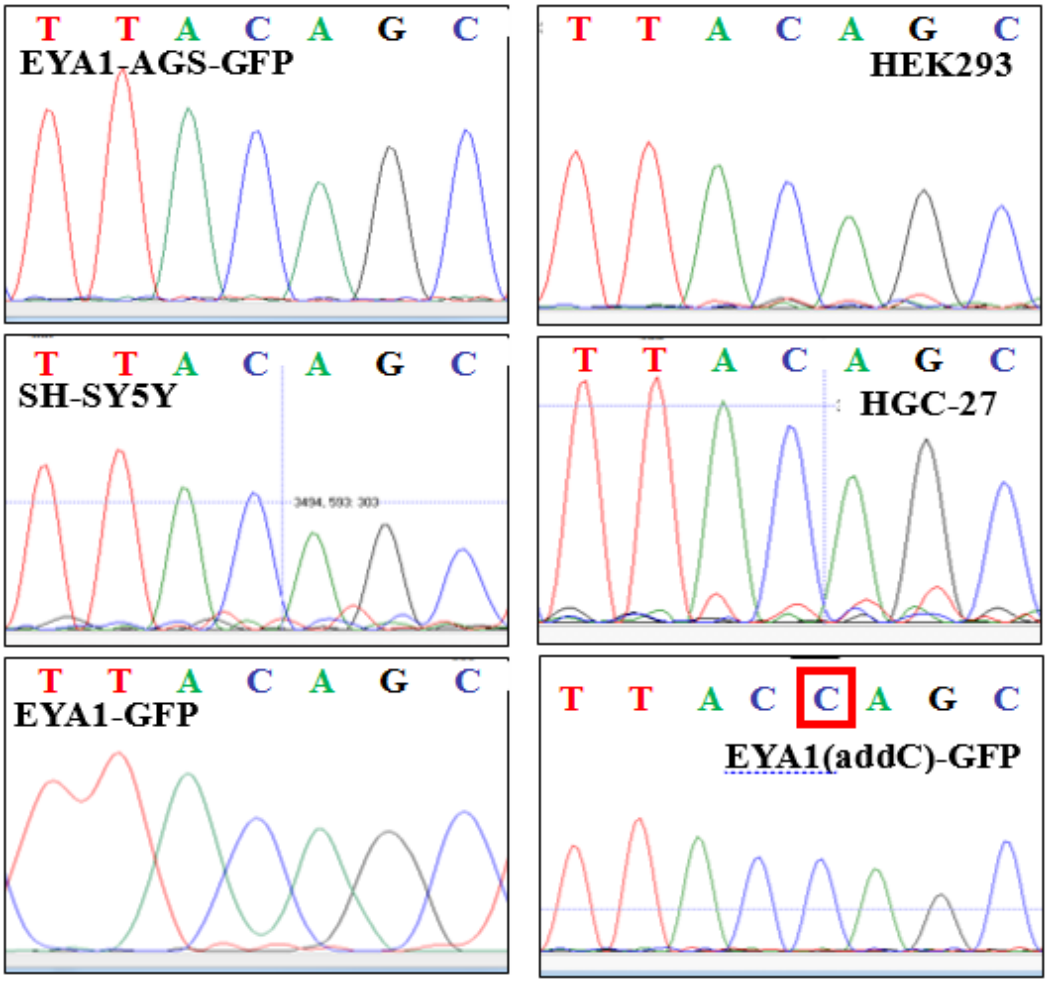

Figure 3.8 Chromatograms showing partial sequence reads of EYA1 cDNA from AGS, HEK, SH-SY5Y and HGC-27 cell lines and the EYA1-GFP and EYA1(addC)-GFP plasmids. The sequences were compared against the reference EYA1 homolog 1 isoform 1 transcript, NM_000503.3. The reference sequence at nucleotides 765-772 should be 'TTACCAGC'. As can been seen above, only the plasmid which was cloned using primers containing the added cytosine (EYA1(addC)-GFP) shows the correct sequence. All other cell lines and plasmids contain the 769delC sequence error.

Overexpressed EYA1 protein showed strong nuclear localisation in HEK cells transiently transfected with EYA1(addC)-GFP (Figure 3.10). In contrast, cells transfected with the EYA1-GFP plasmid containing the single base deletion, showed that the EYA1 protein was localised exclusively in the cytoplasm (Figure 3.10).

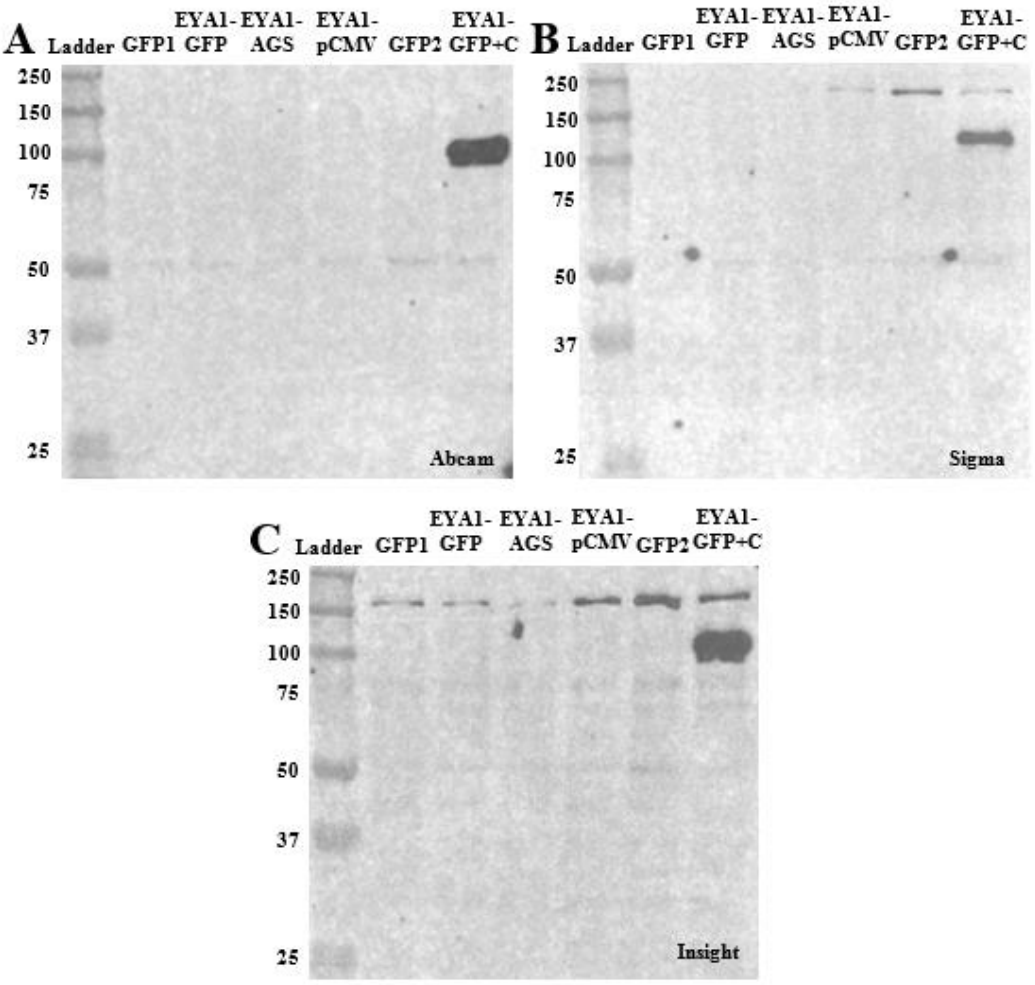

Figure 3.9 EYA1(addC)-GFP transfected HEK cells highly express EYA1 protein. Three polyclonal Anti-EYA1 antibodies targeting internal (A) and C-terminal (B&C) immunogens were used to detect endogenous expression in the control treatments (GFP-transfected cells) and overexpressed EYA1 proteins in lysates from cells transfected with either the EYA1-GFP, EYA1-GFP (AGS cDNA), EYA1-pCMV6-XL5 and EYA1(addC)-GFP plasmids.

AGS cells had a very low transfection efficiency, and therefore the EYA1(addC)-GFP plasmid was transfected into HGC-27 and Hs746T gastric epithelial cell lines. Localisation of the transfected EYA1-GFP protein was nuclear in all cell lines (Figure 3.11A-C); however, transfection efficiency was equally low in the HGC-27 or Hs746T cell lines. Endogenous EYA1 was exclusively localised in the cytoplasm in all cell lines.

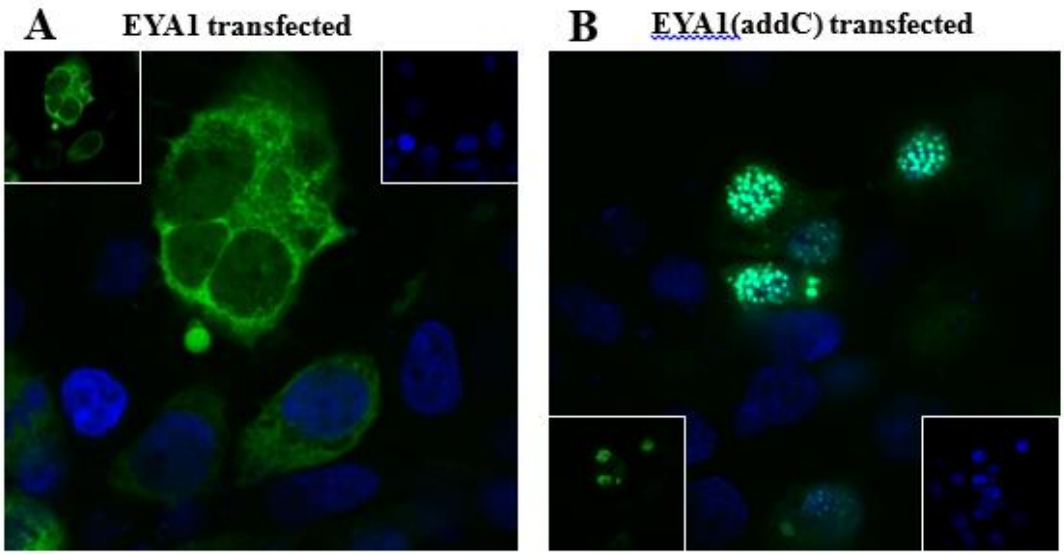

Figure 3.10 Loss of 769C leads to failure of EYA1 nuclear translocation. HEK cells were transiently transfected over 24h with either the EYA1-GFP plasmid (A) containing the 769delC error or the corrected EYA1(addC)-GFP plasmid (B). Images of EYA1(addC)-GFP transfected cells are representative from a group of four images (n=4). Cells were counterstained with a Hoechst nuclear stain and images were obtained using a fluorescence microscope (40X magnification).

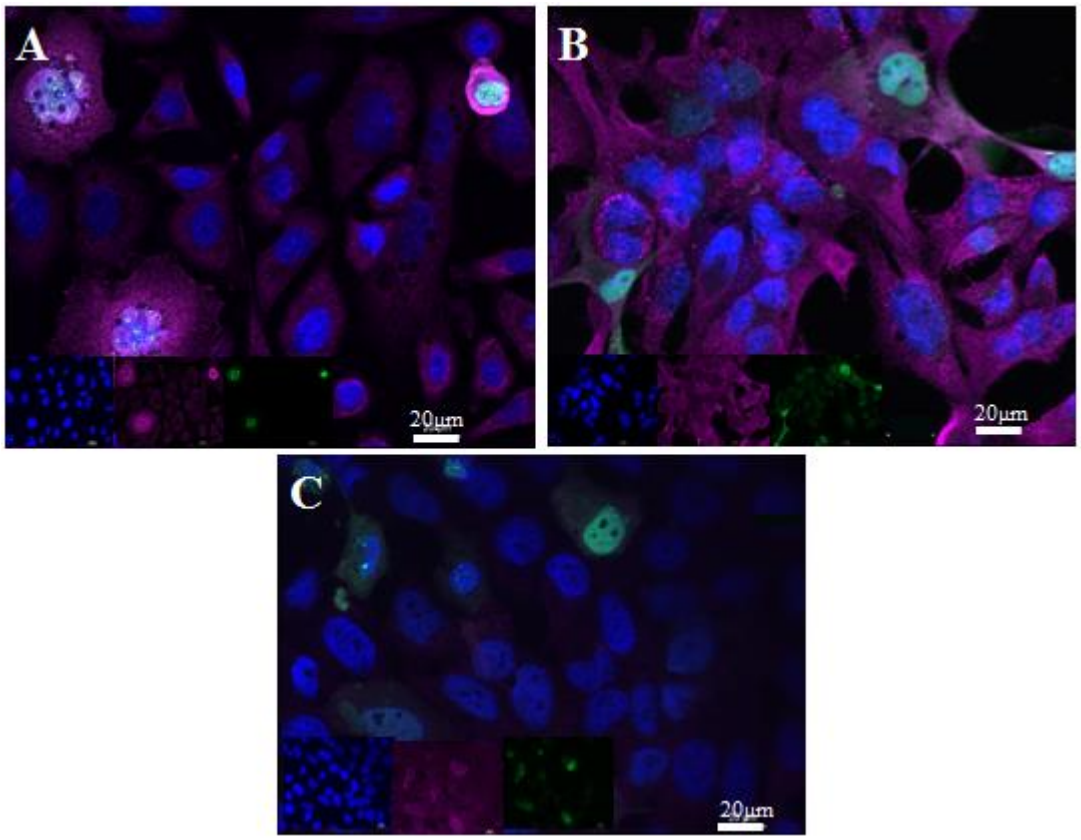

Figure 3.11 Transient transfection of EYA1(addC)-GFP in three gastric cell lines. AGS (A), Hs746T (B) and HGC (C) cells were transiently transfected over 24h with EYA1(addC)-GFP. Fluorescent images taken by combing Z-stack images taken using 349 (nuclei), 488 (EYA1-GFP) and 568nm (endogenous EYA1) excitations. Images are all taken at 40X magnification (n=1).

3.3.3 **Production of an AGS cell line stably expressing EYA1**

To study the effect of overexpressed EYA1 in gastric epithelial toxicity, AGS cells were stably transfected with EYA1 by co-transfecting EYA1(addC)-GFP and pCMV(CAT)T7-SB100 plasmids. Figure 3.12 shows transient expression of EYA1-GFP in AGS cells co-transfected with EYA1(addC)-GFP and pCMV-SB100. Co-transfections with pCMV-SB100 seemed to cause slightly decreased EYA1-GFP protein expression (Figure 3.12G); however, EYA1-GFP localisation remained exclusively nuclear across all transfections/co-transfections (Figure 3.12C-F).

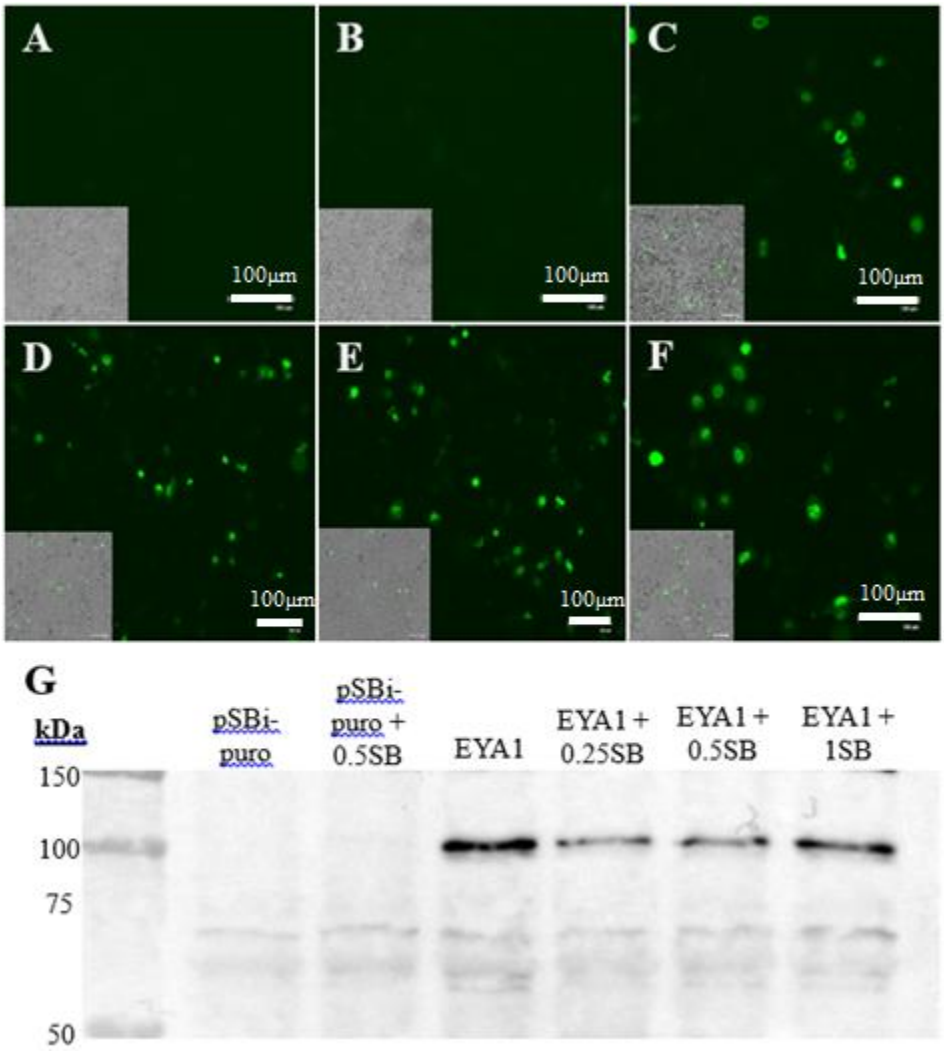

Figure 3.12 Analysis of EYA1 protein expression and localisation in AGS cells transient transfected with EYA1(addC)-GFP and increasing concentrations of pCMV-SB100. Fluorescent (A-F; 20X magnification) and western blotting (G) images showing expression of EYA1-GFP in AGS cells 24h after transient transfection with pSBi-puro (A), pSBi-puro & 0.5µg pCMV-SB100 (B), EYA1(addC)-GFP (C) and EYA1(addC)-GFP with 0.25 (D), 0.5 (E), or 1µg (F) of pCMV-SB100. Overlapping images of white and green channels are shown for each fluorescence image to show transfection efficiency (n=1).

Co-transfection of 2.5µg EYA(addC)-GFP and 1µg pCMV-SB100 per well of a 6 well plate seemed to have the highest EYA1-GFP expression (Figure 3.12G). However, the lack of a loading control and biological replicate for this experiment makes this analysis unreliable. Regarless, these plasmid concentrations were used to produce an AGS cell line stably expressing EYA1-GFP.

AGS cells transfected with pSBi-puro displayed cell death to a similar extent to other 0.25µg/mL puromycin treatments. Resistant colonies could not be demonstrated by

ICF since the pSBi-puro vector contained no GFP tag. Untransfected cells treated with the same concentration of puromycin (0.25µg/mL) had undergone complete cell death (data not shown), demonstrating that cell survival was mediated by the puromycin resistant gene expression in the transfected cells.

As can be seen in figures Figure 3.13A-D, increasing puromycin concentrations caused an increase in selection for transfected cells. After 48h in selective media, native cells were still present in wells treated with 0.025 and 0.25µg/mL puromycin (Figure 3.13A&B). The higher puromycin concentrations (0.5 and 1µg/mL) had however successfully abolished all native cells and left only EYA1-GFP transfected colonies after 48h (Figure 3.13C&D). These cells were grown as a batch culture in selective media for 2 weeks until they could be cultured in T75 flasks.

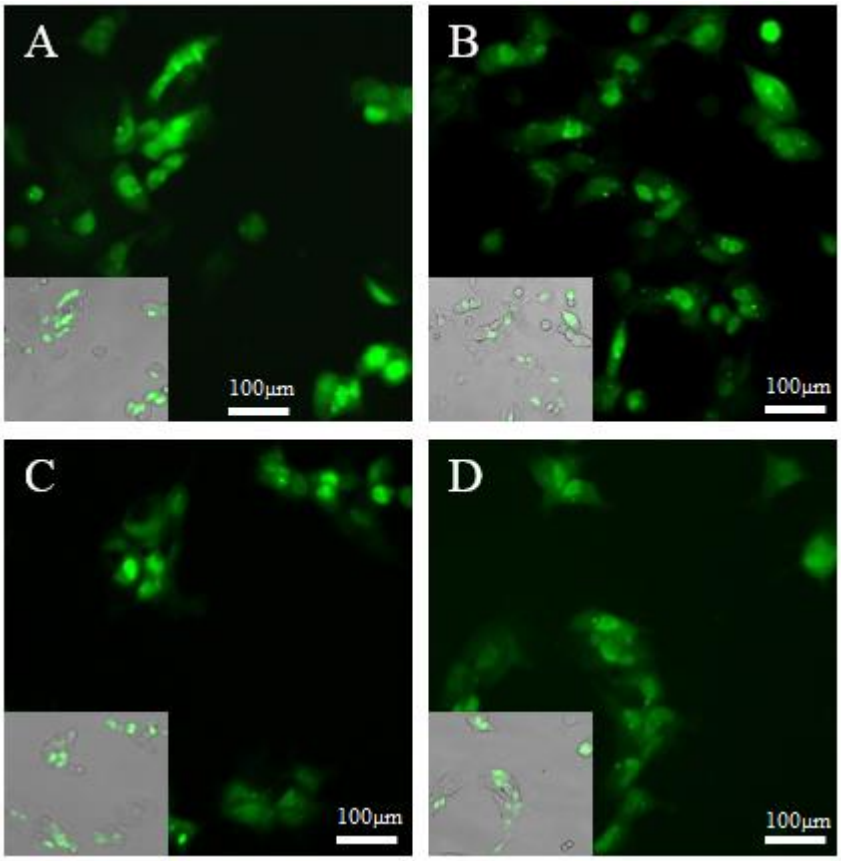

Figure 3.13 Producing an AGS cell line stably transfected with EYA1(addC)-GFP. AGS cells were co-transfected with 250ng pCMV-SB100 and EYA1(addC) (A-D). Cells were exposed to either 0.025 (A), 0.25 (B), 0.5 (C) or 1µg/mL puromycin. Fluorescent images were taken 48h after the first puromycin treatment at 20X magnification using the green (488nm) channel. An overlap of the white and green channel images are shown in the bottom left corner to show puromycin selection.

3.3.4 **Detection of endogenous and overexpressed EYA1 in AGS and AGS-EYA1 cell lines by LC-MS/MS**

Seven tryptic peptides matching the EYA1 protein sequence NP_000494.2[486] were detected by tandem MS in the AGS-EYA1 sample only. This includes the peptides ranging from positions 338-347 with low confidence, 2-12 with medium confidence, 13-43, 351-362, 450-460, 485-492 and 516-531 with high confidence (Table 3.9). A full list of peptide fragments and their confidence values can be found in Appendix 3.1.

A representative XIC for the precursor ion [13]LSGSSESPSGPK[24] is shown to illustrate the difference between EYA1 fragment levels in AGS and AGS-EYA1 (Figure 3.14). The corresponding MS/MS spectra is shown for the [13]LSGSSESPSGPK[24] as well as two other peptides detected in the AGS-EYA1 sample (Figure 3.15), that matched the EYA1 protein sequence. The data together shows that EYA1 is present in higher abundance in AGS-EYA1 cells.

Table 3.9 EYA1 peptide fragments identified by LC-MS/MS in AGS-EYA1 protein lysates. Green text representing high, yellow medium and red low confidence identification. Representative MS/MS spectra are shown above for peptides with underlined text.

M**EMQDLTSPHSR**__**LSGSSESPSGPK**__**LGNSHINSNSMTPNGTEVK**TEPMS
SSETASTTADGSLNNFSGSAIGSSSFSPRPTHQFSPPQIYPSNRPYPHILPTPS
SQTMAAYGQTQFTTGMQQATAYATYPQPGQPYGISSYGALWAGIKTEGG
LSQSQSPGQTGFLSYGTSFSTPQPGQAPYSYQMQGSSFTTSSGIYTGNNSL
TNSSGFNSSQQDYPSYPSFGQGQYAQYYNSSPYPAHYMTSSNTSPTTPST
NATYQLQEPPSGITSQAVTDPTAEYSTIHSPSTPIKDSDSDRLRRGSDGKSR
GRGRRNNNPSPPPDSDLERVFIWDLDETIIVFHSLLTGSYANRYGR__**DPPTS**__
__**VSLGLR**__MEEMIFNLADTHLFFNDLEECDQVHIDDVSSDDNGQDLSTYNF
GTDGFPAAATSANLCLATGVRGGVDWMRKLAFRYRRVKEIYNTYK**NNV**
GGLLGPAKREADWLQLRAEIEALTDSWLTLALK__**ALSLIHSR**__TNCVNILVTT
TQLIPALAKVLLY**GLGIVFPIENIYSATK**IGKESCFERIIQRFGRKVVYVVI
GDGVEEEQGAKKHAMPFWRISSHSDLMALHHALELEYL

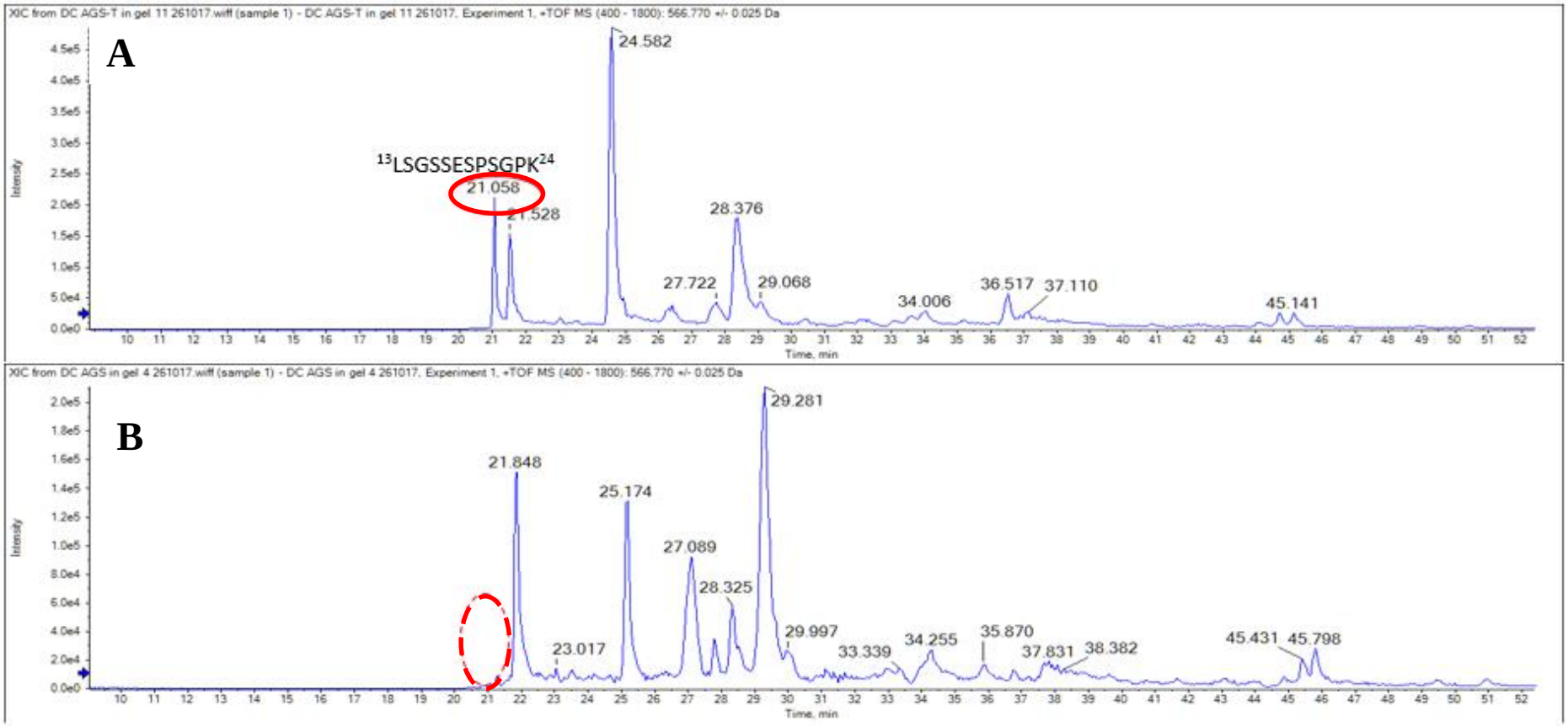

Figure 3.14 Representative extracting ion count (XIC) chromatograms for the detection of EYA1 protein in AGS and AGS-EYA1 protein extracts. Comparison of precursor ions with a mass to charge ratios (m/z) of 566.8 (± 0.1Da) in AGS-EYA1 (A) and AGS (B) cells. In the AGS-EYA1 MS/MS spectrum, a precursor eluted with a peak rention time of 21.1 min was interpreted and shown to match the sequence ^{13}LSGSSESPSGPK^{24}. This peptide could not be detected in the AGS MS/MS spectrum.

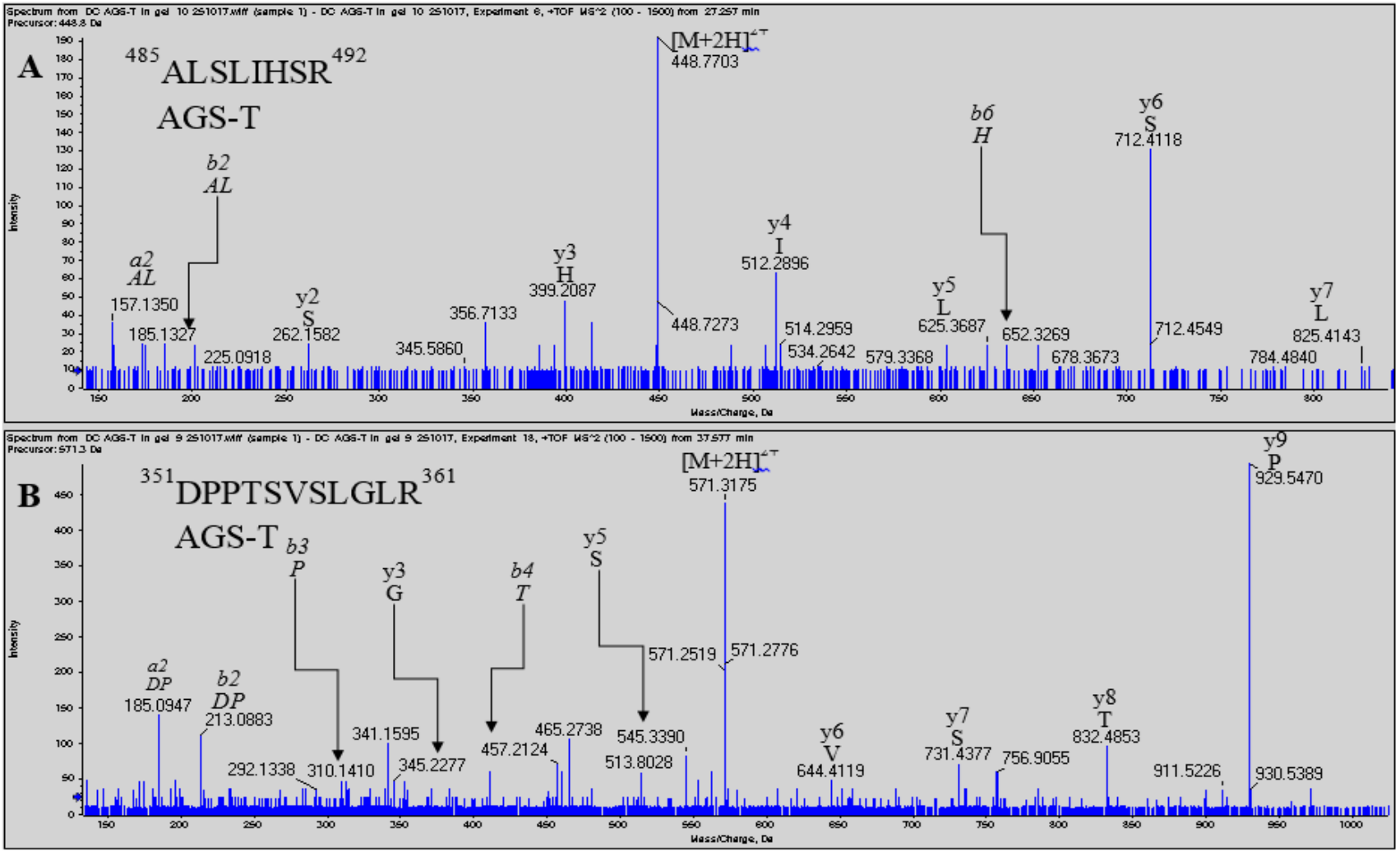
A
485 ALSLIHSR 492
AGS-T
[M+2H]2+
448.7703
b2
AL
b6
H
y6
S
712.4118
a2
AL
157.1350
185.1327
225.0918
y2
S
262.1582
345.5860
356.7133
y3
H
399.2087
448.7273
y4
I
512.2896
514.2959
534.2642
579.3368
y5
L
625.3687
652.3269
678.3673
712.4549
784.4840
y7
L
825.4143
Intensity
Mass/Charge, Da
B
351 DPPTSVSLGLR 361
AGS-T
[M+2H]2+
571.3175
b3
P
y3
G
b4
T
y5
S
y9
P
929.5470
a2
DP
185.0947
b2
DP
213.0883
292.1338
310.1410
341.1595
345.2277
457.2124
465.2738
513.8028
545.3390
571.2519
571.2776
y6
V
644.4119
y7
S
731.4377
756.9055
y8
T
832.4853
911.5226
930.5389
Intensity
Mass/Charge, Da

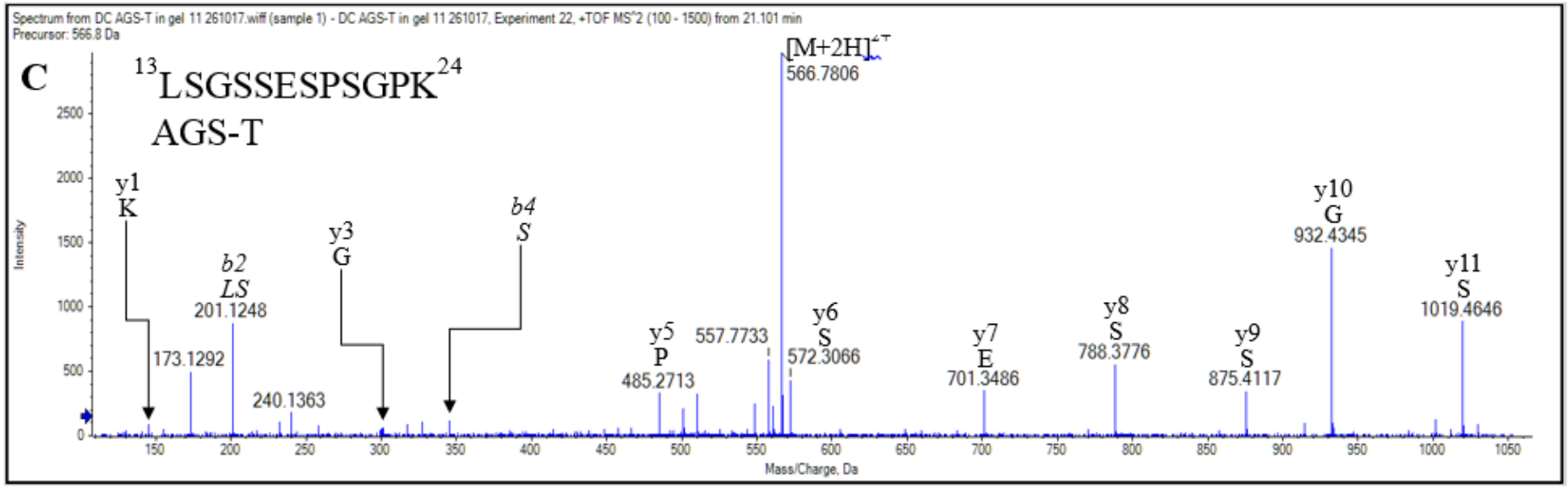

Figure 3.15 Representative MS/MS spectra of EYA1 tryptic peptides detected in AGS-EYA1 extracts. The three peptides presented, ALSLIHSR (A), DPPTSVSLGLR (B) and LSGSSESPSGPK (C), were present without any biological or artefactual modifications and with no missed or non-specific cleavages.

3.4 **Discussion**

As can be seen in Figure 3.3A transient transfection of EYA1-pCMV6-XL5 into AGS cells with lipofectamine was successful in the sense that EYA1 mRNA expression was greatly increased in AGS cells transiently transfected with EYA1 compared to control (empty vector) transfected cells. However, there seemed to be only a minimal change in EYA1 protein between EYA1 and control transfected cells, which could be observed by immunofluorescence (Figure 3.4) but not by western blot (Figure 3.3B).

There is a dose-dependent decrease in endogenous *EYA1* expression from 1-2μL Lipofectamine in the pCMV6-XL5 transfected AGS cells (Figure 3.3A). However, the expression is restored at 2.5μL Lipofectamine (Figure 3.3A). This varying expression pattern could be a consequence of the transfection method or may be caused by a difference in the amount of cDNA loaded into the gel. Whilst it is known that certain transcription factors (Homeobox A2[492] and Nuclear Receptor Subfamily 2 Group F Member 2[493]) and microRNAs (miR-101[385] and miR-562[390]) regulate *EYA1* expression, the mechanism by which *EYA1* is regulated following stress (e.g. chemical transfection) is so far unkwown.

The increased EYA1 mRNA expression, but lack of protein expression, can be explained by the single-base (769C) deletion detected in the EYA1-pCMV-XL5 plasmid (Figure 3.5). The deletion of this nucleic acid from the mRNA sequence causes a frameshift mutation and a truncated C-terminal protein sequence (Table 3.8). This frameshift causes a change in the amino acid (aa) sequence at aa256 and causes an early stop codon at aa365 (Figure 3.16). The truncated protein would theoretically have completely lost the EYA and tyrosine phosphatase domains.

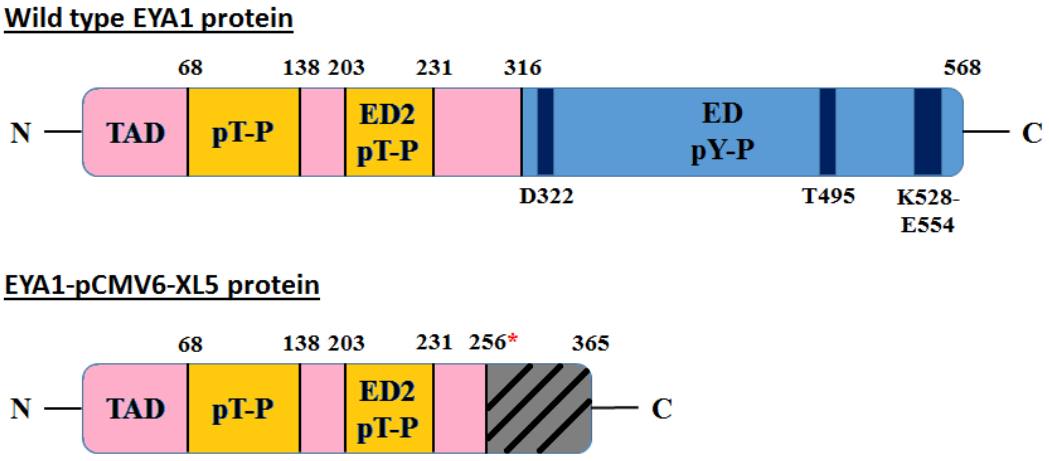

Figure 3.16 Deletion of 769C in the EYA1 mRNA sequence leads to loss of the entire EYA and tyrosine phosphatase domains. Comparison of full-length protein (wild type) with the predicted protein domains of the EYA1 expressed from EYA1-pCMV6-XL5. The highly conserved EYA domain (ED) is highlighted in blue, with the HAD phosphotyrosine phosphatase (pY-P) motifs represented with the darker blue bars. The transactivation domain (TAD) is denoted by the pink N-terminal region with the embedded phosphothreonine phosphatase (pT-P) domains in yellow. The Eya domain 2 (ED2), a poorly conserved and tyrosine-rich domain, partly overlaps with one of the pT-P motifs. The grey area demonstrates the change in amino acid sequence caused by the frameshift and the early truncation at the C-terminus[362].

Several residues on the EYA1 protein, such as serine 454, leucine 472 and leucine 550, have been revealed as being important for stabilisation with SIX proteins[367]. Reduced nuclear translocation and rapid protein ubiquitination with subsequent proteasomal degradation occurs with the BOR-associated L550P mutation due to a loss of interaction with SIX proteins[367]. Since the frameshift mutation at aa256 mutation observed in the original and GFP plasmid would cause a loss of this essential residue, this could explain why very low/no protein expression was observed in cells transfected with this plasmid (Figure 3.3, Figure 3.4 and Figure 3.9).

The same deletion (769delC) was found after sequencing EYA1 cDNA derived from AGS, HEK293, SH-SY5Y and HGC-27 cell lines (Figure 3.8). As with the transfections with the 769delC EYA1 plasmids, this could explain why endogenous EYA1 protein could not be detected in these cell lines (Figure 2.7).

There has been a report of the deletion of this cytosine occurring in a patient with typical BOR syndrome (phenotype: branchial abnormalities, pits, extern ear abnormalities and deafness)[494]. Unfortunately, in this study sequencing of *SIX* genes

was only performed in the absence of discovering an EYA1 mutation or frameshift. Therefore, it is not clear whether this patient presented any other BOR-related mutations. Considering that BOR syndrome is a relatively rare condition (~1 in 40,000), it is unlikely that this mutation alone could lead to BOR phenotypes[494].

The fact that the 769C deletion was present in every cell line tested would suggest that this deletion might be common in, or even necessary to the development of, tumorigenic cell lines. What is less likely, given BOR syndrome is inherited in an autosomal dominant pattern[364], is that the relevance of the EYA domain was lost at some point in evolution on the human EYA1 protein and has since become a pseudogene. A way to study this phenomenon further would be to perform a screening of healthy, cancer and BOR patient's EYA1 gDNA and mRNA.

To study the effect of full-length EYA1, the 769delC EYA1-GFP plasmid was corrected by performing a series of PCR reactions that introduced the missing cytosine nucleic acid into the EYA1 cDNA sequence (Figure 3.1). The principle of this technique is to perform two PCR reactions on EYA1 cDNA using forward and reverse primers that contain the missing base. The second PCR reaction includes mixing the two reactants from the initial PCR and using the overlapping regions of each as 'primers' to extend the rest of the EYA1 fragments. This process produced full-length EYA1 cDNA, which was cloned into the pEGFP-C1 and pSBi-puro plasmids, to be used in transient and stable transfections.

EYA1-GFP protein was highly expressed in HEK cells transfected with the EYA1(addC)-GFP plasmid as shown by western blot (Figure 3.9) and immunofluorescence (Figure 3.10).

The overexpressed EYA1-GFP protein was localised almost exclusively in the nucleus, whereas truncated EYA1 was found exclusively in the cytoplasm (Figure 3.10). This data supports the current reports that the C-terminal EYA1/SIX-binding domains are essential for nuclear localisation[367,462,481].

EYA1 protein fragments could only be detected in AGS-EYA1 (not AGS) cells as shown in Figure 3.14A&B. Several other N- and C-terminal fragments were identified in the AGS-EYA1 protein lysates (Table 3.9), suggesting that the deletion that caused the truncation has be successfully repaired and that full-length EYA1 protein is being

expressed. This data further supports the western blotting results that show EYA1 protein expression is only detected in AGS-EYA1 cell lysates (Figure 3.9).

EYA1/*Eya1* stable cell lines have been developed in a limited number of studies using kidney[373,463,482], breast[373,387] and MEF[463] cells, none of which of been made commercially available. An *EYA1* knockout CML cell line, available from Horizon Discovery (Cambridge, UK), seems to be the only commercially available cell line with altered EYA1 expression. This would therefore make this study the first to produce a gastric epithelial cell line stably expressing *EYA1*.

Now that an EYA1 stably transfected gastric epithelial cell line has been generated with demonstrable significant EYA protein expression, the role of EYA1 can now be studied in aspirin-mediated gastric epithelial toxicity.

Chapter 4

In vitro characterisation of the role of EYA1 in aspirin-induced apoptosis in AGS cells

Contents

4.1 **Introduction**

Though systemic effects are key to aspirin-induced ulcerogenesis, this chapter will focus on the direct, intracellular toxicity cause by aspirin. These 'topical' effects begin with the trapping and accumulation of ionised aspirin within gastric epithelial cells[495]. There have been various *in vitro* studies, using the AGS cell line, that try to elucidate the role of aspirin-induced apoptosis in gastric ulceration[249,250,395,403,496].

As described in section 2.1, the mechanism of aspirin-induced apoptosis has been linked to stimuli originating from disturbances in various intracellular systems including inhibition of proteasome function, oxidative/mitochondrial and ER stress and dysregulation/translocation of several pro- and anti-apoptotic genes and proteins[1]. The mitochondrial pathway seems to play an important role in aspirin mediated apoptosis demonstrated by AIF[250] and SMAC release[249], BAX and BAK relocation[249,418], caspase-8[249,395] and 9[418] activation.

Though not exclusive, the two main routes of apoptosis include the extrinsic pathway, which involves the activation of various cell surface receptors (e.g. FAS receptor, tumor necrosis factor receptor 1, etc.), and the intracellular pathway, which is triggered by intracellular signals. Since EYA1 is involved in DNA repair following genotoxic stress, the hypothesis that EYA1 overexpression could attenuate gastric epithelial apoptosis resulting from aspirin-toxicity was investigated in this chapter.

The intrinsic apoptotic pathway can be triggered by 'negative' and 'positive' signals. Negative signals arise from the absence of signalling from growth factors, hormones and cytokines that suppress death programs. Whereas, examples of positive stimuli are triggers such as DNA damage, hypoxia, free radicals and hyperthermia (Figure 4.1).

Stress-response transcription factors such as p53 activate the transcription of BH3-only genes: *NOXA*, *PUMA*, *BID*, *BIK* and *BIM*. The proteins translated by these genes displace BAX and BAK proteins from BCL-2 proteins such as BCL-2, BCL-X_L, BCL-x, BCL-w and MCL-1. It has also been demonstrated that BH3-only proteins interact with BAX and BAK to expose their hydrophobic BH3 helices, allowing homo-dimerization and subsequent oligomerization of BAX and BAK monomers. Chemical inhibitors of BCL-2 proteins such as A-1331852 and S63845, which inhibit BCL-X_L

and MCL-1 respectively, are also able to release BAX and BAK by mimicking the actions of BH-3 only proteins (BH-3 mimetics)[497].

There are reports that BAX and BAK oligomerization causes mitochondrial outer membrane permeabilization (MOMP) either by opening voltage gated anion channels such as VDAC, or by directly forming pores on the outer mitochondrial membrane. This event allows two groups of pro-apoptotic proteins, normally sequestered in the intermembrane space, to be released into the cytosol.

The first group of proteins released include SMAC/DIABLO and HtrA2/Omi which both inactivate the inhibitor of apoptosis (IAP) proteins such as XIAP. Cytochrome c, which is also released early after BAK/BAX-induced MOMP, binds to and activates Apaf-1 and procaspase-9, forming the apoptosome.

The second group of proteins released include Caspase-Activated DNase (CAD), which is later activated/cleaved by caspase-3, causing DNA fragmentation and chromatin condensation. Caspase-independent proteins, AIF and endonuclease G are simultaneously released during the late-stage commitment to cell death. These proteins act independently, also causing DNA fragmentation.

The initiator caspase, caspase-9, goes on to activate the "executioner" or effector caspases, caspase-3, -6 and -7. Substrates of these caspases, most notably caspase-3, cause:

(i) Activation of dormant killers: protein kinase C-δ and –θ (PKC-δ/θ), mitogen-activated protein kinase kinase kinase-1 (MEKK1), p21 activated kinase 2 (PAK65) and pro-caspases,

(ii) Structural dismantling (nuclear lamins, fodrin, gelsolin, etc.),

(iii) Elimination of death antagonists: BCL-2 proteins, DNA fragmentation factor subunit alpha (DFF-45/ICAD) and p28 Bap31,

(iv) DNA repair proteins: Poly(ADP-ribose) polymerase (PARP) and protein kinase, DNA-activated, catalytic polypeptide (DNA-PK_{CS}), and

(v) Several other types of protein: RB transcriptional corepressor 1 (Rb), protein tyrosine kinase 2 (FAK), MDM2 proto-oncogene (MDM2), etc.

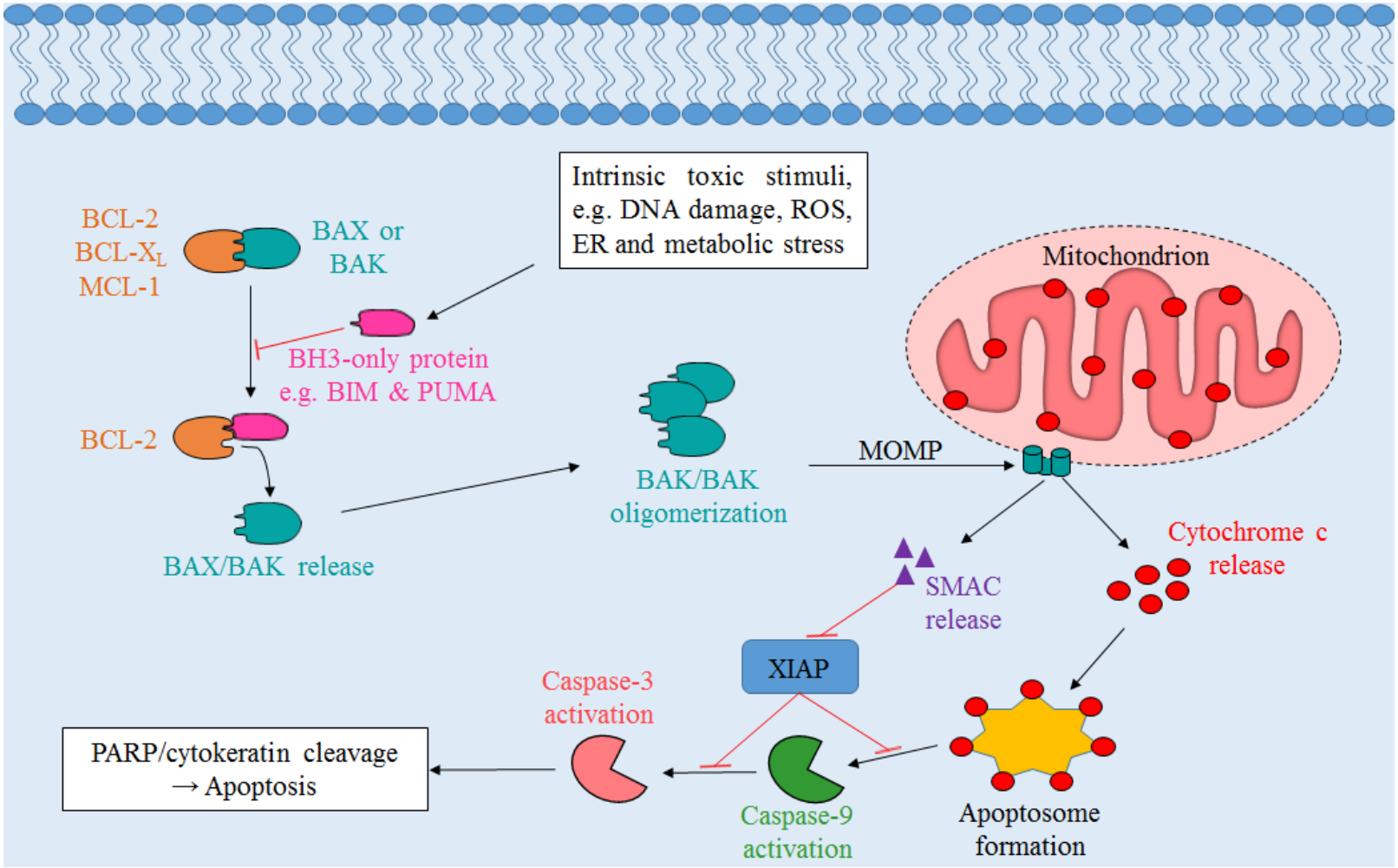
Intrinsic toxic stimuli, e.g. DNA damage, ROS, ER and metabolic stress
BCL-2
BCL-XL
MCL-1
BAX or BAK
BH3-only protein e.g. BIM & PUMA
BCL-2
BAX/BAK release
BAK/BAK oligomerization
Mitochondrion
MOMP
Cytochrome c release
SMAC release
XIAP
Caspase-3 activation
Caspase-9 activation
Apoptosome formation
PARP/cytokeratin cleavage → Apoptosis

Figure 4.1 The intrinsic apoptosis pathway is triggered by intracellular damage or stress. These signals initiate the transcription and translation of BH3-only proteins such as BIM and PUMA which displace pro-apoptotic proteins such as BAX and BAK from anti-apoptotic BCL-2 proteins (BCL-2, BCL-X_L, MCL-1, etc.). This displacement can be imitated by BH-3 mimetics such as A1331852 and S63845. BAX and BAK oligmerize and either open voltage-dependent anion channels or directly form pores on the outter mitochondrial membrane, allowing the release of cytochrome c from the mitochondria. Cytochrome c forms the apoptosome by facilitating the oligomerization of APAF1 proteins. The apoptosome activates the initiator caspase-9 from its zymogen precursor, which in turn activates the executioner caspases-3 and -7. Caspases can be inhibited by IAPs and chemical inhibitors such as z-VAD. Caspase-3/7 go on to cleave various substrates (ICAD, PARP, etc.) that ultimately results in the morphological and biochemical phenotypes of apoptosis.

Throughout the chapter, various small molecular inducers of cell death were used (Table 4.1), either as a positive control (raptinal), or to test the protective effect of EYA1 against various stress stimuli (staurosporine, brefeldin A and tunicamycin).

Raptinal, a small molecule inducer of cell death, has been shown to induce cytochrome c release and cell death within minutes and shows efficacy across various cell types/animal models. The induction of apoptosis of other apoptotic agents such as STS usually takes 6-12h, making raptinal a useful control for studying apoptotic cell death[498].

The aims of this chapter were to (i) determine whether EYA1 overexpression effects aspirin-induced apoptosis in AGS cells, (ii) determine the effects of EYA1 overexpression following incubation with different apoptotic stimuli, and (iii) identify where in the apoptotic pathway EYA1 is exerting its effect.

Table 4.1 Summary of apoptotic inducers used to study the role of EYA1 in aspirin-mediated gastric toxicity.

Apoptotic stimuli	Mechanism of apoptosis	References
Raptinal	Causes cytochrome c release and cell death within minutes and shows efficacy across various cell types/animal models.	498
Staurosporine (STS)	STS inhibits ATP-binding sites of PKC and cyclin-dependent kinases. STS has allow shown to cause caspases-8 and -9 activation and AIF release.	499, 500, 501
Brefeldin A (BFA)	BFA blocks protein transport from the endoplasmic reticulum (ER) to the Golgi. BFA has been shown to activate ER, mitochondria and capase-8 apoptotic pathways and downregulate anti-apoptotic proteins BCL-2 and MCL-1.	69,502,503, 504
Tunicamycin (TUN)	TUN inhibits the post-translational modification (i.e. N-linked glycosylation) of several proteins in the ER. TUN activates ER and mitochondrial pathways including CHOP, caspases-8, -9, -10 and -12.	505,506

4.2 **Materials and methods**

4.2.1 **Materials**

Unless stated otherwise, reagents were purchased from Sigma-Aldrich Co., Dorset, UK. Rabbit Anti-EYA1 primary and Goat Anti-Rabbit Ig HRP secondary antibodies were from Abcam, Cambridge, UK. All other primary antibodies used in this chapter were purchased from Cell Signaling, Hitchin, UK. BH3 mimetics, A1331852 and S63845, were kindly provided by AbbVie Inc. (North Chicago, IL, USA). Pan-caspase inhibitor, z-VAD, was purchased from Selleck Chemicals Co., Houston, TX, USA. PBS, Pierce BCA Protein Assay Kit, LDS sample buffer, NUPAGE sample reducing agent, Tween-20, SeeBlue Plus2 Pre-stained Protein Standard were purchased from Thermo Fisher Scientific. Clarity ECL substrate was purchased from Bio-Rad, Hertfordshire, UK.

4.2.2 **Cell lines and culture conditions**

AGS and EYA1-AGS

AGS cells were cultured as described in section 2.2.2. Following stable selection of the EYA1-AGS cell line in puromycin for 2 weeks, cells were cultured as per AGS cells. For all Sub-G1 and western blotting experiments, AGS and EYA1-AGS cells were plated at 450,000 cells/well across separate 6-well plates and incubated overnight at 37°C and 5% CO_2.

4.2.3 **Preparation of drug solutions**

Stock aspirin concentrations were made in DMSO before being diluted at a ratio of 1 in 138.8 to obtain the final media concentrations. All aspirin-containing media was sonicated for 5 min to ensure full dissolution of the drug.

Apoptotic inducing agents including staurosporine (STS), tunicamycin (TUN) and brefeldin A (BFA) were prepared in DMSO to 5, 10 and 20mM stock solutions. STS was diluted to 5μM in media and TUN and BFA were diluted to 20μM.

Raptinal, a potent apoptotic inducer, was prepared in DMSO to 10mM and diluted to 10μM in media. MCL-1 inhibitor, S63845, and BCL-X_L inhibitor, A-1331852, were prepared in DMSO to 100μM and diluted to 100nM in media.

4.2.4 **Aspirin-induced apoptosis in AGS and EYA1-AGS cell lines**

Flow cytometric analysis

AGS and EYA1-AGS cells were treated with either 10 or 20mM aspirin for 48h. A set of cells treated with 10μM raptinal for 1.5h were added as a positive control for an increased sub-G1 population. A set of 10 and 20mM aspirin-treated cells were also pre-treated for 1h and co-incubated with 30μM of the pan-caspase inhibitor z-VAD.

At the end of the drug treatments, cells were washed with PBS, trypsinized from the wells and pelleted with the supernatant by centrifugation for 5 min at 300g. Cell pellets were washed twice with PBS and fixed in 70% ice-cold ethanol for 30 min on ice. Samples were centrifuged again at 750g for 5 min and washed twice in PBS. Pellets were resuspended in 50μL of 100μg/mL RNase A for 30 min at room temperature and 200μL of 50μg/mL propidium iodide (PI) was added to each sample.

The levels of sub-G1 content in each sample was measured by FACS analysis (Attune NxT Acoustic Focusing Cytometer, Life Technologies) using the BL-3 fluorescence channel. Representative images of forward and side scatter gating are provided for both control and aspirin treated cells (Appendix 4.1).

Western blots

AGS and EYA1-AGS cells were treated with 0, 10 and 20mM aspirin for 48h and raptinal for 1.5h as a positive control. Cells were lysed in 120μL RIPA buffer containing 1% protease inhibitor and lysates were sonicated to homogenize samples. Sample concentrations were determined by BCA and samples denatured as described in section 2.2.6.

Samples were treated with reducing buffer, heat treated at 85°C for 5 min and placed on ice for 5 min. Next, 20μg of protein from each sample was loaded into 7% (EYA1), 10% (caspase-9, PARP, cleaved PARP and GAPDH) and 15% (cleaved caspase-3) acrylamide gels and separated by electrophoresis. Proteins from the gels were transferred to nitrocellulose membranes, which were stained with Ponceau Red solution, cut and blocked in 5% skimmed milk.

Membranes were washed in TBST and incubated separately with caspase-9, cleaved caspase-3, PARP, cleaved PARP, EYA1 and GAPDH polyclonal antibodies overnight

at 4°C. Blots for loading controls (GAPDH) were performed on membranes separate to the other target proteins. Membranes were washed again in TBST before incubating each with Goat Anti-Rabbit Ig HRP secondary antibody for 1h at room temperature. Bands were visualised using the ECL and ChemiDoc Imaging System described in section 2.2.6.

4.2.5 **Effect of other apoptosis-inducing compounds on caspase processing and BCL-2/BH3-only proteins in AGS and EYA1-AGS cell lines**

Western blots

AGS and EYA1-AGS cells were exposed to either DMSO (control), 20mM aspirin, 5μM STS, 20μM TUN or 20μM BFA for 24h. Protein lysates were collected, quantified, electrophoresed and transferred as described in section 4.2.4. Membranes were incubated with XIAP, GAPDH, caspase-3, -7 and 9 primary antibodies overnight at 4°C. Goat anti-Rabbit Ig HRP secondary antibody was added to each membrane for 1h before visualising the bands as described in section 4.2.4.

AGS and EYA1-AGS cells were treated with A1331852 and S63845 alone or in combination for 3h. A 15% polyacrylamide gel was used to separate protein lysates used to analyse caspase-3, BCL-2, BCL-X_L, BAX and BAK. All other proteins analysed were separated in 10% polyacrylamide gels.

Flow cytometric analysis

AGS and EYA1-AGS cells were treated with 10μM raptinal for 2h, 100nM of BCL-X_L inhibitor, A1331852, MCL-1 inhibitor, S63845, alone or in combination for 3h and DMSO as a vehicle control. Cells were processed as described in section 4.2.4 for analysis of sub-G1 DNA content using FACS. Representative images of forward and side scatter gating are provided for both control and BH3- mimetic combination treated cells (Appendix 4.2).

4.2.6 **Statistical analysis**

All statistical analyses were performed using Graphpad Prism 7.04 for Windows. Both sets of sub-G1 data were analysed using two-way ANOVA with Sidak's multiple comparison post-hoc test and the significance threshold was set to $P < 0.05$. Two additional analyses were performed on the results from the aspirin-treated AGS and

EYA1-AGS cells experiment. Firstly, a Two-way ANOVA with Dunnett's correction was performed to compare the effect of increasing aspirin concentrations and raptinal on sub-G1 content. A One-way ANOVA with Sidak's corrections was also performed to determine the effect of blocking caspase-mediated apoptosis on the accumulation of sub-G1 content. Data are shown as means ± standard deviation (SD).

4.3 Results

4.3.1 EYA1 overexpression significantly reduces aspirin-induced AGS apoptosis

Since EYA1-AGS cells contain the corrected (769addC) GFP-tagged EYA1, flow cytometry analysis of apoptosis could not be performed using FITC-bound Annexin-V. Instead, sub-G1 analysis was performed to compare aspirin-induced toxicity between AGS and EYA-AGS cell lines. Cells undergoing apoptosis lose DNA content by fragmented DNA being extracted during the fixation process and through the shedding of apoptotic bodies. This shows as a sub-G1 peak on histograms showing DNA staining levels against number of cells, allowing quantification of apoptotic cells.

When comparing the effect of 20mM aspirin, EYA1-AGS cells had a significantly lower sub-G1 content than the native AGS cells as determined by FACS (Figure 4.2). Though there was no statistical difference in sub-G1 content at 0 and 10mM aspirin between AGS and EYA1-AGS cells, the basal level of sub-G1 content seemed to be lower in EYA1-AGS cells in all treatments except raptinal.

Two additional statistical analyses of this data performed also shown that:

(i) 20mM aspirin (AGS only) and raptinal treatments significantly increased sub-G1 content compared to their respective 0mM aspirin controls calculated using Two-way ANOVA with Dunnett's multiple comparison, $P<0.05$, and,

(ii) zVAD pre- and co-treatment significantly decreased sub-G1 content in only AGS cells treated with 20mM aspirin, determined by independent One-way ANOVAs with Sidak's multiple comparisons, $P<0.05$).

The mechanism of protection in EYA1-AGS cells was further investigated by comparing proteins involved in apoptotic pathway. A dose dependent cleavage of the initiator caspase, caspase-9, effector caspase, caspase-3, inactivation of

Poly(ADP-Ribose) polymerase (PARP), and cleavage of cytokeratin-18 (M30) can be observed in AGS cells treated with 10 and 20mM aspirin (Figure 4.3).

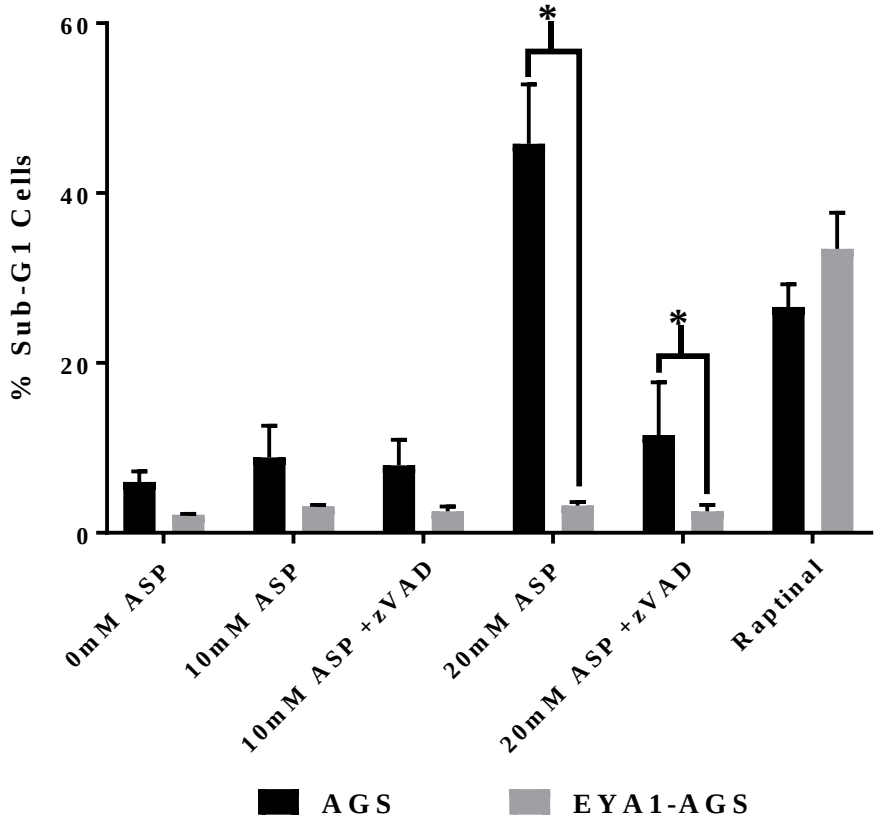

Figure 4.2 Flow cytometric analysis of sub-G1 cell cycle DNA content in AGS and EYA1-AGS cells, following treatment with either DMSO (vehicle control), 10/20mM aspirin for 48h or 10μM raptinal for 1.5h. For combination treatments, cells were pre-treated with 30μM zVAD for 1h and co-incubated with aspirin and zVAD for 48h. For each measurement, 40,000 cells were analysed using the BL-3 fluorescence channel. Error bars indicate standard deviation for each set of data (n=3) and '*' denotes a $p<0.05$.

Conversely, the same concentrations of aspirin did not cause cleavage of any of the aforementioned markers of apoptosis in EYA1-AGS cells. EYA1 overexpression could not however prevent the cleavage of cytokeratin-18, PARP and caspases when treated with raptinal.

To determine whether the EYA1-mediated protection was exclusive to aspirin-mediated cytotoxicity, the effect of other pro-apoptotic compounds, covering a diverse set of mechanisms, was assessed in AGS and EYA1-AGS cells. This included a kinase inhibitor (staurosporine), ER/proteasome inhibitor (tunicamycin) and ROS inducing

agent (brefeldin A). After 24h of drug exposure, the caspase cascade was only activated in AGS cells treated with aspirin and brefeldin A (Figure 4.4). All pro-apoptotic agents had no effect on XIAP protein expression in both cell lines except staurosporine, which caused a 25% decrease in AGS cells.

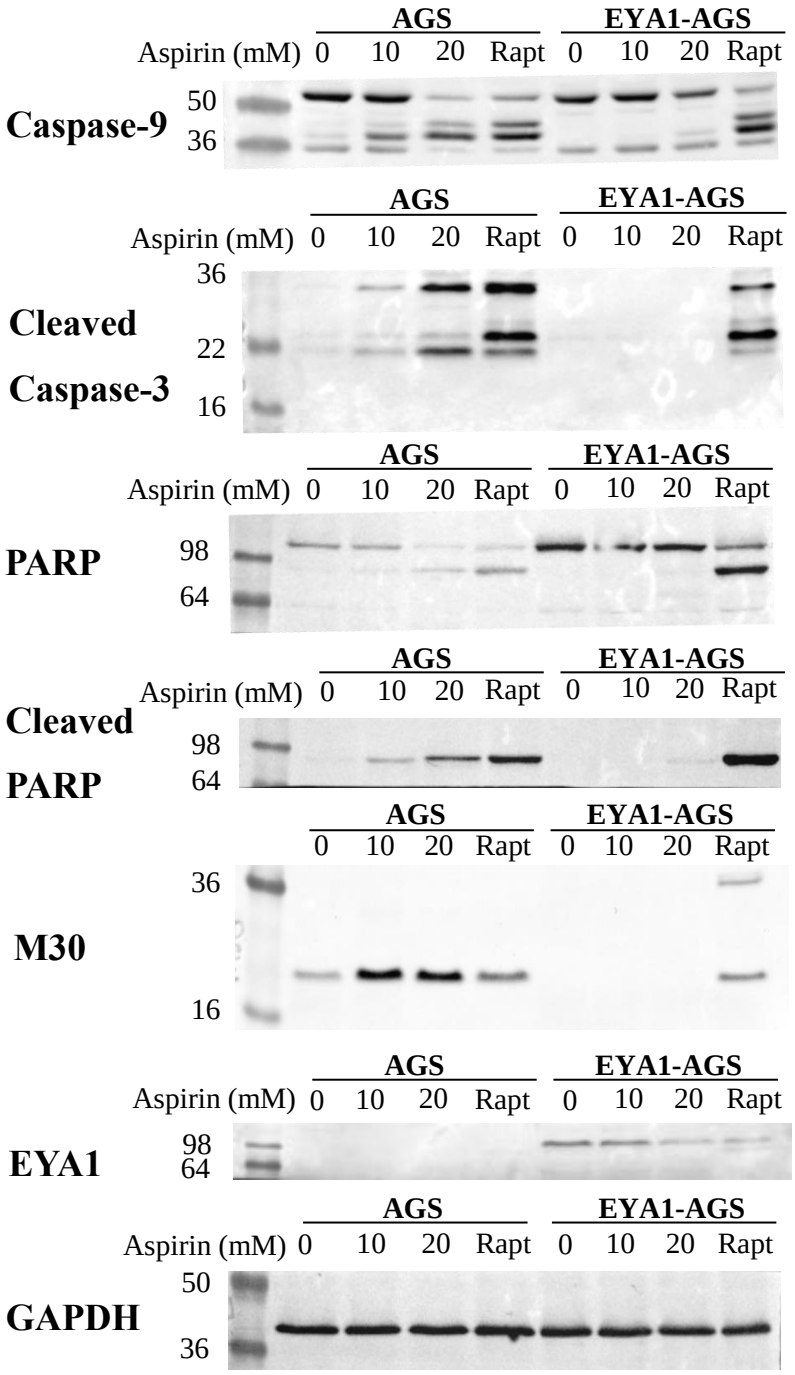

Figure 4.3 EYA1 overexpression protects against aspirin-induced activation of the caspase cascade. AGS and EYA1-AGS cells were treated with aspirin (10 and 20mM) for 48h or 10μM raptinal for 1.5h. Protein lysates from each sample were analysed by western blotting for eyes absent homolog 1 (EYA1), Glyceraldehyde 3-phosphate dehydrogenase (GAPDH), cleaved poly ADP ribose polymerase (PARP), full length PARP, cleaved cytokeratin-18 (M30), caspases-3 and caspase-9.

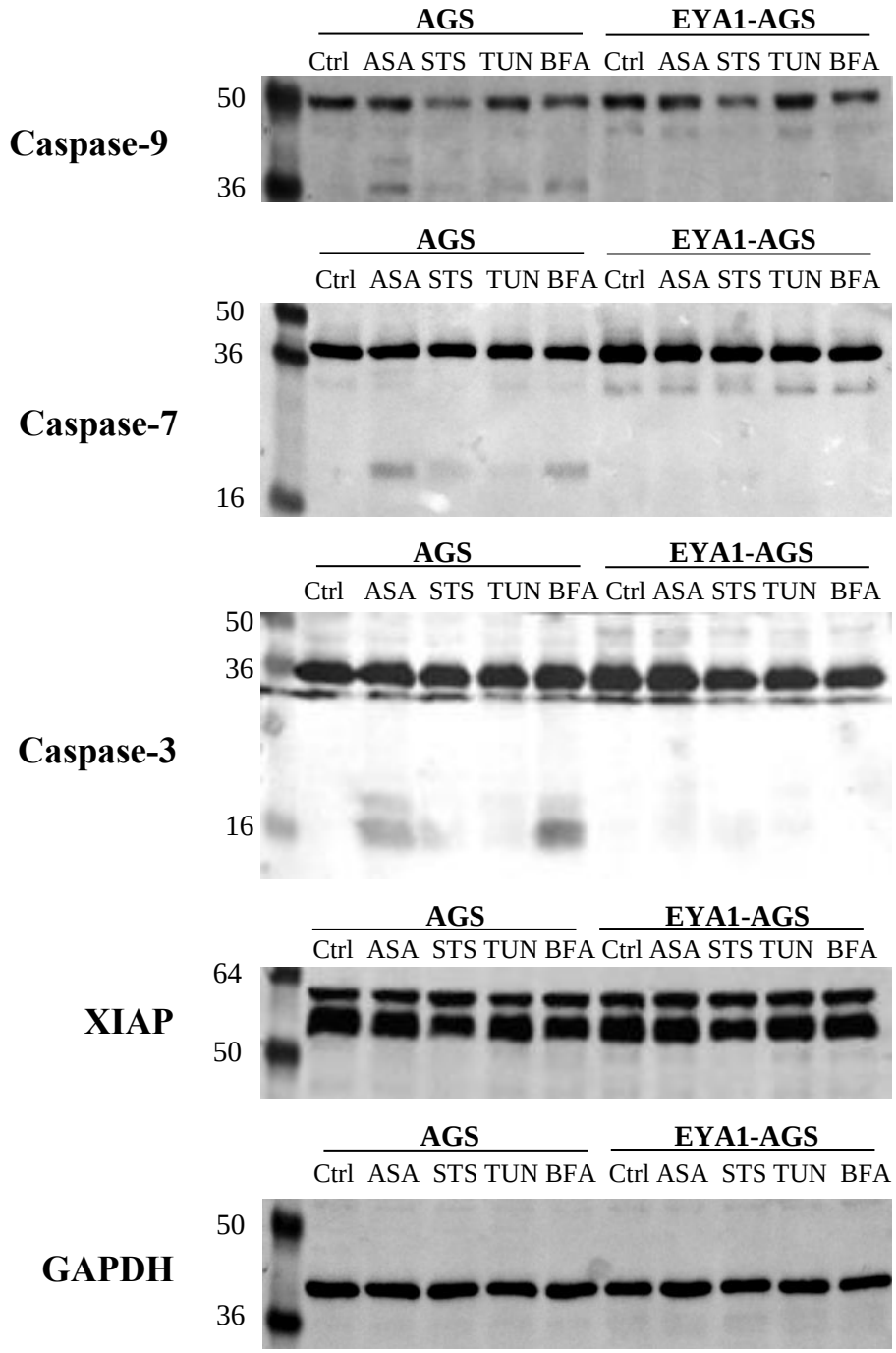

Figure 4.4 Aspirin and brefeldin A triggers the apoptotic pathway in AGS but not EYA1-AGS cells. Cells were exposed to 20mM aspirin (ASA), 5μM staurosporine (STS), 20μM tunicamycin A (TUN) and 20μM brefeldin A (BFA) for 24h. Levels of X-linked inhibitor of apoptosis protein (XIAP), cleaved caspase-9, -7 and -3 were measured by western blot. GAPDH was used as a loading control (n=1).

4.3.2 **Apoptosis induced by BCL-X_L and MCL-1 inhibition is abated by EYA1 overexpression**

Since the mode of aspirin-induced death is at least partly caused by caspase-9 activation, the role of the BCL-2 family (pro- and anti-apoptotic) proteins was investigated between AGS and EYA1-AGS cell lines. BCL-X_L (A-1331852) and MCL-1 (S63845) inhibitors were both shown to be ineffective in inducing apoptosis in EYA1-AGS cells. A statistically significant reduction in sub-G1 content was observed in EYA1-AGS cells treated with A-1331852 and A-1331852 in combination with S63845 compared to native AGS cells (Figure 4.5). These findings were mirrored by caspase-3 and PARP western blots demonstrating that cleavage of these apoptotic markers was only observed in AGS cells treated with A1331852 and A1331852-S63845 combination (Figure 4.6). S63845 alone did cause slight cleavage of caspase-3 and PARP in AGS cells, which supports the slight increase in sub-G1 shown in Figure 4.5.

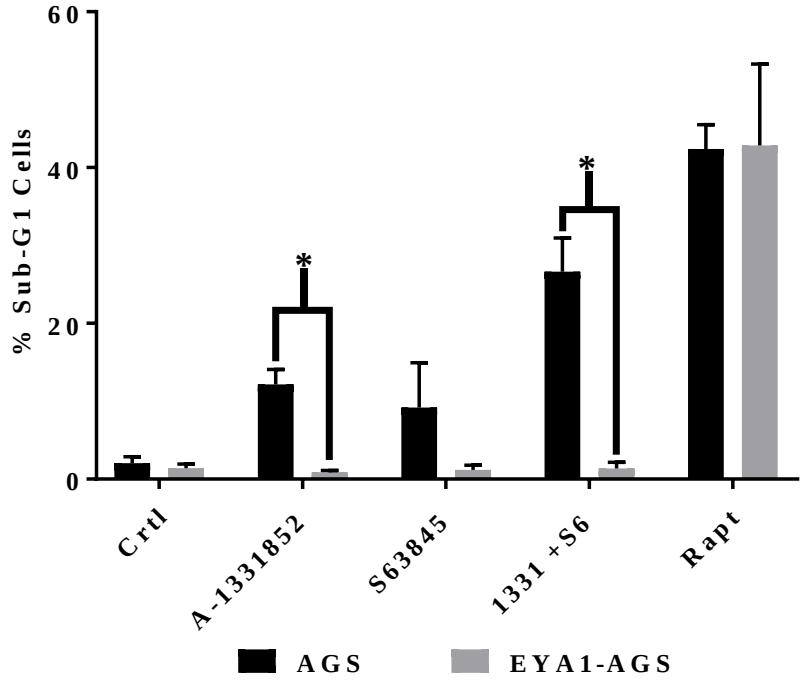

Figure 4.5 Sub-G1 analysis of AGS and EYA1-AGS cells treated with 100nM of either A-1331852 (BCL-X_L inhibitor) or S63845 (MCL-1 inhibitor) alone and combined for 3h. Raptinal (10μM) was used as a positive control. The percentage of cells in sub-G1 were analysed using 40,000 cells from each treatment and the BL-3 fluorescence channel. Error bars indicate standard deviation for each set of data (n=3) and "*" denotes a $p<0.05$.

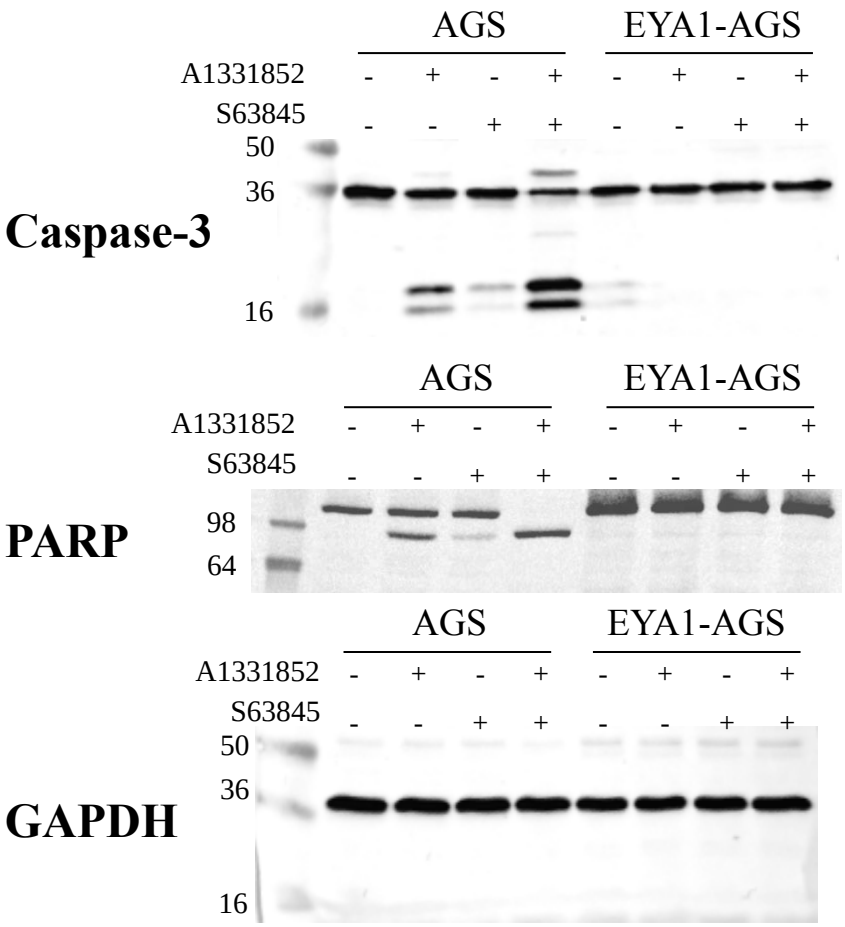

Figure 4.6 EYA1 overexpression in AGS cells protects against BH3-mimetic induced caspase-3 and PARP processing. AGS and EYA1-AGS cells were treated with 100nM of either A1331852 (BCL-X_L inhibitor) or S63845 (MCL-1 inhibitor) alone or in combination for 3h. Caspase-3 and PARP cleavage was measured using western blotting, using GAPDH as a loading control (n=1).

To identify the point at which the protective effect of EYA1 expression intercepts the apoptotic signalling caused by aspirin, proteins further upstream of caspase-9 cleavage were investigated. Generally, A1331852 and S63945 treatment did not cause a change in expression of any BCL-2 family proteins.

4.3.3 Effect of EYA1 overexpression on BAX, BCL-2 and BCL-X_L protein expression

Pro-apoptotic protein, BAX, was significantly decreased in EYA1-AGS cells compared to AGS cells. BAK (25kDa band) expression was however comparable between the two cell lines. In regards to the anti-apoptotic BCL-2-family proteins, MCL-1 expression remained constant between cell lines, except for a significantly

reduced expression in AGS cells co-treated with both BH3-mimetics. Unexpectedly, expression of BCL-2 and BCL-X_L protein was markedly reduced in EYA1-AGS cells (Figure 4.7).

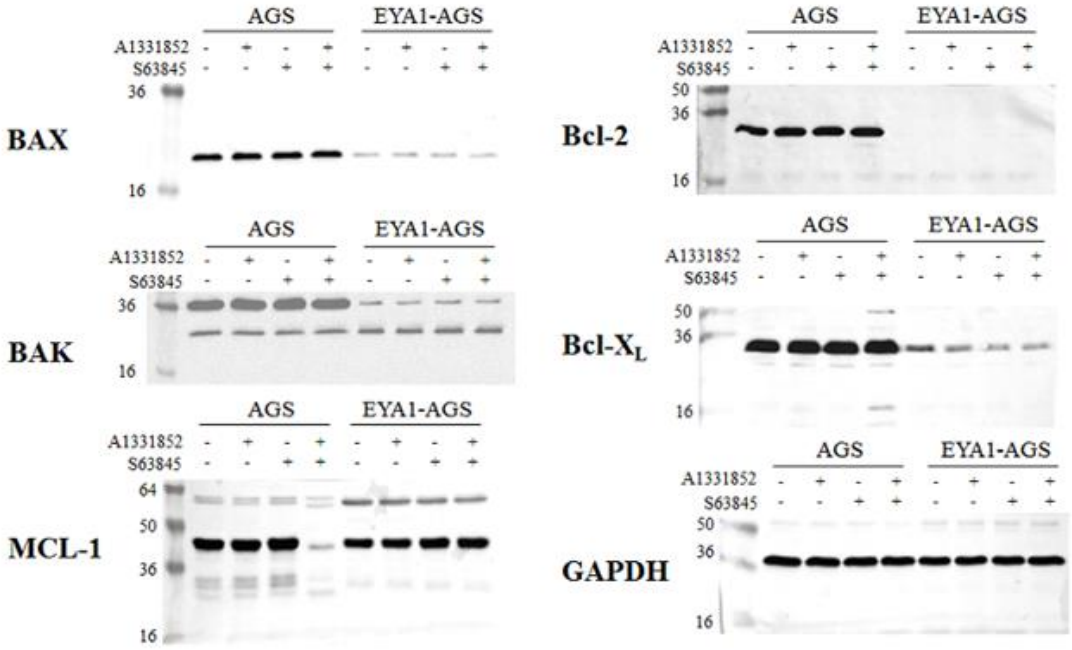

Figure 4.7 Over-expression of EYA1 in AGS cells causes reduced expression of both the pro-apoptotic protein BAX, and anti-apoptotic proteins BCL-2 and BCL-X_L. AGS and EYA1-AGS cells were treated with BH3 mimetics alone or in combination for 3h.BCL-2 and BH3-only protein levels were measured by western blot.

4.4 **Discussion**

Aspirin-induced AGS toxicity was abated by both zVAD co-treatment and EYA1 overexpression, as determined by sub-G1 analysis (Figure 4.2). This suggests that both aspirin toxicity and the protective effect of EYA1 are heavily linked to apoptotic cell death. By contrast, although raptinal-induced apoptosis can also be blocked by the pan-caspase inhibitor Q-VD-OPh[498], EYA1 over-expression did not have any effect. The lack of protection against raptinal toxicity was either because the mechanism of apoptosis is not through the same pathway, or because the induction of apoptosis is so rapid.

EYA1-AGS cells seemed to have a lower basal sub-G1 count compared to native AGS cells (Figure 4.2). This is initial evidence that the protective effects of EYA1 overexpression occurs upstream of any apoptotic machinery such as caspase activation

or MOMP. This hypothesis was supported by the absence of aspirin-induced caspase 3/9, keratin (M30) and PARP cleavage in EYA1-AGS cells (Figure 4.3).

Staurosporine and tunicamycin failed to induce apoptosis in the native AGS cell line (Figure 4.4). These results contradict previous findings that show staurosporine causes toxicity to AGS cells at nanomolar concentrations as early as 3 hours[507,508]. Tunicamycin alone has been shown to cause only minimal toxicity in BGC823 and SGC7901 gastric cell lines[509,510], but potently sensitizes cells to TRAIL induced apoptosis[509-511]. Higher concentrations and longer treatment times will need to be tested to optimise the use of these apoptotic agents with AGS cells.

Brefeldin A and aspirin caused partial caspase-7 and 9 activation and noticeable caspase-3 activation (Figure 4.4). This finding supports previous reports that brefeldin A causes cytotoxicity to gastric carcinoma cell lines, MKN-1 and KATOIII, at nanomolar concentrations[512]. Caspase cleavage was however blocked in EYA1-AGS cells with both aspirin and brefeldin A treatments. This could suggest that EYA1 may play a part in alleviating ER stress. To test this hypothesis, ER stress protein levels (e.g. C/EBP homologous transcription factor (CHOP), glucose-regulated protein (GRP) 78 and GRP94) could be compared in EYA1 overexpressed and native AGS cells. Aspirin causes ER stress by initiating PERK-mediated phosphorylation and inhibition of eukaryotic initiation factor 2α (eIF2α), a protein that catalyses the initiation of protein synthesis[513]. Given that EYA1 acts as a phosphatase[360], it could theoretically dephosphorylate and therefore inactivate PERK. However, since EYA1 localises to the nucleus, not the ER, it is more likely to exert its protective effect by promoting repair pathways.

Since EYA1 overexpression inhibits apoptosis upstream of caspase-9 activation (Figure 4.3), BH3-mimetics were used to determine the role of EYA1 during BAX/BAK activation and MOMP. The BCL-X_L inhibitor, A133152, alone and in combination with MCL-1 inhibitor, S63845, caused significantly less apoptotic cell death in EYA1-AGS cells compared to AGS cells as shown by both reduced sub-G1 content (Figure 4.5) and the absence of caspase-3 and PARP cleavage (Figure 4.6). This suggests that MOMP plays a crucial role in aspirin-induced gastric epithelial cell death and that overexpression of EYA1 somehow blocks the activity of either BAX/BAX and/or BH-3 only proteins. EYA1 may therefore play a role in the

transcriptional or post-translational regulation of these pro-apoptotic proteins. To test these hypotheses, the expression and transcriptional activity of transcription factors that regulate pro-apoptotic genes could be studied in the response to aspirin-induced AGS cytotoxicity. A closer look at BAX/BAX activation and the release of mitochondrial proteins involved in apoptosis will also help to determine the role of EYA1 overexpression in aspirin-induced gastric cell death.

BCL-X_L and MCL-1 are members of the BCL-2 family of proteins that prevent apoptosis by binding to pro-apoptotic proteins such as BAX, BAX, BID and BH3-only activators/sensitizers[514]. As can be seen in Figure 4.7, EYA1 overexpression caused a reduction in BAX and BCL-X_L protein expression. Surprisingly, BCL-2 protein expression had also been completely abolished in EYA1-AGS cells. Whether this is a consequence of the method of transfection or a real effect of EYA1 overexpression is unclear; however it is unusual that a reduction in both BCL-X_L and BCL-2 proteins is seen in the cell line, which has shown to be more resistant to aspirin-induced apoptosis.

BCL-X_L protein levels do vary, increasing acutely following intra-and extracellular stress signalling[515]. This does not however explain why the basal levels of BCL-X_L are higher in AGS cells in the absence of any BH mimetic (Figure 4.7). Jak-mediated STAT phosphorylation promotes BCL-X_L expression[516]. Over expression of EYA1, a phosphatase, could theoretically downregulate BCL-X_L expression via STAT dephosphorylation.

BCL-2 is a protein with a notably more stable expression level[514] and, as shown in AGS cells, does not change following treatment with BH3 mimetics. BCL-2 mRNA is stabilised by nucleolin[517], a member of the ribonucleoprotein-containing family. Nucleolin binds to the ARE-1 instability element in the 3'-UTR of BCL-2 mRNA, preventing enzymatic degradation by ribonuclease. BCL-2 translation is also downregulated by two miRNAs, miR-15a and miR-16-1[517]. There are currently no reports on whether EYA1 regulates nucleolin or either of these miRNAs.

BAX expression is regulated at the transcriptional level by p53 and p73 following stress signalling. This, again, does not explain why the basal protein expression is lower in EYA1-AGS cells in the absence of BH3 mimetic treatment compared with the parental cell line (Figure 4.7). E3 ligases, such as parkin, also regulate BAX expression at the protein level by initiating ubiquitin-mediated proteasomal

degradation[518,519]. Parkin requires phosphorylation to become active[520], and so would therefore be unlikely to be the target of EYA1-mediated BAX degradation.

MCL-1 protein expression is reduced in AGS cells treated with both BH3 mimetics (Figure 4.7). The likely explanation is that MCL-1 is inactivated by caspases during apoptosis[521], potentiating release of pro-apoptotic factors. This is supported by the extensive caspase-3 cleavage observed in AGS cells and lack of cleavage of either caspase-3 or MCL-1 in EYA1-AGS cells co-treated with A1331852 and S63845 (Figure 4.6 and Figure 4.7).

Aspirin mediated gastric epithelial toxicity has shown to be mediated by the upregulation of BAX and BAK[396] and the downregulation of BCL-2[249] proteins. The decreased levels of both BAX and BCL-2 in EYA1-AGS cells may explain why aspirin seem to cause less apoptosis in the EYA1 overexpressed cell line compared to AGS cells, but further work will be needed to delineate the interactions between EYA1 and the apoptotic pathways.

There are several limitations of the work undertaken in this chapter. The EYA1 cDNA clone was transfected into the AGS genome by random insertion using transposases. This variable remains uncontrolled throughout the chapter since all comparisons are made against the parental cell line (i.e. AGS cells). A more suitable control would have been to use an AGS cell line stably transfected following the same method but using a blank vector (i.e. pSBi-puro) instead of EYA1-GFP-pSBi-puro. It will also be important to determine whether the effect of EYA1 overexpression on BCL-2 family protein can be replicated in other cell lines and to determine the mechanism of how EYA1 dysregulates the expression of these central apoptotic regulators.

Another follow-up experiment with AGS and EYA1-AGS cell lines should include comparing the extent of DNA damage and repair caused by aspirin treatment. A report by Cook *et al.* revealed that EYA1 phosphatase activity was essential for modulating apoptosis following genotoxic stress. The study found that EYA1 promotes survival by dephosphorylating histone H2AX at Tyr142 and allowing repair complexes to bind to phosphorylated Ser139[360]. Assays that assess DNA damage (e.g. COMET assays) and the phosphorylation status at Ser139 and Tyr142 on histone H2AX (analysable by western blot) should be carried out to connect aspirin toxicity to EYA1-mediated H2AX dephosphorylation. These studies should compare the effect of aspirin against

agents that are known to cause DNA damage and dephosphorylate Tyr142 on histone H2AX such as etoposide, bleomycin or gamma-irradiation[522].

In this chapter, it has been demonstrated that EYA1 overexpression provides protection to aspirin-induced apoptosis in gastric epithelial cells. This could be explained, at least in part, by the ability of EYA1 overexpression to protect against apoptosis caused by ER stress or downregulate pro-apoptotic BCL-2 family proteins. The role EYA1 plays in the other aspirin-mediated apoptotic pathways remains unclear. However, it seems that the protective effect(s) occur upstream of mitochondrial outer membrane permeabilization.

Chapter 5

Database analysis of *EYA1* and gastric injury

Contents

5.1 Introduction

An unpublished genome-wide association study (GWAS) performed at the University of Liverpool has identified an association between aspirin-induced peptic ulcer disease and an intronic SNP localised to the *EYA1* locus (Bourgeois *et al*., unpublished data).

Eyes absent homolog 1 (*EYA1*) is located in the 8q13.3 (chromosome 8, *q* arm, region 1 band 3, sub-band 3) region after positional cloning identified a family-inherited BOR-causing mutation[364]. The *EYA1* gene consists of 16 exons that, to date, encode four known isoforms (Table 5.1). EYA1B and EYA1C, both referred to as isoform 1, share the same amino acid sequence and are the longest isoforms, each consist of 592 amino acids. EYA1D, alternately named isoform 3, and EYA1 isoform 4 are both 586 amino acids long but do not share the same amino acid sequence. EYA1 isoform 5, the shortest isoform, containing 470 amino acids due to a much shorter N-terminus than the other EYA1 isoforms[486]. The *EYA1* gene also has fourteen predicted transcripts, eleven of which encode a protein with a slightly longer N-terminus.

Though the EYA1 orthologue, *eya1*, and other genes within the retinal determination gene network (RDGN) were originally defined by their role in Drosophila eye morphogenesis, studies of metazoan EYA1 has unveiled its role in a wide variety of signalling pathways. These include the development and homeostasis of the eye[523,524], ear[368,525,526], kidney[364,368,526,527], lungs[528], muscle[364,528,529] and nervous system[530,531].

EYA proteins contain a highly conserved 271 amino acids C-terminal motif (Table 5.2) named the EYA domain (ED). The ED interacts with SIX and DACH proteins to form a composite transcription factor[355,481,532,533]. The genes that encode these proteins, along with the *PAX* family genes (most notably *PAX2* and *PAX6*), consist of the core genes that form the retinal determination network[534]. The ED was more recently found to possess motifs characteristic of the haloacid dehalogenase class of enzymes that provide phosphatase activity. This enzymatic motif demonstrates dual specificity for phospho-threonine residues on MYC[386] (cell cycle progression vs. growth arrest) and phospho-tyrosine residues on H2AX[355-357] (DNA-damage repair vs. apoptosis) and ERβ[535] (Six-independent transcriptional regulation).

Table 5.1 Comparison between the amino acid sequences of each EYA1 isoform. The longest isoform, isoform 1 (NP_000494.2), was used as the reference sequence to compare against isoforms 3 (NP_742056.2), 4 (NP_001275503.1) and 5 (NP_001275504.1). Alterations in the sequences are represented by highlighted substitutions, insertions or deletions (-).

EYA1 isoform	**1**	**3**	**4**	**5**
Amino acid comparison	MEMQDLTSPHSRLSGSSESPSG PKLGNSHINSNSMTPNGTEVKT EPMSSSETASTTADGSLNNFSG SAIGSSSFSPRPTHQFSPPQIYPS NRPYPHILPTPSSQTMAAYGQT QFTTGMQQATAYATYPQPGQP YGISSYGALWAGIKTEGGLSQS QSPGQTGFLSYGTSFSTPQPGQ APYSYQMQGSSFTTSSGIYTGN NSLTNSSGFNSSQQDYPSYPSF GQGQYAQYYNSSPYPAHYMTS SNTSPTTPSTNATYQLQEPPSGI TSQAVTDPTAEYSTIHSPSTPIK DSDSDRLRRGSDGKSRGRGRR NNNPSPPPDSDLERVFIWDLDE TIIVFHSLLTGSYANRYGRDPPT SVSLGLRMEEMIFNLADTHLFF NDLEECDQVHIDDVSSDDNGQ DLSTYNFGTDGFPAAATSANLC LATGVRGGVDWMRKLAFRYR RVKEIYNTYKNNVGGLLGPAK REAWLQLRAEIEALTDSWLTL ALKALSLIHSRTNCVNILVTTTQ LIPALAKVLLYGLGIVFPIENIYS ATKIGKESCFERIIQRFGRKVVY VVIGDGVEEEQGAKKHAMPFW RISSHSDLMALHHALELEYL	MEDPRGINGQSVQTSQASSDVA VSSSCRSMEMQDLTSPHSRLSGS SESPSGPKLGNSHINSNSMTPNGT EVKTEPMSSSETASTTADGSLNN FSGSAIGSSSFSPRPTHQFSPPQIY PSNRPYPHILPTPSSQTMAAYGQ TQFTTGMQQATAYATYPQPGQP YGISSY-----GIKTEGGLSQSQSP GQTGFLSYGTSFSTPQPGQAPYS YQMQGSSFTTSSGIYTGNNSLTN SSGFNSSQQDYPSYPSFGQGQYA QYYNSSPYPAHYMTSSNTSPTTP STNATYQLQEPPSGITSQAVTDPT AEYSTIHSPSTPIKDSDSDRLRRG SDGKSRGRGRRNNNPSPPPDSDL ERVFIWDLDETIIVFHSLLTGSYA NRYGR---------- ----------ECDQVHIDDVSSDD NGQDLSTYNFGTDGFPAAATSA NLCLATGVRGGVDWMRKLAFR YRRVKEIYNTYKNNVGGLLGPA KREAWLQLRAEIEALTDSWLTLA LKALSLIHSRTNCVNILVTTTQLIP ALAKVLLYGLGIVFPIENIYSATK IGKESCFERIIQRFGRKVVYVVIG DGVEEEQGAKKHAMPFWRISSH SDLMALHHALELEYL	MEMQDLTSPHSRLSGSSESPSGP KLGNSHINSNSMTPNGTEVKTEP MSSSETASTTADGSLNNFSGSAIG SSSFSPRPTHQFSPPQIYPS--KPY PHILPTPSSQTMAAYGQTQFTTG MQQATAYATYPQPGQPYGISSY- ----GIKTEGGLSQSQSPGQTGFL SYGTSFSTPQPGQAPYSYQMQGS SFTTSSGIYTGNNSLTNSSGFNSS QQDYPSYPSFGQGQYAQYYNSS PYPAHYMTSSNTSPTTPSTNATY QLQEPPSGITSQAVTDPTAEYSTI HSPSTPIKDSDSDRLRRGSDGKSR GRGRRNNNPSPPPDSDLERVFIW DLDETIIVFHSLLTGSYANRYGR DPPTSVSLGLRMEEMIFNLADTH LFFNDLEECDQVHIDDVSSDDNG QDLSTYNFGTDGFPAAATSANLC LATGVRGGVDWMRKLAFRYRR VKEIYNTYKNNVGGLLGPAKRE AWLQLRAEIEALTDSWLTLALK ALSLIHSRTNCVNILVTTTQLIPA LAKVLLYGLGIVFPIENIYSATKI GKESCFERIIQRFGRKVVYVVIGD GVEEEQGAKKHAMPFWRISSHS DLMALHHALELEYL	---------- ---------- ---------- ---------- ----------MQQATAY ATYPQPGQPYGISSY -----GIKT EGGLSQSQSPGQTGFLSYGTSFS TPQPGQAPYSYQMQGSSFTTSS GIYTGNNSLTNSSGFNSSQQDYP SYPSFGQGQYAQYYNSSPYPAH YMTSSNTSPTTPSTNATYQLQEP PSGITSQAVTDPTAEYSTIHSPST PIKDSDSDRLRRGSDGKSRGRG RRNNNPSPPPDSDLERVFIWDLD ETIIVFHSLLTGSYANRYGRDPP TSVSLGLRMEEMIFNLADTHLFF NDLEECDQVHIDDVSSDDNGQD LSTYNFGTDGFPAAATSANLCL ATGVRGGVDWMRKLAFRYRR VKEIYNTYKNNVGGLLGPAKRE AWLQLRAEIEALTDSWLTLALK ALSLIHSRTNCVNILVTTTQLIPA LAKVLLYGLGIVFPIENIYSATKI GKESCFERIIQRFGRKVVYVVIG DGVEEEQGAKKHAMPFWRISSH SDLMALHHALELEYL

Table 5.2 Comparison between the amino acid sequences of the longest EYA1 isoform from humans (NP_000494.2) against chimpanzee (XP_009453767), mice (NP_001297388) and zebrafish (NP_571268) sequences. Alterations in the sequences are represented by highlighted substitutions, insertions or deletions (-). The highly conserved C-terminals are shown in red text and the three HAD motifs have been underlined.

Species	Human (*Homo sapiens)*	Chimpanzee (*Pan troglodytes*)	Mouse (*Mus musculus*)	Zebrafish (*Danio rerio*)
Amino acid comparison	MEMQDLTSPHSRLSGSSESPSG PKLGNSHINSNSMTPNGTEVKT EPMSSSETASTTADGSLNNFSG SAIGSSSFSPRPTHQFSPPQIYPS NRPYPHILPTPSSQTMAAYGQT QFTTGMQQATAYATYPQPGQP YGISSYGALWAGIKTEGGLSQS QSPGQTGFLSYGTSFSTPQPGQ APYSYQMQGSSFTTSSGIYTGN NSLTNSSGFNSSQQDYPSYPSF GQGQYAQYYNSSPYPAHYMTS SNTSPTTPSTNATYQLQEPPSGI TSQAVTDPTAEYSTIHSPSTPIK DSDSDRLRRGSDGKSRGRGRR NNNPSPPPDSDLERVFIWDLDE TIIVFHSLLTGSYANRYGRDPPT SVSLGLRMEEMIFNLADTHLFF NDLEECDQVHIDDVSSDDNGQ DLSTYNFGTDGFPAAATSANLC LATGVRGGVDWMRKLAFRYR RVKEIYNTYKNNVGGLLGPAK REAWLQLRAEIEALTDSWLTL ALKALSLIHSRTNCVNILVTTTQ LIPALAKVLLYGLGIVFPIENIYS ATKIGKESCFERIIQRFGRKVVY VVIGDGVEEEQGAKKHAMPFW RISSHSDLMALHHALELEYL	MEDPRGINGQSVQTSQASSDVA VSSSCRSMEMQDLTSPHSRLSGS SESPSGPKLDNSHINSNSMTPNGT EVKTEPMSSSETASTTADGSLDN FSGSAIGSSSFSPRPTHQFSPPQIY PSNRPYPHILPTPSSQTMAAYGQ TQFTTGMQQATAYATYPQPGQP YGISSYGALWAGIKTEGGLSQSQ SPGQTGFLSYGTSFSTPQPGQAPY SYQMQGSSFTTSSGLYTGNNSLT NSSGFNSSQQDYPSYPSFGQGQY AQYYNSSPYPAHYMTSSNTSPTT PSTNATYQLQEPPSGITSQAVTDP TAEYSTIHSPSTPIKDSDSDRLRR GSDGKSRGRGRRNNNPSPPPDSD LERVFIWDLDETIIVFHSLLTGSY ANRYGRDPPTSVSLGLRMEEMIF NLADTHLFFNDLEECDQVHIDDV SSDDNGQDLSTYNFGTDGFPAA ATSANLCLATGVRGGVDWMRK LAFRYRRVKEIYNTYKNNVGGL LGPAKREAWLQLRAEIEALTDS WLTLALKALSLIHSRTNCVNILV TTTQLIPALAKVLLYGLGIVFPIE NIYSATKIGKESCFERIIQRFGRKV VYVVIGDGVEEEQGAKKHAMPF WRISSHSDLMALHHALELEYL	MEMQDLTSPHSRLSGSSESPSGP KLDSSHINSTSMTPNGTEVKTEP MSSSEIASTAADGSLDSFSGSALG SSSFSPRPAHPFSPPQIYPS–KSYP HILPTPSSQTMAAYGQTQFTTGM QQATAYATYPQPGQPYGISSYGA LWAGIKTESGLSQSQSPGQTGFL SYGTSFGTPQPGQAPYSYQMQGS SFTTSSGLYSGNNSLTNSSGFNSS QQDYPSYPGFGQGQYAQYYNSS PYPAHYMTSSNTSPTTPSTNATY QLQEPPSGVTSQAVTDPTAEYSTI HSPSTPIKETDSERLRRGSDGKSR GRGRRNNNPSPPPDSDLERVFIW DLDETIIVFHSLLTGSYANRYGR DPPTSVSLGLRMEEMIFNLADTH LFFNDLEECDQVHIDDVSSDDNG QDLSTYNFGTDGFPAAATSANLC LATGVRGGVDWMRKLAFRYRR VKEIYNTYKNNVGGLLGPAKRE AWLQLRAEIEALTDSWLTLALK ALSLIHSRTNCVNILVTTTQLIPA LAKVLLYGLGIVFPIENIYSATKI GKESCFERIIQRFGRKVVYVVIGD GVEEEQGAKKHAMPFWRVSSHS DLMALHHALELEYL	MEMQDLASPHSRVSGSSESPNG PNIDNSHINNNSMTPNGTEGDNI TMLTTADWLLSSSSQSAAVKTE PMSSSEIATSVADGSLDSFSGSAI GTSGFSPRQTHQFSPQIYPSNRA YPHILPTPSAQNMAAYGQTQYT TGMQQAAAAYGTYPQPVQPYGIS AY- - - - -GIKTEGGLTQAQSPG QSGFLSYSSSFSTPQTGQAPYSY QMQGGSFTTTSGLYAGSNSLTN STGFNSTQQDYPSYPTFGQSQY AQYYNSSPYTSPYMTSNNTSPT TPSTTATYTLQEPPSGITSQALTE QPTGEYSTIHSPSTPIKDSDSDRL RRATDVKARGRGRRNNNPSPPP DSDLERVFIWDLDETIIVFHSLLT GSYANRFGRDPPTSVSLGLRME EMIFNLADTHFFFNDLEECDQV HIDDVSSDDNGQDLSTYNFSTD GFHAAATSANLCLATGVRGGV DWMRKLAFRYRRVKEIYTTYK NNVGGLLGPAKREAWLQLRAEI EALTDSWLTLALKALTLIHSRSN CVNILVTTTQLIPALAKVLLYGL GVVFPIENIYSATKIGKESCFERV IQRFGRKVVYVVVVGDGVEEEQ GSKKHNMPFWRISSHSDLMALH HALDLEYL

The N-terminal domain (NTD) of EYA proteins, though poorly conserved, contains residues pertaining to transactivation domains[481,536] and threonine phosphatase motifs[359,537]. The currently accepted theory is that mammalian Eya1 is initially cytoplasmic and is translocated to the nucleus by interaction with Six proteins[481,538].

Though BOR-related mutations in the ED have been associated with loss of Six interaction and reduced nuclear translocation[462], the ED alone is not sufficient for nuclear translocation[481], suggesting that the N-terminal of EYA1 is also involved in nuclear translocation.

The advent of next generation sequencing and the advancement of mass spectrometric[539] techniques have allow for faster, cheaper, more precise and higher throughput methods of annotating the human genome, transcriptome and proteome. These technologies paved the way for the creation of various open-source online databases. Defining the expression, structure, function, localization and interactions of the roughly 20,000 human proteins (and their isoforms) is made possible by the openly accessible DNA[540,541], RNA[461,542-545] and protein[461,546-548] databases. These databases process large datasets from self-generated datasets and/or public archives and present the transformed data freely online for the advancement of biomedical research.

The databases used to characterise EYA1 in this chapter are The Human Protein Atlas (HPA), EMBL-EBI Expression Atlas and GTEx portal for gene expression data. HPA, ProteomicsDB and the Human Proteome Map for tissue protein expression. ProteomicsDB, PeptideAtlas and Global Proteome Machine Database (GPMdb) were used to describe peptide-based identifications of the human EYA1 protein. Finally, the Gene Atlas Phenome-wide association study (PheWAS) database was used for identifying associations between SNPs and gastric injury phenotypes (Table 5.3).

Using the search term "EYA1" in the NCBI ClinVar database[549] (https://www.ncbi.nlm.nih.gov/clinvar/), over 150 causative variants have been identified in *EYA1* for BOR and BOR-like syndromes. There is also a growing area of research in elucidating the roles of ectopic *EYA1* expression and *EYA1* mutations in the development of a plethora of cancers[370].

Table 5.3 Online database resources used to gather information on gene/protein expression and disease causing variants of *EYA1*/EYA1.

Database type	Database name	URL	Reference
Gene expression	The Human Protein Atlas (HPA)	https://www.proteinatlas.org	[461]
	EMBL-EBI Expression Atlas	https://www.ebi.ac.uk/gxa	[545]
	Genotype-Tissue Expression (GTEx) Portal	https://www.gtexportal.org	[542]
	Functional ANnoTation Of Mammalian Genome (FANTOM)	http://fantom.gsc.riken.jp/5	[550]
Protein Expression	HPA	https://www.proteinatlas.org	[461]
	ProteomicsDB	https://www.proteomicsdb.org	[548]
	Human Proteome Map (HPM)	http://www.humanproteomemap.org	[547]
	PeptideAtlas	http://www.peptideatlas.org	[551]
	Global Proteome Machine Database (GPMdb)	https://gpmdb.thegpm.org/	[552]
GWAS/ PHEWAS	Gene Atlas	http://geneatlas.roslin.ed.ac.uk	[553]

The aims of this chapter was to utilise publically available online databases to (i) characterize the gene and protein expression of EYA1 across different human tissues, (ii) determine the association of EYA1 SNPs with gastric injury phenotypes and (iii) characterise the top hit from the aspirin-gastric ulcer GWAS, (rs12678747), in relation to its genomic context, population diversity and effects on transcript and protein expression. A haplotype analysis was performed using the HaploReg database to assess other variants in linkage disequilibrium with rs12678747.

5.2 **Databases**

5.2.1 **Human Protein Atlas (HPA)**

Transcriptomic data collection

The HPA is a Swedish-based program started in 2003 that use various technologies to generate RNA and protein expression data of all human proteins in healthy human tissue. Within the HPA Tissue Atlas, data is sourced from three gene expression databases, namely HPA, GTEx and FANTOM. RNA-seq data from HPA covers 64 cell lines (Cell Atlas) and 37 tissue samples (Tissue Atlas) using Illumina HiSeq2000 and 2500. More information about the cell lines and tissue samples can be found at the following sites: www.proteinatlas.org/learn/cellines and www.proteinatlas.org/ about/assays+annotation. Averaged abundance is reported as 'Transcripts Per Million' (TPM) and represents the sum of all protein coding transcripts for EYA1. RNA-seq data from GTEx and FANTOM5 CAGE that measure EYA1 transcript levels in various tissues are also displayed in the HPA Tissue Atlas (described in section 5.2.2).

The final set of collated data available from the Pathology Atlas section of HPA is EYA1 RNA expression data from 17 of the most common cancer types (representing 21 cancer subtypes). The data was generated in systems-based analysis of the transcriptome of 7932 patients (Table 5.4). Survival analysis for low (<0.069 FPKM, n=193) and high (>0.069 FPKM, n=161) *EYA1* expression in 354 stomach cancer patients was also obtain from the Pathology Atlas dataset (Table 5.5). The publicly available information was obtained from The Cancer Genome Atlas Genomic Data Commons (TCGA-GDC) project and expressed as 'number Fragments Per Kilobase of exon per Million reads' (FPKM).

Table 5.4 Sample sizes for each of the 21 cancer subtypes included in the analysis of EYA1 expression from the Pathology Atlas on Human Protein Atlas (n=7932). Data was sourced from the TCGA-GDC Data Portal [date accessed 03/08/18].

HPA cancer type	TCGA cancer	No. of samples in TCGA
Breast cancer	Breast Invasive Carcinoma (BRCA)	1075
Cervical cancer	Cervical Squamous Cell Carcinoma and Endocervical Adenocarcinoma (CESC)	291
Colorectal cancer	Colon Adenocarcinoma (COAD)	438
	Rectum Adenocarcinoma (READ)	159
Endometrial cancer	Uterine Corpus Endometrial Carcinoma (UCEC)	541
Glioma	Glioblastoma Multiforme (GBM)	153
Head and neck cancer	Head and Neck Squamous Cell Carcinoma (HNSC)	499
Liver cancer	Liver Hepatocellular Carcinoma (LIHC)	365
Lung cancer	Lung Adenocarcinoma (LUAD)	500
	Lung Squamous Cell Carcinoma (LUSC)	494
Melanoma	Skin Cutaneous Melanoma (SKCM)	102
Ovarian cancer	Ovary Serous Cystadenocarcinoma (OV)	373
Pancreatic cancer	Pancreatic Adenocarcinoma (PAAD)	176
Prostate cancer	Prostate Adenocarcinoma (PRAD)	494
Renal cancer	Kidney Chromophobe (KICH)	64
	Kidney Renal Clear Cell Carcinoma (KIRC)	528
	Kidney Renal Papillary Cell Carcinoma (KIRP)	285
Stomach cancer	Stomach Adenocarcinoma (STAD)	354
Testis cancer	Testicular Germ Cell Tumor (TGCT)	134
Thyroid cancer	Thyroid Carcinoma (THCA)	501
Urothelial cancer	Bladder Urothelial Carcinoma (BLCA)	406

Table 5.5 Patient information for those included in the survival analysis dataset from the Pathology Atlas on Human Protein Atlas [date accessed 03/08/18]. Data was sourced from the TCGA-GDC Data Portal (Project ID, TCGA-STAD).

Patient metric		Number of samples in TCGA
State	**Alive**	208
	Dead	146
Gender	**Male**	229
	Female	125
Cancer stage	**i**	48
	ii	110
	iii	146
	iv	35
	n/a	15

The search term ‘EYA1’ was entered into the HPA search function with the ‘Field’ set to ‘All’. All HPA data and figures were extracted from the EYA1 HPA profile on 03/08/18 (https://www.proteinatlas.org/ENSG00000104313-EYA1).

Proteomic data collection

As well as hosting extensive transcriptomic data, the HPA provides a map of 90% of the putative human proteome by comparing its transcriptomic data with microarray-based immunohistochemistry and immunocytochemistry using samples representing all major tissues and organs (n=44). The immunofluorescent (IF) images obtained from the HPA ‘Cell Atlas’ (date accessed [03/08/18]) provide information on the intensity, subcellular localisation and variations observed across different cell lines (termed single-cell variations) of stained EYA1 protein at the single cell level.

The rhabdomyosarcoma cell line RH-30 was selected for IF staining of EYA1 due to having one of the highest RNA expression profiles (Figure 5.1D). Though displaying a relatively low RNA expression for EYA1 (Figure 5.1D), the U-2 OS cell line was selected as part of a project at HPA to characterise the entire human proteome in one cell line. To aid in determining the subcellular localisation of target proteins, cells are also counter-stained for nuclei (DAPI), microtubules (anti-tubulin) and the endoplasmic reticulum (anti-calreticulin/anti-KDEL). The EYA1 primary antibody used for this experiment was used at a dilution of 1:44. The ‘Protein Epitope Signature Tag’ (PrEST)-produced antibody is available from Abcam, Cambridge, UK (HPA028917) and targets amino acid 155-300 of the EYA1 peptide sequence (NP_000494.2). A colorimetric view showing intensity is provided for each IF stain and ranked negative, weak, moderate or strong depending on laser power/detector gain settings required to capture optimal images, as well as the visual appearance of the stain.

HPA also has a repository of immunohistochemical images of up to 44 normal and 20 cancer tissues as a part of the Tissue Atlas and Pathology Atlas of each protein. Unfortunately, the images for EYA1-stained healthy and cancer tissue are currently ‘Pending normal/cancer tissue analysis’.

5.2.2 **Other transcriptomic databases**

Genotype-Tissue Expression (GTEx) Portal

The GTEx project, funded by the National Institute of Health (NIH), provides a resource that describes how genetic variations alter gene expression by comparing global RNA expression within individual tissues. Identified correlations between expression and genetic variation are termed expression quantitative trait loci (eQTLs).

The GTEx data acquired from the HPA 'Tissue Atlas' (see section 5.2.1) included RNA-seq (Illumina HiSeq 2000) analysis of 5798 samples from 31 tissues. Like HPA, GTEx data is based on a 'Collapsed Gene Model', where expression is given as the sum of all EYA1 transcripts in 'Read Per Kilobase of transcript per Million' (RPKM).

A search using the 'Single-Tissue eQTLs' function was performed firstly to identify eQTLs for EYA1 in all tissues types, as well as only stomach tissue, from the GTEx Analysis Release V7 (dbGaP Accession phs000424.v7.p2) data source. A second search using the 'Single-Tissue eQTLs' function was performed to identify eQTLs associated with the EYA1 single nucleotide polymorphism, rs12678747.

Functional ANnoTation Of Mammalian Genome (FANTOM)

The FANTOM5 project utilises both high-throughput Cap Analysis of Gene Expression (CAGE) and next-generation sequencing techniques to provide extensive tissue-specific expression profiles[554]. The FANTOM data, originating from the FANTOM5 repository, was obtained from the HPA 'Tissue Atlas' (see section 5.2.1) and included EYA1 transcriptomic analysis from 36 distinct tissues, presented as 'Tags Per Million' (TPM).

EMBL-EBI Expression Atlas

The Expression Atlas is another open source database that acts as a central resource for expression profiles, collating results from other tissue archives including HPA (https://www.ebi.ac.uk/gxa/experiments/E-PROT-3/Results), GTEx (https://www.ebi.ac.uk/gxa/experiments/E-MTAB-5214) and FANTOM5 (https://www.ebi.ac.uk/gxa/experiments/E-MTAB-3358/Results). Other projects in the Expression Atlas database include the Human Developmental Biology Resource (HBDR; https://www.ebi.ac.uk/gxa/experiments/E-MTAB-4840/Results) which shows foetal expression of EYA1

from 26 days post-conception to 20 weeks post-conception, NIH Roadmap Epigenomics (https://www.ebi.ac.uk/gxa/experiments/E-MTAB-3871/Results), ENCODE (https://www.ebi.ac.uk/gxa/experiments/E-MTAB-4344/Results), Illumina Body Map (https://www.ebi.ac.uk/gxa/experiments/E-MTAB-513/Results).

All datasets are converted to 'Transcripts Per Million' (TPM) to allow for cross comparison between studies. Any reads below the minimum thresholds for detection were designated as having expression values of zero. EYA1 expression data was obtained from Expression Atlas by searching for the 'EYA1' gene and selecting 'Homo sapiens' under the 'Organism' tab.

Raw expression was extracted from the 'Baseline expression' tab (date accessed [04/08/18]) and average TPMs for each tissue were determined by taking the sum of all reported TPMs for that tissue and dividing by the number of studies that contained EYA1 expression data for that tissue.

5.2.3 **Other proteomic databases**

To characterise EYA1 protein expression, this subsection will focus on three databases with information on tissue-specific expression, HPA[461], Human Proteome Map[547] and ProteomicsDB[548], as well as two of the largest human peptide-based resources, namely Peptide Atlas[551] and GPMDB[552].

Human Proteome Map (HPM)

The HPM provides a 'draft map' of 17,294 protein-coding genes within the human proteome, which accounts for >84% of all annotated proteins. The project involved performing proteomic profiling of 30 histologically healthy tissues (17 adult, 7 foetal and 6 primary haematopoietic cells) using high resolution and accuracy Fourier transform LC-MS/MS and Orbitrap mass analyser. Data from the mass spectroscopy analysis can be searched for on the HPM online web tool. The tissue-based protein expression is also summarized in a heatmap-style image for each gene entered into the query. More detailed information of the methods used can be found in the article publish by Kim *et al.*, 2014[547].

Human adult samples were harvested post-mortem from three donors for lung, heart, liver, gall bladder, adrenal gland, kidney, urinary bladder, prostate, testis, ovary, rectum, colon, pancreas, oesophagus, retina and frontal cortex tissue. Samples from

foetuses consist of heart, liver, testis, ovary, gut, placenta and brain tissue. Haematopoietic cells were obtained by leukapheresis from healthy volunteers undergoing routine blood tests and include platelets, monocytes, natural killer (NK) cells, B cells, CD4+ and CD8+ T cells.

Queries were made on the HPM web tool (date accessed [05/08/18]) to view tissue-based protein expression of EYA1 and GAPDH. For comparison, GAPDH expression was included alongside EYA1 in the tissue-based profiling.

ProteomicsDB

Though PRIDE[555] is the current community-standard for publishing raw peptide and protein identification results, it does not provide an intuitive interface for comparing and visualising proteomic datasets. Other proteomic databases such as neXtProt[556] PaxDb[557] and MaxQB[558] lack peptide identification information, contain less comprehensive repositories, do not allow cross dataset comparisons or storage of other data types (transcriptomics, interaction networks, etc.) and experimental setups (treatments and other conditions).

ProteomicsDB was released in 2014 to fill this gap by providing a means to store and visualise large collections of quantitative mass spectrometry. The online web tool contains data from 408 experiments from 78 projects, with 19,000 LC-MS/MS results that covers 80% of the human proteome. The expression feature can be used to explore protein abundance across hundreds of tissues, body fluids and cell lines through both a body heatmap and cell type bar chart.

Proteomic results were obtained from the ProteomicsDB online web tool by entering "EYA1" into the "Human Proteins" database and selecting information from the "Sequence coverage" and "Expression" tabs of the Eyes absent homolog 1 (Q99502) profile (date accessed [05/07/18]). References to the projects that identified peptides of EYA1 are listed in Table 5.6.

PeptideAtlas

In 2004, PeptideAtlas published their first set proteomic data, which identified peptides mapping to 27% of human genes with false discovery rates (FDR) reaching over 10%[559]. PeptideAtlas now contains LC-MS/MS proteomic data for various eukaryotes, with all experimental data published in the public domain. The human

database being a compendium of 1426 distinct experiments from laboratories around world. The latest 'Human all proteome' build (database reference: THISP_2017-10-01) available from the PeptideAtlas website now reports a coverage of over 85% of the human proteome with an FDR of around 1% reported in their latest general publication[560].

Unlike other large, community-shaping proteomic data repositories, such as PRIDE and the Global Proteome Machine Database (GPMDB), PeptideAtlas includes only high quality datasets with high confidence peptide identifications, as assessed by PeptideProphet[561]. The data are then searched against a contaminant database (e.g. cRAP, common Repository of Adventitious Proteins, www.thegpm.org/crap) and reprocessed through a stringent pipeline with a PSM FDR threshold of 0.0002.

A query for the EYA1 protein accession "Q99502" was searched within the "Human" build type and data on distinct observed peptides was extracted from the results (date accessed [07/08/18]). Peptides are each denoted by an accession number that can be searched on the PeptideAtlas home page to provide more information on the data sources, spectra images and genomic and proteomic mapping of the observed sequence.

Global Proteome Machine Database (GPMDB)

The main limitation of proteomic data is that the rate that it can be produced, far out paces the rate at which it can be analysed. Hundreds of thousands of spectra for tens of thousands of proteins are routinely produced by high performance mass spectrometry experiments. Vast amounts of this data is submitted to public databases and remains untouched aside from being used for proteomic mapping[552].

Table 5.6 ProteomicsDB projects that reported EYA1 peptides using LC-MS/MS. Information for projects without a PubMed ID can be found at the following links: [a]https://www.proteomicsdb.org/proteomicsdb/#projects/12, [b]https://www.proteomicsdb.org/proteomicsdb/#projects/4048 and [c]https://www.proteomicsdb.org/proteomicsdb/#projects/4155. The [d]CPTAC_phaseII_ovarian_cancer_tissue project is a private project meaning the experimental information is not available.

Project Name	PubMed ID/ project link	Experiment Name	Unique Peptides	Unique peptide spectra matches (PSM)	Sequence coverage (%)
Pirmoradian_MCP_2013[562]	23878402	Full proteome	2	5	5
Shiromizu_JPR_2013[563]	23312004	SW_SILAC	1	28	1
Geiger_MCP_2012[564]	22278370	Proteome profiling of 11 cell lines	1	1	1
Moghaddas_CellReports_2013[565]	23933261	deep proteome of 9 cell lines	1	3	1
Mertins_NatMethods_2013[566]	23749302	High coverage pSTY proteome	1	4	1
Cutler_PeptideAtlas_TissueProteomes	[a]	Roche_human_platelets_lysate	1	9	1
PeptideAtlas_Build2012_SpecLib	[b]	Consensus data	1	1	3
Cellzome_adopted	[c]	Placenta (P76637)	1	1	3
Cho_ClinProteomics_2013[567]	23394617	Quantitative proteomic analysis of primary amniocytes	1	14	4
Phanstiel_NatMethods_2011[568]	21983960	8plex_phospho_biorep3	1	448	4
Nagaraj_MSB_2011[569]	22068331	Deep proteome of HeLa cells	2	10	6
Mertins_TCGA_Nature_2015[570]	23000897	TCGA_A7-A0CD-01A_C8-A12W-01A_AN-A0AL-01A_Proteome_BI_20130913	1	9	1
CPTAC_phaseII_ovarian_cancer_tissue	[d]	IschemiaOC_Proteome_PNNL	1	1	1
Pandey_Nature_2014[547]	24870542	Retina	1	9	1

The GPMDB provides a repository of the largest curation of publically available proteomic information derived from user-submitted tandem mass spectrometry. The database allows for the comparison of original spectrum-to-peptide sequence correlations with a list of previously reported spectra showing the same observed sequences and makes available the accompanying experimental information. The repository also serves as a useful tool to record the observed coverage of a protein sequence and increase confidence in consistently produced signals[571].

A search on the GPMDB web page was made by entering 'EYA' under 'Keywords' and 'Homo sapiens' under 'Data source' and selecting the profile for the accession number 'ENSP00000373394'. Images showing information on the EYA1 peptide coverage in various cell lines and cell types, as well as healthy and malignant tissues were extracted from the EYA1 proteomic profile (date accessed [08/08/18]).

5.2.4 **PheWAS database**

GeneAtlas

Where GWAS tries to find causal genotypes for a selected phenotype, the increasing application of electronic health/medical records (EHRs/EMRs) and "Real-World Data" (RWD) has allowed for an accompanying 'genotype-to-phenotypes' approach. Phenome-wide association studies (PheWAS) are analyses that allow for the comparison of pre-defined genetic variants on one or several human phenomes. The phenome of an individual is characterised by the information available within the EHRs. These documents include basic information on a patient's profile (height, age, weight, etc.), measurements of vital signs (heart rate, blood pressure, respiratory rate, etc.) and current and past health conditions (heart disease, cancer, metabolic disease, etc.) but also diagnostic results and measurements including x-rays and blood screening[572].

PheWAS can help to examine the pleiotropic effects of genetic variants in the context of interindividual variation and different environmental exposures. This data could then be used to reveal previously unidentified pathophysiological connections that will improve knowledge of disease[573,574], direct stratification efforts[575,576] (in terms of avoiding ADRs and selecting most effective treatments) and potentially provide reason for the repurposing of well characterised drugs[576,577].

GeneAtlas is a publically available PheWAS database, containing associations made using a Linear Mixed Model for 778 traits and 31,415,476 polymorphisms (623,944 genotyped and 30,798,054 imputed from Haplotype Reference Consortium) in a cohort of 452,264 UK Biobank White British individuals[578]. The study also involved collecting individual measurements from the UK Biobank repository[578] such as baseline measurements (height, age, etc.), self-reported traits (e.g. self-reported depression), hospital admissions data and cancer diagnoses from the UK Cancer Registries. Information for each successfully tested polymorphism is available to download on the database. Since the cohort contains both related and unrelated individuals, this open access approach allows researchers to apply study-specific quality control measures.

The 'Trait Info' and 'By Significance' search functions were used to identify genome-wide significant associations ($p<1x10^{-8}$) between SNPs on all chromosomes and medically diagnosed 'K25 Gastric ulcer' or self-reported 'gastric/stomach ulcer' (date accessed [09/07/18]). A second search was performed using the 'Region or Gene' function looking for associations in polymorphism specifically at the 'EYA1' genomic loci (Chromosome 8 of the GRCh37.p13 assembly, 72,059kb – 72,325kb,) with the aforementioned gastric traits (date accessed [24/07/18]).

As part of the analysis of the rs12678747 SNP (described in section 5.2.5), a PheWAS search using the 'By Variant' function was performed to assess the association between rs12678747 and gastric ulcer phenotypes (medically diagnosed 'K25 Gastric ulcer' and self-reported 'gastric/stomach ulcer') and all traits available on GeneAtlas (date accessed (data accessed [01/08/18]).

5.2.5 **EYA1 genomics**

Aspirin-peptic ulcer genome-wide association study and replication cohort

Caucasian patients suspected of PUD were recruited both retrospectively from endoscopic databases and prospectively from 15 UK hospitals. Of the 1478 recruited patients, genomic DNA (gDNA) was extracted from whole blood of 723 patients, that matched three distinct phenotypes (one case and two control groups), using a Chemagen 5mL whole-blood DNA extraction kit on the Chemagic Magnetic Separation Module I (PerkinElmer Chemagen Technologie, Baesweiler, Germany).

Cases were defined as patients with endoscopically confirmed PUD within 2 weeks of using aspirin (n=247). The control group comprised of two subgroups, 245 patients with endoscopically confirmed peptic ulcer disease (PUD) with no history of NSAID use in the past 3 months prior to diagnosis (group A) and 231 patients with no PUD that either were or were not taking NSAIDs (group B).

Genotypes of all patient gDNA were determined using the Illumina Omni 2.5 single nucleotide polymorphism (SNP) array and Illuminus genotype calling algorithm[579] (Illumina, San Diego, CA, USA). After imputation and application of quality controls, 5,548,084 single nucleotide variants were used for association analysis using a logistic regression model.

SNP signals that reached a nominal significance of 10^{-6} in the discovery cohort were typed in a replication cohort containing 515 individuals of which 206 were cases and 309 were controls (124 group A and 184 group B) as defined above. Genotyping was performed using the Agena MassArray iPLEX platform (Agena Bioscience Inc, San Diego, CA, USA) and the same logistic regression model used in the discovery cohort. Meta-analysis combing the statistical results from both cohorts was performed using GWAMA software[580].

The lead variant, rs12678747 ($p=1.65x10^{-7}$), fell short of genome-wide significance ($1x10^{-8}$), however the association was replicated in cohort of 84 PUD patients (p=0.002). Meta-analysis combining data from discovery and replication cohorts determined an odds ratio of 2.03 ($p=3.12x10^{-11}$) for carriers of the rs12678747 polymorphism (Bourgeois *et al*., unpublished data).

Carbamazepine hypersensitivity study

Whole genome sequencing was performed on gDNA from 28 cases (carbamazepine (CBZ)-induced hypersensitivity) and 20 controls (CBZ, no hypersensitivity). Sequencing was outsourced to Illumina Inc., where samples were analysed on an Illumina HiSeq 2000. Sequences were aligned to UCSC human genome build 37 (hg37). Single nucleotide variants (n=1107), short insertions (n=43) and deletions (n=57) that mapped to the EYA1 locus were analysed to determine their region within the gene (e.g. intronic, exonic, etc.), allelic frequency and zygosity between case and control groups (unpublished data).

Encyclopaedia of DNA Elements (ENCODE)

Regulatory regions provide key information on the control of gene expression and are important targets for the study of human biology and disease. The goal of the ENCODE project is to systematically map all functional elements scattered across the human genome. Regulatory regions were identified using ChIP-seq (Chromatin immunoprecipitation followed by sequencing) technology to determine the binding locations of 119 DNA binding proteins in 72 cell types[581], as well as determining the methylation/acetylation states of histones flanking these regions.

The variant 'rs12678747' was entered into the 'Candidate Regulatory Elements' search function on the ENCODE online web tool. Information regarding regional sensitivity to DNase and CCCTC-binding factor (CTCF) were extracted along with the methylation/acetylation scores for histones (H3K4me3 and H3K27ac) proximal to the rs12678747 loci (date accessed [31/07/18]).

HaploReg

The combination of genetic variants at a chromosomal region that are inherited together (haplotypes) have allowed for the identification of loci involved in common disease by family- and population-based linkage studies[582]. Statistics for linkage disequilibrium (denoted as r^2) define the difference in the observed and expected frequencies of alleles at discrete loci. Haplotype screening is an essential method used clinically in bone marrow transplantation. Several markers in the major histocompatibility complex genes are genotyped in transplant recipients and unrelated donors. Higher haplotype homology, determined by human leukocyte antigen (HLA) matching, is correlated with more successful transplant outcomes[583].

Outside of HLA matching, haplotyping does not provide greater clinical validity or utility than genotyping causative mutation directly. However, haplotype screening can help predict disease severity, such certain β-globin haplotypes being related to less severe phenotypes in sickle cell disease[584,585] and reports of a specific *IL10* promoter haplotype being associated to reduced disease and death rates in hematopoietic-cell transplants[586]. Finally haplotype analysis plays a significant role in the area of pharmacogenomics, such as in the cases of asthmatics response to *β*-agonists (ADRB2

haplotypes)[587] and the hypersensitivity reactions caused by various classes of drugs (HLA haplotypes)[588].

HaploReg is an online tool for interrogating the haplotype blocks of genomic variants. A query for 'rs12678747' was submitted on the HaploReg v4.1 database with the following specifications: LD threshold (r^2) = 0.8, 1000G Phase 1 population for LD calculation = EUR (European), Source of epigenomes = ChromHMM (Core 15-state model), and Mammalian conservation algorithm = SiPhy-omega. The following information was extracted from variants in LD with rs12678747 from the HaploReg results (date accessed [01/08/18]]): Chromosomal location, LD (r^2), rs identification number, frequency of variant in the European population, GENCODE genes linked to the variant loci and the dbSNP functional annotation of the variant (e.g. synonymous, non-synonymous, intronic, etc.).

5.3 **Results**

5.3.1 **EYA1 transcriptomic analysis**

From the tissue-specific data, *EYA1* seems to be expressed highest in brain/nerve, endocrine, prostate and retinal tissue. Moderate to low expression was also observed in muscle, gastrointestinal, kidney/urinary bladder tissue and tissues of the female reproductive system (Figure 5.1A-C and Figure 5.4A&B).

Though generally only weakly expressed in cancer tissue, expression is highest in glioma and prostate cancers (Figure 5.2). From the immortalized cell line dataset from HPA (Figure 5.1D), *EYA1* expression is shown to be highest in neuroblastoma (SH-SY5Y), uterus (AN3-CA) and rhabdomyosarcoma (RH-30) cell lines. Weak *EYA1* expression is also detected in lymphoid, lung, renal, prostate, fibroblast and skeletal muscle cell lines.

Based on the information available from the HPA, GTEx and NIH Roadmap Epigenomics datasets, *EYA1* shows very low expression in stomach tissue with 0.3TPM (n=4), 0.5 RPKM (n=193) and 2TPM (n=4) respectively (Figure 5.1A&B and Figure 5.4B). Expression of *EYA1* detected in stomach cancer tissues ranged from undetected to 7.8 FPKM, with an average FPKM of 0.1 (Figure 5.2). Higher *EYA1* expression was found to be associated with a lower 5-year survival probability (Figure 5.3).

A GTEx portal search for eQTLs of EYA1 in all tissues revealed over 700 SNPs that alter EYA1 gene expression. However, no significant eQTLs are reported for EYA1 in stomach tissue[542] (GTEx Analysis Release V7, dbGaP Accession phs000424.v7.p2).

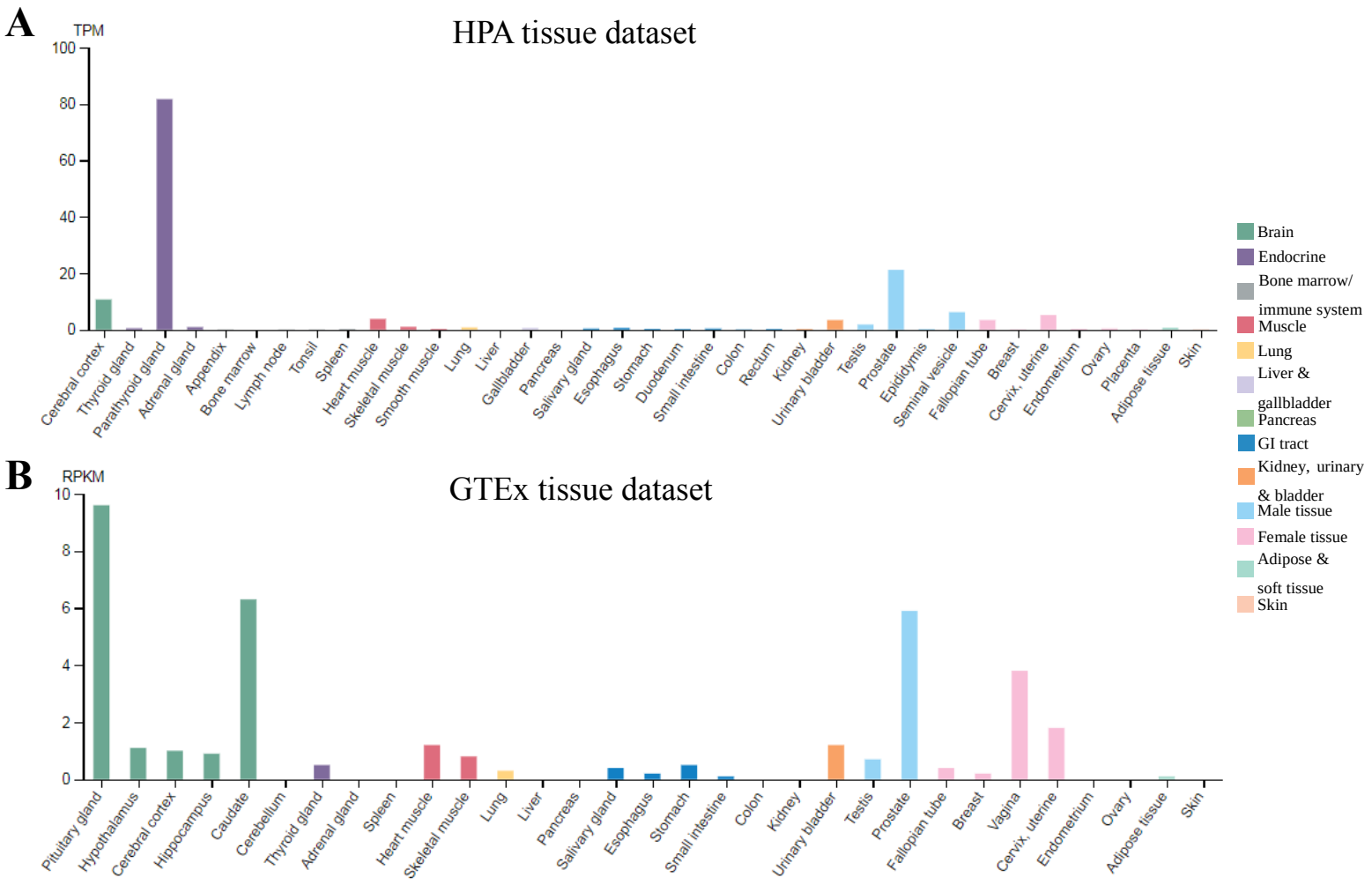
A
TPM
HPA tissue dataset
100
80
60
40
20
0
Cerebral cortex
Thyroid gland
Parathyroid gland
Adrenal gland
Appendix
Bone marrow
Lymph node
Tonsil
Spleen
Heart muscle
Skeletal muscle
Smooth muscle
Lung
Liver
Gallbladder
Pancreas
Salivary gland
Esophagus
Stomach
Duodenum
Small intestine
Colon
Rectum
Kidney
Urinary bladder
Testis
Prostate
Epididymis
Seminal vesicle
Fallopian tube
Breast
Cervix, uterine
Endometrium
Ovary
Placenta
Adipose tissue
Skin
Brain
Endocrine
Bone marrow/ immune system
Muscle
Lung
Liver & gallbladder
Pancreas
GI tract
Kidney, urinary & bladder
Male tissue
Female tissue
Adipose & soft tissue
Skin
B
RPKM
GTEx tissue dataset
10
8
6
4
2
0
Pituitary gland
Hypothalamus
Cerebral cortex
Hippocampus
Caudate
Cerebellum
Thyroid gland
Adrenal gland
Spleen
Heart muscle
Skeletal muscle
Lung
Liver
Pancreas
Salivary gland
Esophagus
Stomach
Small intestine
Colon
Kidney
Urinary bladder
Testis
Prostate
Fallopian tube
Breast
Vagina
Cervix, uterine
Endometrium
Ovary
Adipose tissue
Skin

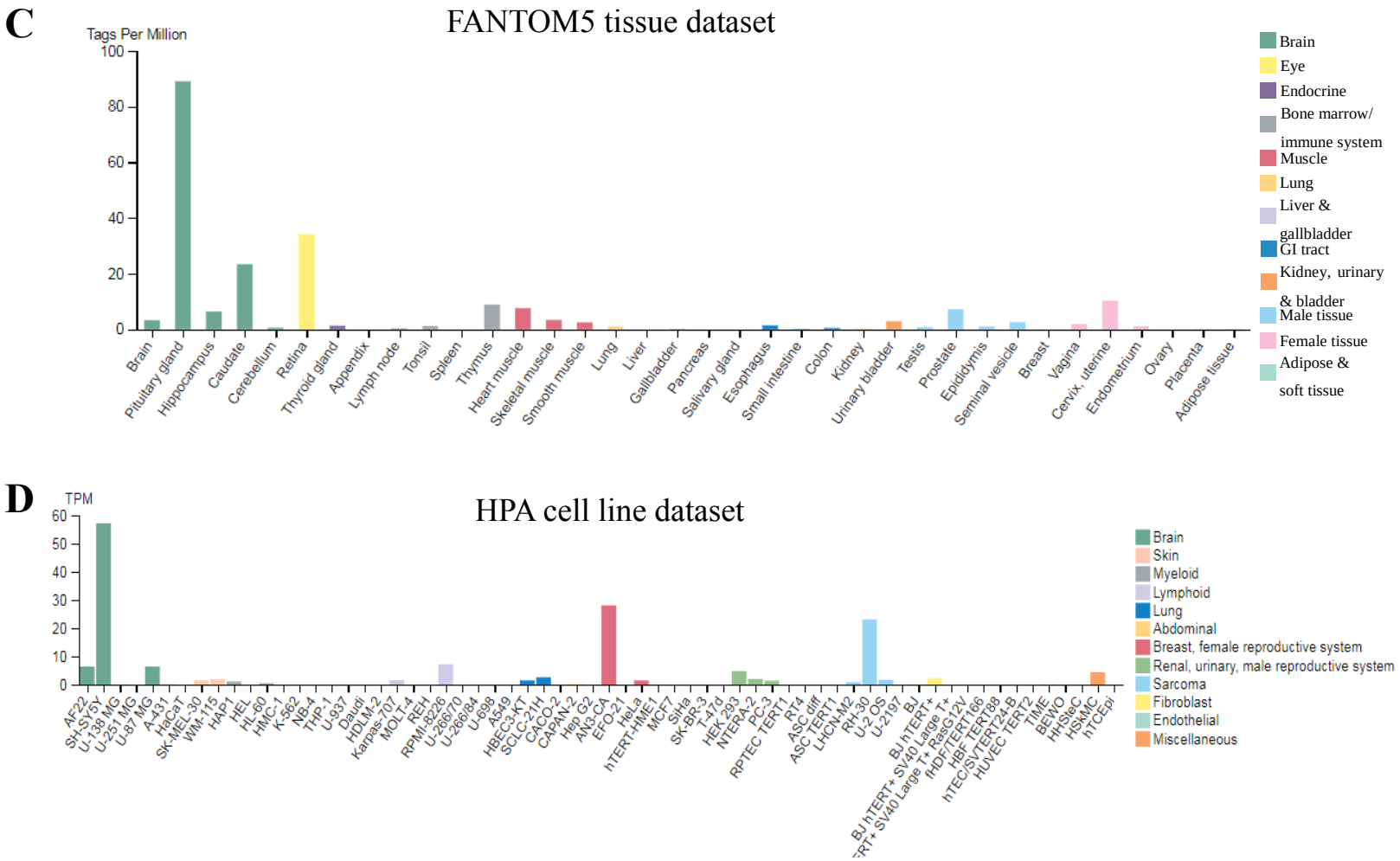

Figure 5.1 EYA1 RNA expression across different tissue types (A-C) and cell lines (D). For both HPA datasets (A & D) mRNA was sequenced using Illumina HiSeq2000 and 2500 machines, with abundance measured in 'Transcripts Per Million' (TPM). RNA abundance from the GTEx (B) and FANTOM5 (C) datasets as represented as 'number Reads Per Kilobase gene model and Million mapped reads' (RPKMs) and 'Tags Per Million' respectively.

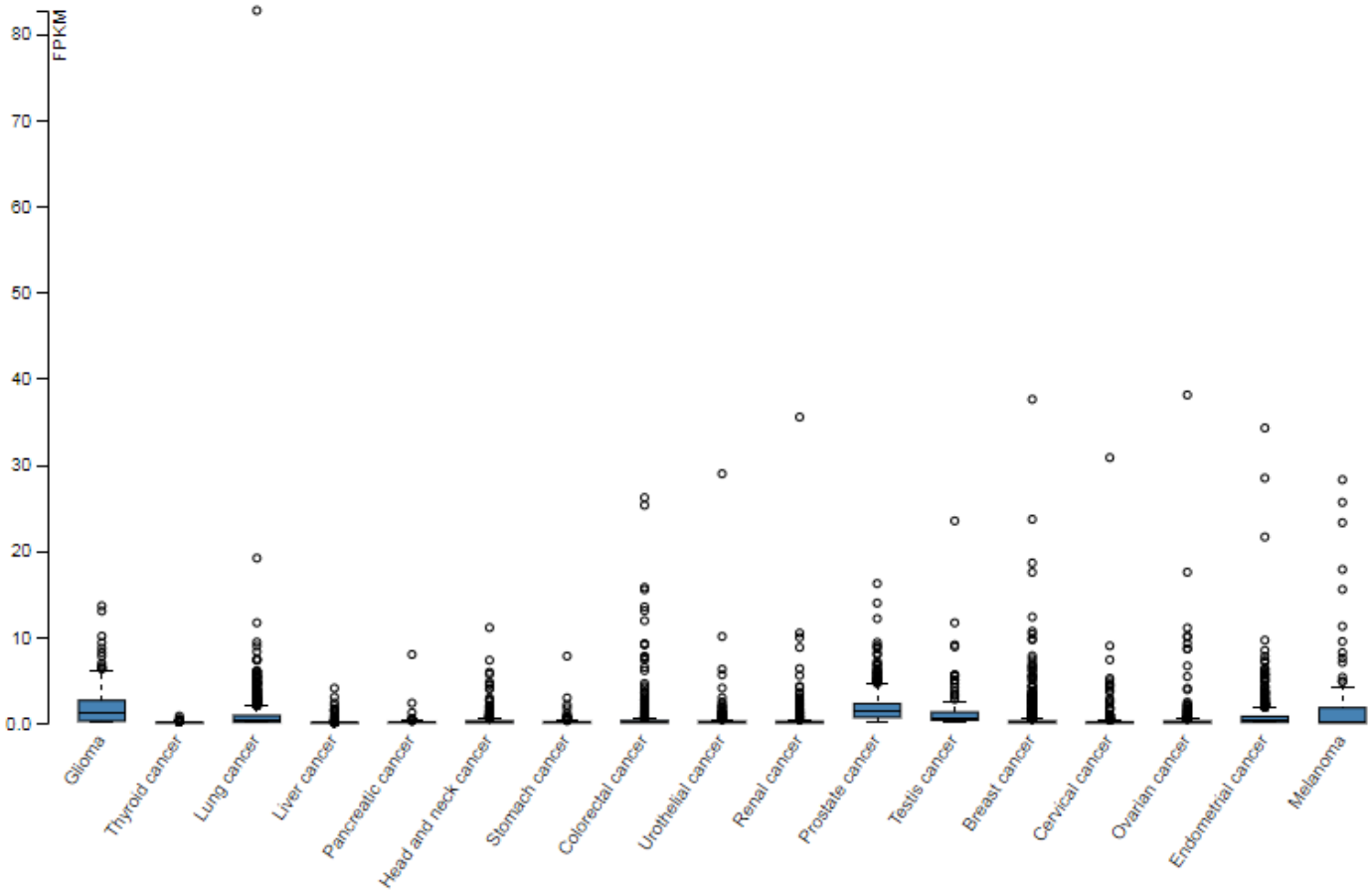

Figure 5.2 EYA1 RNA expression across 17 distinct types of cancers. RNA-seq data is shown as number Fragments Per Kilobase of exon per Million reads (FPKMs) to represent quantification of expression. Data was generated and held in the Genomic Data Commons (GDC) Data Portal under The Cancer Genome Atlas project. Figure was extracted from the HPA 'Pathology Atlas' profile for EYA1 [date accessed 03/08/18].

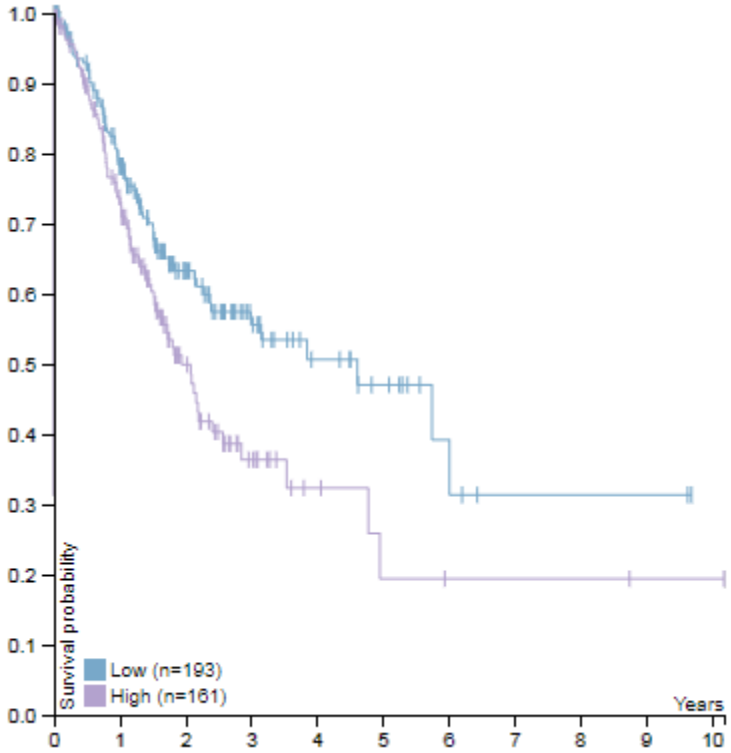

Expression cut-off	0.1 FPKM
5-year survival: high expression	19%
5-year survival: low expression	47%
Log-rank P value	1.06E-02

Figure 5.3 Kaplan-Meier plot and correlation statistics showing survival analysis of 354 stomach cancer patients with either high (>0.069 FPKM, n=161) or low (<0.069 FPKM, n=193) EYA1 expression. The log-rank statistic performed defined prognostic genes as those with P values <0.001. Figure and table information were extracted from the HPA 'Pathology Atlas' profile for EYA1 [date accessed 03/08/18].

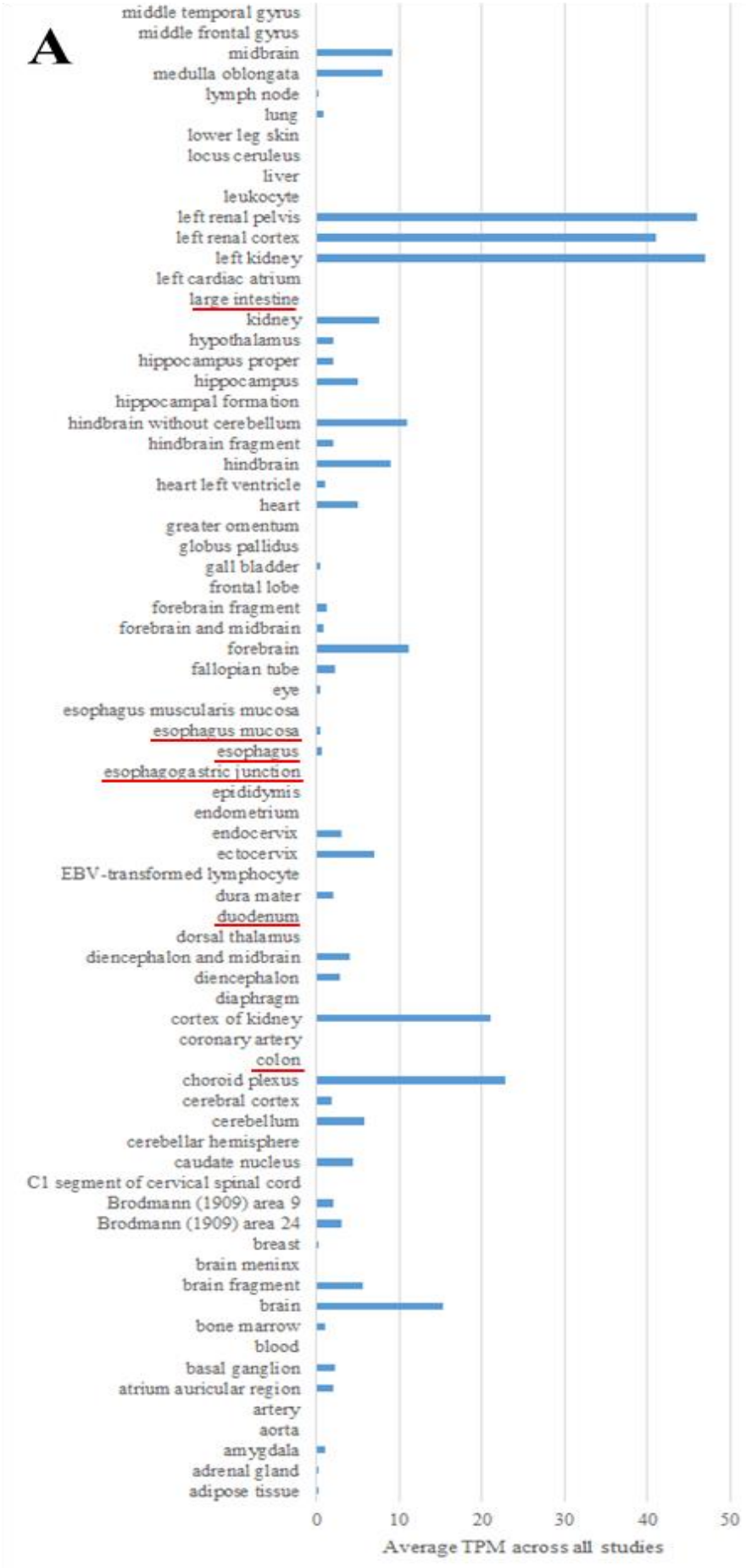
A
middle temporal gyrus
middle frontal gyrus
midbrain
medulla oblongata
lymph node
lung
lower leg skin
locus ceruleus
liver
leukocyte
left renal pelvis
left renal cortex
left kidney
left cardiac atrium
large intestine
kidney
hypothalamus
hippocampus proper
hippocampus
hippocampal formation
hindbrain without cerebellum
hindbrain fragment
hindbrain
heart left ventricle
heart
greater omentum
globus pallidus
gall bladder
frontal lobe
forebrain fragment
forebrain and midbrain
forebrain
fallopian tube
eye
esophagus muscularis mucosa
esophagus mucosa
esophagus
esophagogastric junction
epididymis
endometrium
endocervix
ectocervix
EBV-transformed lymphocyte
dura mater
duodenum
dorsal thalamus
diencephalon and midbrain
diencephalon
diaphragm
cortex of kidney
coronary artery
colon
choroid plexus
cerebral cortex
cerebellum
cerebellar hemisphere
caudate nucleus
C1 segment of cervical spinal cord
Brodmann (1909) area 9
Brodmann (1909) area 24
breast
brain meninx
brain fragment
brain
bone marrow
blood
basal ganglion
atrium auricular region
artery
aorta
amygdala
adrenal gland
adipose tissue
0
10
20
30
40
50
Average TPM across all studies

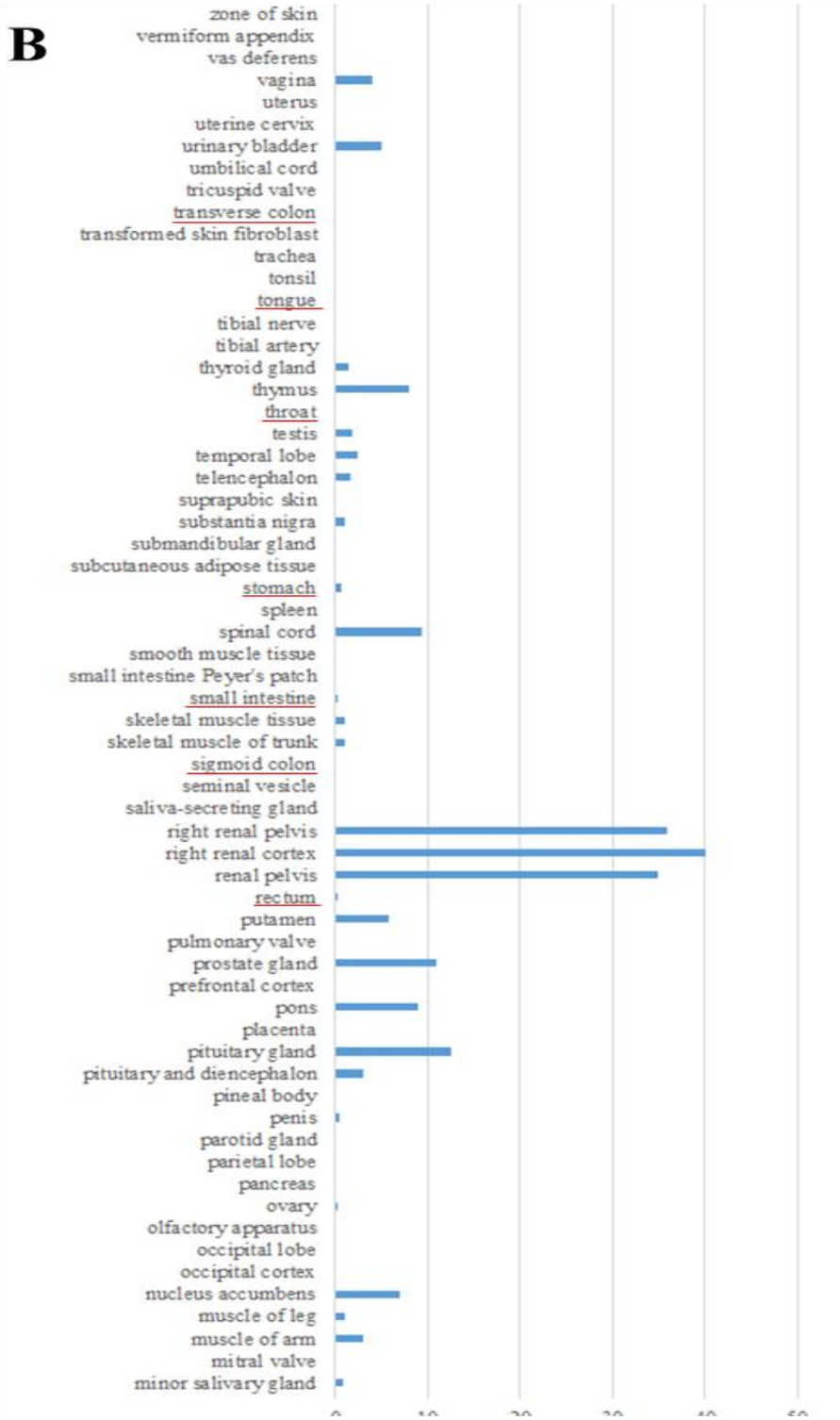

Figure 5.4 Expression Atlas overview of EYA1 gene expression in 136 human tissues arranged alphabetic-ally from (A) a-mid to (B) min-z. Values, shown as Transcripts Per Million (TPM), represent the average expression which was calculated by taking the sum of all recorded expression values for each tissue and dividing by the number of studies that tissue data was available across the HPA, GTEx, FAN-TOM5, HBDR NIH Epigenomic Road-map ENCODE and Illumina Body Map studies. All areas that are liable to develop ulceration due to NSAID therapy are underlined in red.

5.3.2 **EYA1 protein expression**

Immunofluorescent imaging of EYA1 protein is localised exclusively in the nuclei of the RH-30 rhabdomyosarcoma cells and mostly nuclei/weakly cytoplasmic in U-2 OS osteosarcoma cells as can be seen in Figure 5.5. Colorimetric grading of EYA1 staining (Figure 5.5C1 & 2) detected low to medium staining in RH-30 cells and a slightly higher expression in U-2 OS cells (Figure 5.5C3).

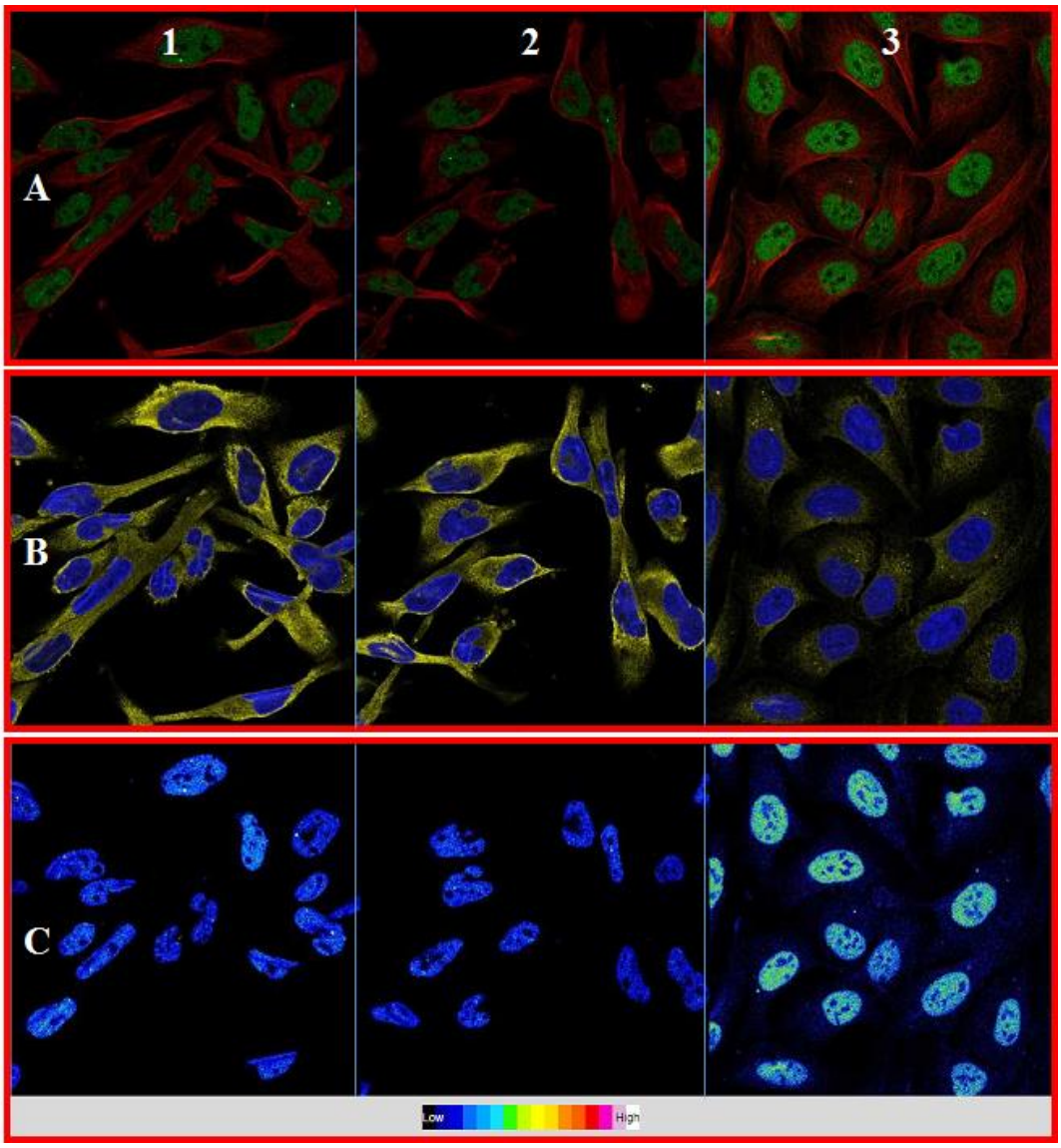

Figure 5.5 HPA-Cell Atlas EYA1 protein expression in RH-30 and U-2 OS cell lines. Immunofluorescent staining of RH-30 (columns 1 & 2) and U-2 OS (column 3) cells for (A) EYA1 (green) & microtubules (red) and (B) nuclei (blue) & endoplasmic reticulum (yellow). A colometric ranking of EYA1 staining is also provided (C), which is determined by the strength of laser and detector settings used to visualise the green staining. Original images available from the HPA Cell Atlas profile for EYA1, [Date accessed 03/08/18].

No western blot data is available from the HPA website due to a 'low RNA count' (https://www.proteinatlas.org/ENSG00000104313-EYA1/anti body), which presumably means that the protein signal is too weak to detect using immunoblotting techniques.

The HPM dataset shows that EYA1 protein expression could only be detected in foetal brain tissue (Figure 5.6). The EYA1 peptide detected by tandem mass spectrometry, LLFPQVAVK, represents the very start of the N-terminus of the predicted EYA1 isoforms X10 (XP_016868700.1) and X11 (XP_016868701.1). As expected glyceraldehyde-3-phosphate dehydrogenase (GAPDH), a housekeeping protein stably and constitutively expressed in most tissues[589], was present in all samples.

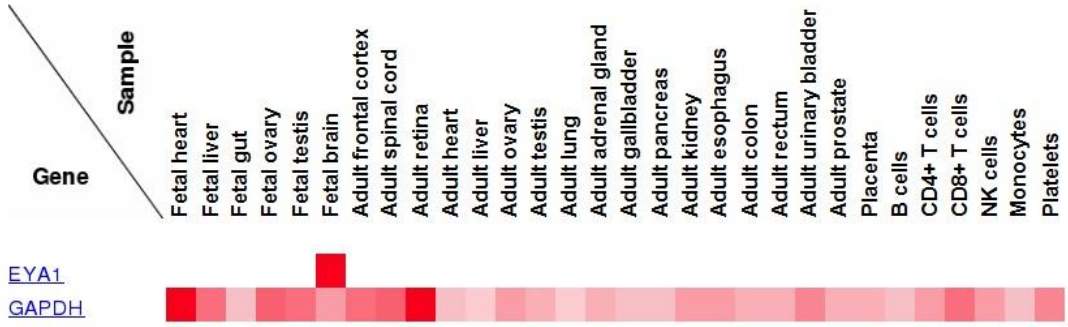

Figure 5.6 Tissue-based expression analysis of EYA1 and GAPDH in 30 healthy human tissue/cell samples. Data are shown as a heat map of low to high expression (light to dark red) and were obtained using tandem mass spectrometry. Data was obtained from HPM database, [Date accessed 05/08/18].

Between all the projects that have detected unique EYA1 peptides, 20.1% of the protein sequence has been reported from projects within ProteomicsDB. The projects cover various cell lines and tissues. However, the only quantitative data available detected low expression of EYA1 in blood platelets and a higher expression in the A-375 epithelial skin cell line (Figure 5.7). Values are shown as $\log_{10}$ transformed normalized iBAQ intensities, which represent value converted from absolute copy numbers of the detected protein within each sample.

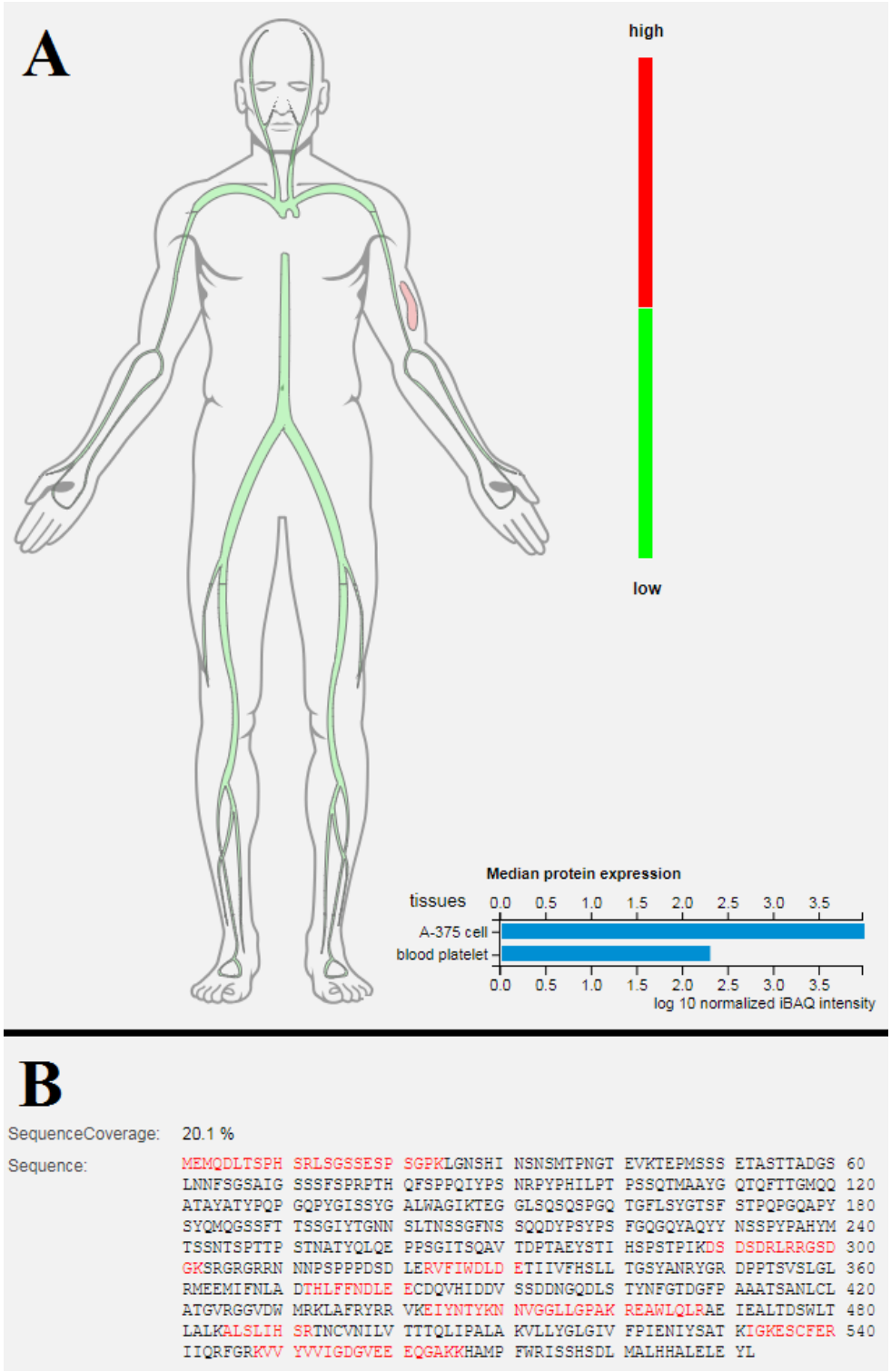

Figure 5.7 Proteomic analysis of EYA1 in human tissues from the ProteomicsDB online web tool, [Date accessed 05/07/18]. (A) Body heat map showing relative expression levels of EYA1 protein in human tissue and cell lines. Expression is shown as a colorimetric scale from high (red) to low (green) denoting peptide levels. A quantitative view of median expression is also provided in terms of $\log_{10}$ normalised iBAQ intensity. (B) EYA1 peptide sequence (NP_000494.2) showing detected unique peptides detected by tandem mass spectrometry highlighted in red.

PeptideAtlas only reports a coverage of 7.9% of the EYA1 protein sequence; however all detected peptides had a 100% confidence score as assessed by PeptideProphet. Two of six peptides mapped exclusively to the EYA1/*EYA1* protein and genomic sequences (Table 5.7). The peptide, AVYVVIGDGVEEEQGAKK (highlighted red), matches with the EYA2 protein sequence (NP_005235.3); however only differs by one peptide (495A in EYA2 and 549V in EYA1) to the longest EYA1 protein sequence (NP_000494.2). As can be seen in Figure 5.8, the observed peptides are located at the start, middle and end of the peptide chain, with the majority of peptide identification being made in the region of the EYA1 domain.

Table 5.7 Table of distinct observed peptides that match the EYA1 (Q99502) protein sequence. All peptide sequences are given from the N-terminal to the C-terminal amino acids. More information on the peptide spectra analysis, proteomic/genomic mapping and data sources can be found by searching the accession number of each peptide on the PeptideAtlas database, [Date accessed 07/08/18]. Green rows highlight EYA1 specific sequences, red rows denote peptides that map to predicted EYA1 protein assemblies and grey rows represent peptides that map to various proteins/genes as well as EYA1. Best Prob: Highest PeptideProphet probability (as a ratio from 0-1) for observed sequence. N Obs: total observations of peptide in all modified forms and charge states. N Prot Map: number of proteins in the reference database to which the peptide maps. N Gen Loc: number of discrete genome locations that encode this amino acid sequence. N experiments: number of experiments in which the peptide was identified. [1] EYA1 peptides identified by LC-MS/MS in AGS lysates (section 3.3.4).

Accession	Sequence	Best Prob	N Obs	N Prot Map	N Gen Loc	N Experiments
PAp03124809	LSGSSESPSGPK[1]	1.0	12	13	1	11
PAp01525796	NNNPSPPPDSDLER	1.0	17	18	1	2
PAp04660071	AVYVVIGDGVEEEQGAKK	1.0	1	9	1	1
PAp02163712	THLFFNDLEE	1.0	10	53	4	2
PAp00810671	NNVGGLLGPAK[1]	1.0	3	38	2	3
PAp01525833	NNPSPPPDSDLER	1.0	263	39	2	16

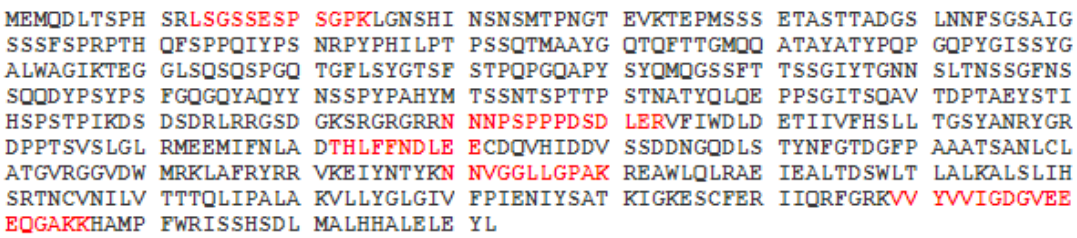

Figure 5.8 PeptideAtlas coverage of EYA1 protein sequence (NP_000494.2) based on peptides identified by tandem mass spectrometry. Image obtain from the PeptideAtlas Human Build archive for EYA1 (Q99502) [Date accessed 07/08/18].

Information on identified EYA1 peptides are available in 306 datasets that are stored in the GPM database with experiments reporting individual coverage from 1 to 60% of the EYA1 protein sequence[590]. These proteomic results available on GPMDB were obtained from datasets in the following open access repositories: Broad Institute, ProteomeXchange, CPTAC Portal, MassIVE and Tranche.

The GPMDB reports an overall coverage of 72.8% of the EYA1 protein sequence from peptides identified by tandem mass spectrometry (Figure 5.9). EYA1 peptides were identified in various tissues, cell lines and cancer tissues (Figure 5.10), occurring most frequently in breast tissue, HeLa cell line and melanoma respectively. Though most commonly observed in epithelial cells, there were no reports of EYA1 peptides identified in gastric epithelial tissue, cells lines or cancer tissue.

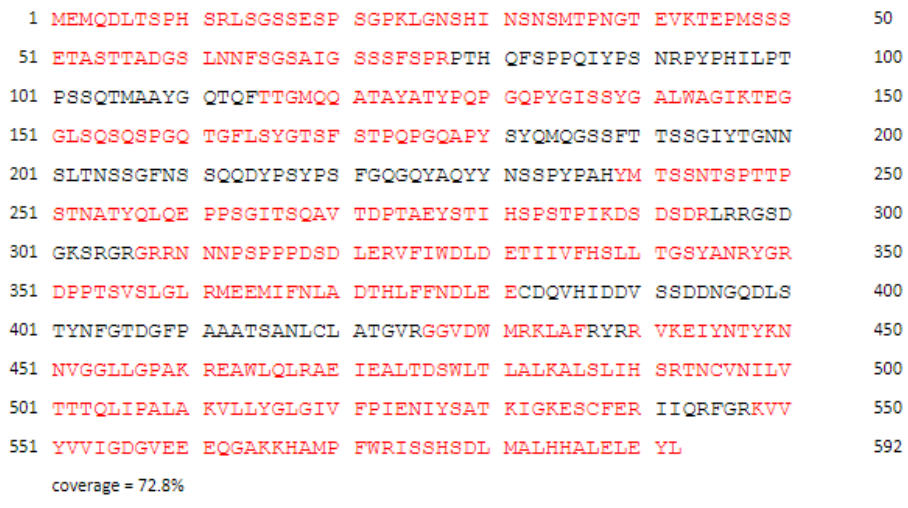

Figure 5.9 Overview of all peptides identified by mass spectrometry that map to the human EYA1 isoform 1 protein sequence (NP_742055.1, also ENSP00000373394.4). Image obtained by using the GPMDB Homo sapiens database to access proteomic information on EYA1 isoform 1, [Date accessed 08/08/18].

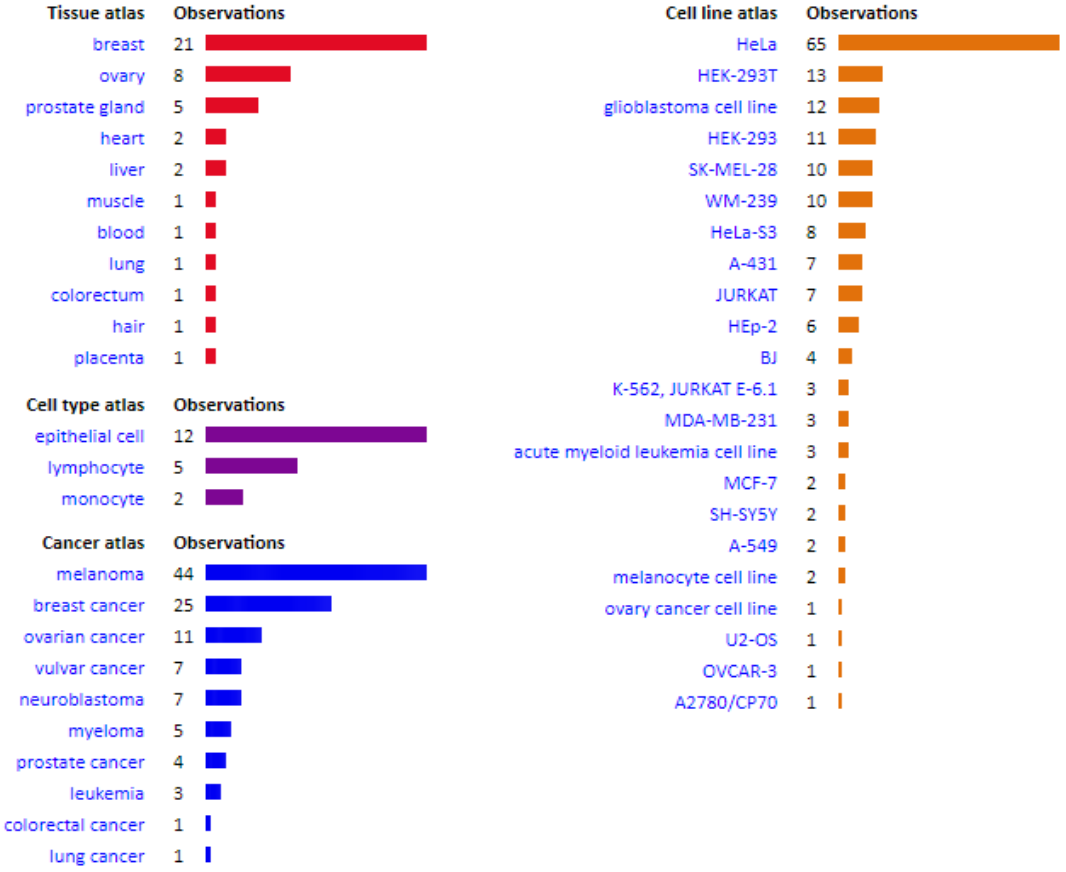

Figure 5.10 Number of EYA1 peptide identifications in different tissues, cell lines, cell types and cancer tissue across all datasets from the GPMDB proteomic analysis, [Data accessed 08/08/18].

5.3.3 **PheWAS analysis**

From the trait analysis (Figure 5.11A-D), three SNPs were identified to have a genome-wide significant association with the ulcer phenotypes (Table 5.8). One SNP was identified for self-reported gastric/stomach ulcer, rs199912782, which maps to an exonic region of the *PRRC2A* gene (4148G>C, NM_004638.3) causing a missense mutation (E1288Q, NP_004629.3) of unknown effects. PRRC2A maps within the 'major histocompatibility complex (MHC) class III' region and potentially plays a role in the inflammatory response. So far, there have been no reports of the gene being involved in gastric ulcer pathogenesis. However, PRRC2A has been shown to be overexpressed in PBMCs of patients with Behçet Disease, a disease defined by oral aphthosis, ocular lesions and genital ulcers[591].

Medically recorded K25 gastric ulceration was associated with missense mutations in the SLIT1 (rs150920866, 2617G>A, NM_003061.2; V789M, NP_003052.2) and NFE2L1 (rs202183954, 779C>T, NM_001330261.1; P37S, NP_001317190.1) genes. Slit guidance ligand 1 (SLIT1) is one of a highly conserved family of secreted glycoproteins. SLIT1 binds to roundabout receptors (ROBOs) to promote axon guidance, angiogenesis, cell migration and motility[592,593]. All SLIT family genes are highly methylated in both early and late stage gastric cancer[593]. NFE2L1 is a CNC-bZIP transcription factor ubiquitously expressed in all tissue and cell types. Nuclear Factor Erythroid-2 Like-1 (NFE2L1; also referred to as Nrf1) is induced by various stress signals, regulating cellular homeostasis, differentiation, and responses to oxidative stress and inflammation[594]. Though having no other reported links with gastric ulceration, Nrf1 has been implicated in the progression of many diseases including cancer, degenerative and metabolic disorders[595].

No SNPs in the region of the EYA1 gene (72109668-72459888, NC_000008.10) were associated with medically recorded K25 gastric ulcer or self-reported gastric/stomach ulcer (Figure 5.12A-B). A search for an association between all EYA1 SNPs and any trait in Gene Atlas database also presented no results at a p-value threshold of $1x10^{-8}$.

Table 5.8 SNPs across all autosomal chromosomes with p-values that reach genome-wide significance for association with medically recorded K25 gastric ulceration and self-reported gastric/stomach ulceration. Variant loci given based on the NC_000006.12 genome reference sequence. Chr.: Chromosome. Eff. allele: Effect allele and MAF: Minor allele frequency.

Trait	Variant	Chr.	Loci	Eff. allele	Functional annotation	P value	MAF
gastric/stomach ulcers	rs199912782	6	31600312	G	c.4148G>C, p.E1288Q	2.22E-09	1.63E-04
K25 Gastric ulcer	rs150920866	10	46128589	C	c.2617G>A, p.V789M	8.99E-09	1.14E-04
K25 Gastric ulcer	rs202183954	17	98797456	C	c.779C>T, p.P37S	2.85E-09	2.03E-04

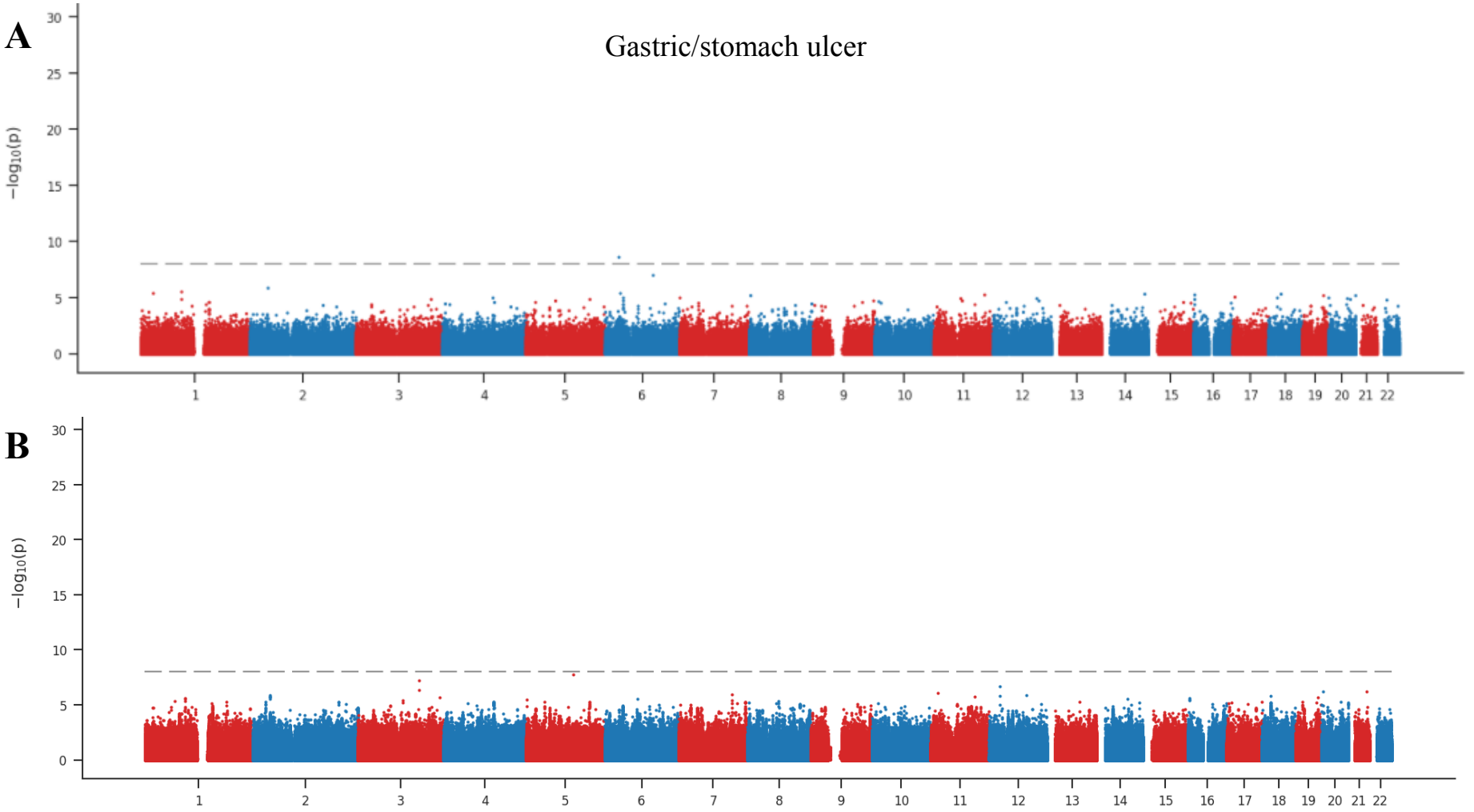
A
Gastric/stomach ulcer
−log10(p)
30
25
20
15
10
5
0
1 2 3 4 5 6 7 8 9 10 11 12 13 14 15 16 17 18 19 20 21 22
B
−log10(p)
30
25
20
15
10
5
0
1 2 3 4 5 6 7 8 9 10 11 12 13 14 15 16 17 18 19 20 21 22

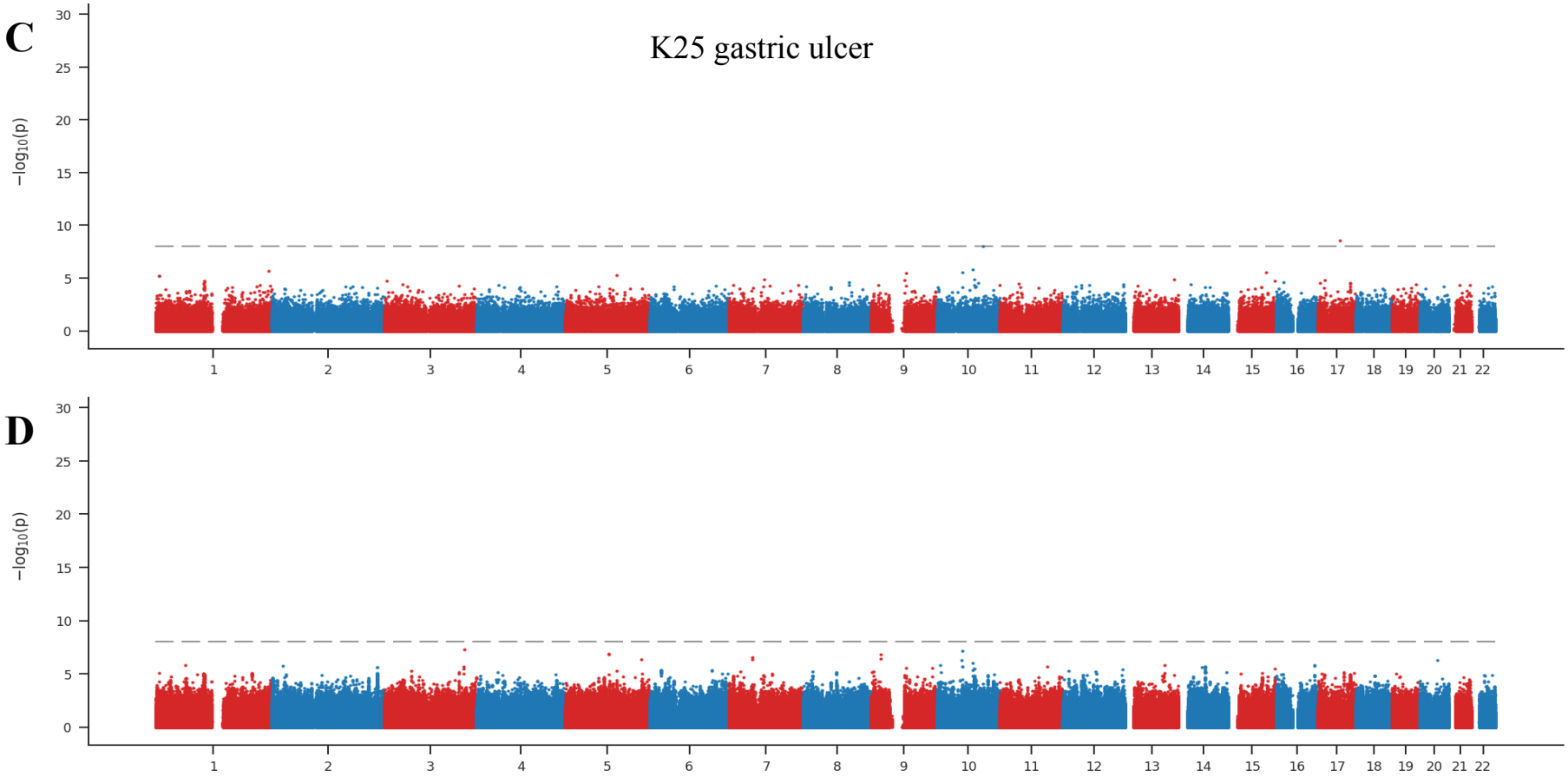

Figure 5.11 Genome- wide association study showing the statistical significance (y-axis; -log10(p)) of 62,394 genotyped (A & C) and 9,113,133 imputed (B & D) SNPs across chromosomes 1-22 (x-axis) on the development of self-reported gastric/stomach ulceration (A & B) and medically recorded K25 gastric ulcer (C & D). Figures were obtained from the Gene ATLAS database, http://geneatlas.roslin.ed.ac.uk [date accessed 09/07/18]. Genome-wide significance, -$\log_{10}$(p) = 8, is shown as a grey dotted line on all figures.

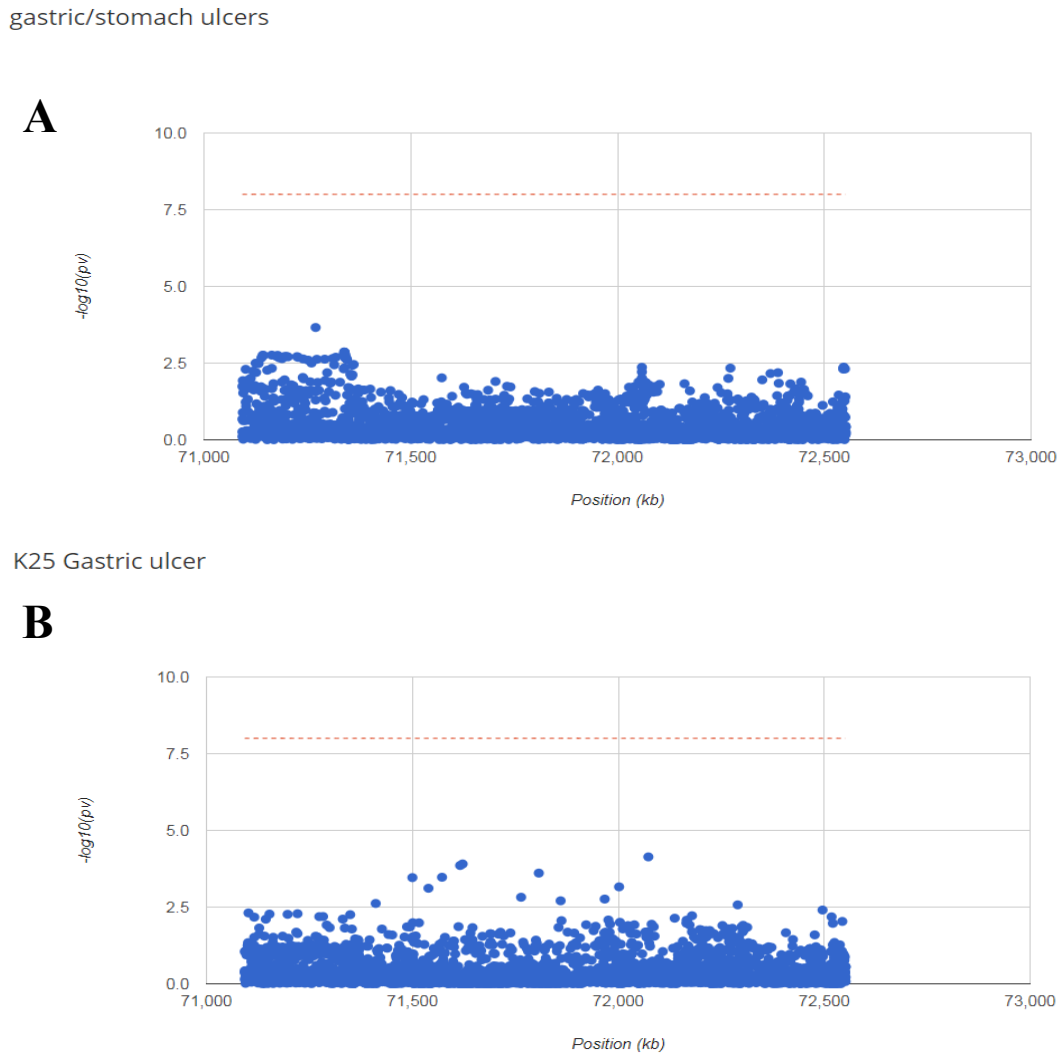

Figure 5.12 Genome- wide association study showing the statistical significance (y-axis; -log10(pv)) of SNPs across the genomic loci of *EYA1* on chromosome 8 (x-axis; NC_000008.10, position 72109668.. 72459888) on the development of self-reported gastric/stomach ulceration (A) and medically recorded K25 gastric ulcer (B). Figures were obtained from the Gene ATLAS database, http://geneatlas.roslin.ed.ac.uk [date accessed 24/07/18]. Genome-wide significance, $-\log_{10}(pv) = 8$, is shown as a grey dotted line on all figures.

5.3.4 **Population frequency, genomic loci, GWAS, PheWAS and haplotype analysis of rs12678747**

The rs12678747 variant (NC_000008.11:g.71202541A>T) is located in the intronic space between the last two exons in the EYA1 gene (exons 15 & 16). The prevalence for this variant ranges from being common in East Asian populations (0.237) to the allele found in the majority of African populations (0.757) (Table 5.9).

Table 5.9 Prevalence of rs12678747 variant allele (A) and reference allele (T) in East Asian (EAS), European (EUR), African (AFR), Mixed American (AMR) and South Asian (SAS) populations. Data obtained from the dbSNP database, [Date accessed 31/07/18].

Population	Chromosome Sample Count	Allele	
		A	T
EAS	1008	0.237	0.763
EUR	1006	0.692	0.308
AFR	1322	0.757	0.243
AMR	694	0.555	0.445
SAS	978	0.492	0.508

From the carbamazepine-hypersensitivity cohort, 1207 genetic variants in the *EYA1* gene were identified including single nucleotide variations (SNV), short insertions and deletions (Table 5.10). Most variants mapped to intronic regions (Table 5.10), though several also fell within regulatory regions (3'-UTR, 5'-UTR and promoter regions). Four exonic SNPs were identified that each caused synonymous codon changes (Table 5.11). The minor allele frequency (MAF) of the rs12678747 variant (1699T>A) was found to be 0.302 (Table 5.11).

Table 5.10 Description of EYA1 variants detected in 28 carbamazepine-hypersensitivity cases and 20 controls. The frequency of the types and regional locations of the variants in the gene are provided. SNV: Single nucleotide variation. UTR: Untranslated region.

Gene Region	Variation type			Total
	Insertions	Deletions	SNV	
3'UTR	1	0	66	67
5'UTR	0	0	7	7
Promoter	2	2	5	9
Intronic	40	55	1025	1120
Exonic	0	0	4	4
Total	43	57	1107	1207

Table 5.11 Prevalence of rs12678747 and exonic EYA1 SNVs. Variants are shown for the EYA1 transcripts NM_000503.5/NM_172058.3; NM_172059.3; NM_172060.3; NM_001288575.1; NM_001288574.1. Minor allele frequency: MAF. A_1/A_1: Homozygous for wild type alleles. A_1/A_2: Heterozygous for variant allele. A_2/A_2: Homozygous for variant alleles.

Rs number	Position	Transcript Var	Protein Var	MAF (A_2)	Genotype freq
rs10103397	72,111,599	c.1656T>C; c.1650T>C; c.1755T>C; c.1737T>C; c.1389T>C	p.H585H; p.H552H; p.H550H; p.H579H; p.H463H	0.302	A_1/A_1: 0.698
					A_1/A_2: 0.198
					A_2/A_2: 0.104
rs12678747	72,114,776	c.1699-3121T>A; c.1594-3121T>A; c.1600-3121T>A; c.1333-3121T>A; c.1681-3121T>A	intronic	0.302	A_1/A_1: 0.698
					A_1/A_2: 0.198
					A_2/A_2: 0.104
rs4738118	72,129,009	c.1173C>T; c.1179C>T; c.912C>T; c.1260C>T; c.1278C>T	p.G304G; p.G426G; p.G393G; p.G391G; p.G420G	0.115	A_1/A_1: 0.885
					A_1/A_2: 0.115
					A_2/A_2: 0
rs55972891	72,184,119	c.840C>A; c.825C>A; c.822C>A; c.741C>A; c.474C>A	p.I274I; p.I275I; p.I247I; p.I158I; p.I280I	0.010	A_1/A_1: 0.990
					A_1/A_2: 0.010
					A_2/A_2: 0
rs1445398	72,211,295	c.447A>G; c.714A>G; c.795A>G; c.798A>G; c.813A>G	p.T266T; p.T265T; p.T149T; p.T238T; p.T271T	0.135	A_1/A_1: 0.865
					A_1/A_2: 0.094
					A_2/A_2: 0.042

The rs12678747 variant is found to be in an intronic region of the EYA1 gene. According to the ENCODE-SCREEN database[581], this SNP may fall within a CCCTC-binding factor region (Table 5.12). No eQTL data is available for rs12678747 in any tissue type on the GTEx database[542] (GTEx Analysis Release V7, dbGaP Accession phs000424.v7.p2).

Table 5.12 ENCODE-SCREEN analysis of candidate cis-regulatory elements at the intronic region around rs12678747 (NC_000008.10:g.72,114,776A>T). Z-scores represent the highest detected signal intensities for (i) the sensitivity of regions of chromatin to cleavage by DNase I, (ii) methylation/acetylation states of histone H3 flanking the suspected regulatory site and (iii) CTCF binding affinity. A Z-score >1.64 is determined to be significant ($p<0.05$). [Date accessed 31/07/18]

Accession	Z-scores				Chr.	start	length
	DN-ase	H3K-4me3	H3K-27ac	CTCF			
EH37E00 56345	2.02	1.61	1.22	1.73	8	72,114,554	350

A query for rs12678747 returned a list of 27 single nucleotide variations (1 synonymous and 26 intronic SNVs) with r^2 values greater than 0.8 (Table 5.13). All SNPs in strong LD with rs12678747 mapped to the EYA1 gene and, as would be expected, had similar allelic frequencies in European populations (0.3-0.31). Five SNPs that were in strong LD with the lead variant were also found in regulatory regions according to a search using ENCODE-SCREEN (highlighted green in Table 5.13).

Associations between rs12678747 and self-reported/medically recorded gastric ulceration were searched using the 'By Variant' search function on GeneAtlas. As can be seen in Table 5.14, rs12678747 did not show a significant association with either gastric ulcer traits. A PheWAS search for associations between rs12678747 and all traits in the GeneAtlas catalogue also provided no significant associations.

Table 5.13 HaploReg analysis of SNPs in strong linkage disequilibrium (LD) with rs12678747 (highlight red). LD was performed using genotype information from the 1000 Genomes Project pilot release. A minimum LD threshold of 0.8 and range of 200kb was applied to the caluations. SNPs in LD with the lead variant that also map to regulatory regions, according to ENCODE-SCREEN, are highlighed green Chromosome (Chr.) positions are stated for the GRCh38.p12 (hg38) primary assembly. Prevalence of SNPs in the European population (EUR freq), genomic mapping and functional annotation (dbSNP func annot) information for each SNP is also provided. [Data accessed from HaploReg v4.1 on 01/08/18]

Chr.	Position (hg38)	LD (r^2)	Variant	EUR freq	GENCODE genes	dbSNP func annot
8	71199364	0.97	rs10103397	0.31	EYA1	synonymous
8	71199443	0.97	rs10090382	0.31	EYA1	intronic
8	71199504	0.98	rs10103852	0.31	EYA1	intronic
8	71199989	0.96	rs10104263	0.30	EYA1	intronic
8	71200914	0.98	rs900109	0.31	EYA1	intronic
8	71200936	0.98	rs875380	0.31	EYA1	intronic
8	71202049	0.96	rs4738114	0.31	EYA1	intronic
8	71202541	1	rs12678747	0.31	EYA1	intronic
8	71203992	0.95	rs6472568	0.31	EYA1	intronic
8	71204667	0.96	rs2380713	0.31	EYA1	intronic
8	71204731	0.96	rs2380714	0.31	EYA1	intronic
8	71205109	0.94	rs7016766	0.30	EYA1	intronic
8	71205170	0.96	rs6472569	0.31	EYA1	intronic
8	71205270	0.95	rs6472570	0.31	EYA1	intronic
8	71206912	0.94	rs7828754	0.30	EYA1	intronic
8	71206935	0.94	rs10539572	0.30	EYA1	intronic
8	71211978	0.94	rs4738116	0.30	EYA1	intronic
8	71212548	0.96	rs4612370	0.30	EYA1	intronic
8	71213066	0.96	rs11993577	0.30	EYA1	intronic
8	71213214	0.97	rs11785838	0.30	EYA1	intronic
8	71214404	0.94	rs9298164	0.30	EYA1	intronic
8	71215044	0.91	rs4738117	0.30	EYA1	intronic
8	71215328	0.93	rs7846086	0.30	EYA1	intronic
8	71215529	0.94	rs3735935	0.30	EYA1	intronic
8	71216242	0.94	rs7834524	0.30	EYA1	intronic
8	71216388	0.87	rs139399702	0.28	EYA1	intronic
8	71216639	0.94	rs4737312	0.30	EYA1	intronic

Table 5.14 PheWAS analysis of the association between rs12678747 and self-reported gastric/stomach and medically reported K25 gastric ulcer. Chromosomal position is given based on the NC_000008.10 reference sequence. Effect allele (Eff. Allele) is the variant allele that the effect on the selected traits is being examined. [Data accessed 01/08/18].

Trait	Variant	Chromosome	Position	Eff. allele	p-value
gastric/stomach ulcers	rs12678747	8	72114776	T	0.424
K25 Gastric ulcer	rs12678747	8	72114776	T	0.351

5.4 Discussion

5.4.1 *EYA1* gene expression analysis

EYA1 gene expression was shown to be highest in various brain/nerve, endocrine, prostate and retinal tissues/cell lines (Figure 5.1 and Figure 5.4). EYA1 acts as key transcriptional regulator in the development of multiple organs. Eya1 phosphatase activity, along with Six1, drives hindbrain growth and development in response to Sonic Hedgehog (Shh) signalling by promoting Gli transcription[376]. Eya1 gene expression is high in human Shh-subtype medulloblastoma[377-379] and promotes medulloblastoma growth *in vitro* and *in vivo*[376].

During embryonic development, neural crest cells found in the cranial placodes give rise to various sensory and endocrine features. Several studies have reported that EYA1 and SIX1 drive the early steps of neurogenesis and morphogenesis of these features[526,530,596,597]. Loss of function mutations in EYA1 causes a spectrum of Mendelian branchiootorenal (BOR) disorders in humans[369]. EYA1 knockdown/knockout studies in mice that present pituitary, thymus and parathyroid hypoplasia, as well as phenotypes homologous to people with BOR syndrome[223,354,526].

No reports have described the role of EYA1 in prostate development but the RDGN has been implicated in the regulation of androgen-dependent and –independent prostate cancer cellular proliferation and tumorigenesis[598].

Optic malformations are not observed in mammalian EYA1 deficiency, possibly due to the presence of EYA isoforms (EYA2-4) not present in invertebrates that rely on a single eya isoform (e.g. Drosophila). However, EYA1 mutations may also have a role

in the development of congenital cataracts and ocular anterior segment anomalies[523,524].

According to the HPA Pathology profile, EYA1 expression is very low in cancer tissue, with average expression across all cancer types less than 2 FPKM (Figure 5.2). Focusing on stomach cancer, increased EYA1 expression was associated with a lower 5-year survival (Figure 5.3), though this result did not reach statistical significance. This potential association could be due to the ability of EYA1 to promote DNA repair, providing a resistance mechanism against chemotherapeutic agents[599], and cellular proliferation[355]. This data resonates with the findings made in Chapter 4 showing that overexpression of EYA1 in gastric epithelial cells (AGS), promotes survival.

Across all databases, expression of EYA1 was consistently very low in stomach tissue. Few studies have researched the expression of EYA1 in gastric epithelial cell. A study by Nikpour *et al*. discovered EYA1 expression is downregulated in gastric tumor and negatively correlated with tumour size, lymphatic invasion and distant metastasis[375]. This finding contradicts the observation made in HPA stomach cancer tissue (Figure 5.2), but is supported by an epigenetic study showing that *EYA1* is hyper-methylated in Epstein-Barr Virus-positive and -negative gastric cancers[374]. However, despite the low expression of EYA1 in gastric tissue, it is not possible to exclude a biologically important role because of the multiple functions of EYA1 and interactions with other signalling systems, which despite low expression, may be associated with an amplified response, both physiologically and pathologically.

5.4.2 **EYA1 protein expression analysis**

Immunostaining of endogenous EYA1 in human rhabdomyosarcoma (RH-30) and osteosarcoma (U-2 OS) cell lines indicated weak and moderate nuclear expression respectively (Figure 5.5). Interestingly U-2 OS cells seemed to have higher EYA1 protein expression than RH-30 cells, despite having 13.5 times lower *EYA1* gene expression (U-2 OS: 1.7 TPM vs. RH-30: 23.1 TPM, Figure 5.1D). This discrepancy may be due to differences in the translational efficiency of EYA1 mRNA in these cell lines, such as the expression of mi-RNAs that regulate EYA1 mRNA translation (e.g. miR-101[385] and miR-562[390]). In studies overexpressing murine[355,367,462,481] and human[463] Eya1/EYA1 cDNA clones, translocation to the nucleus is dependent on co-expression with Six. The endogenous expression of EYA1 observed in RH-30 and U-

2 OS nuclei may suggest that sufficient levels of endogenous SIX proteins are available in these cell lines.

No tissue-based protein expression data was available for EYA1 in the HPA 'Tissue/Pathology Atlas'. HPM and ProteomicsDB report expression of EYA1 protein in foetal brain, blood platelets and the A-375 epithelial skin cell line. Though protein expression of EYA1 in brain tissue correlates with the gene expression profiles, blood and skin tissue shown consistently low EYA1 gene expression (Figure 5.1 and Figure 5.4).

The scarcity of information regarding EYA1 protein expression may suggest that EYA1 is mostly expressed during embryogenesis, after which the gene is silenced in the majority of tissues. This would explain why high EYA1 expression is mostly associated with developmental disorders with loss-of-function mutations and tumorigenesis when expressed ectopically[354] (Table 1.8). Alternatively, difficulty in detection of EYA1 peptide fragments could be due to, transient expression, low protein abundance or insufficient amounts of detectable peptides[560].

Coverage of the EYA1 peptide sequence is low (7.9%) in PeptideAtlas (Figure 5.8) but data are much more thoroughly processed than other proteomic databases, allowing for results that are more trustworthy. Peptides that map to a single genomic locus (LSGSSESPSGPK and NNNPSPPPDSDLER) were only found outside of the EYA domain, which is unexpected given the EYA domain is canonically much more highly conserved than the N-terminal region. One peptide unique to EYA1 (LSGSSESPSGPK), and one not unique (NNVGGLLGPAK), reported in the Peptide Atlas database were also identified in LC-MS/MS analysis of AGS proteome performed in Chapter 3 (section 3.3.4).

The coverage of EYA1 protein sequence is much higher in the GPMdb database (72.8%) but does not omit non-unique peptide sequences. As can be seen in Table 5.15, EYA2, EYA3 and EYA4 share several homologous amino acid sequences with EYA1 (mostly in the EYA domain). This could result in various false positive identifications in the EYA1 peptide coverage.

Table 5.15 Comparison between the amino acid sequences of all human EYA isoforms. EYA1 (NP_000494.2) was used as the reference sequence to compare the EYA2 (NP_005235.3), EYA3 (NP_001981.2) and EYA4 (NP_001287942.1) protein sequences. Each EYA1-4 isoform was chosen based on containing the longest amino acid sequence. Alterations in the sequences are represented by highlighted substitutions, insertions or deletions.

Isoform	EYA1	EYA2	EYA3	EYA4
Amino acid comparison	MEMQDLTSPHSRLSGSSESPSG PKLGNSHINSNSMTPNGTEVKT EPMSSSETASTTADGSLNNFSG SAIGSSSFSPRPTHQFSPPQIYPS NRPYPHILPTPSSQTMAAYGQT QFTTGMQQATAYATYPQPGQP YGISSYGALWAGIKTEGGLSQS QSPGQTGFLSYGTSFSTPQPGQ APYSYQMQGSSFTTSSGIYTGN NSLTNSSGFNSSQQDYPSYPSF GQGQYAQYYNSSPYPAHYMTS SNTSPTTPSTNATYQLQEPPSGI TSQAVTDPTAEYSTIHSPSTPIK DSDSDRLRRGSDGKSRGRGRR NNNPSPPPDSDLERVFIWDLDE TIIVFHSLLTGSYANRYGRDPPT SVSLGLRMEEMIFNLADTHLFF NDLEECDQVHIDDVSSDDNGQ DLSTYNFGTDGFPAAATSANLC LATGVRGGVDWMRKLAFRYR RVKEIYNTYKNNVGGLLGPAK REAWLQLRAEIEALTDSWLTL ALKALSLIHSRTNCVNILVTTTQ LIPALAKVLLYGLGIVFPIENIYS ATKIGKESCFERIIQRFGRKVVY VVIGDGVEEEQGAKKHAMPFW RISSHSDLMALHHALELEYL	MVELVISPSLTVNSDCLDKLKFN RADAAVWTLSDRQGITKSAPLR VSQLFSRSCPRVLPRQPSTAMAA YGQTQYSAGIQQATPYTAYPPPA QAYGIPSYSIKTEDSLNHSPGQSG FLSYGSSFSTSPTGQSPYTYQMH GTTGFYQGGNGLGNAAGFGSVH QDYPSYPGFPQSQYPQYYGSSYN PPYVPASSICPSPLSTSTYVLQEAS HNVPNQSSESLAGEYNTHNGPST PAKEGDTDRPHRASDGKLRGRS KRSSDPSPAGDNEIERVFVWDLD ETIIIFHSLLTGTFASRYGKDTTTS VRIGLMMEEMIFNLADTHLFFND LEDCDQIHVDDVSSDDNGQDLST YNFSADGFHSSAPGANLCLGSGV HGGVDWMRKLAFRYRRVKEMY NTYKNNVGGLIGTPKRETWLQL RAELEALTDLWLTHSLKALNLIN SRPNCVNVLVTTTQLIPALAKVL LYGLGSVFPIENIYSATKTGKESC FERIMQRFGRKAVYVVIGDGVEE EQGAKKHNMPFWRISCHADLEA LRHALELEYL	MEEEQDLPEQPVKKAKMQESGE QTISQVSNPDVSDQKPETSSLASN LPMSEEIMTCTDYIPRSSNDYTSQ MYSAKPYAHILSVPVSETAYPGQ TQYQTLQQTQPYAVYPQATQTY GLPPFGALWPGMKPESGLIQTPS PSQHSVLTCTTGLTTSQPSPAHYS YPIQASSTNASLISTSSTIANIPAA AVASISNQDYPTYTILGQNQYQA CYPSSSFGVTGQTNSDAESTTLA ATTYQSEKPSVMAPAPAAQRLSS GDPSTSPSLSQTTPSKDTDDQSRK NMTSKNRGKRKADATSSQDSEL ERVFLWDLDETIIIFHSLLTGSYA QKYGKDPTVVIGSGLTMEEMIFE VADTHLFFNDLEECDQVHVEDV ASDDNGQDLSNYSFSTDGFSGSG GSGSHGSSVGVQGGVDWMRKL AFRYRKVREIYDKHKSNVGGLLS PQRKEALQRLRAEIEVLTDSWLG TALKSLLLIQSRKNCVNVLITTTQ LVPALAKVLLYGLGEIFPIENIYS ATKIGKESCFERIVSRFGKKVTY VVIGDGRDEEIAAKQHNMPFWRI TNHGDLVSLHQALELDFL	MEDSQDLNEQSVKKTCTESDVS QSQNSRSMEMQDLASPHTLVG GGDTPGSSKLEKSNLSSTSVTTN GTGGENMTVLNTADWLLSCNT PSSATMSLLAVKTEPLNSSETTA TTGDGALDTFTGSVITSSGYSPR SAHQYSPQLYPSKPYPHILSTPA AQTMSAYAGQTQYSGMQQPAV YTAYSQTGQPYSLPTYDLGVML PAIKTESGLSQTQSPLQSGCLSY SPGFSTPQPGQTPYSYQMPGSSF APSSTIYANNSVSNSTNFSGSQQ DYPSYTAFGQNQYAQYYSASTY GAYMTSNNTADGTPSSTSTYQL QESLPGLTNQPGTDLHPGEFDT MQSPSTPIKDLDERTCRSSGSKS RGRGRKNNPSPPPDSDLERVFV WDLDETIIVFHSLLTGSYAQKY GKDPPMAVTLGLRMEEMIFNLA DTHLFFNDLEECDQVHIDDVSS DDNGQDLSTYSFATDGFHAAAS SANLCLPTGVRGGVDWMRKLA FRYRRVKELYNTYKNNVGGLL GPAKRDAWLQLRAEIEGLTDSW LTNALKSLSIISTRSNCINVLVTT TQLIPALAKVLLYSLGGAFPIENI YSATKIGKESCFERIMQRFGRKV VYVVIGDGVEEEQAAKKHNMP FWRISSHSDLLALHQALELEYL

5.4.3 **PheWAS analysis**

No association between EYA1 SNPs and gastric ulceration traits (or any traits) were observed using PheWAS analysis. The lack of association may be because the phenotype is very loosely defined. As described in section 1.1.4, gastric ulceration has various aetiologies. Refining the phenotype to gastric ulcers caused by NSAID- or even aspirin-induced gastric ulcer may prevent the dilution of associations between the ulcer phenotype and EYA1 polymorphisms. However, simultaneous analyses of the GWAS study that identified associations between aspirin therapy and PUD (see section 5.2.5) found no association between non-aspirin/any NSAID therapy and PUD (Bourgeois *et al*., unpublished data). Therefore, genetic associations between NSAID therapy and PUD may be limited to aspirin therapy, at least in the Caucasian population in the UK.

It is important to note that the results of GWAS studies performed by Tanikawa *et al*., which identified associations between a variant allele (rs2294008, chromosome 8) of the prostate stem cell antigen (*PSCA*) gene and both gastric[600] and duodenal[601] ulceration, were not identified in the PheWAS analysis. PSCA is a cell surface protein involved in cellular proliferation. Individuals with the C allele at rs2294008 express a PSCA protein with a shorter N-terminal region, which is predicted to have cytoplasmic localisation and higher susceptibility to proteasomal degradation. Therefore, the longer isoform (T allele) may facilitate mucosal repair by enhancing epithelial cellular proliferation[600].

Searching for associations by ulcer traits, SNPs were identified in genes that have not yet been studied in the context of ulcer pathogenesis. These novel associations suggest potential ulcer-related roles for genes encoding MHC class III (*PRRC2A*), stress-signal induced transcription factors (*NFE2L1*) and glycoproteins involved in angiogenesis and metastasis (*SLIT1*).

Counterintuitively, the immune system plays a pivotal role in *H. pylori*-induced gastric ulceration. Defective immune signalling proteins may potentiate immune-mediated gastric inflammation and subsequent ulcer formation[38].

Oxidative stress is a major contributor to the development of stomach ulcer following psychological and physical stress[602]. NSAIDs cause mitochondrial uncoupling, which

dissipates the mitochondrial transmembrane potential. This leads to the release of pro-apoptotic factors and ROS such as superoxide ($O_2^{\bullet-}$) and hydrogen peroxide (H_2O_2), ultimately resulting in gastric mucosal damage. Genes that regulate the anti-oxidative response are therefore very important to the defence against NSAID-induced gastric ulceration[118].

Healing of ulcerative tissue depends on the regrowth of blood vessels (via angiogenesis) to allow the supply of nutrients required for mucosal repair[603]. Both selective[604] and non-selective[605] NSAIDs have demonstrated impaired ulcer healing by reducing angiogenesis and down regulating expression of VEGF/bFGF growth factors.

Interpretation of the results from self-reported gastric/stomach ulcer must be handled with caution as this trait was defined retrospectively by medically trained interviewers from anecdotal evidence (UK Biobank[578], Data-Field: 20002). However, clinically obtained measurements can also cause incorrect assignment of phenotype codes, such as hypercholesterolaemia (ICD9 272.0) and atherosclerosis (ICD9 440). Conclusions made from associations are also limited by the low granularity of the phenotypes integrated into PheWAS approach. Subcategorizing gastric ulcer into infection-, chemical- and psychological-induced gastric ulceration would allow for better-defined associations. However, subdividing traits will lower average case numbers, which will negatively affect the power to detect associations[606].

5.4.4 **Genomic and functional characterisation of rs12678747**

The lead variant, rs12678747, from the aspirin-ulcer GWAS is a common intronic SNP that may fall within a CTCF regulatory region between the last two exons of the *EYA1* gene (Table 5.12). CTCF is a protein that regulates transcriptional activation, repression and insulation by acting as a transcription factor and by remodelling the three-dimensional structure of the genome[607]. The variant may consequently alter the binding or activity of CTCF, thereby increasing or decreasing transcriptional regulation of *EYA1*.

At the time of writing this thesis, a search for single nucleotide polymorphisms in the *'EYA1'* gene on the dbSNP database produces 76,696 results. EYA1 polymorphisms recorded in this database display a uniform distribution across the gene, a feature also

observed in the carbamazepine-hypersensitivity cohort. According to dbSNP, there is a high prevalence of this variant in European populations (MAF: 0.692). However, the variant appeared to be much less common (MAF: 0.302) in the carbamazepine-hypersensitivity cohort (Table 5.11). This discrepancy may be indicative of the low number of patients in the carbamazepine hypersensitive cohort.

Since no eQTL data was available for this variant, the functional effects on *EYA1* gene and protein expression should therefore be determined in stomach tissue (e.g. by RNA-Seq). An explanation for the absence of eQTL data for rs12678747 may be that the effect on EYA1 expression may only be observed in haplotypes containing other SNPs that also map to regulatory regions.

Indeed, the rs12678747 variant is in strong LD with five other *EYA1* SNPs as reported in ENCODE-SCREEN[581] to also fall within regulatory regions (Table 5.13). The ENCODE-SCREEN profiles of two of the five SNPs, rs2380713 and rs2380714, are located in a binding site for the transcription factor MAF bZIP transcription factor K (MAFK).

Another variant found in strong LD with rs12678747, namely rs10103397, causes a synonymous change from a CAT to CAC codon (p.H585H). Using the information available for Homo sapiens on the Codon Usage Database[608], the latter codon has a higher translational efficiency compared to the wild type (0.58 vs. 0.42 respectively), which could therefore lead to an increase in the expression of EYA1 protein. Despite this, no eQTL data was available for any of the variants identified in LD with rs12678747.

Together, this shows that rs12678747, along with various other variants that are commonly co-inherited, may have a cumulative effect on the transcriptional and translational expression of EYA1. However, further experimental work is required to determine whether rs12678747 is the causal variant. This is important as identifying the functional effects of either rs12678747 or causative haplotypes could translate to better clinical decision making for predicting ulcer risk in the administration of NSAIDs.

5.4.5 **Conclusions**

Based on the database analyses, the following conclusions about EYA1 can be made, *EYA1* gene expression is very low in healthy and tumorigenic stomach tissue. This is represented by the apparent lack of EYA1 protein detected in stomach tissue in publically available tissue-based proteomic databases. This may be due to undetectable levels in healthy stomach tissue, but does not provide adequate information on variability in expression, or whether expression is induced in ulcer tissue. Furthermore, because of the complexity of action of EYA1 and interaction with other genes, even low level of expression may lead to significant downstream effects. Further work using functional approaches is needed, including identifying the causal variant, and characterising the SNPs found in regulatory regions within the *EYA1* gene.

PheWAS analysis also uncovered potentially novel associations of genes yet to be defined in ulcer pathogenesis (Table 5.8). Like with GWAS, any PheWAS associations reported herein will need to be validated in replication cohorts. This could be achieved by case-control studies, which will allow for direct hypothesis testing and lower the burden of multiple comparison testing. However, rare alleles such as the variants identified from the PheWAS analysis must be considered with caution as SNPs with low MAFs are more prone to genotyping errors, lack power for making genotype-phenotype associations and demand a much larger sample size[609].

PheWAS studies could also be used in the future to find novel associations between prescribed medications and clinical outcomes (MedWAS), such as pharmacokinetic, pharmacodynamics and adverse drug reactions. Emergence of this EHR-based data approach faces many challenges stemming from unstructured medication records being entered incorrectly (misspelt) or incomplete (dosage, frequency, route of administration, etc.)[572]. Patient compliance to treatment regimen is another variable that is difficult to both incorporate into EHRs and account for in PheWAS analysis. However, tools are being developed that can extract and normalized medication information into a format that can be used for downstream MedWAS analysis[610,611]. A proof-of-concept study using the MedWAS approach has been performed on clinical trial data and proved a plausible method to identify previously reported and novel associations[612], despite having a sample size relatively smaller that than commonly used in GWAS. These types of therapeutic-based PheWAS studies may

increase the power to detect associations between genotypes and drug-induced phenotypes.

Updates to the UK Biobank database include exome sequencing of 50,000 participants and more detailed clinical and primary care information[578]. Another large-scale research initiative, named the 'All of Us' research program, aimed at the advancement of precision medicine was recently started by the NIH[613]. The program plans to retrieve various biological specimens and behavioural data linked the EHRs of a cohort of 1 million American citizens, in order to produce an extensive multi-omics resource for the scientific community[614]. The addition of these longitudinal data sources will allow for more powerful and rigorous studies that will ultimately lead to advancements in personalised healthcare.

Chapter 6

Final discussion

Contents

6.1 **EYA1 in aspirin-induced gastric epithelial damage**

The upper gastrointestinal ADRs associated with NSAIDs are a major clinical burden that demand significant resources from the healthcare providers; prevent effective management of chronic inflammatory conditions; and carry a high risk for mortality (section 1.4.1). Several genetic variants have been reported to alter the risk of developing gastric ulcers (section 1.5.1), but none so far have provided a robust, replicable predictive biomarker.

A GWAS performed by our group (unpublished) identified a novel association between an intronic variant in the *EYA1* gene and aspirin-induced gastric ulceration. The motive behind this project was to investigate the role of this gene in aspirin-mediated gastric epithelial toxicity using an *in vitro* model.

Aspirin and other non-selective inhibitors have been shown to induce direct cytotoxicity of gastric epithelial cells and cause indirect damage through systemic mechanisms compromising repair and gastroprotective processes. In a report by Cook et al., induction of pro-survival pathways by EYA1-mediated histone H2AX dephosphorylation was observed following hypoxia and ionizing radiation-induced genotoxic stress[360]. Aspirin has been shown to cause ATM auto-phosphorylation in colorectal cancer cells, leading to a ROS-independent phosphorylation of p53, CHK2 and H2AX. These events coincide with G_1 cell cycle arrest, mediated mostly by CHK2-induced $p21^{Waf1/Clip1}$, double stranded DNA breaks and activation of DNA repair pathways. However, the study did not show activation of repair pathways beyond aspirin-induced H2AX serine-139 phosphorylation[430].

There have been conflicting reports on the association between aspirin and DNA damage. One report states that aspirin increases DNA damage, assessed by the COMET assay, in lymphocytes from healthy, asthmatic and chronic obstructive pulmonary disorder (COPD) individuals[615]. Similarly, a major metabolite of aspirin, namely 2,3-dihydroxybenzoic acid (2,3-DHBA), caused simultaneous increases to ROS levels and DNA damage in pancreatic and leukaemia cell lines[616].

In contrast, aspirin suppressed genotoxicity caused by the anticancer agent mitomycin in mice[617] and DNA damage in lymphocytes from breast cancer patients[618]; effects supposedly related to the ability of aspirin to act as a radical scavenger. At tolerable

doses of sulindac, scavenger enzymes are activated following oxidative DNA damage. It is therefore likely that tolerable doses of aspirin can also inhibit genotoxic stimuli by activating oxidative response pathways[433]. There have also been mixed reports on the clastogenic potential of aspirin, with some *in vitro* and *in vivo* reports of aspirin-induced chromosome aberrations and sister-chromatid exchange[619].

The experiments carried out in this thesis are the first to examine whether the anti-apoptotic effects of EYA1 tyrosine phosphatase activity displayed in radiation-induced genotoxic stress in HEK cells, translate to aspirin-induced gastric epithelial cytotoxicity. Overexpression of EYA1 in the gastric epithelial AGS cell line attenuated aspirin-induced, caspase-dependent apoptosis (Chapter 4). Based on currently known functions of EYA1, the most likely mechanism of this protective effect is that EYA1 steers H2AX activity towards survival responses following aspirin toxicity (Figure 6.1).

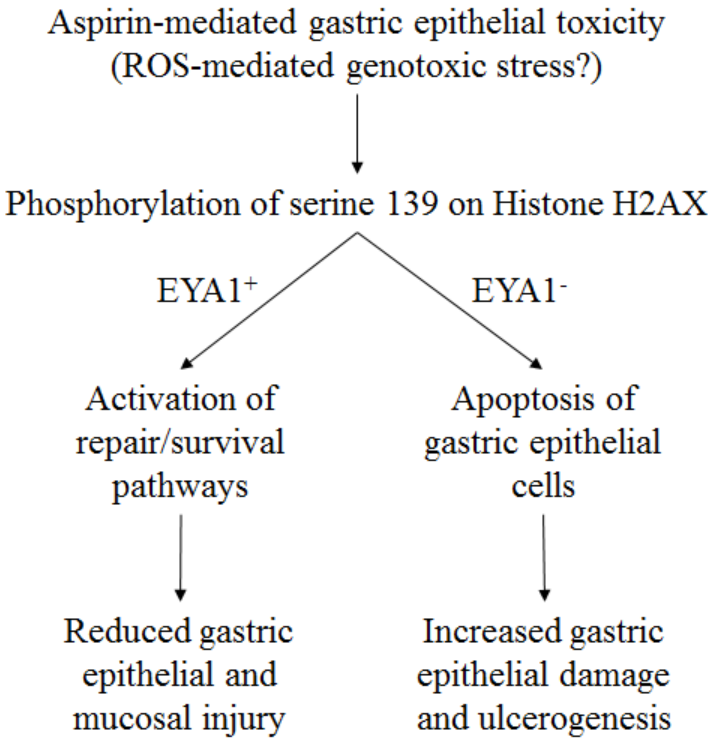

Figure 6.1 Proposed mechanism of EYA1-mediated protection against aspirin-induced gastric epithelial toxicity and ulcerogenesis. During aspirin-induced gastric epithelial toxicity, genotoxic stress causes ATM-mediated phosphorylation of histone H2AX. The degree of EYA1-mediated tyrosine 142 dephosphorylation will determine whether the cell will undergo apoptosis or repair and survival. This may be an important factor in the risk of developing gastric ulcers during aspirin therapy.

This raises several new research questions, such as ‘Does aspirin-induced gastric epithelial toxicity lead to activation of repair pathways via EYA1-H2AX interactions?’, ‘If so, how does aspirin cause H2AX activation?’, ‘Does the transcriptional activity of EYA1 contribute to its protective effects?’ and ‘Does the protective effect of EYA1 observed *in vitro* translate to an *in vivo* model of gastric ulceration?’.

Answering these questions will allow for the testing of novel therapeutic agents that promote EYA1-mediated protection against NSAID-induced gastric epithelial toxicity. EYA1 activity is regulated at least in part by SUMO1-mediated proteolysis[482]. Inhibitors of SUMO1 may therefore increase EYA1 activity and gastric epithelial resilience against aspirin/NSAIDs; however, SUMO1 inhibition would also likely cause various adverse effects given that it regulates several cellular pathways including of cell cycle progression[620,621].

6.2 **Models of NSAID-induced gastric ulceration**

Before filling in the knowledge gaps between aspirin-induced gastric epithelial toxicity and the protective actions of EYA1, several concerns identified during the experimental process must first be addressed. The first obstacle will be to identify a gastric epithelial cell line that expresses endogenous EYA1 protein. As determined in Chapter 2, endogenous EYA1 could not be identified in seven cell lines, consisting of 5 distinct tissue types. This includes two cell lines that have previously shown to express endogenous EYA1 (MDA-MB-231[373] and HEK293[387,463]) and the SH-SY5Y neuroblastoma cell line, which displayed the highest EYA1 gene expression in the HPA cell line database (Figure 5.1D).

EYA1 downregulation seems to be common to human cancer development (Table 1.8) and expression at both the gene and protein levels is scarce in human cancers/cancer cell lines (sections 5.3.1 and 5.3.2). It will therefore be necessary to test other non-tumour-derived gastric epithelial models, such as JOK-1 and GES-1 immortalised cell lines, induced pluripotent stem cells (iPSCs) or primary gastric epithelial cells[622], for endogenous EYA1 expression.

The lack of EYA1 expression in the tested cell lines is likely due to the recurrent 769-cytosine deletion identified by sequencing cell line EYA1 cDNAs (Figure 3.8). It will

be important to sequence the RNA of healthy patient samples to determine whether this frameshift mutation is observable outside of tumorigenic sources. Overexpression of the reference EYA1 did provide a protection against aspirin-induced gastric epithelial toxicity; however, it is important to remember that this was protection has only so far been observed at greatly upregulated levels of ectopic EYA1. Identifying a model that endogenously expresses EYA1 protein will allow for a better understanding of EYA1 activity *in situ*, perhaps by using siRNA techniques.

It was unclear whether the reduction in BAX, BCL-2 and BCL-X_L protein expression (Figure 4.7) was a consequence of the transfection process or by the activity of overexpressed EYA1 protein. Therefore, future experiments will include subcloning untagged EYA1 into a *pac*-containing plasmid for stable expression in AGS, HGC-27 and Hs746T gastric epithelial cell lines using non-transposase transfection methods. This will clarify whether the downregulation of BAX, BCL-2 and BCL-X_L can be replicated both by using a transfection method less likely to cause genome alterations and by eliminating any changes to EYA1 function caused by protein tags.

6.2.1 **Limitations of traditional models of GI toxicity**

In vitro models

Though not commonly used in drug development as a pre-clinical screening tool for GI toxicity, *in vitro* models are useful in looking closer at the mechanisms of tissue-specific toxicities[622]. *In vitro* models also have the advantage of being easy to handle, an infinite source of replication and an even cheaper and more rapid method of studying toxicity than *in vivo* and clinical studies.

Drawbacks of *in vitro* studies are that cell lines are made by isolating tissues, which are usually derived from late-stage metastatic tumours or immortalised by transfection, and culturing them in ways that causes further genotypic and phenotypic shifts from healthy tissue. This could cause the tissue to respond differently to stimuli over time and does not allow for an understanding of how other cell types/bodily systems respond to the stimuli[623]. Primary resected tissue on the other hand can often be difficult to obtain, has limited replicability and is more prone to contamination. Lastly, most gastric cell lines are derived from epithelial cells (Table 2.1). As

described in section 1.2.2, several glandular cells are important in ulcer pathogenesis, a factor that is not accounted for in tumour-derived and immortalised cell lines.

In vivo models

Various *in vivo* models exist for the study of NSAID-induced peptic ulceration[624]. Using these techniques in *EYA1* knockout rodents, or rodents with specific *EYA1* mutations, may provide further insight into the role of EYA1 in NSAID-induced peptic ulceration. However, as with all models, *in vivo* models of NSAID-induced peptic ulceration present various limitations and may only be predictive of 70% of clinical drug toxicities when combining rodent and non-rodent models[625].

These include high costs, ethical considerations and various physiological and environmental differences between humans and *in vivo* models of disease[625]. For example, animal studies use young adults whereas ulceration occurs in a wide age range in humans. Secondly, healthy animals are used *in vivo*, whereas patients can have a variety of comorbidities that may affect ulcer pathology. Concomitant therapy is also another consideration that cannot be fully controlled for in animal studies. Genetic variability is another factor present in human disease that cannot be replicated in genetically homogenous animal models. Lastly, animals are kept in uniform environmental conditions during *in vivo* studies. As described in section 1.2.3, environmental factors such as housing, nutrition and lifestyle play major roles in human ulcer pathogenesis[625].

6.2.2 **Emerging models of GI toxicity**

More recently developed models of drug-induced GI toxicity overcome some of these limitations and provide new ways to evaluate disease progression *in vitro*/*ex vivo*[622]. Recent studies have used a trans-well model, consisting of a monolayer of NCI-N87 cells, to study drug permeability[626] and the effect of *H. pylori* infection on gastric epithelial permeability, pro-inflammatory cytokine secretion and apical/basolateral events[627]. A model like this would be useful to study the topical effects of NSAIDs, such as ion trapping, and their role in inflammation and epithelial integrity.

In vitro grown organoids are near-physiological models of *in vivo* biological processes that have quickly become an essential tool in researching human disease. Since the development of intestinal organoid culture systems circa 2009[628], several other tissue

models have been created[629]. Gastric organoid models were developed a year later by the same group[630] and have since been used to model diseases, such as *H. pylori* infection and gastric cancer, and study gastric physiology and development[622].

The process involves *de novo* generation of 3D cellular clusters from human and mouse-derived primary tissue, embryonic stem cells or iPSCs[631]. These spheroids can be grown indefinitely in extracellular matrix substitutes (e.g. Matrigel) and differentiated into mature organoids by manipulating growth signalling pathways to mimic the functionality of various tissues[629].

Mature gastric organoids can maintain morphological and macromolecular markers of both oxyntic and pyloric glands, such as E-cadherin/catenin positive endocrine (pepsinogen, gastrin and ghrelin) and mucous (mucin 5AC) cells[632]. Unfortunately, corpus-type organoids do not possess parietal cells and therefore lack the acidic luminal environment[631,632].

Other limitations to organoid models include the lack of several local gastric cellular components (immune cells, ENS, etc.) and physiologically relevant mechanical effects (gastric motility). The utility for screening assays may also be limited by the difficulty in accessing the luminal surface of organoids for drug treatments/sampling, as well as the fact that it is a relatively low-throughput method due to the higher level of complexity of the model. Phenotypic differences exist with both intra-individual and inter-individual gastric organoids, which presents yet another barrier. Organoids within the same culture are heterogeneous due to variability in their viability, size and shape[629]. Whereas, inter-individual variability within and between populations will demand large collections of organoids from different social and demographic backgrounds[622].

Nevertheless, *in vitro* gastric organoids could provide useful tools for the future of GI toxicity models as they are more physiologically relevant than 2D culture models, are easier to manipulate than *in vivo* models and reduce the cost and questions of animal welfare associated with them[33,629]. To date, there seems to be no published accounts of gastric organoids being used to study NSAID-induced peptic ulceration. However, pilot studies performed by our group have shown that aspirin induces dose-dependent toxicity in gastric organoids generated from murine stomach.

6.3 **Novel solutions to NSAID-induced gastropathy**

6.3.1 **NSAID conjugates**

Though COX-2 selective inhibitors have found a niche use, there remains a need to search for novel strategies to dissociate analgesic, anti-inflammatory and anti-platelet therapy from gastrointestinal, renal and cardiovascular ADRs. One alternative therapy being explored is the use of NSAIDs that are conjugated to gastroprotective agents (also termed NSAID prodrugs), such as phosphatidylcholine (PC) and gaseous mediators, NO and H_2S[99,633].

PC-conjugated NSAIDs

PC constitutes 50% of the phospholipids found in most eukaryotic cell membranes[634] and are also an important component of the mucous gel layer, as described in section 1.2.2. A study combining several non-selective NSAIDs with exogenous phospholipids prevented mucosal damage and the GI side effects associated with the parent drugs, whilst enhancing their therapeutic effects[635].

Subsequent studies in rats demonstrated that PC-conjugation accelerated ulcer healing[636], probably through the maintenance of mucosal surface hydrophobicity, and increased NSAID bioavailability and potency (COX-inhibition)[637]. The gastroprotective effects of PC-conjugated NSAIDs were also observed in a small human study, with the number of gastric erosions being significantly lower in the PC-associated aspirin group compared to aspirin group and the level of PG inhibition being equivalent in both groups[638].

COX-inhibiting nitric oxide donors (CINODs)

The gastroprotective effects of NO and H_2S include vasodilation, inhibition of leukocyte adherence, and accelerated ulcer healing[99] (covered in section 1.4.2). CINODs, previously called NO-releasing NSAIDs or NO-NSAIDs, are non-steroidal anti-inflammatory agents conjugated to a single NO-donating group.

The first CINOD to be developed, Naproxcinod, is a nitroxybutyl ester-conjugated naproxen selected by NicOx that reached phase III clinical trials for the treatment of osteoarthritis[639]. Studies in rats show that Naproxcinod exhibited significantly less

gastric and small intestinal damage, superior analgesic and comparable anti-inflammatory effects, and did not impair ulcer healing[640].

Naproxcinod also displayed promising results in early stage clinical trials, significantly reducing GI erosions and small intestinal permeability compared to diclofenac and naproxen respectively, whilst maintaining comparable bioavailability[641]. However, after entering Phase II and III clinical trials, the reduced GI toxicity of Naproxcinod was found to be less profound than what was observed in animal studies[642].

The use of Naproxcinod for the treatment of osteoarthritis was later rejected by the U.S. Food and Drug Administration (FDA) in 2010 based on the lack of studies in high-risk populations, e.g. elderly and those at increased CV and GI risk, drug-drug interactions, e.g. vasoactive, platelet-active, anti-coagulant or GI related agents, and GI, CV and renal safety[643]. Naproxcinod was also rejected by the European Medicines Agency after the committee raised concerns that the benefits did not sufficiently outweigh the risks, including the effects on blood pressure and hepatotoxicity[644].

Interestingly, a study of the cytotoxic mechanisms of NO-aspirin shown that the NO moiety induced DNA damage through oxidative stress. DNA damage assessed by COMET assay was accompanied by activation of ATM, increased phosphorylation of histone H2AX and apoptosis[645]. This suggests that EYA1 activity may also prove important in the toxicity of future NSAID therapies.

Hydrogen Sulphide-releasing NSAIDs

Similar to NO-NSAIDs, several H_2S-donating NSAIDs are in development, with preclinical tests displaying promising safety profiles. H_2S-releasing versions of diclofenac and indomethacin prevented gastric damage and leukocyte adherence observed with the parent compounds in rats[646]. Additionally, H_2S-conjugated diclofenac can reduce the expression and synthesis of various pro-inflammatory cytokines[647,648] and H2S-conjugated salicylate significantly accelerates ulcer healing in rats[296].

6.3.2 **Prostaglandin synthase inhibitors and receptor agonists/antagonists**

The adverse cardiovascular effects of COX-2 selective NSAIDs are suggested to be a consequence of PGI_2 inhibition, a PG with potent antithrombotic properties (see

section 1.3.2). Since PGE_2 is the PG mostly commonly associated with inflammation, specific inhibitors of PGE_2 synthase and ligands of the four PGE_2 receptors (EP1-4) may provide anti-inflammatory properties with safer CV and GI profiles than current NSAIDs.

mPGES-1 inhibitors

To this end, an inducible PGE synthase that preferentially metabolises COX-2-derived PGH_2 in inflammatory cells, mPGES-1, presents an attractive target. Selective inhibitors of this isomerase are in development by pharmaceutical companies, two of which have entered clinical trials[649].

PTGES knockout mice do not develop febrile response following lipopolysaccharide injection[650] and exhibit a 40% reduction in pain response compared to normal mice[651,652]. Studies PTGES knockout mice have also shown that the severity of joint pain is significantly reduced in collagen and carrageenan-induced arthritis models compared to wild-type phenotypes[653]. Taken together, these studies suggest that inhibition of PGE_2 synthases could be used to treat fever, pain and inflammatory conditions.

Several animal studies have shown comparable efficiencies The adverse GI events associated with currently available NSAIDs are so far not apparent with mPGES-1 inhibitors[654]. There is also evidence that mPGES-1 inhibition may confer positive cardiovascular effects, perhaps due to the "shunting" of PGH_2 towards PGI_2 synthesis[655]. However, increased PGI_2 levels may concurrently override the analgesic effects of inhibited PGE_2 synthesis[656]. Other factors withholding the development of mPGES-1 inhibitors include interspecies differences in efficacy, poor pharmacokinetic properties and selectivity issues against other mPGES isoforms[657].

EP receptor agonists/antagonists

EP4 receptors are the most common PGE_2 receptors found in humans. EP4 receptors exhibit both pro-inflammatory and anti-inflammatory roles depending on tissue and disease states[658]. Activation of EP2 receptors has also demonstrated pro-inflammatory properties[659]. EP2 and EP4 receptor agonists and antagonists may consequently become valuable novel drug classes.

6.3.3 **Alternative approaches to reduce GI toxicity**

Dual COX/5-LOX inhibitors

In addition to conversion to prostanoids by COX enzymes, arachidonic acid is also a substrate for lipoxygenase (LOX) metabolism into lipoxins (12-LOX and 15-LOX) and leukotrienes (5-LOX). Inhibition of COX enzymes can divert arachidonic acid metabolism to increased production of leukotrienes. Leukotrienes are a group of eicosanoid mediators that regulate pro-inflammatory responses. Inappropriate leukotriene production is associated with various inflammatory conditions including arthritic conditions, gout, psoriasis, inflammatory bowel disease, allergic responses, COPD and gastric ulceration[660].

Dual inhibitors of both the COX and 5-LOX pathways were therefore developed as a strategy to maintain the anti-inflammatory and anti-thrombotic, whilst avoiding the adverse effects of leukotriene build-up. The leading agent in this novel drug class, Licofelone, is the first to progress to phase III human studies and has shown similar efficacy as naproxen and celecoxib[661]. The GI tolerability of Licofelone is similar to that of celecoxib, and shows no apparent decrease when combined with aspirin therapy. Licofelone also demonstrated lower incidences of peripheral oedema, compared to celecoxib and naproxen, and hypertension, compared to naproxen[662].

In summary, dual LOX/COX inhibitors have shown encouraging results from preliminary studies and may provide safer alternative than current NSAIDs.

Lactoferrin and NSAID sequestering

Studies to test the effect of growth factors present in bovine colostrum have shown that colostrum preparations reduced NSAID-induced gastric injury[663,664]. Recent studies have also shown that lactoferrin, a constituent of various secretory fluids (including milk), can reduce gastric ulcer and bleeding. The mechanism behind this protective action was found to be that the C-lobe of lactoferrin sequesters unbound COX inhibitors[665,666]. This highlights the potential of growth factor supplements and lactoferrin in the prevention of NSAID-induced gastric injury.

6.4 **Conclusions**

Despite the advances in NSAID development, non-selective NSAIDs, will likely remain the mainstay therapy for anti-inflammatory, analgesic and antipyretic conditions for the near future. Furthermore, low-dose aspirin remains an important agent for secondary prevention of cardiovascular disease. Even with current preventative measures, GI complications caused by NSAIDs are, and will surely continue to be, a major global health burden. Accordingly, improved preventative and therapeutic strategies are required, the development of which will progress through utilising advanced models of GI toxicity and better characterising the mechanisms of NSAID-induced GI injury.

The association between the *EYA1* SNP, rs12678747, and gastric ulceration is intriguing but needs further validation in additional replication cohorts, and functional analysis to determine mechanisms. The findings present in this thesis start to provide a better mechanistic understanding of aspirin-induced gastric epithelial toxicity.

The next steps will be to:

(i) Validate the protective effects of EYA1 overexpression during aspirin-induced gastric epithelial toxicity.

(ii) More clearly connect aspirin-induced gastric epithelial toxicity to EYA1-mediated survival/repair responses.

(iii) Identify the functional effects of the aforementioned SNP and other SNPs within its haplogroup.

Appendices

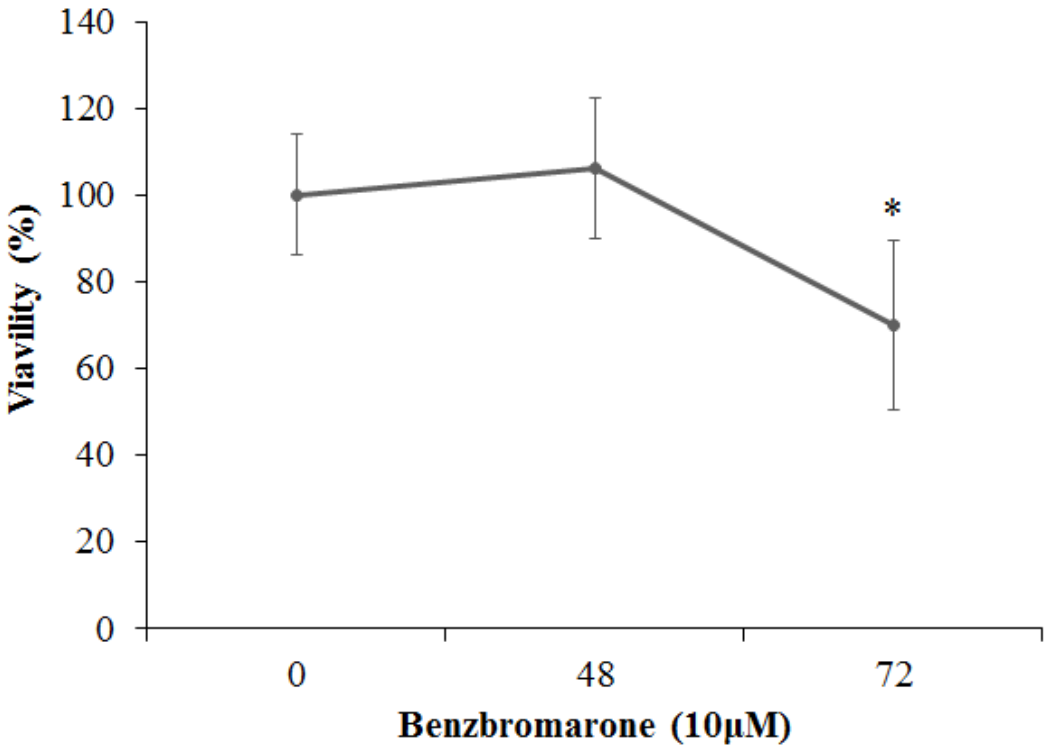

Appendix 2.1 The effect of 10µM benzbromarone on AGS cell viability after 48 and 72h treatment. Data represents means ± SD (n=3). A one-way ANOVA with Dunnett's correction was performed to compare the means of each time point with the untreated control. * denotes $p < 0.05$.

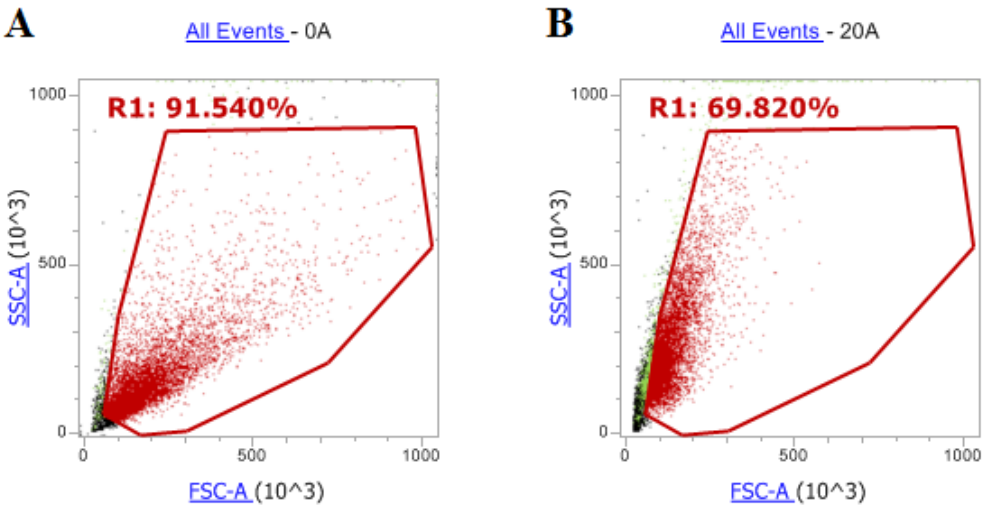

Appendix 2.2 Representative images of forward (FSC-A) and side (SSC-A) scatter plots to show gating of AGS cells included in the annexin-V/propidium iodide flow cytometry analysis. Plots for both control (A) and aspirin (B) treated cells are shown.

Appendix 3.1 Confidence values for EYA1 peptide fragments identified in the mass spectrometric analysis of AGS and AGS-EYA1 protein lysates. Calulations for the confidence values are based on the mass accuracy of the parent and fragment ions, the number of b- and y-ions matched to the theoretical spectrum, the absence of missed or non-specific tryptic cleavages, and the absence of biological or artefactual modifications. The maximum possible confidence value attainable is 99%.

Sequence	Confidence value
ALSLIHSR	99.00
ALSLIHSR	62.70
DPPTSVSLGLR	99.00
DPPTSVSLGLR	97.83
DPPTSVSLGLR	97.57
DPPTSVSLGLR	97.05
EMQDLTSPHSR	73.38
EMQDLTSPHSR	27.79
GLGIVFPIENIYSATK	99.00
GLGIVFPIENIYSATK	99.00
GLGIVFPIENIYSATK	99.00
GLGIVFPIENIYSATK	99.00
LGNSHINSNSMTPNGTEVK	99.00
LSGSSESPSGPK	99.00
LSGSSESPSGPK	99.00
LSGSSESPSGPK	99.00
LSGSSESPSGPK	99.00
LSGSSESPSGPK	44.41
NNVGGLLGPAK	99.00
NNVGGLLGPAK	99.00
NNVGGLLGPAK	98.88
NNVGGLLGPAK	21.34
NNVGGLLGPAK	21.34

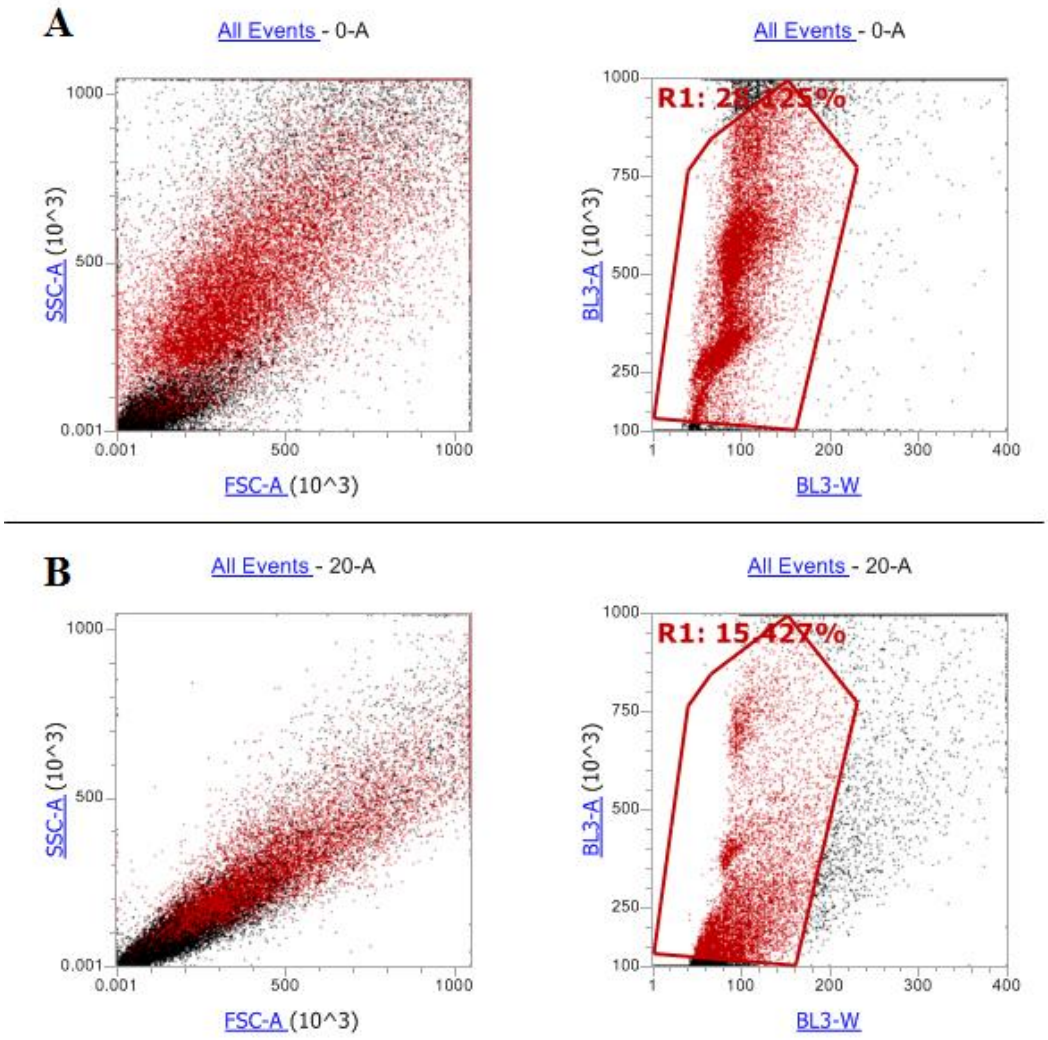

Appendix 4.1 Representative images of forward and side scatter plots to show gating of AGS and AGS-EYA1 cells included in the sub-G1 flow cytometry analysis. Gating was performed by selecting around the area of cells on the dot plot of BL3 channel width (BL3-W) vs. BL3 channel area (BL3-A). Plots for both control (A) and aspirin (B) treated cells are shown.

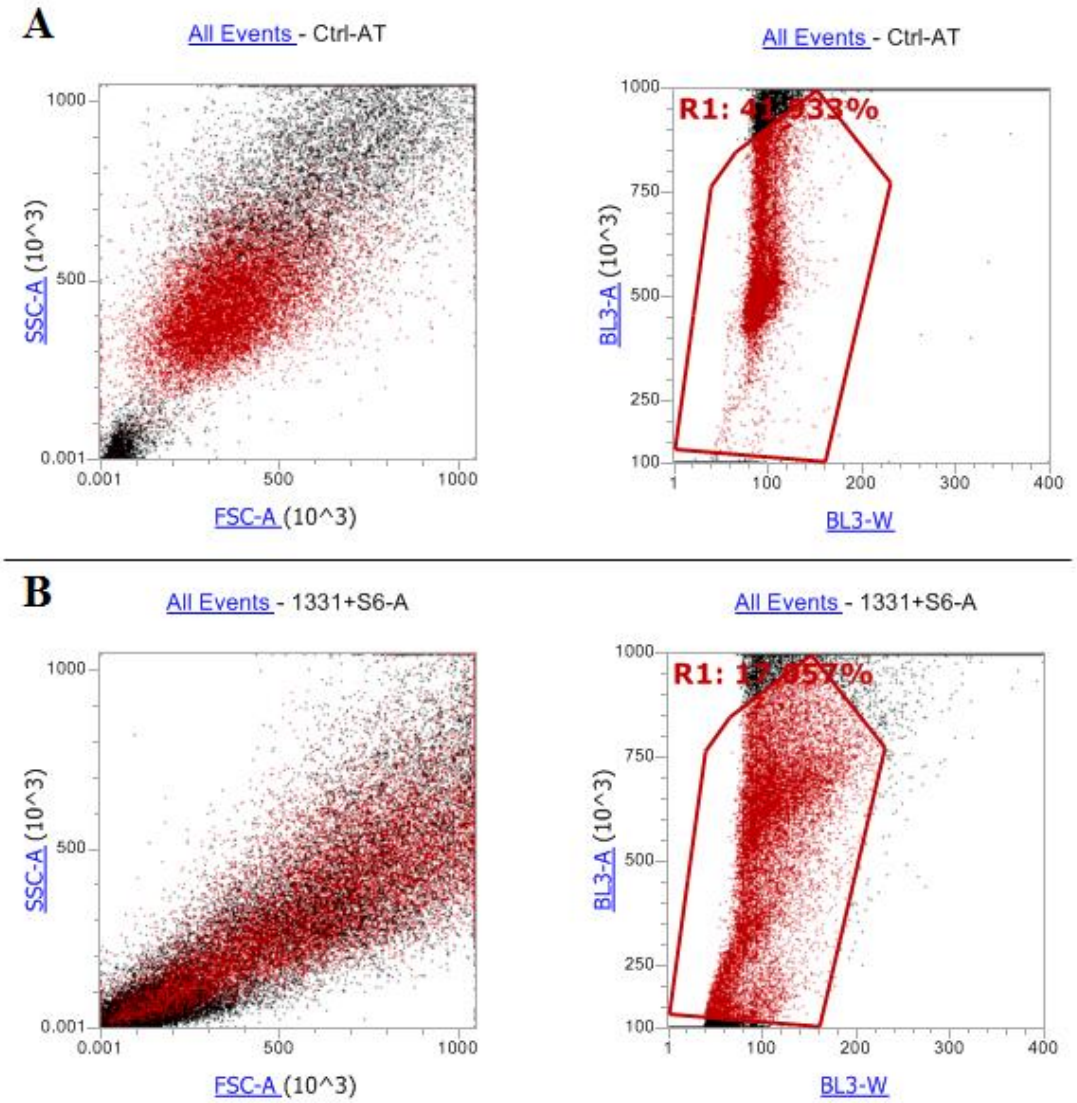

Appendix 4.2 Representative images of forward and side scatter plots to show gating of AGS and AGS-EYA1 cells included in the sub-G1 flow cytometry analysis. Gating was performed by selecting around the area of cells on the dot plot of BL3 channel width (BL3-W) vs. BL3 channel area (BL3-A). Plots for cells treated with control (A) and A1331853 with S63845 (B) are shown.

Bibliography

1 Musumba, C., Pritchard, D. M. & Pirmohamed, M. Review article: cellular and molecular mechanisms of NSAID-induced peptic ulcers. *Alimentary pharmacology & therapeutics* **30**, 517-531, doi:10.1111/j.1365-2036.2009.04086.x (2009).

2 Mahadevan, V. Anatomy of the stomach. *Surgery (Oxford)* **32**, 571-574 (2014).

3 Wilson, R. L. & Stevenson, C. E. in *Shackelford's Surgery of the Alimentary Tract, 2 Volume Set* 634-646 (Elsevier, 2019).

4 Drake, R. L., Vogl, W., Mitchell, A. W. M. & Gray, H. *Gray's anatomy for students*. (Philadelphia, PA : Churchill Livingstone/Elsevier, 2010 [i.e. 2009]. 2nd ed., 2010).

5 Ekblad, E., Mei, Q. & Sundler, F. Innervation of the gastric mucosa. *Microscopy research and technique* **48**, 241-257 (2000).

6 Browning, K. N. & Travagli, R. A. Central nervous system control of gastrointestinal motility and secretion and modulation of gastrointestinal functions. *Comprehensive physiology* **4**, 1339-1368 (2011).

7 Scharoun, S., Barone, F., Wayner, M. & Jones, S. Vagal and gastric connections to the central nervous system determined by the transport of horseradish peroxidase. *Brain research bulletin* **13**, 573-583 (1984).

8 Furness, J. B. The enteric nervous system and neurogastroenterology. *Nature reviews Gastroenterology & hepatology* **9**, 286 (2012).

9 Humphreys, G., Davison, J. & Veale, W. Hypothalamic neuropeptide Y inhibits gastric acid output in rat: role of the autonomic nervous system. *American Journal of Physiology-Gastrointestinal and Liver Physiology* **263**, G726-G732 (1992).

10 Powley, T. L., Holst, M. C., Boyd, D. B. & Kelly, J. B. Three-dimensional reconstructions of autonomic projections to the gastrointestinal tract. *Microscopy research and technique* **29**, 297-309 (1994).

11 Schemann, M. & Grundy, D. Electrophysiological identification of vagally innervated enteric neurons in guinea pig stomach. *American Journal of Physiology-Gastrointestinal and Liver Physiology* **263**, G709-G718 (1992).

12 Travagli, R. A., Hermann, G. E., Browning, K. N. & Rogers, R. C. Brainstem circuits regulating gastric function. *Annu. Rev. Physiol.* **68**, 279-305 (2006).

13 White Jr, R. L. *et al.* Excitation of neurons in the medullary raphe increases gastric acid and pepsin production in cats. *American Journal of Physiology-Gastrointestinal and Liver Physiology* **260**, G91-G96 (1991).

14 Coceani, F., Pace-Asciak, C., Volta, F. & Wolfe, L. Effect of nerve stimulation on prostaglandin formation and release from the rat stomach. *American Journal of Physiology-Legacy Content* **213**, 1056-1064 (1967).

15 Nezamis, J. E., Robert, A. & Stowe, D. F. Inhibition by prostaglandin E1 of gastric secretion in the dog. *The Journal of physiology* **218**, 369-383 (1971).

16 Tache, Y. Brainstem neuropeptides and vagal protection of the gastric mucosal against injury: role of prostaglandins, nitric oxide and calcitonin-gene related peptide in capsaicin afferents. *Current medicinal chemistry* **19**, 35-42 (2012).

17 Schubert, M. L. & Peura, D. A. Control of gastric acid secretion in health and disease. *Gastroenterology* **134**, 1842-1860 (2008).

18 Snell, R. S. *Clinical anatomy by regions*. (Philadelphia ;London : Lippincott Williams & Wilkins, 2008. 8th ed., 2008).

19 Barrett, K. E. *et al. Physiology of the Gastrointestinal Tract. [electronic book]*. Vol. 4th ed. (Elsevier Science, 2006).
20 Choi, E. *et al.* Cell lineage distribution atlas of the human stomach reveals heterogeneous gland populations in the gastric antrum. *Gut*, gutjnl-2013-305964 (2014).
21 Hirschowitz, B. Pepsinogen. *Postgraduate medical journal* **60**, 743 (1984).
22 Gray, J. L., Bunnett, N. W., Orloff, S. L., Mulvihill, S. J. & Debas, H. T. A role for calcitonin gene-related peptide in protection against gastric ulceration. *Annals of surgery* **219**, 58 (1994).
23 Green, T. & Dockray, G. Calcitonin gene-related peptide and substance P in afferents to the upper gastrointestinal tract in the rat. *Neuroscience letters* **76**, 151-156 (1987).
24 Hansen, P., Stadil, F. & Rehfeld, J. Hepatic and intestinal elimination of endogenous gastrin in pigs. *Digestion* **57**, 356-361 (1996).
25 Hansen, C. P., Stadil, F., Yucun, L. & Rehfeld, J. Pharmacokinetics and organ metabolism of carboxyamidated and glycine-extended gastrins in pigs. *American Journal of Physiology-Gastrointestinal and Liver Physiology* **271**, G156-G163 (1996).
26 Vuyyuru, L. & Schubert, M. L. Histamine, acting via H3 receptors, inhibits somatostatin and stimulates acid secretion in isolated mouse stomach. *Gastroenterology* **113**, 1545-1552 (1997).
27 Yeomans, N. D. & Naesdal, J. Systematic review: ulcer definition in NSAID ulcer prevention trials. *Alimentary pharmacology & therapeutics* **27**, 465-472 (2008).
28 Warren, J. R. & Marshall, B. Unidentified curved bacilli on gastric epithelium in active chronic gastritis. *The lancet* **321**, 1273-1275 (1983).
29 Malfertheiner, P., Chan, F. K. & McColl, K. E. Peptic ulcer disease. *The Lancet* **374**, 1449-1461 (2009).
30 Ramakrishnan, K. & Salinas, R. C. Peptic ulcer disease. *American family physician* **76** (2007).
31 Pirmohamed, M. *et al.* Adverse drug reactions as cause of admission to hospital: prospective analysis of 18 820 patients. *Bmj* **329**, 15-19 (2004).
32 Musumba, C. *et al.* The relative contribution of NSAIDs and H elicobacter pylori to the aetiology of endoscopically-diagnosed peptic ulcer disease: observations from a tertiary referral hospital in the UK between 2005 and 2010. *Alimentary pharmacology & therapeutics* **36**, 48-56 (2012).
33 Burkitt, M. D., Duckworth, C. A., Williams, J. M. & Pritchard, D. M. Helicobacter pylori-induced gastric pathology: insights from in vivo and ex vivo models. *Disease models & mechanisms* **10**, 89-104 (2017).
34 Vos, T. *et al.* Global, regional, and national incidence, prevalence, and years lived with disability for 328 diseases and injuries for 195 countries, 1990–2016: a systematic analysis for the Global Burden of Disease Study 2016. *The Lancet* **390**, 1211-1259 (2017).
35 Cai, S., García Rodríguez, L., Masso-Gonzalez, E. & Hernandez-Diaz, S. Uncomplicated peptic ulcer in the UK: trends from 1997 to 2005. *Alimentary pharmacology & therapeutics* **30**, 1039-1048 (2009).
36 Lanas, A. & Chan, F. K. Peptic ulcer disease. *The Lancet* **390**, 613-624 (2017).
37 Miller, A. & Schwaitzberg, S. Surgical and endoscopic options for benign and malignant gastric outlet obstruction. *Current Surgery Reports* **2**, 48 (2014).
38 Kusters, J. G., van Vliet, A. H. & Kuipers, E. J. Pathogenesis of Helicobacter pylori infection. *Clinical microbiology reviews* **19**, 449-490 (2006).

39 Garcia Rodriguez, L. A. & Hernández-Díaz, S. Risk of uncomplicated peptic ulcer among users of aspirin and nonaspirin nonsteroidal antiinflammatory drugs. *American journal of epidemiology* **159**, 23-31 (2004).
40 Donahue, J. G. *et al.* Gastric and duodenal safety of daily alendronate. *Archives of internal medicine* **162**, 936-942 (2002).
41 Graham, D. & Malaty, H. Alendronate gastric ulcers. *Alimentary pharmacology & therapeutics* **13**, 515-519 (1999).
42 Lanza, F. L. Gastrointestinal Adverse Effects of Bisphosphonates. *Treatments in endocrinology* **1**, 37-43 (2002).
43 Grove, E. L., Würtz, M., Schwarz, P., Jørgensen, N. R. & Vestergaard, P. Gastrointestinal events with clopidogrel: a nationwide population-based cohort study. *Journal of general internal medicine* **28**, 216-222 (2013).
44 Vella, V. Drug-induced peptic ulcer disease. *Journal of the Malta College of Pharmacy Practise* **10**, 15-19 (2005).
45 Shike, M., Gillin, J. S., Kemeny, N., Daly, J. M. & Kurtz, R. C. Severe gastroduodenal ulcerations complicating hepatic artery infusion chemotherapy for metastatic colon cancer. *American Journal of Gastroenterology* **81** (1986).
46 Schuster, K. M., Feuer, W. J. & Barquist, E. S. Outcomes of cocaine-induced gastric perforations repaired with an omental patch. *Journal of Gastrointestinal Surgery* **11**, 1560-1563 (2007).
47 Ito, T., Igarashi, H. & Jensen, R. T. Pancreatic neuroendocrine tumors: clinical features, diagnosis and medical treatment: advances. *Best practice & research Clinical gastroenterology* **26**, 737-753 (2012).
48 Lee, J. K., Whittaker, S. J., Enns, R. A. & Zetler, P. Gastrointestinal manifestations of systemic mastocytosis. *World journal of gastroenterology: WJG* **14**, 7005 (2008).
49 Grant, C. S. & Van Heerden, J. A. Anastomotic ulceration following subtotal and total pancreatectomy. *Annals of surgery* **190**, 1 (1979).
50 Higa, K. D., Boone, K. B. & Ho, T. Complications of the laparoscopic Roux-en-Y gastric bypass: 1,040 patients-what have we learned? *Obesity surgery* **10**, 509-513 (2000).
51 Kefalas, C. H. in *Baylor University Medical Center Proceedings.* 147-151 (Taylor & Francis).
52 Ingle, S. B. & Hinge, C. R. Eosinophilic gastroenteritis: an unusual type of gastroenteritis. *World journal of gastroenterology: WJG* **19**, 5061 (2013).
53 Gromski, M. A. *et al.* Multifocal Gastric Ulcers Caused by Diffuse Large B Cell Lymphoma in a Patient With Significant Weight Loss. *Journal of investigative medicine high impact case reports* **4**, 2324709616683721 (2016).
54 Cárdenas-Mondragón, M. G. *et al.* Epstein-Barr virus association with peptic ulcer disease. *Analytical Cellular Pathology* **2015** (2015).
55 Debongnie, J.-C. *et al.* Gastric ulcers and Helicobacter heilmannii. *European journal of gastroenterology & hepatology* **10**, 251-254 (1998).
56 Weston, A. P. Hiatal hernia with Cameron ulcers and erosions. *Gastrointestinal endoscopy clinics of North America* **6**, 671-679 (1996).
57 Ziegler, A. B. The role of proton pump inhibitors in acute stress ulcer prophylaxis in mechanically ventilated patients. *Dimensions of Critical Care Nursing* **24**, 109-114 (2005).
58 Chung, C.-S., Chiang, T.-H. & Lee, Y.-C. A systematic approach for the diagnosis and treatment of idiopathic peptic ulcers. *The Korean journal of internal medicine* **30**, 559 (2015).
59 Lichtenberger, L. M. Gastroduodenal mucosal defense. *Current opinion in gastroenterology* **15**, 463 (1999).

60 Corfield, A. P. Mucins: a biologically relevant glycan barrier in mucosal protection. *Biochimica et Biophysica Acta (BBA)-General Subjects* **1850**, 236-252 (2015).
61 Taupin, D. & Podolsky, D. K. Trefoil factors: initiators of mucosal healing. *Nature reviews Molecular cell biology* **4**, 721 (2003).
62 Lacy, E. & Ito, S. Rapid epithelial restitution of the rat gastric mucosa after ethanol injury. *Laboratory investigation; a journal of technical methods and pathology* **51**, 573-583 (1984).
63 Svanes, K., Ito, S., Takeuchi, K. & Silen, W. Restitution of the surface epithelium of the in vitro frog gastric mucosa after damage with hyperosmolar sodium chloride: morphologic and physiologic characteristics. *Gastroenterology* **82**, 1409-1426 (1982).
64 Ho, S. B. *et al.* The adherent gastric mucous layer is composed of alternating layers of MUC5AC and MUC6 mucin proteins. *Digestive diseases and sciences* **49**, 1598-1606 (2004).
65 Kawakubo, M. *et al.* Natural antibiotic function of a human gastric mucin against Helicobacter pylori infection. *Science* **305**, 1003-1006 (2004).
66 Lindén, S. *et al.* Strain-and blood group–dependent binding of Helicobacter pylori to human gastric MUC5AC glycoforms. *Gastroenterology* **123**, 1923-1930 (2002).
67 Allen, A. & Flemström, G. Gastroduodenal mucus bicarbonate barrier: protection against acid and pepsin. *American Journal of Physiology-Cell Physiology* **288**, C1-C19 (2005).
68 Ham, M., Akiba, Y., Takeuchi, K., Montrose, M. H. & Kaunitz, J. D. in *Physiology of the Gastrointestinal Tract (Fifth Edition)* 1169-1208 (Elsevier, 2012).
69 Han, T. *et al.* Novel hybrids of brefeldin A and nitrogen mustards with improved antiproliferative selectivity: design, synthesis and antitumor biological evaluation. *European journal of medicinal chemistry* **150**, 53-63 (2018).
70 Laine, L., Takeuchi, K. & Tarnawski, A. Gastric mucosal defense and cytoprotection: bench to bedside. *Gastroenterology* **135**, 41-60 (2008).
71 Yoshikawa, T. & Arakawa, T. *Bioregulation and Its Disorders in the Gastrointestinal Tract*. (Blackwell Science Japan, 1998).
72 Nguyen, T. *et al.* Novel roles of local insulin-like growth factor-1 activation in gastric ulcer healing: promotes actin polymerization, cell proliferation, re-epithelialization, and induces cyclooxygenase-2 in a phosphatidylinositol 3-kinase-dependent manner. *The American journal of pathology* **170**, 1219-1228 (2007).
73 Pai, R. *et al.* Prostaglandin E 2 transactivates EGF receptor: a novel mechanism for promoting colon cancer growth and gastrointestinal hypertrophy. *Nature medicine* **8**, 289 (2002).
74 Hase, K. *et al.* Expression of LL-37 by human gastric epithelial cells as a potential host defense mechanism against Helicobacter pylori. *Gastroenterology* **125**, 1613-1625 (2003).
75 Yang, Y. H. *et al.* The cationic host defense peptide rCRAMP promotes gastric ulcer healing in rats. *Journal of Pharmacology and Experimental Therapeutics* **318**, 547-554 (2006).
76 Holzer, P. in *Physiology of the Gastrointestinal Tract (Fifth Edition)* 817-845 (Elsevier, 2012).
77 Berndt, G., Grosser, N., Hoogstraate, J. & Schröder, H. AZD3582 increases heme oxygenase-1 expression and antioxidant activity in vascular endothelial and gastric mucosal cells. *European journal of pharmaceutical sciences* **25**, 229-235 (2005).

78 Oh, G.-S. *et al.* Hydrogen sulfide inhibits nitric oxide production and nuclear factor-κB via heme oxygenase-1 expression in RAW264. 7 macrophages stimulated with lipopolysaccharide. *Free Radical Biology and Medicine* **41**, 106-119 (2006).
79 Cai, W.-J. *et al.* The novel proangiogenic effect of hydrogen sulfide is dependent on Akt phosphorylation. *Cardiovascular research* **76**, 29-40 (2007).
80 Calatayud, S., Barrachina, D. & Esplugues, J. V. Nitric oxide: relation to integrity, injury, and healing of the gastric mucosa. *Microscopy research and technique* **53**, 325-335 (2001).
81 Fiorucci, S., Distrutti, E., Cirino, G. & Wallace, J. L. The emerging roles of hydrogen sulfide in the gastrointestinal tract and liver. *Gastroenterology* **131**, 259-271 (2006).
82 Chatzaki, E. *et al.* Corticotropin-releasing factor (CRF) receptor type 2 in the human stomach: Protective biological role by inhibition of apoptosis. *Journal of cellular physiology* **209**, 905-911 (2006).
83 Yoneda, M. & Taché, Y. Central thyrotropin-releasing factor analog prevents ethanol-induced gastric damage through prostaglandins in rats. *Gastroenterology* **102**, 1568-1574 (1992).
84 Konturek, S. J., Brzozowski, T., Bielanski, W. & Schally, A. V. Role of endogenous gastrin in gastroprotection. *European journal of pharmacology* **278**, 203-212 (1995).
85 Stroff, T., Plate, S., Respondek, M., Müller, K.-M. & Peskar, B. M. Protection by gastrin in the rat stomach involves afferent neurons, calcitonin gene-related peptide, and nitric oxide. *Gastroenterology* **109**, 89-97 (1995).
86 Konturek, S. J., Brzozowski, T., Pytko-Polonczyk, J. & Drozdowicz, D. Exogenous and endogenous cholecystokinin protects gastric mucosa against the damage caused by ethanol in rats. *European journal of pharmacology* **273**, 57-62 (1995).
87 Stroff, T., Lambrecht, N. & Peskar, B. M. Nitric oxide as mediator of the gastroprotection by cholecystokinin-8 and pentagastrin. *European journal of pharmacology* **260**, R1-R2 (1994).
88 Mercer, D. W., Cross, J. M., Chang, L. & Lichtenberger, L. M. Bombesin prevents gastric injury in the rat: role of gastrin. *Digestive diseases and sciences* **43**, 826-833 (1998).
89 Stroff, T. & Peskar, B. in *Gastroenterology.* A227-A227 (WB SAUNDERS CO INDEPENDENCE SQUARE WEST CURTIS CENTER, STE 300, PHILADELPHIA, PA 19106-3399).
90 Yang, H., Kawakubo, K. & Taché, Y. Intracisternal PYY increases gastric mucosal resistance: role of cholinergic, CGRP, and NO pathways. *American Journal of Physiology-Gastrointestinal and Liver Physiology* **277**, G555-G562 (1999).
91 Stroff, T. *et al.* Tachykinin-induced increase in gastric mucosal resistance: role of primary afferent neurons, CGRP, and NO. *American Journal of Physiology-Gastrointestinal and Liver Physiology* **271**, G1017-G1027 (1996).
92 Brzozowski, T. *et al.* Role of central and peripheral ghrelin in the mechanism of gastric mucosal defence. *Inflammopharmacology* **13**, 45-62 (2005).
93 Konturek, S. *et al.* Transforming growth factor alpha and epidermal growth factor in protection and healing of gastric mucosal injury. *Scandinavian journal of gastroenterology* **27**, 649-655 (1992).
94 Filaretova, L., Bagaeva, T., Podvigina, T. & Makara, G. Various ulcerogenic stimuli are potentiated by glucocorticoid deficiency in rats. *Journal of Physiology-Paris* **95**, 59-65 (2001).
95 Filaretova, L., Filaretov, A. & Makara, G. Corticosterone increase inhibits stress-induced gastric erosions in rats. *American Journal of Physiology-Gastrointestinal and Liver Physiology* **274**, G1024-G1030 (1998).

96 Filaretova, L., Podvigina, T., Bagaeva, T., Bobryshev, P. & Takeuchi, K. Gastroprotective role of glucocorticoid hormones. *Journal of pharmacological sciences* **104**, 195-201 (2007).
97 Takezono, Y. *et al.* Role of prostaglandins in maintaining gastric mucus-cell permeability against acid exposure. *Journal of Laboratory and Clinical Medicine* **143**, 52-58 (2004).
98 Araki, H. *et al.* The roles of prostaglandin E receptor subtypes in the cytoprotective action of prostaglandin E2 in rat stomach. *Alimentary Pharmacology & Therapeutics: Cytoprotection* **14**, 116-124 (2000).
99 Wallace, J. L. Prostaglandins, NSAIDs, and gastric mucosal protection: why doesn't the stomach digest itself? *Physiological reviews* **88**, 1547-1565 (2008).
100 Taira, K. *et al.* Roles of cyclooxygenase-2 and prostaglandin E receptors in gastric mucosal defense in Helicobacter pylori-infected mice. *Inflammopharmacology* **15**, 132-138 (2007).
101 Takahashi, M., Maeda, S., Ogura, K., Terano, A. & Omata, M. The possible role of vascular endothelial growth factor (VEGF) in gastric ulcer healing: effect of sofalcone on VEGF release in vitro. *Journal of clinical gastroenterology* **27**, S178-S182 (1998).
102 Wallace, J. L. Lipid mediators of inflammation in gastric ulcer. *American Journal of Physiology-Gastrointestinal and Liver Physiology* **258**, G1-G11 (1990).
103 Ham, E. A. *et al.* Inhibition by prostaglandins of leukotriene B4 release from activated neutrophils. *Proceedings of the National Academy of Sciences* **80**, 4349-4353 (1983).
104 Haurand, M. & Flohé, L. Leukotriene formation by human polymorphonuclear leukocytes from endogenous arachidonate: Physiological triggers and modulation by prostanoids. *Biochemical pharmacology* **38**, 2129-2137 (1989).
105 Wertheim, W. A. *et al.* Regulation of neutrophil-derived IL-8: the role of prostaglandin E2, dexamethasone, and IL-4. *The Journal of Immunology* **151**, 2166-2175 (1993).
106 Hogaboam, C. M., Bissonnette, E. Y., Chin, B. C., Befus, A. D. & Wallace, J. L. Prostaglandins inhibit inflammatory mediator release from rat mast cells. *Gastroenterology* **104**, 122-129 (1993).
107 Kunkel, S., Chensue, S. & Phan, S. Prostaglandins as endogenous mediators of interleukin 1 production. *The Journal of Immunology* **136**, 186-192 (1986).
108 Kunkel, S. L., Wiggins, R., Chensue, S. W. & Larrick, J. Regulation of macrophage tumor necrosis factor production by prostaglandin E2. *Biochemical and biophysical research communications* **137**, 404-410 (1986).
109 Rouzer, C. A. & Marnett, L. J. Cyclooxygenases: structural and functional insights. *Journal of lipid research* **50**, S29-S34 (2009).
110 Rang, H. P., Ritter, J., Flower, R. J. & Henderson, G. *Rang & Dale's pharmacology.*, ([Edinburgh?] : Elsevier/Churchill Livingstone, [2016]. Eighth edition., 2016).
111 Tanaka, A., Araki, H., Hase, S., Komoike, Y. & Takeuchi, K. Up-regulation of COX-2 by inhibition of COX-1 in the rat: a key to NSAID-induced gastric injury. *Alimentary pharmacology & therapeutics* **16**, 90-101 (2002).
112 Wallace, J. L., McKnight, W., Reuter, B. K. & Vergnolle, N. NSAID-induced gastric damage in rats: requirement for inhibition of both cyclooxygenase 1 and 2. *Gastroenterology* **119**, 706-714 (2000).
113 Ehrlich, K., Sicking, C., Respondek, M. & Peskar, B. M. Interaction of cyclooxygenase isoenzymes, nitric oxide, and afferent neurons in gastric mucosal defense in rats. *Journal of Pharmacology and Experimental Therapeutics* **308**, 277-283 (2004).
114 Gretzer, B., Maricic, N., Respondek, M., Schuligoi, R. & Peskar, B. M. Effects of specific inhibition of cyclo-oxygenase-1 and cyclo-oxygenase-2 in the rat stomach with

normal mucosa and after acid challenge. *British journal of pharmacology* **132**, 1565-1573 (2001).

115 Chan, F. *et al.* in *Gastroenterology.* A24-A25 (WB SAUNDERS CO INDEPENDENCE SQUARE WEST CURTIS CENTER, STE 300, PHILADELPHIA, PA 19106-3399 USA).

116 Schmassmann, A. *et al.* Role of the different isoforms of cyclooxygenase and nitric oxide synthase during gastric ulcer healing in cyclooxygenase-1 and-2 knockout mice. *American journal of physiology-gastrointestinal and liver physiology* **290**, G747-G756 (2006).

117 Silva, M. I. G. & de Sousa, F. C. F. in *Peptic ulcer disease* (InTech, 2011).

118 Matsui, H. *et al.* The pathophysiology of non-steroidal anti-inflammatory drug (NSAID)-induced mucosal injuries in stomach and small intestine. *Journal of clinical biochemistry and nutrition* **48**, 107-111 (2011).

119 Watanabe, T. *et al.* Mechanisms of peptic ulcer recurrence: role of inflammation. *Inflammopharmacology* **10**, 291-302 (2002).

120 Zamani, M. *et al.* Systematic review with meta-analysis: the worldwide prevalence of Helicobacter pylori infection. *Alimentary pharmacology & therapeutics* **47**, 868-876 (2018).

121 Schultze, V. *et al.* Differing patterns of Helicobacter pylori gastritis in patients with duodenal, prepyloric, and gastric ulcer disease. *Scandinavian journal of gastroenterology* **33**, 137-142 (1998).

122 Saul, C., Teixeira, C. R., Pereira-Lima, J. C. & Torresini, R. J. S. Prevalence reduction of duodenal ulcer: a Brazilian study.(retrospective analysis in tha last decade: 1996-2005). *Arquivos de gastroenterologia* **44**, 320-324 (2007).

123 Sipponen, P. *et al.* Chronic antral gastritis, Lewisa+ phenotype, and male sex as factors in predicting coexisting duodenal ulcer. *Scandinavian journal of gastroenterology* **24**, 581-588 (1989).

124 Sipponen, P. *et al.* Cumulative 10-year risk of symptomatic duodenal and gastric ulcer in patients with or without chronic gastritis: a clinical follow-up study of 454 outpatients. *Scandinavian journal of gastroenterology* **25**, 966-973 (1990).

125 Suzuki, R. B. *et al.* Different risk factors influence peptic ulcer disease development in a Brazilian population. *World Journal of Gastroenterology: WJG* **18**, 5404 (2012).

126 Alaja, R. *et al.* Psychiatric referrals associated with substance use disorders: prevalence and gender differences. *Alcoholism: Clinical and Experimental Research* **21**, 620-626 (1997).

127 Dawson, D. Gender differences in the risk of alcohol dependence: United States, 1992. *Addiction* **91**, 1831-1842 (1996).

128 Nitsche, W. Alcoholism. Classification, epidemiology, etiology. *Fortschritte der Medizin* **100**, 1111-1115 (1982).

129 Liu, E. S., Wong, B. C. & Cho, C. H. Influence of gender difference and gastritis on gastric ulcer formation in rats. *Journal of gastroenterology and hepatology* **16**, 740-747 (2001).

130 Sakaguchi, T., Yamazaki, M., Itoh, S., Okamura, N. & Bando, T. Gastric acid secretion controlled by oestrogen in women. *Journal of international medical research* **19**, 384-388 (1991).

131 Liou, J.-M., Lin, J.-T., Lee, Y.-C., Wu, C.-Y. & Wu, M.-S. Helicobacter pylori infection in the elderly. *International Journal of Gerontology* **2**, 145-153 (2008).

132 Lee, M. & Feldman, M. The aging stomach: implications for NSAID gastropathy. *Gut* **41**, 425-426 (1997).

133 Weiskopf, D., Weinberger, B. & Grubeck-Loebenstein, B. The aging of the immune system. *Transplant international* **22**, 1041-1050 (2009).

134 Hernández-Díaz, S. & Rodríguez, L. A. G. a. Incidence of serious upper gastrointestinal bleeding/perforation in the general population:: Review of epidemiologic studies. *Journal of clinical epidemiology* **55**, 157-163 (2002).
135 Lau, J. Y. *et al.* Systematic review of the epidemiology of complicated peptic ulcer disease: incidence, recurrence, risk factors and mortality. *Digestion* **84**, 102-113 (2011).
136 Garrow, D. & Delegge, M. H. Risk factors for gastrointestinal ulcer disease in the US population. *Digestive diseases and sciences* **55**, 66 (2010).
137 Åhsberg, K., Höglund, P. & Staël von Holstein, C. Mortality from peptic ulcer bleeding: the impact of comorbidity and the use of drugs that promote bleeding. *Alimentary pharmacology & therapeutics* **32**, 801-810 (2010).
138 Liang, C.-C. *et al.* Peptic ulcer disease risk in chronic kidney disease: ten-year incidence, ulcer location, and ulcerogenic effect of medications. *PloS one* **9**, e87952 (2014).
139 Sheu, B.-S. *et al.* Consensus on control of risky nonvariceal upper gastrointestinal bleeding in Taiwan with National Health Insurance. *BioMed research international* **2014** (2014).
140 Levenstein, S., Kaplan, G. A. & Smith, M. Sociodemographic characteristics, life stressors, and peptic ulcer. A prospective study. (1995).
141 Kim, H.-S. *et al.* Tissue plasminogen activator and plasminogen activator inhibitor type 1 gene polymorphism in patients with gastric ulcer complicated with bleeding. *Journal of Korean medical science* **18**, 58 (2003).
142 Sugimoto, M. *et al.* Different effects of polymorphisms of tumor necrosis factor-alpha and interleukin-1 beta on development of peptic ulcer and gastric cancer. *Journal of gastroenterology and hepatology* **22**, 51-59 (2007).
143 Hwang, I.-R. *et al.* Effect of interleukin 1 polymorphisms on gastric mucosal interleukin 1β production in Helicobacter pylori infection. *Gastroenterology* **123**, 1793-1803 (2002).
144 Sugimoto, M., Yamaoka, Y. & Furuta, T. Influence of interleukin polymorphisms on development of gastric cancer and peptic ulcer. *World journal of gastroenterology: WJG* **16**, 1188 (2010).
145 Yin, Y.-W. *et al.* Association between interleukin-8 gene− 251 T/A polymorphism and the risk of peptic ulcer disease: A meta-analysis. *Human immunology* **74**, 125-130 (2013).
146 Zhang, B.-B., Wang, J., Bian, D.-L. & Chen, X.-Y. No association between IL-1β− 31 C/T polymorphism and the risk of duodenal ulcer: a meta-analysis of 3793 subjects. *Human immunology* **73**, 1200-1206 (2012).
147 Edgren, G. *et al.* Risk of gastric cancer and peptic ulcers in relation to ABO blood type: a cohort study. *American journal of epidemiology* **172**, 1280-1285 (2010).
148 Wang, P.-Y. *et al.* Impact of blood type, functional polymorphism (T-1676C) of the COX-1 gene promoter and clinical factors on the development of peptic ulcer during cardiovascular prophylaxis with low-dose aspirin. *BioMed research international* **2014** (2014).
149 Keller, R., Dinkel, K.-C., Christl, S. & Fischbach, W. Interrelation between ABH blood group 0, Lewis (B) blood group antigen, Helicobacter pylori infection, and occurrence of peptic ulcer. *Zeitschrift für Gastroenterologie* **40**, 273-276 (2002).
150 Umlauft, F. *et al.* Helicobacter pylori infection and blood group antigens: lack of clinical association. *American Journal of Gastroenterology* **91** (1996).
151 Marmot, M. G. *et al.* Health inequalities among British civil servants: the Whitehall II study. *The Lancet* **337**, 1387-1393 (1991).

152 Bytzer, P. *et al.* Low socioeconomic class is a risk factor for upper and lower gastrointestinal symptoms: a population based study in 15 000 Australian adults. *Gut* **49**, 66-72 (2001).
153 Levenstein, S. & Kaplan, G. A. Socioeconomic status and ulcer: a prospective study of contributory risk factors. *Journal of clinical gastroenterology* **26**, 14-17 (1998).
154 Buckley, M. J. *et al.* A community-based study of the epidemiology of Helicobacter pylori infection and associated asymptomatic gastroduodenal pathology. *European journal of gastroenterology & hepatology* **10**, 375-379 (1998).
155 Graham, D. Y. *et al.* Epidemiology of Helicobacter pylori in an asymptomatic population in the United States: effect of age, race, and socioeconomic status. *Gastroenterology* **100**, 1495-1501 (1991).
156 Bujanda, L. The effects of alcohol consumption upon the gastrointestinal tract. *The American journal of gastroenterology* **95**, 3374 (2000).
157 Bode, C., Maute, G. & Bode, J. Prostaglandin E2 and prostaglandin F2 alpha biosynthesis in human gastric mucosa: effect of chronic alcohol misuse. *Gut* **39**, 348-352 (1996).
158 Chou, S. P. An examination of the alcohol consumption and peptic ulcer association—Results of a national survey. *Alcoholism: Clinical and Experimental Research* **18**, 149-153 (1994).
159 Li, L. *et al.* Cigarette smoking and gastrointestinal diseases: the causal relationship and underlying molecular mechanisms. *International journal of molecular medicine* **34**, 372-380 (2014).
160 Bhatt, D. L. *et al.* ACCF/ACG/AHA 2008 expert consensus document on reducing the gastrointestinal risks of antiplatelet therapy and NSAID use: a report of the American College of Cardiology Foundation Task Force on Clinical Expert Consensus Documents. *Journal of the American College of Cardiology* **52**, 1502-1517 (2008).
161 Guslandi, M. Steroid ulcers: Any news? *World journal of gastrointestinal pharmacology and therapeutics* **4**, 39 (2013).
162 Thomopoulos, K. C. *et al.* Acute upper gastrointestinal bleeding in patients on long-term oral anticoagulation therapy: endoscopic findings, clinical management and outcome. *World journal of gastroenterology: WJG* **11**, 1365 (2005).
163 NICE. *Managing peptic ulcer disease in adults*, <http://pathways.nice.org.uk/pathways/dyspepsia-and-gastro-oesophageal-refluxdisease> (2018).
164 Rostom, A., Moayyedi, P., Hunt, R. & Group, C. A. o. G. C. Canadian consensus guidelines on long-term nonsteroidal anti-inflammatory drug therapy and the need for gastroprotection: benefits versus risks. *Alimentary pharmacology & therapeutics* **29**, 481-496 (2009).
165 Scheiman, J. M. & Fendrick, A. M. Practical approaches to minimizing gastrointestinal and cardiovascular safety concerns with COX-2 inhibitors and NSAIDs. *Arthritis Research & Therapy* **7**, S23 (2005).
166 Sandler, R. S. *et al.* The burden of selected digestive diseases in the United States. *Gastroenterology* **122**, 1500-1511 (2002).
167 Everhart, J. E. & Ruhl, C. E. Burden of digestive diseases in the United States part I: overall and upper gastrointestinal diseases. *Gastroenterology* **136**, 376-386 (2009).
168 de Leest, H. *et al.* Costs of treating bleeding and perforated peptic ulcers in The Netherlands. *The Journal of rheumatology* **31**, 788-791 (2004).
169 Al-Sohaily, S. Long-term management of patients taking proton pump inhibitors. *Australian Prescriber* **31**, 5-7 (2008).

170 Cheung, K. S. *et al.* Long-term proton pump inhibitors and risk of gastric cancer development after treatment for Helicobacter pylori: a population-based study. *Gut*, gutjnl-2017-314605 (2017).
171 Organization, W. H. International drug monitoring: the role of national centres, report of a WHO meeting [held in Geneva from 20 to 25 September 1971]. (1972).
172 Alomar, M. J. Factors affecting the development of adverse drug reactions. *Saudi Pharmaceutical Journal* **22**, 83-94 (2014).
173 Rang, H. P., Ritter, J. M., Flower, R. J. & Henderson, G. *Rang & Dale's Pharmacology*. 8th ed. edn, 317-323 (Elsevier Health Sciences, 2014).
174 Pirmohamed, M. *et al.* Carbamazepine-hypersensitivity: assessment of clinical and in vitro chemical cross-reactivity with phenytoin and oxcarbazepine. *British journal of clinical pharmacology* **32**, 741-749 (1991).
175 Sultana, J., Cutroneo, P. & Trifirò, G. Clinical and economic burden of adverse drug reactions. *Journal of pharmacology & pharmacotherapeutics* **4**, S73 (2013).
176 Kola, I. & Landis, J. Can the pharmaceutical industry reduce attrition rates? *Nature reviews Drug discovery* **3**, 711 (2004).
177 Need, A. C., Motulsky, A. G. & Goldstein, D. B. Priorities and standards in pharmacogenetic research. *Nature genetics* **37**, 671 (2005).
178 Guengerich, F. P. Mechanisms of drug toxicity and relevance to pharmaceutical development. *Drug metabolism and pharmacokinetics* **26**, 3-14 (2011).
179 Al-Saffar, A. *et al.* in *Principles of Safety Pharmacology* 291-321 (Springer, 2015).
180 NICE. *Non-steroidal anti-inflammatory drugs*, <https://bnf.nice.org.uk/treatment-summary/non-steroidal-anti-inflammatory-drugs.html> (2018).
181 Cathcart, M. K. Signal-activated phospholipase regulation of leukocyte chemotaxis. *Journal of lipid research* **50**, S231-S236 (2009).
182 Zarghi, A. & Arfaei, S. Selective COX-2 inhibitors: a review of their structure-activity relationships. *Iranian journal of pharmaceutical research: IJPR* **10**, 655 (2011).
183 Hata, A. N. & Breyer, R. M. Pharmacology and signaling of prostaglandin receptors: multiple roles in inflammation and immune modulation. *Pharmacology & therapeutics* **103**, 147-166 (2004).
184 Kawabata, A. Prostaglandin E2 and pain—an update. *Biological and Pharmaceutical Bulletin* **34**, 1170-1173 (2011).
185 Ricciotti, E. & FitzGerald, G. A. Prostaglandins and inflammation. *Arteriosclerosis, thrombosis, and vascular biology* **31**, 986-1000 (2011).
186 Gilroy, D. W. *et al.* Inducible cyclooxygenase may have anti-inflammatory properties. *Nature medicine* **5**, 698 (1999).
187 Reijman, M. *et al.* Is there an association between the use of different types of nonsteroidal antiinflammatory drugs and radiologic progression of osteoarthritis?: The rotterdam study. *Arthritis & Rheumatism: Official Journal of the American College of Rheumatology* **52**, 3137-3142 (2005).
188 Vane, J. R. Inhibition of Prostaglandin Synthesis as a Mechanism of Action for Aspirin-like Drugs. *Nature New Biology* **231**, 232, doi:10.1038/newbio231232a0 (1971).
189 Ong, C., Lirk, P., Tan, C. & Seymour, R. An evidence-based update on nonsteroidal anti-inflammatory drugs. *Clinical medicine & research* **5**, 19-34 (2007).
190 Pelletier, J.-P., Martel-Pelletier, J., Rannou, F. & Cooper, C. in *Seminars in arthritis and rheumatism.* S22-S27 (Elsevier).
191 Zhang, X., Donnan, P. T., Bell, S. & Guthrie, B. Non-steroidal anti-inflammatory drug induced acute kidney injury in the community dwelling general population and people with chronic kidney disease: systematic review and meta-analysis. *BMC nephrology* **18**, 256 (2017).

192 Whelton, A. Nephrotoxicity of nonsteroidal anti-inflammatory drugs: physiologic foundations and clinical implications. *The American journal of medicine* **106**, 13S-24S (1999).
193 Hörl, W. H. Nonsteroidal anti-inflammatory drugs and the kidney. *Pharmaceuticals* **3**, 2291-2321 (2010).
194 Bombardier, C. *et al.* Comparison of upper gastrointestinal toxicity of rofecoxib and naproxen in patients with rheumatoid arthritis. *New England Journal of Medicine* **343**, 1520-1528 (2000).
195 Schnitzer, T. J. *et al.* Comparison of lumiracoxib with naproxen and ibuprofen in the Therapeutic Arthritis Research and Gastrointestinal Event Trial (TARGET), reduction in ulcer complications: randomised controlled trial. *The Lancet* **364**, 665-674 (2004).
196 Silverstein, F. E. *et al.* Gastrointestinal toxicity with celecoxib vs nonsteroidal anti-inflammatory drugs for osteoarthritis and rheumatoid arthritis: the CLASS study: a randomized controlled trial. *Jama* **284**, 1247-1255 (2000).
197 Singh, G. *et al.* Celecoxib versus naproxen and diclofenac in osteoarthritis patients: SUCCESS-I Study. *The American journal of medicine* **119**, 255-266 (2006).
198 Husband, M. & Mehta, V. Cyclo-oxygenase-2 inhibitors. *Continuing Education in Anaesthesia, Critical Care & Pain* **13**, 131-135 (2013).
199 Varga, Z., rafay ali Sabzwari, S. & Vargova, V. Cardiovascular risk of nonsteroidal anti-inflammatory drugs: an under-recognized public health issue. *Cureus* **9** (2017).
200 Hinz, B., Renner, B. & Brune, K. Drug insight: cyclo-oxygenase-2 inhibitors—a critical appraisal. *Nature Reviews Rheumatology* **3**, 552 (2007).
201 Szczeklik, A. Mechanism of aspirin-induced asthma. *Allergy* **52**, 613-619 (1997).
202 Auriel, E., Regev, K. & Korczyn, A. D. in *Handbook of clinical neurology* Vol. 119 577-584 (Elsevier, 2014).
203 Chang, J.-K. *et al.* Effects of anti-inflammatory drugs on proliferation, cytotoxicity and osteogenesis in bone marrow mesenchymal stem cells. *Biochemical pharmacology* **74**, 1371-1382 (2007).
204 Sriuttha, P., Sirichanchuen, B. & Permsuwan, U. Hepatotoxicity of Nonsteroidal Anti-Inflammatory Drugs: A Systematic Review of Randomized Controlled Trials. *International journal of hepatology* **2018** (2018).
205 Rostom, A., Goldkind, L. & Laine, L. Nonsteroidal anti-inflammatory drugs and hepatic toxicity: a systematic review of randomized controlled trials in arthritis patients. *Clinical Gastroenterology and Hepatology* **3**, 489-498 (2005).
206 Kishida, T., Onozato, T., Kanazawa, T., Tanaka, S. & Kuroda, J. Increase in covalent binding of 5-hydroxydiclofenac to hepatic tissues in rats co-treated with lipopolysaccharide and diclofenac: involvement in the onset of diclofenac-induced idiosyncratic hepatotoxicity. *The Journal of toxicological sciences* **37**, 1143-1156 (2012).
207 Aithal, G. P. Hepatotoxicity related to antirheumatic drugs. *Nature Reviews Rheumatology* **7**, 139 (2011).
208 Goldkind, L. & Laine, L. A systematic review of NSAIDs withdrawn from the market due to hepatotoxicity: lessons learned from the bromfenac experience. *Pharmacoepidemiology and drug safety* **15**, 213-220 (2006).
209 Singer, J. B. *et al.* A genome-wide study identifies HLA alleles associated with lumiracoxib-related liver injury. *Nature genetics* **42**, 711 (2010).
210 Mahdi, J. G. Medicinal potential of willow: A chemical perspective of aspirin discovery. *Journal of Saudi Chemical Society* **14**, 317-322 (2010).
211 Piper, P. J. & Vane, J. R. Release of additional factors in anaphylaxis and its antagonism by anti-inflammatory drugs. *Nature* **223**, 29 (1969).

212 Warner, T. D., Nylander, S. & Whatling, C. Anti-platelet therapy: cyclo-oxygenase inhibition and the use of aspirin with particular regard to dual anti-platelet therapy. *British journal of clinical pharmacology* **72**, 619-633 (2011).
213 Chiang, N., Arita, M. & Serhan, C. N. Anti-inflammatory circuitry: lipoxin, aspirin-triggered lipoxins and their receptor ALX. *Prostaglandins, leukotrienes and essential fatty acids* **73**, 163-177 (2005).
214 Ittaman, S. V., VanWormer, J. J. & Rezkalla, S. H. The role of aspirin in the prevention of cardiovascular disease. *Clinical medicine & research*, cmr. 2013.1197 (2014).
215 Baigent, C. *et al.* (Elsevier, 2009).
216 Elwood, P. C. *et al.* Aspirin in the treatment of cancer: reductions in metastatic spread and in mortality: a systematic review and meta-analyses of published studies. *PloS one* **11**, e0152402 (2016).
217 Wang, J. *et al.* Anti-inflammatory drugs and risk of Alzheimer's disease: an updated systematic review and meta-analysis. *Journal of Alzheimer's Disease* **44**, 385-396 (2015).
218 Pedersen, A. K. & FitzGerald, G. A. Dose-related kinetics of aspirin: presystemic acetylation of platelet cyclooxygenase. *New England Journal of Medicine* **311**, 1206-1211 (1984).
219 Patrignani, P. *et al.* Reappraisal of the clinical pharmacology of low-dose aspirin by comparing novel direct and traditional indirect biomarkers of drug action. *Journal of Thrombosis and Haemostasis* **12**, 1320-1330 (2014).
220 Ai, G., Dachineni, R., Muley, P., Tummala, H. & Bhat, G. J. Aspirin and salicylic acid decrease c-Myc expression in cancer cells: a potential role in chemoprevention. *Tumor Biology* **37**, 1727-1738 (2016).
221 Gupta, S. C., Sundaram, C., Reuter, S. & Aggarwal, B. B. Inhibiting NF-κB activation by small molecules as a therapeutic strategy. *Biochimica et Biophysica Acta (BBA)-Gene Regulatory Mechanisms* **1799**, 775-787 (2010).
222 Abramson, S. B. & Weissmann, G. The mechanisms of action of nonsteroidal antiinflammatory drugs. *Arthritis & Rheumatology* **32**, 1-9 (1989).
223 Xu, X.-M. *et al.* Suppression of inducible cyclooxygenase 2 gene transcription by aspirin and sodium salicylate. *Proceedings of the National Academy of Sciences* **96**, 5292-5297 (1999).
224 NICE. *Aspirin*, <https://bnf.nice.org.uk/drug/aspirin.html> (2018).
225 Levy, G. Clinical pharmacokinetics of aspirin. *Pediatrics* **62**, 867-872 (1978).
226 Dahlen, B., Boreus, L., Anderson, P., Andersson, R. & Zetterström, O. Plasma acetylsalicylic acid and salicylic acid levels during aspirin provocation in aspirin-sensitive subjects. *Allergy* **49**, 43-49 (1994).
227 Yamashita, S. *et al.* Measurement of drug concentration in the stomach after intragastric administration of drug solution to healthy volunteers: analysis of intragastric fluid dynamics and drug absorption. *Pharmaceutical research* **30**, 951-958, doi:10.1007/s11095-012-0931-1 (2013).
228 Niv, Y. *et al.* Endoscopy in asymptomatic minidose aspirin consumers. *Digestive diseases and sciences* **50**, 78-80 (2005).
229 Sostres, C. & Lanas, A. Should prophylactic low-dose aspirin therapy be continued in peptic ulcer bleeding? *Drugs* **71**, 1-10 (2011).
230 Cayla, G. *et al.* Prevalence and clinical impact of upper gastrointestinal symptoms in subjects treated with low dose aspirin: the UGLA survey. *International journal of cardiology* **156**, 69-75 (2012).
231 Herlitz, J., Tóth, P. P. & Næsdal, J. Low-Dose Aspirin Therapy for Cardiovascular Prevention. *American journal of cardiovascular drugs* **10**, 125-141 (2010).

232 Biondi-Zoccai, G. G. *et al.* A systematic review and meta-analysis on the hazards of discontinuing or not adhering to aspirin among 50 279 patients at risk for coronary artery disease. *European heart journal* **27**, 2667-2674 (2006).
233 Sostres, C., Gargallo, C. J., Arroyo, M. T. & Lanas, A. Adverse effects of non-steroidal anti-inflammatory drugs (NSAIDs, aspirin and coxibs) on upper gastrointestinal tract. *Best practice & research Clinical gastroenterology* **24**, 121-132 (2010).
234 McCarthy, D. Nonsteroidal anti-inflammatory drug-related gastrointestinal toxicity: definitions and epidemiology. *The American journal of medicine* **105**, 3S-9S (1998).
235 Lanas, A. *et al.* Time trends and impact of upper and lower gastrointestinal bleeding and perforation in clinical practice. *The American journal of gastroenterology* **104**, 1633 (2009).
236 Sostres, C., Gargallo, C. J. & Lanas, A. Nonsteroidal anti-inflammatory drugs and upper and lower gastrointestinal mucosal damage. *Arthritis research & therapy* **15**, S3 (2013).
237 Rostom, A. *et al.* Gastrointestinal safety of cyclooxygenase-2 inhibitors: a Cochrane Collaboration systematic review. *Clinical Gastroenterology and Hepatology* **5**, 818-828. e815 (2007).
238 Castellsague, J. *et al.* Individual NSAIDs and upper gastrointestinal complications. *Drug safety* **35**, 1127-1146 (2012).
239 Gabriel, S. E., Jaakkimainen, L. & Bombardier, C. Risk for serious gastrointestinal complications related to use of nonsteroidal anti-inflammatory drugs: a meta-analysis. *Annals of internal medicine* **115**, 787-796 (1991).
240 Huang, J.-Q., Sridhar, S. & Hunt, R. H. Role of Helicobacter pylori infection and non-steroidal anti-inflammatory drugs in peptic-ulcer disease: a meta-analysis. *The Lancet* **359**, 14-22 (2002).
241 Cryer, B. NSAID-associated deaths: the rise and fall of NSAID-associated GI mortality. *The American journal of gastroenterology* **100**, 1694 (2005).
242 Hawkey, C. & Langman, M. Non-steroidal anti-inflammatory drugs: overall risks and management. Complementary roles for COX-2 inhibitors and proton pump inhibitors. *Gut* **52**, 600-608 (2003).
243 Ligumsky, M., Golanska, E. M., Hansen, D. G. & Kauffman, G. L. Aspirin can inhibit gastric mucosal cyclo-oxygenase without causing lesions in rat. *Gastroenterology* **84**, 756-761 (1983).
244 Ligumsky, M. *et al.* Rectal Administration of Nonsteroidal Andinflammatory Drugs: Effect on Rat Gastric Ulcerogenicity and Prostaglandin E2 Synthesis. *Gastroenterology* **98**, 1245-1249 (1990).
245 Bjarnason, I. *et al.* Mechanisms of damage to the gastrointestinal tract from non-steroidal anti-inflammatory drugs. *Gastroenterology* (2017).
246 Goddard, P. J., Hills, B. A. & Lichtenberger, L. M. Does aspirin damage canine gastric mucosa by reducing its surface hydrophobicity? *American Journal of Physiology-Gastrointestinal and Liver Physiology* **252**, G421-G430 (1987).
247 Handa, O. *et al.* The role of mitochondria-derived reactive oxygen species in the pathogenesis of non-steroidal anti-inflammatory drug-induced small intestinal injury. *Free radical research* **48**, 1095-1099 (2014).
248 Madara, J. L. Tight junction dynamics: is paracellular transport regulated? *Cell* **53**, 497-498 (1988).
249 Redlak, M. J., Power, J. J. & Miller, T. A. Role of mitochondria in aspirin-induced apoptosis in human gastric epithelial cells. *American Journal of Physiology-Gastrointestinal and Liver Physiology* **289**, G731-G738 (2005).

250 Leung, A. M., Redlak, M. J. & Miller, T. A. Aspirin-induced mucosal cell death in human gastric cells: role of a caspase-independent mechanism. *Digestive diseases and sciences* **54**, 28-35 (2009).
251 Orrenius, S. Reactive oxygen species in mitochondria-mediated cell death. *Drug metabolism reviews* **39**, 443-455 (2007).
252 Somasundaram, S. *et al.* Mitochondrial damage: a possible mechanism of the "topical" phase of NSAID induced injury to the rat intestine. *Gut* **41**, 344-353 (1997).
253 Krause, M. M. *et al.* Nonsteroidal antiinflammatory drugs and a selective cyclooxygenase 2 inhibitor uncouple mitochondria in intact cells. *Arthritis & Rheumatism* **48**, 1438-1444 (2003).
254 Mügge, F. L. & Silva, A. M. Endoplasmic reticulum stress response in the roadway for the effects of non-steroidal anti-inflammatory drugs. *Endoplasmic Reticulum Stress in Diseases* **2** (2015).
255 Flamment, M., Hajduch, E., Ferré, P. & Foufelle, F. New insights into ER stress-induced insulin resistance. *Trends in Endocrinology & Metabolism* **23**, 381-390 (2012).
256 Yu, C., Li, W. b., Liu, J. b., Lu, J. w. & Feng, J. f. Autophagy: novel applications of nonsteroidal anti-inflammatory drugs for primary cancer. *Cancer medicine* **7**, 471-484 (2018).
257 Chiou, S.-K., Hoa, N. & Hodges, A. Sulindac sulfide induces autophagic death in gastric epithelial cells via survivin down-regulation: a mechanism of NSAIDs-induced gastric injury. *Biochemical pharmacology* **81**, 1317-1323 (2011).
258 Chiou, S.-K. *et al.* Survivin: a novel target for indomethacin-induced gastric injury. *Gastroenterology* **128**, 63-73 (2005).
259 Lichtenberger, L. M. Where is the evidence that cyclooxygenase inhibition is the primary cause of nonsteroidal anti-inflammatory drug (NSAID)-induced gastrointestinal injury?: Topical injury revisited. *Biochemical pharmacology* **61**, 631-637 (2001).
260 Tomisato, W. *et al.* Role of direct cytotoxic effects of NSAIDs in the induction of gastric lesions. *Biochemical pharmacology* **67**, 575-585 (2004).
261 Redfern, J. S. & Feldman, M. Role of endogenous prostaglandins in preventing gastrointestinal ulceration: induction of ulcers by antibodies to prostaglandins. *Gastroenterology* **96**, 596-605 (1989).
262 Komoike, Y., Takeeda, M., Tanaka, A., Kato, S. & Takeuchi, K. Prevention by parenteral aspirin of indomethacin-induced gastric lesions in rats: mediation by salicylic acid. *Digestive diseases and sciences* **47**, 1538-1545 (2002).
263 Wallace, J. L. & McKnight, G. W. Characterization of a simple animal model for nonsteroidal anti-inflammatory drug induced antral ulcer. *Canadian journal of physiology and pharmacology* **71**, 447-452 (1993).
264 Estes, L. L., Fuhs, D. W., Heaton, A. H. & Butwinick, C. S. Gastric ulcer perforation associated with the use of injectable ketorolac. *Annals of Pharmacotherapy* **27**, 42-43 (1993).
265 Hansen, D. G., Aures, D. & Grossman, M. I. Histamine augments gastric ulceration produced by intravenous aspirin in cats. *Gastroenterology* **74**, 540-543 (1978).
266 Takeuchi, K. Pathogenesis of NSAID-induced gastric damage: importance of cyclooxygenase inhibition and gastric hypermotility. *World journal of gastroenterology: WJG* **18**, 2147 (2012).
267 Tanaka, A., Matsumoto, M., Hayashi, Y. & Takeuchi, K. Functional mechanism underlying cyclooxygenase-2 expression in rat small intestine following

administration of indomethacin: Relation to intestinal hypermotility. *Journal of gastroenterology and hepatology* **20**, 38-45 (2005).

268 Barnett, K. *et al.* Role of cyclooxygenase-2 in modulating gastric acid secretion in the normal and inflamed rat stomach. *American Journal of Physiology-Gastrointestinal and Liver Physiology* **279**, G1292-G1297 (2000).

269 Kato, S., Aihara, E., Yoshii, K. & Takeuchi, K. Dual action of prostaglandin E2 on gastric acid secretion through different EP-receptor subtypes in the rat. *American Journal of Physiology-Gastrointestinal and Liver Physiology* **289**, G64-G69 (2005).

270 Nishio, H., Terashima, S., Aihara, M. N. E. & Takeuchi, K. INVOLVEMENT OF PROSTAGLANDIN E RECEPTOR EP3 SUBTYPE. *Journal of Physiology and Pharmacology* **58**, 407-421 (2007).

271 Yokotani, K., Okuma, Y. & Osumi, Y. Inhibition of vagally mediated gastric acid secretion by activation of central prostanoid EP3 receptors in urethane-anaesthetized rats. *British journal of pharmacology* **117**, 653-656 (1996).

272 Feldman, M. & Colturi, T. J. Effect of indomethacin on gastric acid and bicarbonate secretion in humans. *Gastroenterology* **87**, 1339-1343 (1984).

273 Rodriguez-Stanley, S., Redinger, N. & Miner Jr, P. Effect of naproxen on gastric acid secretion and gastric pH. *Alimentary pharmacology & therapeutics* **23**, 1719-1724 (2006).

274 Ichikawa, T. *et al.* Nitric oxide synthase activity in rat gastric mucosa contributes to mucin synthesis elicited by calcitonin gene-related peptide. *Biomedical Research* **27**, 117-124 (2006).

275 Okajima, K. & Harada, N. Regulation of inflammatory responses by sensory neurons: molecular mechanism (s) and possible therapeutic applications. *Current medicinal chemistry* **13**, 2241-2251 (2006).

276 Kim, H.-K. *et al.* Preventive effects of rebamipide on NSAID-induced gastric mucosal injury and reduction of gastric mucosal blood flow in healthy volunteers. *Digestive diseases and sciences* **52**, 1776-1782 (2007).

277 Ohno, T. *et al.* Roles of Calcitonin Gene–Related Peptide in Maintenance of Gastric Mucosal Integrity and in Enhancement of Ulcer Healing and Angiogenesis. *Gastroenterology* **134**, 215-225 (2008).

278 Appleyard, C., McCafferty, D., Tigley, A., Swain, M. & Wallace, J. Tumor necrosis factor mediation of NSAID-induced gastric damage: role of leukocyte adherence. *American Journal of Physiology-Gastrointestinal and Liver Physiology* **270**, G42-G48 (1996).

279 Milani, S. & Calabrò, A. Role of growth factors and their receptors in gastric ulcer healing. *Microscopy research and technique* **53**, 360-371 (2001).

280 Szabo, S. & Vincze, Á. Growth factors in ulcer healing: lessons from recent studies. *Journal of Physiology-Paris* **94**, 77-81 (2000).

281 Schmassmann, A. Mechanisms of ulcer healing and effects of nonsteroidal anti-inflammatory drugs. *The American journal of medicine* **104**, 43S-51S (1998).

282 Wang, J.-Y. & Casero, R. A. *Polyamine cell signaling: physiology, pharmacology, and cancer research*. (Springer, 2006).

283 Saunders, F., Hughes, A. & Wallace, H. M. Investigating the effects of NSAIDs on the expression of regulatory components of the polyamine pathway. *Toxicology* **253**, 22-23 (2008).

284 Motawi, T. K., Abd Elgawad, H. M. & Shahin, N. N. Modulation of indomethacin-induced gastric injury by spermine and taurine in rats. *Journal of biochemical and molecular toxicology* **21**, 280-288 (2007).

285 Ganguly, K., Kundu, P., Banerjee, A., Reiter, R. J. & Swarnakar, S. Hydrogen peroxide-mediated downregulation of matrix metalloprotease-2 in indomethacin-induced acute gastric ulceration is blocked by melatonin and other antioxidants. *Free Radical Biology and Medicine* **41**, 911-925 (2006).
286 Lempinen, M., Inkinen, K., Wolff, H. & Ahonen, J. Matrix metalloproteinases 2 and 9 in indomethacin-induced rat gastric ulcer. *European surgical research* **32**, 169-176 (2000).
287 Ito, A., Nose, T., Takahashi, S. & Mori, Y. Cyclooxygenase inhibitors augment the production of pro-matrix metalloproteinase 9 (progelatinase B) in rabbit articular chondrocytes. *Febs Letters* **360**, 75-79 (1995).
288 Miralles, M., Wester, W., Sicard, G. A., Thompson, R. & Reilly, J. M. Indomethacin inhibits expansion of experimental aortic aneurysms via inhibition of the cox2 isoform of cyclooxygenase. *Journal of vascular surgery* **29**, 884-893 (1999).
289 Ganguly, K. & Swarnakar, S. Induction of matrix metalloproteinase-9 and-3 in nonsteroidal anti-inflammatory drug-induced acute gastric ulcers in mice: regulation by melatonin. *Journal of pineal research* **47**, 43-55 (2009).
290 Swarnakar, S. *et al.* Curcumin regulates expression and activity of matrix metalloproteinases 9 and 2 during prevention and healing of indomethacin-induced gastric ulcer. *Journal of Biological Chemistry* **280**, 9409-9415 (2005).
291 Lanas, A. Role of nitric oxide in the gastrointestinal tract. *Arthritis Research & Therapy* **10**, S4 (2008).
292 Slomiany, B. & Slomiany, A. Role of endothelin-converting enzyme-1 in the suppression of constitutive nitric oxide synthase in rat gastric mucosal injury by indomethacin. *Scandinavian journal of gastroenterology* **35**, 1131-1136 (2000).
293 Imamine, S., Akbar, S. M. f., Mizukami, Y., Matsui, H. & Onji, M. Apoptosis of rat gastric mucosa and of primary cultures of gastric epithelial cells by indomethacin: role of inducible nitric oxide synthase and interleukin-8. *International journal of experimental pathology* **82**, 221-229 (2001).
294 Piotrowski, J., Slomiany, A. & Slomiany, B. Activation of apoptotic caspase-3 and nitric oxide synthase-2 in gastric mucosal injury induced by indomethacin. *Scandinavian journal of gastroenterology* **34**, 129-134 (1999).
295 Souza, M., Mota, J., Oliveira, R. & Cunha, F. Gastric damage induced by different doses of indomethacin in rats is variably affected by inhibiting iNOS or leukocyte infiltration. *Inflammation Research* **57**, 28-33 (2008).
296 Wallace, J. L., Dicay, M., McKnight, W. & Martin, G. R. Hydrogen sulfide enhances ulcer healing in rats. *The FASEB Journal* **21**, 4070-4076 (2007).
297 Łowicka, E. & Bełtowski, J. Hydrogen sulfide (H2S)-the third gas of interest for pharmacologists. *Pharmacological reports: PR* **59**, 4-24 (2007).
298 Fiorucci, S. *et al.* Inhibition of hydrogen sulfide generation contributes to gastric injury caused by anti-inflammatory nonsteroidal drugs. *Gastroenterology* **129**, 1210-1224 (2005).
299 Jaworek, J., Brzozowski, T. & Konturek, S. J. Melatonin as an organoprotector in the stomach and the pancreas. *Journal of pineal research* **38**, 73-83 (2005).
300 Allegra, M. *et al.* The chemistry of melatonin's interaction with reactive species. *Journal of pineal research* **34**, 1-10 (2003).
301 Poeggeler, B. *et al.* Melatonin—A Highly Potent Endogenous Radical Scavenger and Electron Donor: New Aspects of the Oxidation Chemistry of this Indole Accessed in vitroa. *Annals of the New York Academy of Sciences* **738**, 419-420 (1994).
302 Rodriguez, C. *et al.* Regulation of antioxidant enzymes: a significant role for melatonin. *Journal of pineal research* **36**, 1-9 (2004).

303 Sewerynek, E., Melchiorri, D., Chen, L. & Reiter, R. J. Melatonin reduces both basal and bacterial lipopolysaccharide-induced lipid peroxidation in vitro. *Free Radical Biology and Medicine* **19**, 903-909 (1995).
304 Gitto, E. *et al.* Melatonin reduces oxidative stress in surgical neonates. *Journal of pediatric surgery* **39**, 184-189 (2004).
305 Brzozowska, I. *et al.* Role of prostaglandins, nitric oxide, sensory nerves and gastrin in acceleration of ulcer healing by melatonin and its precursor, L-tryptophan. *Journal of pineal research* **32**, 149-162 (2002).
306 Kato, K. *et al.* Circadian rhythm of melatonin and prostaglandin in modulation of stress-induced gastric mucosal lesions in rats. *Alimentary pharmacology & therapeutics* **16**, 29-34 (2002).
307 Kato, K. *et al.* Central nervous system action of melatonin on gastric acid and pepsin secretion in pylorusligated rats. *Neuroreport* **9**, 2447-2450 (1998).
308 Sjöblom, M. & Flemström, G. Melatonin in the duodenal lumen is a potent stimulant of mucosal bicarbonate secretion. *Journal of pineal research* **34**, 288-293 (2003).
309 Ganguly, K., Maity, P., Reiter, R. J. & Swarnakar, S. Effect of melatonin on secreted and induced matrix metalloproteinase-9 and-2 activity during prevention of indomethacin-induced gastric ulcer. *Journal of pineal research* **39**, 307-315 (2005).
310 Konturek, P. *et al.* Melatonin and its precursor L-tryptophan prevent acute gastric mucosal damage induced by aspirin in humans. *Journal of Physiology and Pharmacology* **59**, 67-75 (2008).
311 Bandyopadhyay, D., Ghosh, G., Bandyopadhyay, A. & Reiter, R. J. Melatonin protects against piroxicam-induced gastric ulceration. *Journal of pineal research* **36**, 195-203 (2004).
312 Khan, D. A. Pharmacogenomics and adverse drug reactions: Primetime and not ready for primetime tests. *Journal of Allergy and Clinical Immunology* **138**, 943-955 (2016).
313 Wyatt, J., Pettit, W. & Harirforoosh, S. Pharmacogenetics of nonsteroidal anti-inflammatory drugs. *The pharmacogenomics journal* **12**, 462 (2012).
314 Ulrich, C. M., Bigler, J. & Potter, J. D. Non-steroidal anti-inflammatory drugs for cancer prevention: promise, perils and pharmacogenetics. *Nature Reviews Cancer* **6**, 130 (2006).
315 Gaedigk, A. *et al.* The Pharmacogene Variation (PharmVar) Consortium: incorporation of the human cytochrome P450 (CYP) allele nomenclature database. *Clinical Pharmacology & Therapeutics* **103**, 399-401 (2018).
316 Kirchheiner, J. *et al.* Enantiospecific effects of cytochrome P450 2C9 amino acid variants on ibuprofen pharmacokinetics and on the inhibition of cyclooxygenases 1 and 2. *Clinical Pharmacology & Therapeutics* **72**, 62-75 (2002).
317 Krasniqi, V., Dimovski, A., Klarica Domjanović, I., Bilić, I. & Božina, N. How polymorphisms of the cytochrome P450 genes affect ibuprofen and diclofenac metabolism and toxicity. *Arhiv za higijenu rada i toksikologiju* **67**, 1-7 (2016).
318 Dai, D. *et al.* Polymorphisms in human CYP2C8 decrease metabolism of the anticancer drug paclitaxel and arachidonic acid. *Pharmacogenetics and Genomics* **11**, 597-607 (2001).
319 Musumba, C. *et al.* CYP2C19* 17 gain-of-function polymorphism is associated with peptic ulcer disease. *Clinical Pharmacology & Therapeutics* **93**, 195-203 (2013).
320 Ishihara, M. *et al.* Risk factors of symptomatic NSAID-induced small intestinal injury and diaphragm disease. *Alimentary pharmacology & therapeutics* **40**, 538-547 (2014).
321 López-Rodríguez, R. *et al.* Influence of CYP2C8 and CYP2C9 polymorphisms on pharmacokinetic and pharmacodynamic parameters of racemic and enantiomeric

forms of ibuprofen in healthy volunteers. *Pharmacological research* **58**, 77-84 (2008).

322 Ma, J., Yang, X. Y., Qiao, L., Liang, L. Q. & Chen, M. H. CYP2C9 polymorphism in non-steroidal anti-inflammatory drugs-induced gastropathy. *Journal of digestive diseases* **9**, 79-83 (2008).

323 Martin, J. H., Begg, E. J., Kennedy, M. A., Roberts, R. & Barclay, M. L. Is cytochrome P450 2C9 genotype associated with NSAID gastric ulceration? *British journal of clinical pharmacology* **51**, 627-630 (2001).

324 Vonkeman, H. E., van de Laar, M. A., van der Palen, J., Brouwers, J. R. & Vermes, I. Allele variants of the cytochrome P450 2C9 genotype in white subjects from The Netherlands with serious gastroduodenal ulcers attributable to the use of NSAIDs. *Clinical therapeutics* **28**, 1670-1676 (2006).

325 Van Oijen, M. G. *et al.* Polymorphisms in genes encoding acetylsalicylic acid metabolizing enzymes are unrelated to upper gastrointestinal health in cardiovascular patients on acetylsalicylic acid. *British journal of clinical pharmacology* **60**, 623-628 (2005).

326 Shiotani, A. *et al.* The preventive factors for aspirin-induced peptic ulcer: aspirin ulcer and corpus atrophy. *Journal of gastroenterology* **44**, 717-725 (2009).

327 Figueiras, A. *et al.* CYP2C9 variants as a risk modifier of NSAID-related gastrointestinal bleeding: a case–control study. *Pharmacogenetics and genomics* **26**, 66 (2016).

328 Blanco, G., Martínez, C., García-Martín, E. & Agúndez, J. A. Cytochrome P450 gene polymorphisms and variability in response to NSAIDs. *Clinical Research and Regulatory Affairs* **22**, 57-81 (2005).

329 Shiotani, A. *et al.* Novel single nucleotide polymorphism markers for low dose aspirin-associated small bowel bleeding. *PloS one* **8**, e84244 (2013).

330 Shiotani, A. *et al.* Association of SLCO1B1* 1b with peptic ulcer amongst Japanese patients taking low-dose aspirin. *Digestive and Liver Disease* **44**, 201-205 (2012).

331 Shiotani, A. *et al.* Single nucleotide polymorphism markers for low-dose aspirin-associated peptic ulcer and ulcer bleeding. *Journal of gastroenterology and hepatology* **29**, 47-52 (2014).

332 Lee, S. J., Park, M. K., Shin, D.-S. & Chun, M. H. Variability of the drug response to nonsteroidal anti-inflammatory drugs according to cyclooxygenase-2 genetic polymorphism. *Drug design, development and therapy* **11**, 2727 (2017).

333 Saxena, A. *et al.* Polymorphism of-765G> C COX-2 is a risk factor for gastric adenocarcinoma and peptic ulcer disease in addition to H pylori infection: a study from northern India. *World Journal of Gastroenterology: WJG* **14**, 1498 (2008).

334 Halushka, M. K., Walker, L. P. & Halushka, P. V. Genetic variation in cyclooxygenase 1: effects on response to aspirin. *Clinical Pharmacology & Therapeutics* **73**, 122-130 (2003).

335 van Oijen, M. G. *et al.* Effect of a specific cyclooxygenase-gene polymorphism (A-842G/C50T) on the occurrence of peptic ulcer hemorrhage. *Digestive diseases and sciences* **51**, 2348-2352 (2006).

336 Arisawa, T. *et al.* Association between genetic polymorphisms in thecyclooxygenase-1 gene promoter and peptic ulcers in Japan. *International journal of molecular medicine* **20**, 373-378 (2007).

337 Arisawa, T. *et al.* Genetic polymorphisms of cyclooxygenase-1 (COX-1) are associated with functional dyspepsia in Japanese women. *Journal of women's health* **17**, 1039-1043 (2008).

338 Martínez, C. *et al.* Genetic predisposition to acute gastrointestinal bleeding after NSAIDs use. *British journal of pharmacology* **141**, 205-208 (2004).
339 Pilotto, A. *et al.* Genetic susceptibility to nonsteroidal anti-inflammatory drug–related gastroduodenal bleeding: role of cytochrome P450 2C9 polymorphisms. *Gastroenterology* **133**, 465-471 (2007).
340 Bhat, I. A. *et al.* Association of interleukin 1 beta (IL-1β) polymorphism with mRNA expression and risk of non small cell lung cancer. *Meta gene* **2**, 123-133 (2014).
341 Cho, J. H. *et al.* The IL-1B genetic polymorphism is associated with aspirin-induced peptic ulcers in a Korean ethnic group. *Gut and liver* **10**, 362 (2016).
342 Hayashi, R. *et al.* Association of genetic polymorphisms in IL17A and IL17F with gastro-duodenal diseases. *Journal of gastrointestinal and liver diseases : JGLD* **21**, 243-249 (2012).
343 Rolandelli, A. *et al.* The IL-17A rs2275913 single nucleotide polymorphism is associated with protection to tuberculosis but related to higher disease severity in Argentina. *Scientific reports* **7**, 40666 (2017).
344 Piazuelo, E., Fuentes, J., Garcfa-González, M. A., Jiménez, P. & Lanas, A. A case-control study of the association between polymorphisms of the endothelial nitric oxide synthase and glycoprotein IIIa genes and upper gastrointestinal bleeding in users of low-dose aspirin. *Clinical therapeutics* **30**, 121-130 (2008).
345 Jeerooburkhan, N. *et al.* Genetic and environmental determinants of plasma nitrogen oxides and risk of ischemic heart disease. *Hypertension* **38**, 1054-1061 (2001).
346 Song, J. *et al.* Genotype-specific influence on nitric oxide synthase gene expression, protein concentrations, and enzyme activity in cultured human endothelial cells. *Clinical chemistry* **49**, 847-852 (2003).
347 Tsukada, T. *et al.* Evidence of association of the ecNOS gene polymorphism with plasma NO metabolite levels in humans. *Biochemical and biophysical research communications* **245**, 190-193 (1998).
348 Wang, X. L. *et al.* Genetic contribution of the endothelial constitutive nitric oxide synthase gene to plasma nitric oxide levels. *Arteriosclerosis, thrombosis, and vascular biology* **17**, 3147-3153 (1997).
349 Negovan, A. *et al.* AGT A-20C (rs5050) gene polymorphism and ulcer occurrence in patients treated with low-dose aspirin: a case-control study/Polimorfismul AGT A-20C și ulcerele gastro-duodenale la pacienții sub tratament cu aspirină în doze antiagregante: studiu caz-control. *Romanian Review of Laboratory Medicine* **23**, 179-187 (2015).
350 Shiotani, A. *et al.* Renin-angiotensin system associated with risk of upper GI mucosal injury induced by low dose aspirin. *Digestive diseases and sciences* **56**, 465-471 (2011).
351 Garg, M. *et al.* the pathophysiological roles of the renin–angiotensin system in the gastrointestinal tract. *Alimentary pharmacology & therapeutics* **35**, 414-428 (2012).
352 Yanai, K., Nibu, Y., Murakami, K. & Fukamizu, A. A cis-acting DNA element located between TATA box and transcription initiation site is critical in response to regulatory sequences in human angiotensinogen gene. *Journal of Biological Chemistry* **271**, 15981-15986 (1996).
353 Zhao, Y. Y., Zhou, J., Narayanan, C. S., Cui, Y. & Kumar, A. Role of C/A polymorphism at− 20 on the expression of human angiotensinogen gene. *Hypertension* **33**, 108-115 (1999).
354 Tadjuidje, E. & Hegde, R. S. The Eyes Absent proteins in development and disease. *Cellular and Molecular Life Sciences* **70**, 1897-1913 (2013).

355 Li, X. *et al.* Eya protein phosphatase activity regulates Six1–Dach–Eya transcriptional effects in mammalian organogenesis. *Nature* **426**, 247 (2003).
356 Rayapureddi, J. P. *et al.* Eyes absent represents a class of protein tyrosine phosphatases. *Nature* **426**, 295 (2003).
357 Tootle, T. L. *et al.* The transcription factor Eyes absent is a protein tyrosine phosphatase. *Nature* **426**, 299 (2003).
358 Rayapureddi, J. P., Kattamuri, C., Chan, F. H. & Hegde, R. S. Characterization of a plant, tyrosine-specific phosphatase of the aspartyl class. *Biochemistry* **44**, 751-758 (2005).
359 Okabe, Y., Sano, T. & Nagata, S. Regulation of the innate immune response by threonine-phosphatase of Eyes absent. *Nature* **460**, 520 (2009).
360 Cook, P. J. *et al.* Tyrosine dephosphorylation of H2AX modulates apoptosis and survival decisions. *Nature* **458**, 591-596 (2009).
361 Chang, E. H. *et al.* Branchio-oto-renal syndrome: The mutation spectrum in EYA1 and its phenotypic consequences. *Human mutation* **23**, 582-589 (2004).
362 Rebay, I. Multiple functions of the Eya phosphotyrosine phosphatase. *Molecular and cellular biology* **36**, 668-677 (2016).
363 Abdelhak, S. *et al.* Clustering of mutations responsible for branchio-oto-renal (BOR) syndrome in the eyes absent homologous region (eyaHR) of EYA1. *Human molecular genetics* **6**, 2247-2255 (1997).
364 Abdelhak, S. *et al.* A human homologue of the Drosophila eyes absent gene underlies branchio-oto-renal (BOR) syndrome and identifies a novel gene family. *Nature genetics* **15**, 157 (1997).
365 Vincent, C. *et al.* BOR and BO syndromes are allelic defects of EYA1. *European journal of human genetics: EJHG* **5**, 242-246 (1997).
366 Morisada, N., Nozu, K. & Iijima, K. Branchio-oto-renal syndrome: Comprehensive review based on nationwide surveillance in J apan. *Pediatrics International* **56**, 309-314 (2014).
367 Musharraf, A. *et al.* BOR-syndrome-associated EYA1 mutations lead to enhanced proteasomal degradation of EYA1 protein. *PloS one* **9**, e87407 (2014).
368 Xu, P.-X. *et al.* Eya1-deficient mice lack ears and kidneys and show abnormal apoptosis of organ primordia. *Nature genetics* **23**, 113 (1999).
369 Orten, D. J. *et al.* Branchio-oto-renal syndrome (BOR): novel mutations in the EYA1 gene, and a review of the mutational genetics of BOR. *Human mutation* **29**, 537-544 (2008).
370 Zhou, H., Zhang, L., Vartuli, R. L., Ford, H. L. & Zhao, R. The Eya phosphatase: Its unique role in cancer. *The international journal of biochemistry & cell biology* (2017).
371 Tadjuidje, E. *et al.* The EYA tyrosine phosphatase activity is pro-angiogenic and is inhibited by benzbromarone. *PloS one* **7**, e34806 (2012).
372 Cai, S. *et al.* EYA1 promotes tumor angiogenesis by activating the PI3K pathway in colorectal cancer. *Experimental cell research* **367**, 37-46 (2018).
373 Wu, K. *et al.* EYA1 phosphatase function is essential to drive breast cancer cell proliferation through cyclin D1. *Cancer research* (2013).
374 Matsusaka, K. *et al.* Classification of Epstein–Barr virus–positive gastric cancers by definition of DNA methylation epigenotypes. *Cancer research* (2011).
375 Nikpour, P., Emadi-Baygi, M., Emadi-Andani, E. & Rahmati, S. EYA1 expression in gastric carcinoma and its association with clinicopathological characteristics: a pilot study. *Medical Oncology* **31**, 955 (2014).
376 Eisner, A. *et al.* The Eya1 phosphatase promotes Shh signaling during hindbrain development and oncogenesis. *Developmental cell* **33**, 22-35 (2015).

377 Kool, M. *et al.* Integrated genomics identifies five medulloblastoma subtypes with distinct genetic profiles, pathway signatures and clinicopathological features. *PloS one* **3**, e3088 (2008).
378 Northcott, P. A. *et al.* Medulloblastoma comprises four distinct molecular variants. *Journal of Clinical Oncology* **29**, 1408 (2011).
379 Thompson, M. C. *et al.* Genomics identifies medulloblastoma subgroups that are enriched for specific genetic alterations. *Journal of Clinical Oncology* **24**, 1924-1931 (2006).
380 Hansen, J. N., Lotta Jr, L. T., Eberhardt, A., Schor, N. F. & Li, X. EYA1 expression and subcellular localization in neuroblastoma and its association with prognostic markers. *Journal of cancer research & therapy* **4**, 11 (2016).
381 Albino, D. *et al.* Identification of low intratumoral gene expression heterogeneity in neuroblastic tumors by genome-wide expression analysis and game theory. *Cancer: Interdisciplinary International Journal of the American Cancer Society* **113**, 1412-1422 (2008).
382 Syed, P. *et al.* Autoantibody profiling of glioma serum samples to identify biomarkers using human proteome arrays. *Scientific reports* **5**, 13895 (2015).
383 Miller, S. J. *et al.* Inhibition of Eyes Absent Homolog 4 expression induces malignant peripheral nerve sheath tumor necrosis. *Oncogene* **29**, 368 (2010).
384 Zhou, J. J. *et al.* Eyes absent gene (EYA1) is a pathogenic driver and a therapeutic target for melanoma. *Oncotarget* **8**, 105081 (2017).
385 Guan, H. *et al.* MicroRNA-101 inhibits cell proliferation and induces apoptosis by targeting EYA1 in breast cancer. *International journal of molecular medicine* **37**, 1643-1651 (2016).
386 Li, J. *et al.* EYA1's conformation-specificity in dephosphorylating phosphothreonine in Myc and its activity on Myc stabilization in breast cancer. *Molecular and cellular biology*, MCB. 00499-00416 (2016).
387 Sun, Y., Kaneko, S., Li, X. & Li, X. The PI3K/Akt signal hyperactivates Eya1 via the SUMOylation pathway. *Oncogene* **34**, 2527-2537 (2015).
388 Sun, Y. & Li, X. The canonical wnt signal restricts the glycogen synthase kinase 3/fbw7-dependent ubiquitination and degradation of eya1 phosphatase. *Molecular and cellular biology* **34**, 2409-2417 (2014).
389 Pandey, R. N. *et al.* The Eyes Absent phosphatase-transactivator proteins promote proliferation, transformation, migration, and invasion of tumor cells. *Oncogene* **29**, 3715 (2010).
390 Drake, K. M. *et al.* Loss of heterozygosity at 2q37 in sporadic Wilms' tumor: putative role for miR-562. *Clinical Cancer Research*, 1078-0432. CCR-1009-1065 (1909).
391 Li, C.-M. *et al.* Gene expression in Wilms' tumor mimics the earliest committed stage in the metanephric mesenchymal-epithelial transition. *The American journal of pathology* **160**, 2181-2190 (2002).
392 Huang, C. C. *et al.* Classification of malignant pediatric renal tumors by gene expression. *Pediatric blood & cancer* **46**, 728-738 (2006).
393 Gao, Q. *et al.* Activating mutations in PTPN3 promote cholangiocarcinoma cell proliferation and migration and are associated with tumor recurrence in patients. *Gastroenterology* **146**, 1397-1407 (2014).
394 Esume, C. *Pharmacogenomics of non-steroidal anti-inflammatory drug-induced gastrointestinal complications*, University of Liverpool, (2016).
395 Power, J. J., Dennis, M. S., Redlak, M. J. & Miller, T. A. Aspirin-induced mucosal cell death in human gastric cells: evidence supporting an apoptotic mechanism. *Digestive diseases and sciences* **49**, 1518-1525 (2004).

396 Zhou, X. M. *et al.* Non-steroidal anti-inflammatory drugs induce apoptosis in gastric cancer cells through up-regulation of bax and bak. *Carcinogenesis* **22**, 1393-1397 (2001).
397 Collaboration, A. T. Collaborative meta-analysis of randomised trials of antiplatelet therapy for prevention of death, myocardial infarction, and stroke in high risk patients. *BMJ* **324**, 71-86 (2002).
398 Bruna Kempfer Bassoli, P. C. G. R. B.-M. J. C., Clairce Luzia Salgueiro-Pagadigorria, R. B. B., Souza, R. S. r. d. S. F. d. S. & Helenir Medri, d. Chlorogenic acid reduces the plasma glucose peak in the oral glucose tolerance test: effects on hepatic glucose release and glycaemia. *Cell biochemistry and function* **26**, 320-328, doi:10.1002/cbf (2008).
399 Deidda, S., Cabras, F. & Restivo, A. Aspirin: a new old anticancer drug. *Annals of Research Hospitals* **1** (2017).
400 Williams, J. L. *et al.* Nitric Oxide-releasing Nonsteroidal Anti-inflammatory Drugs (NSAIDs) Alter the Kinetics of Human Colon Cancer Cell Lines More Effectively than Traditional NSAIDs. *Cancer Research* **61**, 3285-3289 (2001).
401 Xu, H. *et al.* Establishment and characterization of an expanding-type gastric cancer cell line by Ming's classification. *Oncology reports* **36**, 3030-3036 (2016).
402 Cimini, A. *et al.* Gastroprotective Effects of L-Lysine Salification of Ketoprofen in Ethanol-Injured Gastric Mucosa. *Journal of cellular physiology* **230**, 813-820 (2015).
403 Lichtenberger, L. M. *et al.* Insight into NSAID-induced membrane alterations, pathogenesis and therapeutics: characterization of interaction of NSAIDs with phosphatidylcholine. *Biochimica et Biophysica Acta (BBA)-Molecular and Cell Biology of Lipids* **1821**, 994-1002 (2012).
404 Ishizuka, J., Martinez, J., Townsend Jr, C. M. & Thompson, J. C. The effect of gastrin on growth of human stomach cancer cells. *Annals of surgery* **215**, 528 (1992).
405 Basque, J. R., Chénard, M., Chailler, P. & Ménard, D. Gastric cancer cell lines as models to study human digestive functions. *Journal of cellular biochemistry* **81**, 241-251 (2001).
406 Barranco, S. *et al.* Establishment and characterization of an in vitro model system for human adenocarcinoma of the stomach. *Cancer research* **43**, 1703-1709 (1983).
407 Akagi, T. & Kimoto, T. Human cell line (HGC-27) derived from the metastatic lymph node of gastric cancer. *Acta medica Okayama* **30** (1976).
408 Smith, H. S. In Vitro Properties of Epithelial Cell Lines Established from Human Carcinomas and Nonmalignant Tissue. *Journal of the National Cancer Institute* **62**, 225-230 (1979).
409 Motoyama, T., Hojo, H. & Watanabe, H. Comparison of seven cell lines derived from human gastric carcinomas. *Pathology International* **36**, 65-83 (1986).
410 Park, J.-G. *et al.* Characteristics of cell lines established from human gastric carcinoma. *Cancer research* **50**, 2773-2780 (1990).
411 Park, J. G. *et al.* Establishment and characterization of human gastric carcinoma cell lines. *International journal of cancer* **70**, 443-449 (1997).
412 Ku, J.-L. *et al.* Establishment and characterization of six human gastric carcinoma cell lines, including one naturally infected with Epstein-Barr virus. *Cellular Oncology* **35**, 127-136 (2012).
413 Akiyama, S. *et al.* Characteristics of three human gastric cancer cell lines, NU-GC-2, NU-GC-3 and NU-GC-4. *Surgery Today* **18**, 438-446 (1988).
414 Wong, B. C.-y. *et al.* Cyclooxygenase-2 inhibitor (SC-236) suppresses activator protein-1 through c-Jun NH2-terminal kinase. *Gastroenterology* **126**, 136-147 (2004).

415 Ivey, K. J., Paone, D. B. & Krause, W. J. Acute effect of systemic aspirin on gastric mucosa in man. *Digestive diseases and sciences* **25**, 97-99 (1980).
416 Bellosillo, B. *et al.* Aspirin and salicylate induce apoptosis and activation of caspases in B-cell chronic lymphocytic leukemia cells. *Blood* **92**, 1406-1414 (1998).
417 Grilli, M., Pizzi, M., Memo, M. & Spano, P. Neuroprotection by aspirin and sodium salicylate through blockade of NF-kappaB activation. *Science* **274**, 1383 (1996).
418 Gu, Q. *et al.* Activation of the caspase-8/Bid and Bax pathways in aspirin-induced apoptosis in gastric cancer. *Carcinogenesis* **26**, 541-546 (2005).
419 Piqué, M. *et al.* Aspirin induces apoptosis through mitochondrial cytochrome c release. *FEBS letters* **480**, 193-196 (2000).
420 Zimmermann, K. C., Waterhouse, N. J., Goldstein, J. C., Schuler, M. & Green, D. R. Aspirin induces apoptosis through release of cytochrome c from mitochondria. *Neoplasia* **2**, 505-513 (2000).
421 Kim, K. M., Song, J. J., An, J. Y., Kwon, Y. T. & Lee, Y. J. Pretreatment of acetylsalicylic acid promotes tumor necrosis factor-related apoptosis-inducing ligand-induced apoptosis by down-regulating BCL-2 gene expression. *Journal of Biological Chemistry* **280**, 41047-41056 (2005).
422 Chan, T. A., Morin, P. J., Vogelstein, B. & Kinzler, K. W. Mechanisms underlying nonsteroidal antiinflammatory drug-mediated apoptosis. *Proceedings of the National Academy of Sciences* **95**, 681-686 (1998).
423 Kopp, E. & Ghosh, S. Inhibition of NF-kappa B by sodium salicylate and aspirin. *Science* **265**, 956-959 (1994).
424 Wong, B. C. Y. *et al.* Suppression of RelA/p65 nuclear translocation independent of I? Ba degradation by cyclooxygenase-2 inhibitor in gastric cancer. *Oncogene* **22** (2003).
425 Yin, M.-J., Yamamoto, Y. & Gaynor, R. B. The anti-inflammatory agents aspirin and salicylate inhibit the activity of IκB kinase-β. *Nature* **396**, 77-80 (1998).
426 Bock, J. M. *et al.* Relative non-steroidal anti-inflammatory drug (NSAID) antiproliferative activity is mediated through p21-induced G1 arrest and E2F inhibition. *Molecular carcinogenesis* **46**, 857-864 (2007).
427 Dikshit, P., Chatterjee, M., Goswami, A., Mishra, A. & Jana, N. R. Aspirin induces apoptosis through the inhibition of proteasome function. *Journal of Biological Chemistry* **281**, 29228-29235 (2006).
428 Ho, C. C. *et al.* Activation of p53 signalling in acetylsalicylic acid-induced apoptosis in oc2 human oral cancer cells. *European journal of clinical investigation* **33**, 875-882 (2003).
429 Huang, Y.-C., Chuang, L.-Y. & Hung, W.-C. Mechanisms underlying nonsteroidal anti-inflammatory drug-induced p27 KIP1 expression. *Molecular pharmacology* **62**, 1515-1521 (2002).
430 Luciani, M. G., Campregher, C. & Gasche, C. Aspirin blocks proliferation in colon cells by inducing a G 1 arrest and apoptosis through activation of the checkpoint kinase ATM. *Carcinogenesis* **28**, 2207-2217 (2007).
431 Piazza, G. A. *et al.* Apoptosis primarily accounts for the growth-inhibitory properties of sulindac metabolites and involves a mechanism that is independent of cyclooxygenase inhibition, cell cycle arrest, and p53 induction. *Cancer research* **57**, 2452-2459 (1997).
432 Zhu, G. *et al.* Non-steroidal anti-inflammatory drug-induced apoptosis in gastric cancer cells is blocked by protein kinase C activation through inhibition of c-myc. *British journal of cancer* **79**, 393 (1999).

433 Adachi, M. *et al.* Nonsteroidal anti-inflammatory drugs and oxidative stress in cancer cells. *Histology and histopathology* **22**, 437-442 (2007).
434 Bhattacharyya, S., Ghosh, S. & Sil, P. C. Amelioration of aspirin induced oxidative impairment and apoptotic cell death by a novel antioxidant protein molecule isolated from the herb Phyllanthus niruri. *PloS one* **9**, e89026 (2014).
435 Gao, J., Liu, X. & Rigas, B. Nitric oxide-donating aspirin induces apoptosis in human colon cancer cells through induction of oxidative stress. *Proceedings of the National Academy of Sciences of the United States of America* **102**, 17207-17212 (2005).
436 Schwenger, P. *et al.* Sodium salicylate induces apoptosis via p38 mitogen-activated protein kinase but inhibits tumor necrosis factor-induced c-Jun N-terminal kinase/stress-activated protein kinase activation. *Proceedings of the National Academy of Sciences* **94**, 2869-2873 (1997).
437 Tsutsumi, S. *et al.* Endoplasmic reticulum stress response is involved in nonsteroidal anti-inflammatory drug-induced apoptosis. *Cell Death & Differentiation* **11**, 1009-1016 (2004).
438 Tanaka, K.-i. *et al.* Involvement of intracellular Ca2+ levels in nonsteroidal anti-inflammatory drug-induced apoptosis. *Journal of Biological Chemistry* **280**, 31059-31067 (2005).
439 Iglesias-Serret, D. *et al.* Aspirin induces apoptosis in human leukemia cells independently of NF-κB and MAPKs through alteration of the Mcl-1/Noxa balance. *Apoptosis* **15**, 219-229 (2010).
440 Gao, J. *et al.* Non-steroidal anti-inflammatory drugs inhibit cellular proliferation and upregulate cyclooxygenase-2 protein expression in endometrial cancer cells. *Cancer science* **95**, 901-907 (2004).
441 Chiou, S.-K. & Mandayam, S. NSAIDs enhance proteasomic degradation of survivin, a mechanism of gastric epithelial cell injury and apoptosis. *Biochemical pharmacology* **74**, 1485-1495 (2007).
442 Subbegowda, R. & Frommel, T. O. Aspirin toxicity for human colonic tumor cells results from necrosis and is accompanied by cell cycle arrest. *Cancer research* **58**, 2772-2776 (1998).
443 Kumar, J. P. Signalling pathways in Drosophila and vertebrate retinal development. *Nature Reviews Genetics* **2**, 846 (2001).
444 Pignoni, F. *et al.* The eye-specification proteins So and Eya form a complex and regulate multiple steps in Drosophila eye development. *Cell* **91**, 881-891 (1997).
445 Silver, S. J. & Rebay, I. Signaling circuitries in development: insights from the retinal determination gene network. *Development* **132**, 3-13 (2005).
446 Krishnan, N. *et al.* Dephosphorylation of the C-terminal tyrosyl residue of the DNA damage-related histone H2A. X is mediated by the protein phosphatase eyes absent. *Journal of Biological Chemistry* **284**, 16066-16070 (2009).
447 Lu, C. *et al.* Cell apoptosis: requirement of H2AX in DNA ladder formation, but not for the activation of caspase-3. *Molecular cell* **23**, 121-132 (2006).
448 Pandey, R. N. *et al.* Structure-activity relationships of benzbromarone metabolites and derivatives as EYA inhibitory anti-angiogenic agents. *PloS one* **8**, e84582 (2013).
449 Lee, M.-H. H., Graham, G. G., Williams, K. M. & Day, R. O. A benefit-risk assessment of benzbromarone in the treatment of gout. *Drug safety* **31**, 643-665 (2008).
450 Felser, A. *et al.* Hepatocellular toxicity of benzbromarone: effects on mitochondrial function and structure. *Toxicology* **324**, 136-146 (2014).
451 Yin, H. *et al.* Cyclooxygenase-independent effects of aspirin on HT-29 human colon cancer cells, revealed by oligonucleotide microarrays. *Biotechnology letters* **28**, 1263-1270 (2006).

452 Qiao, L., Hanif, R., Sphicas, E., Shiff, S. J. & Rigas, B. Effect of aspirin on induction of apoptosis in HT-29 human colon adenocarcinoma cells. *Biochemical pharmacology* **55**, 53-64 (1998).
453 Maity, G. *et al.* Aspirin blocks growth of breast tumor cells and tumor-initiating cells and induces reprogramming factors of mesenchymal to epithelial transition. *Laboratory Investigation* **95**, 702-717 (2015).
454 Ordan, O., Rotem, R., Jaspers, I. & Flescher, E. Stress-responsive JNK mitogen-activated protein kinase mediates aspirin-induced suppression of B16 melanoma cellular proliferation. *British journal of pharmacology* **138**, 1156-1162 (2003).
455 Kepp, O., Galluzzi, L., Lipinski, M., Yuan, J. & Kroemer, G. Cell death assays for drug discovery. *Nature reviews Drug discovery* **10**, 221-237 (2011).
456 Brody, T. M. & Fouts, W. Action of sodium salicylate and related compounds on tissue metabolism in vitro. *Journal of Pharmacology and Experimental Therapeutics* **117**, 39-51 (1956).
457 Mehlman, M. A. & Tobin, R. B. Oxidative phosphorylation and respiration by rat liver mitochondria from aspirin-treated rats. *Biochemical pharmacology* **21**, 3279-3285 (1972).
458 Yukiko, T., Sokpong, L. & Michio, U. In vitro effects of nonsteroidal anti-inflammatory drugs on oxidative phosphorylation in rat liver mitochondria. *Biochemical pharmacology* **26**, 2101-2106 (1977).
459 Kramar, R. & Müller, M. Inhibition of enzymes of the internal mitochondrial membrane by benzbromarone. *Experientia* **29**, 391-392 (1973).
460 Kaufmann, P. *et al.* Mechanisms of benzarone and benzbromarone-induced hepatic toxicity. *Hepatology* **41**, 925-935 (2005).
461 Uhlén, M. *et al.* Tissue-based map of the human proteome. *Science* **347**, 1260419 (2015).
462 Buller, C., Xu, X., Marquis, V., Schwanke, R. & Xu, P.-X. Molecular effects of Eya1 domain mutations causing organ defects in BOR syndrome. *Human molecular genetics* **10**, 2775-2781 (2001).
463 Li, X. *et al.* Methylation of the phosphatase-transcription activator EYA1 by protein arginine methyltransferase 1: mechanistic, functional, and structural studies. *The FASEB Journal* **31**, 2327-2339 (2017).
464 Ardito, F., Giuliani, M., Perrone, D., Troiano, G. & Lo Muzio, L. The crucial role of protein phosphorylation in cell signaling and its use as targeted therapy. *International journal of molecular medicine* **40**, 271-280 (2017).
465 Case, N. *et al.* Mechanical regulation of glycogen synthase kinase 3β (GSK3β) in mesenchymal stem cells is dependent on Akt protein serine 473 phosphorylation via mTORC2 protein. *Journal of Biological Chemistry* **286**, 39450-39456 (2011).
466 Cole, P. A., Shen, K., Qiao, Y. & Wang, D. Protein tyrosine kinases Src and Csk: a tail's tale. *Current opinion in chemical biology* **7**, 580-585 (2003).
467 Kataoka, M., Kuwahara, R., Iwasaki, S., Shoji-Kasai, Y. & Takahashi, M. Nerve growth factor-induced phosphorylation of SNAP-25 in PC12 cells: a possible involvement in the regulation of SNAP-25 localization. *Journal of neurochemistry* **74**, 2058-2066 (2000).
468 Kuwahara, H., Nishizaki, M. & Kanazawa, H. Nuclear localization signal and phosphorylation of Serine350 specify intracellular localization of DRAK2. *Journal of biochemistry* **143**, 349-358 (2007).
469 Hunter, T. The age of crosstalk: phosphorylation, ubiquitination, and beyond. *Molecular cell* **28**, 730-738 (2007).

470 Xu, X. *et al.* The CUL7 E3 ubiquitin ligase targets insulin receptor substrate 1 for ubiquitin-dependent degradation. *Molecular cell* **30**, 403-414 (2008).
471 Alkuraya, F. S. *et al.* SUMO1 haploinsufficiency leads to cleft lip and palate. *Science* **313**, 1751-1751 (2006).
472 Kim, T. K. & Eberwine, J. H. Mammalian cell transfection: the present and the future. *Analytical and bioanalytical chemistry* **397**, 3173-3178 (2010).
473 Hu, S. *et al.* miR-532 promoted gastric cancer migration and invasion by targeting NKD1. *Life sciences* **177**, 15-19 (2017).
474 Safari, F. & Zaer, S. J. Evaluation of Cell-Morphological Changes by Helicobacter pylori CagA and Pragmin in AGS Human Gastric Carcinoma Cells. *Gene, Cell and Tissue* **4** (2017).
475 Vara, J. A., Portela, A., Ortìn, J. & Jimenez, A. Expression in mammalian cells of a gene from Streptomyces alboniger conferring puromycin resistance. *Nucleic acids research* **14**, 4617-4624 (1986).
476 Chen, M.-B. *et al.* AMPKα phosphatase Ppm1E upregulation in human gastric cancer is required for cell proliferation. *Oncotarget* **8**, 31288 (2017).
477 Hagemeier, S. R., Barlow, E. A., Meng, Q. & Kenney, S. C. The cellular ataxia telangiectasia-mutated kinase promotes epstein-barr virus lytic reactivation in response to multiple different types of lytic reactivation-inducing stimuli. *Journal of virology* **86**, 13360-13370 (2012).
478 Kim, K. K., Park, K. S., Song, S. B. & Kim, K. E. Up regulation of GW112 Gene by NFκB promotes an antiapoptotic property in gastric cancer cells. *Molecular carcinogenesis* **49**, 259-270 (2010).
479 Tsai, K. W. *et al.* Aberrant expression of miR-196a in gastric cancers and correlation with recurrence. *Genes, Chromosomes and Cancer* **51**, 394-401 (2012).
480 Zhang, X. *et al.* miR-874 functions as a tumor suppressor by inhibiting angiogenesis through STAT3/VEGF-A pathway in gastric cancer. *Oncotarget* **6**, 1605 (2015).
481 Ohto, H. *et al.* Cooperation of six and eya in activation of their target genes through nuclear translocation of Eya. *Molecular and cellular biology* **19**, 6815-6824 (1999).
482 Sun, J. *et al.* The phosphatase-transcription activator EYA1 is targeted by anaphase-promoting complex/Cdh1 for degradation at M-to-G1 transition. *Molecular and cellular biology* **33**, 927-936 (2013).
483 Mátés, L. *et al.* Molecular evolution of a novel hyperactive Sleeping Beauty transposase enables robust stable gene transfer in vertebrates. *Nature genetics* **41**, 753-761 (2009).
484 Kupershmidt, I. *et al.* Ontology-based meta-analysis of global collections of high-throughput public data. *PloS one* **5**, e13066 (2010).
485 NCBI. *Primer-BLAST, National Center for Biotechnology Information, Bethesda (MD), National Library of Medicine (US)*, <Available from: https://www.ncbi.nlm.nih.gov/tools/primer-blast/> (1988).
486 NCBI. *Gene [Internet], Bethesda (MD): National Library of Medicine (US), National Center for Biotechnology Information*, <Available from: https://www.ncbi.nlm.nih.gov/gene/> (2004).
487 Geurts, A. M. *et al.* Gene transfer into genomes of human cells by the sleeping beauty transposon system. *Molecular Therapy* **8**, 108-117 (2003).
488 Abdullah, A. *et al.* Analysis of the role of Nrf2 in the expression of liver proteins in mice using two-dimensional gel-based proteomics. *Pharmacological reports* **64**, 680-697 (2012).

489 Kitteringham, N. R. *et al.* Proteomic analysis of Nrf2 deficient transgenic mice reveals cellular defence and lipid metabolism as primary Nrf2-dependent pathways in the liver. *Journal of proteomics* **73**, 1612-1631 (2010).
490 Shilov, I. V. *et al.* The Paragon Algorithm, a next generation search engine that uses sequence temperature values and feature probabilities to identify peptides from tandem mass spectra. *Molecular & Cellular Proteomics* **6**, 1638-1655 (2007).
491 Tang, W. H., Shilov, I. V. & Seymour, S. L. Nonlinear fitting method for determining local false discovery rates from decoy database searches. *Journal of proteome research* **7**, 3661-3667 (2008).
492 Minoux, M. *et al.* Mouse Hoxa2 mutations provide a model for microtia and auricle duplication. *Development* **140**, 4386-4397 (2013).
493 Massa, F. M. *The crucial roles played by HNF1β during kidney development*, Université René Descartes-Paris V, (2012).
494 Krug, P. *et al.* Mutation screening of the EYA1, SIX1, and SIX5 genes in a large cohort of patients harboring branchio-oto-renal syndrome calls into question the pathogenic role of SIX5 mutations. *Human mutation* **32**, 183-190 (2011).
495 Bjarnason, I., Scarpignato, C., Takeuchi, K. & Rainsford, K. Determinants of the short-term gastric damage caused by NSAIDs in man. *Alimentary pharmacology & therapeutics* **26**, 95-106 (2007).
496 Tanaka, K.-I. *et al.* Adaptive cytoprotection induced by pretreatment with ethanol protects against gastric cell damage by NSAIDs. *Digestive diseases and sciences* **49**, 210-217 (2004).
497 Milani, M. *et al.* DRP-1 is required for BH3 mimetic-mediated mitochondrial fragmentation and apoptosis. *Cell death & disease* **8**, e2552 (2017).
498 Palchaudhuri, R. *et al.* A small molecule that induces intrinsic pathway apoptosis with unparalleled speed. *Cell reports* **13**, 2027-2036 (2015).
499 Zhang, X. D., Gillespie, S. K. & Hersey, P. Staurosporine induces apoptosis of melanoma by both caspase-dependent and-independent apoptotic pathways. *Molecular cancer therapeutics* **3**, 187-197 (2004).
500 Bertrand, R., Solary, E., O'Connor, P., Kohn, K. W. & Pommier, Y. Induction of a common pathway of apoptosis by staurosporine. *Experimental cell research* **211**, 314-321 (1994).
501 Antonsson, A. & Persson, J. L. Induction of apoptosis by staurosporine involves the inhibition of expression of the major cell cycle proteins at the G2/M checkpoint accompanied by alterations in Erk and Akt kinase activities. *Anticancer research* **29**, 2893-2898 (2009).
502 Anadu, N. O., Davisson, V. J. & Cushman, M. Synthesis and anticancer activity of brefeldin A ester derivatives. *Journal of medicinal chemistry* **49**, 3897-3905 (2006).
503 Paek, S.-M. Recent Synthesis and Discovery of Brefeldin A Analogs. *Marine drugs* **16**, 133 (2018).
504 Lee, S. A., Kim, Y. J. & Lee, C. S. Brefeldin A Induces Apoptosis by Activating the Mitochondrial and Death Receptor Pathways and Inhibits Focal Adhesion Kinase-Mediated Cell Invasion. *Basic & clinical pharmacology & toxicology* **113**, 329-338 (2013).
505 Jiang, C. C. *et al.* Tunicamycin sensitizes human melanoma cells to tumor necrosis factor–related apoptosis-inducing ligand–induced apoptosis by up-regulation of trail-r2 via the unfolded protein response. *Cancer research* **67**, 5880-5888 (2007).
506 Shiraishi, T. *et al.* Tunicamycin enhances tumor necrosis factor–related apoptosis-inducing ligand–induced apoptosis in human prostate cancer cells. *Cancer research* **65**, 6364-6370 (2005).

507 Oldani, A. *et al.* Helicobacter pylori counteracts the apoptotic action of its VacA toxin by injecting the CagA protein into gastric epithelial cells. *PLoS pathogens* **5**, e1000603 (2009).
508 Zhaleh, M., Azadbakht, M. & Bidmeshki, A. P. Inhibitory effects of mouse bone marrow mesenchymal stem cell soup on staurospurine-induced cell death in MCF-7 and AGS. *Bratislavske lekarske listy* **118**, 34-43 (2017).
509 WU, P., WANG, J.-y., ZHANG, X.-d., ZHU, X.-f. & ZHANG, L.-j. Tunicamycin enhances the sensitivity to TRAIL in gastric cancer cells by up-regulation of TRAIL-R2. *TUMOR* **33**, 15-20 (2013).
510 Zhou, Y. *et al.* Casticin potentiates TRAIL-induced apoptosis of gastric cancer cells through endoplasmic reticulum stress. *PloS one* **8**, e58855 (2013).
511 Zhang, H.-Y. *et al.* Tunicamycin enhances TRAIL-induced apoptosis by inhibition of cyclin D1 and the subsequent downregulation of survivin. *Experimental & molecular medicine* **41**, 362 (2009).
512 ISHII, S., NAGASAWA, M., KARIYA, Y. & YAMAMOTO, H. Selective cytotoxic activity of brefeldin A against human tumor cell lines. *The Journal of antibiotics* **42**, 1877-1878 (1989).
513 Silva, A. M., Wang, D., Komar, A. A., Castilho, B. A. & Williams, B. R. Salicylates trigger protein synthesis inhibition in a protein kinase R-like endoplasmic reticulum kinase-dependent manner. *Journal of Biological Chemistry* **282**, 10164-10171 (2007).
514 Shamas-Din, A., Kale, J., Leber, B. & Andrews, D. W. Mechanisms of action of Bcl-2 family proteins. *Cold Spring Harbor perspectives in biology* **5**, a008714 (2013).
515 Grad, J. M., Zeng, X.-R. & Boise, L. H. Regulation of Bcl-xL: a little bit of this and a little bit of STAT. *Current opinion in oncology* **12**, 543-549 (2000).
516 Grandis, J. R. *et al.* Constitutive activation of Stat3 signaling abrogates apoptosis in squamous cell carcinogenesis in vivo. *Proceedings of the National Academy of Sciences* **97**, 4227-4232 (2000).
517 Willimott, S. & Wagner, S. D. (Portland Press Limited, 2010).
518 Johnson, B. N., Berger, A. K., Cortese, G. P. & LaVoie, M. J. The ubiquitin E3 ligase parkin regulates the proapoptotic function of Bax. *Proceedings of the National Academy of Sciences* **109**, 6283-6288 (2012).
519 Li, B. & Dou, Q. P. Bax degradation by the ubiquitin/proteasome-dependent pathway: involvement in tumor survival and progression. *Proceedings of the National Academy of Sciences* **97**, 3850-3855 (2000).
520 Zhang, C.-W., Hang, L., Yao, T.-P. & Lim, K.-L. Parkin regulation and neurodegenerative disorders. *Frontiers in aging neuroscience* **7**, 248 (2016).
521 Herrant, M. *et al.* Cleavage of Mcl-1 by caspases impaired its ability to counteract Bim-induced apoptosis. *Oncogene* **23**, 7863 (2004).
522 Burma, S., Chen, B. P., Murphy, M., Kurimasa, A. & Chen, D. J. ATM phosphorylates histone H2AX in response to DNA double-strand breaks. *Journal of Biological Chemistry* **276**, 42462-42467 (2001).
523 Azuma, N., Hirakiyama, A., Inoue, T., Asaka, A. & Yamada, M. Mutations of a human homologue of the Drosophila eyes absent gene (EYA1) detected in patients with congenital cataracts and ocular anterior segment anomalies. *Human molecular genetics* **9**, 363-366 (2000).
524 Reis, L. M. *et al.* Whole exome sequencing in dominant cataract identifies a new causative factor, CRYBA2, and a variety of novel alleles in known genes. *Human genetics* **132**, 761-770 (2013).

525 Ahmed, M. *et al.* Eya1-Six1 interaction is sufficient to induce hair cell fate in the cochlea by activating Atoh1 expression in cooperation with Sox2. *Developmental cell* **22**, 377-390 (2012).
526 Xu, P.-X. *et al.* Eya1 is required for the morphogenesis of mammalian thymus, parathyroid and thyroid. *Development* **129**, 3033-3044 (2002).
527 Sajithlal, G., Zou, D., Silvius, D. & Xu, P.-X. Eya1 acts as a critical regulator for specifying the metanephric mesenchyme. *Developmental biology* **284**, 323-336 (2005).
528 El-Hashash, A. H., Al Alam, D., Turcatel, G., Bellusci, S. & Warburton, D. Eyes absent 1 (Eya1) is a critical coordinator of epithelial, mesenchymal and vascular morphogenesis in the mammalian lung. *Developmental biology* **350**, 112-126 (2011).
529 Bui, Q. T., Zimmerman, J. E., Liu, H. & Bonini, N. M. Molecular analysis of Drosophila eyes absent mutants reveals features of the conserved Eya domain. *Genetics* **155**, 709-720 (2000).
530 Ahmed, M., Xu, J. & Xu, P.-X. EYA1 and SIX1 drive the neuronal developmental program in cooperation with the SWI/SNF chromatin-remodeling complex and SOX2 in the mammalian inner ear. *Development*, dev. 071670 (2012).
531 Riddiford, N. & Schlosser, G. Six1 and Eya1 both promote and arrest neuronal differentiation by activating multiple Notch pathway genes. *Developmental biology* **431**, 152-167 (2017).
532 Ikeda, K., Watanabe, Y., Ohto, H. & Kawakami, K. Molecular interaction and synergistic activation of a promoter by Six, Eya, and Dach proteins mediated through CREB binding protein. *Molecular and cellular biology* **22**, 6759-6766 (2002).
533 Ozaki, H., Watanabe, Y., Ikeda, K. & Kawakami, K. Impaired interactions between mouse Eya1 harboring mutations found in patients with branchio-oto-renal syndrome and Six, Dach, and G proteins. *Journal of human genetics* **47**, 107 (2002).
534 Pappu, K. & Mardon, G. in *Drosophila eye development* 5-20 (Springer, 2002).
535 Yuan, B. *et al.* A phosphotyrosine switch determines the antitumor activity of ERβ. *The Journal of clinical investigation* **124**, 3378-3390 (2014).
536 Xu, P.-X., Cheng, J., Epstein, J. A. & Maas, R. L. Mouse Eya genes are expressed during limb tendon development and encode a transcriptional activation function. *Proceedings of the National Academy of Sciences* **94**, 11974-11979 (1997).
537 Sano, T. & Nagata, S. Characterization of the threonine–phosphatase of mouse eyes absent 3. *FEBS letters* **585**, 2714-2719 (2011).
538 Zhang, Y., Knosp, B. M., Maconochie, M., Friedman, R. A. & Smith, R. J. A comparative study of Eya1 and Eya4 protein function and its implication in branchio-oto-renal syndrome and DFNA10. *Journal of the Association for Research in Otolaryngology* **5**, 295-304 (2004).
539 Bensimon, A., Heck, A. J. & Aebersold, R. Mass spectrometry–based proteomics and network biology. *Annual review of biochemistry* **81**, 379-405 (2012).
540 Haft, D. H. *et al.* RefSeq: an update on prokaryotic genome annotation and curation. *Nucleic acids research* **46**, D851-D860 (2017).
541 Zerbino, D. R. *et al.* Ensembl 2018. *Nucleic acids research* **46**, D754-D761 (2017).
542 Consortium, G. Genetic effects on gene expression across human tissues. *Nature* **550**, 204 (2017).
543 Noguchi, S. *et al.* FANTOM5 CAGE profiles of human and mouse samples. *Scientific data* **4**, 170112 (2017).
544 O'Leary, N. A. *et al.* Reference sequence (RefSeq) database at NCBI: current status, taxonomic expansion, and functional annotation. *Nucleic acids research* **44**, D733-D745 (2015).

545 Papatheodorou, I. *et al.* Expression Atlas: gene and protein expression across multiple studies and organisms. *Nucleic acids research* **46**, D246-D251 (2017).
546 Consortium, U. UniProt: the universal protein knowledgebase. *Nucleic acids research* **45**, D158-D169 (2016).
547 Kim, M.-S. *et al.* A draft map of the human proteome. *Nature* **509**, 575 (2014).
548 Schmidt, T. *et al.* ProteomicsDB. *Nucleic acids research* **46**, D1271-D1281 (2017).
549 Landrum, M. J. *et al.* ClinVar: improving access to variant interpretations and supporting evidence. *Nucleic acids research* **46**, D1062-D1067 (2017).
550 Lizio, M. *et al.* Gateways to the FANTOM5 promoter level mammalian expression atlas. *Genome biology* **16**, 22 (2015).
551 Desiere, F. *et al.* The peptideatlas project. *Nucleic acids research* **34**, D655-D658 (2006).
552 Craig, R., Cortens, J. P. & Beavis, R. C. Open source system for analyzing, validating, and storing protein identification data. *Journal of proteome research* **3**, 1234-1242 (2004).
553 Canela-Xandri, O., Rawlik, K. & Tenesa, A. An atlas of genetic associations in UK Biobank. *bioRxiv*, 176834 (2017).
554 Takahashi, H., Lassmann, T., Murata, M. & Carninci, P. 5′ end–centered expression profiling using cap-analysis gene expression and next-generation sequencing. *Nature protocols* **7**, 542 (2012).
555 Vizcaíno, J. A. *et al.* 2016 update of the PRIDE database and its related tools. *Nucleic acids research* **44**, D447-D456 (2015).
556 Gaudet, P. *et al.* The neXtProt knowledgebase on human proteins: 2017 update. *Nucleic acids research* **45**, D177-D182 (2016).
557 Wang, M., Herrmann, C. J., Simonovic, M., Szklarczyk, D. & von Mering, C. Version 4.0 of PaxDb: protein abundance data, integrated across model organisms, tissues, and cell-lines. *Proteomics* **15**, 3163-3168 (2015).
558 Schaab, C., Geiger, T., Stoehr, G., Cox, J. & Mann, M. Analysis of high-accuracy, quantitative proteomics data in the MaxQB database. *Molecular & Cellular Proteomics*, mcp. M111. 014068 (2012).
559 Desiere, F. *et al.* Integration with the human genome of peptide sequences obtained by high-throughput mass spectrometry. *Genome biology* **6**, R9 (2005).
560 Farrah, T. *et al.* The state of the human proteome in 2012 as viewed through PeptideAtlas. *Journal of proteome research* **12**, 162-171 (2012).
561 Keller, A., Nesvizhskii, A. I., Kolker, E. & Aebersold, R. Empirical statistical model to estimate the accuracy of peptide identifications made by MS/MS and database search. *Analytical chemistry* **74**, 5383-5392 (2002).
562 Pirmoradian, M. *et al.* Rapid and deep human proteome analysis by single-dimension shotgun proteomics. *Molecular & Cellular Proteomics*, mcp. O113. 028787 (2013).
563 Shiromizu, T. *et al.* Identification of missing proteins in the neXtProt database and unregistered phosphopeptides in the PhosphoSitePlus database as part of the Chromosome-centric Human Proteome Project. *Journal of proteome research* **12**, 2414-2421 (2013).
564 Geiger, T., Wehner, A., Schaab, C., Cox, J. & Mann, M. Comparative proteomic analysis of eleven common cell lines reveals ubiquitous but varying expression of most proteins. *Molecular & Cellular Proteomics*, mcp. M111. 014050 (2012).
565 Gholami, A. M. *et al.* Global proteome analysis of the NCI-60 cell line panel. *Cell reports* **4**, 609-620 (2013).
566 Mertins, P. *et al.* Integrated proteomic analysis of post-translational modifications by serial enrichment. *Nature methods* **10**, 634 (2013).

567 Cho, C.-K. J. *et al.* Quantitative proteomic analysis of amniocytes reveals potentially dysregulated molecular networks in Down syndrome. *Clinical proteomics* **10**, 2 (2013).
568 Phanstiel, D. H. *et al.* Proteomic and phosphoproteomic comparison of human ES and iPS cells. *Nature methods* **8**, 821 (2011).
569 Nagaraj, N. *et al.* Deep proteome and transcriptome mapping of a human cancer cell line. *Molecular systems biology* **7**, 548 (2011).
570 Network, C. G. A. Comprehensive molecular portraits of human breast tumours. *Nature* **490**, 61 (2012).
571 Zhang, C.-C. *et al.* In silico protein interaction analysis using the global proteome machine database. *Journal of proteome research* **10**, 656-668 (2010).
572 Bush, W. S., Oetjens, M. T. & Crawford, D. C. Unravelling the human genome–phenome relationship using phenome-wide association studies. *Nature Reviews Genetics* **17**, 129 (2016).
573 Hu, J. X., Thomas, C. E. & Brunak, S. Network biology concepts in complex disease comorbidities. *Nature Reviews Genetics* **17**, 615 (2016).
574 Solovieff, N., Cotsapas, C., Lee, P. H., Purcell, S. M. & Smoller, J. W. Pleiotropy in complex traits: challenges and strategies. *Nature Reviews Genetics* **14**, nrg3461 (2013).
575 Denny, J. C., Bastarache, L. & Roden, D. M. Phenome-wide association studies as a tool to advance precision medicine. *Annual review of genomics and human genetics* **17**, 353-373 (2016).
576 Pulley, J. M. *et al.* Accelerating precision drug development and drug repurposing by leveraging human genetics. *Assay and drug development technologies* **15**, 113-119 (2017).
577 Rastegar-Mojarad, M., Ye, Z., Kolesar, J. M., Hebbring, S. J. & Lin, S. M. Opportunities for drug repositioning from phenome-wide association studies. *Nature biotechnology* **33**, 342 (2015).
578 Sudlow, C. *et al.* UK biobank: an open access resource for identifying the causes of a wide range of complex diseases of middle and old age. *PLoS medicine* **12**, e1001779 (2015).
579 Teo, Y. Y. *et al.* A genotype calling algorithm for the Illumina BeadArray platform. *Bioinformatics* **23**, 2741-2746 (2007).
580 Mägi, R. & Morris, A. P. GWAMA: software for genome-wide association meta-analysis. *BMC bioinformatics* **11**, 288 (2010).
581 Consortium, E. P. An integrated encyclopedia of DNA elements in the human genome. *Nature* **489**, 57 (2012).
582 Crawford, D. C. & Nickerson, D. A. Definition and clinical importance of haplotypes. *Annu. Rev. Med.* **56**, 303-320 (2005).
583 McCluskey, J. & Peh, C. A. The human leucocyte antigens and clinical medicine: an overview. *Reviews in immunogenetics* **1**, 3-20 (1999).
584 Nagel, R. L. *et al.* The Senegal DNA haplotype is associated with the amelioration of anemia in African-American sickle cell anemia patients. *Blood* **77**, 1371-1375 (1991).
585 Nagel, R. L. *et al.* Hematologically and genetically distinct forms of sickle cell anemia in Africa: the Senegal type and the Benin type. *New England Journal of Medicine* **312**, 880-884 (1985).
586 Lin, M.-T. *et al.* Relation of an interleukin-10 promoter polymorphism to graft-versus-host disease and survival after hematopoietic-cell transplantation. *New England Journal of Medicine* **349**, 2201-2210 (2003).

587 Marson, F. A., Bertuzzo, C. S., Ribeiro, A. F. & Ribeiro, J. D. Polymorphisms in ADRB2 gene can modulate the response to bronchodilators and the severity of cystic fibrosis. *BMC pulmonary medicine* **12**, 50 (2012).
588 Yip, V., Alfirevic, A. & Pirmohamed, M. Genetics of immune-mediated adverse drug reactions: a comprehensive and clinical review. *Clinical reviews in allergy & immunology* **48**, 165-175 (2015).
589 Aldridge, G. M., Podrebarac, D. M., Greenough, W. T. & Weiler, I. J. The use of total protein stains as loading controls: an alternative to high-abundance single-protein controls in semi-quantitative immunoblotting. *Journal of neuroscience methods* **172**, 250-254 (2008).
590 Craig, R. & Beavis, R. C. *GPM Database*, <https://gpmdb.thegpm.org/> (2003).
591 Puccetti, A. *et al.* Gene Expression Profiling in Behcet's Disease Indicates an Autoimmune Component in the Pathogenesis of the Disease and Opens New Avenues for Targeted Therapy. *Journal of immunology research* **2018** (2018).
592 Kidd, T., Bland, K. S. & Goodman, C. S. Slit is the midline repellent for the robo receptor in Drosophila. *Cell* **96**, 785-794 (1999).
593 Kim, M., Kim, J.-H., Baek, S.-J., Kim, S.-Y. & Kim, Y. S. Specific expression and methylation of SLIT1, SLIT2, SLIT3, and miR-218 in gastric cancer subtypes. *International journal of oncology* **48**, 2497-2507 (2016).
594 Biswas, M. & Chan, J. Y. Role of Nrf1 in antioxidant response element-mediated gene expression and beyond. *Toxicology and applied pharmacology* **244**, 16-20 (2010).
595 Kim, H. M., Han, J. W. & Chan, J. Y. Nuclear factor erythroid-2 like 1 (NFE2L1): structure, function and regulation. *Gene* **584**, 17-25 (2016).
596 Schlosser, G. *et al.* Eya1 and Six1 promote neurogenesis in the cranial placodes in a SoxB1-dependent fashion. *Developmental biology* **320**, 199-214 (2008).
597 Zou, D., Silvius, D., Fritzsch, B. & Xu, P.-X. Eya1 and Six1 are essential for early steps of sensory neurogenesis in mammalian cranial placodes. *Development* **131**, 5561-5572 (2004).
598 Wang, J. *et al.* (AACR, 2013).
599 Robin, T. P. *et al.* EWS/FLI1 regulates EYA3 in Ewing sarcoma via modulation of miRNA-708, resulting in increased cell survival and chemoresistance. *Molecular Cancer Research* (2012).
600 Tanikawa, C. *et al.* Impact of PSCA variation on gastric ulcer susceptibility. *PloS one* **8**, e63698 (2013).
601 Tanikawa, C. *et al.* A genome-wide association study identifies two susceptibility loci for duodenal ulcer in the Japanese population. *Nature genetics* **44**, 430 (2012).
602 Suzuki, H., Nishizawa, T., Tsugawa, H., Mogami, S. & Hibi, T. Roles of oxidative stress in stomach disorders. *Journal of clinical biochemistry and nutrition* **50**, 35-39 (2011).
603 Kang, J. M. *et al.* Enhancement of gastric ulcer healing and angiogenesis by cochinchina Momordica seed extract in rats. *Journal of Korean medical science* **25**, 875-881 (2010).
604 Guo, J. S. *et al.* Antiangiogenic effect of a highly selective cyclooxygenase-2 inhibitor on gastric ulcer healing in rats. *Toxicology and applied pharmacology* **183**, 41-45 (2002).
605 Amagase, K., Yokota, M., Tsukimi, Y. & Okabe, S. Characterization of" unhealed gastric ulcers" produced with chronic exposure of acetic acid ulcers to indomethacin in rats. *Journal of physiology and pharmacology* **54**, 349-360 (2003).
606 Hebbring, S. J. The challenges, advantages and future of phenome-wide association studies. *Immunology* **141**, 157-165 (2014).

607 Kim, S., Yu, N.-K. & Kaang, B.-K. CTCF as a multifunctional protein in genome regulation and gene expression. *Experimental & molecular medicine* **47**, e166 (2015).
608 Nakamura, Y., Gojobori, T. & Ikemura, T. Codon usage tabulated from international DNA sequence databases: status for the year 2000. *Nucleic acids research* **28**, 292-292 (2000).
609 Marees, A. T. *et al.* A tutorial on conducting genome-wide association studies: Quality control and statistical analysis. *International journal of methods in psychiatric research*, e1608 (2018).
610 Sohn, S. *et al.* MedXN: an open source medication extraction and normalization tool for clinical text. *Journal of the American Medical Informatics Association* **21**, 858-865 (2014).
611 Xu, H. *et al.* MedEx: a medication information extraction system for clinical narratives. *Journal of the American Medical Informatics Association* **17**, 19-24 (2010).
612 Moore, C. B. *et al.* in *Open forum infectious diseases.* ofu113 (Oxford University Press).
613 Health, N. I. o. (ed U.S. Department of Health and Human Services (HHS)) 69 (NIH, https://allofus.nih.gov/, 2018).
614 Collins, F. S. & Varmus, H. A new initiative on precision medicine. *New England Journal of Medicine* **372**, 793-795 (2015).
615 Najafzadeh, M. *et al.* DNA damage in healthy individuals and respiratory patients after treating whole blood in vitro with the bulk and nano forms of NSAIDs. *Frontiers in molecular biosciences* **3**, 50 (2016).
616 Oikawa, S., Kobayashi, H., Tada-Oikawa, S., Isono, Y. & Kawanishi, S. Damage to cellular and isolated DNA induced by a metabolite of aspirin. *Mutation Research/Fundamental and Molecular Mechanisms of Mutagenesis* **661**, 93-100 (2009).
617 Niikawa, M., Okamura, T., Sugiura, K. & Nagase, H. Aspirin intake suppresses MMC-induced genotoxicity in mice. *Asian Pac. J. Cancer Prev* **9**, 279-282 (2008).
618 Dandah, O. *et al.* Aspirin and ibuprofen, in bulk and nanoforms: Effects on DNA damage in peripheral lymphocytes from breast cancer patients and healthy individuals. *Mutation Research/Genetic Toxicology and Environmental Mutagenesis* **826**, 41-46 (2018).
619 Giri, A. The genetic toxicology of paracetamol and aspirin: a review. *Mutation Research/Reviews in Genetic Toxicology* **296**, 199-210 (1993).
620 Bellail, A. C., Olson, J. J. & Hao, C. SUMO1 modification stabilizes CDK6 protein and drives the cell cycle and glioblastoma progression. *Nature communications* **5**, 4234 (2014).
621 Hughes, D. J. *et al.* Generation of specific inhibitors of SUMO-1–and SUMO-2/3–mediated protein-protein interactions using Affimer (Adhiron) technology. *Sci. Signal.* **10**, eaaj2005 (2017).
622 Carr, D. F. *et al.* Towards better models and mechanistic biomarkers for drug-induced gastrointestinal injury. *Pharmacology & therapeutics* (2017).
623 Devlin, R. B., Frampton, M. L. & Ghio, A. J. In vitro studies: What is their role in toxicology? *Experimental and Toxicologic Pathology* **57**, 183-188 (2005).
624 Adinortey, M. B., Ansah, C., Galyuon, I. & Nyarko, A. In Vivo Models Used for Evaluation of Potential Antigastroduodenal Ulcer Agents. *Ulcers* **2013**, 1-12, doi:10.1155/2013/796405 (2013).
625 Olson, H. *et al.* Concordance of the toxicity of pharmaceuticals in humans and in animals. *Regulatory Toxicology and Pharmacology* **32**, 56-67 (2000).

626 Lemieux, M., Bouchard, F., Gosselin, P., Paquin, J. & Mateescu, M. A. The NCI-N87 cell line as a gastric epithelial barrier model for drug permeability assay. *Biochemical and biophysical research communications* **412**, 429-434 (2011).
627 Fiorentino, M. *et al.* Helicobacter pylori-induced disruption of monolayer permeability and proinflammatory cytokine secretion in polarized human gastric epithelial cells. *Infection and immunity* **81**, 876-883 (2013).
628 Sato, T. *et al.* Single Lgr5 stem cells build crypt–villus structures in vitro without a mesenchymal niche. *Nature* **459**, 262 (2009).
629 Fatehullah, A., Tan, S. H. & Barker, N. Organoids as an in vitro model of human development and disease. *Nature cell biology* **18**, 246 (2016).
630 Barker, N. *et al.* Lgr5+ ve stem cells drive self-renewal in the stomach and build long-lived gastric units in vitro. *Cell stem cell* **6**, 25-36 (2010).
631 McCracken, K. W. *et al.* Modelling human development and disease in pluripotent stem-cell-derived gastric organoids. *Nature* **516**, 400 (2014).
632 Schlaermann, P. *et al.* A novel human gastric primary cell culture system for modelling Helicobacter pylori infection in vitro. *Gut* **65**, 202-213 (2016).
633 Sinha, M. *et al.* Current perspectives in NSAID-induced gastropathy. *Mediators of inflammation* **2013** (2013).
634 Van Meer, G., Voelker, D. R. & Feigenson, G. W. Membrane lipids: where they are and how they behave. *Nature reviews Molecular cell biology* **9**, 112 (2008).
635 Lichtenberger, L. M. *et al.* Non-steroidal anti-inflammatory drugs (NSAIDs) associate with zwitterionic phospholipids: insight into the mechanism and reversal of NSAID-induced gastrointestinal injury. *Nature medicine* **1**, 154 (1995).
636 Kurinets, A. & Lichtenberger, L. M. Phosphatidylcholine-associated aspirin accelerates healing of gastric ulcers in rats. *Digestive diseases and sciences* **43**, 786-790 (1998).
637 Lichtenberger, L. M. *et al.* Phosphatidylcholine association increases the anti-inflammatory and analgesic activity of ibuprofen in acute and chronic rodent models of joint inflammation: relationship to alterations in bioavailability and cyclooxygenase-inhibitory potency. *Journal of Pharmacology and Experimental Therapeutics* **298**, 279-287 (2001).
638 Anand, B. S., Romero, J. J., Sanduja, S. K. & Lichtenberger, L. M. Phospholipid association reduces the gastric mucosal toxicity of aspirin in human subjects. *The American journal of gastroenterology* **94**, 1818 (1999).
639 Baerwald, C., Verdecchia, P., Duquesroix, B., Frayssinet, H. & Ferreira, T. Efficacy, safety, and effects on blood pressure of naproxcinod 750 mg twice daily compared with placebo and naproxen 500 mg twice daily in patients with osteoarthritis of the hip: A randomized, double-blind, parallel-group, multicenter study. *Arthritis & Rheumatism* **62**, 3635-3644 (2010).
640 Davies, N. *et al.* NO-naproxen vs. naproxen: ulcerogenic, analgesic and anti-inflammatory effects. *Alimentary pharmacology & therapeutics* **11**, 69-79 (1997).
641 Hawkey, C. *et al.* Gastrointestinal safety of AZD3582, a cyclooxygenase inhibiting nitric oxide donator: proof of concept study in humans. *Gut* **52**, 1537-1542 (2003).
642 Lohmander, L. *et al.* A randomised, placebo controlled, comparative trial of the gastrointestinal safety and efficacy of AZD3582 versus naproxen in osteoarthritis. *Annals of the rheumatic diseases* **64**, 449-456 (2005).
643 (FDA), U. S. F. a. D. A. Summary Minutes of the for the Joint Meeting of the Arthritis Advisory Committee and the Drug Safety and Risk Management Advisory Committee. (https://www.archive-it.org/collections/7993, 2010).

644 (EMA), E. M. A. Withdrawal of the marketing authorisation application for Beprana (naproxcinod) (https://www.ema.europa.eu/, 2011).
645 Tanaka, T. *et al.* Nitrogen oxide-releasing aspirin induces histone H2AX phosphorylation, ATM activation and apoptosis preferentially in S-phase cells: involvement of reactive oxygen species. *Cell Cycle* **5**, 1669-1674 (2006).
646 Wallace, J. L. Hydrogen sulfide-releasing anti-inflammatory drugs. *Trends in pharmacological sciences* **28**, 501-505 (2007).
647 Li, L. *et al.* Anti-inflammatory and gastrointestinal effects of a novel diclofenac derivative. *Free Radical Biology and Medicine* **42**, 706-719 (2007).
648 Wallace, J. L., Caliendo, G., Santagada, V., Cirino, G. & Fiorucci, S. Gastrointestinal safety and anti-inflammatory effects of a hydrogen sulfide–releasing diclofenac derivative in the rat. *Gastroenterology* **132**, 261-271 (2007).
649 Psarra, A., Nikolaou, A., Kokotou, M. G., Limnios, D. & Kokotos, G. Microsomal prostaglandin E2 synthase-1 inhibitors: a patent review. *Expert opinion on therapeutic patents* **27**, 1047-1059 (2017).
650 Engblom, D. *et al.* Microsomal prostaglandin E synthase-1 is the central switch during immune-induced pyresis. *Nature neuroscience* **6**, 1137 (2003).
651 Kamei, D. *et al.* Reduced pain hypersensitivity and inflammation in mice lacking microsomal prostaglandin e synthase-1. *Journal of Biological Chemistry* **279**, 33684-33695 (2004).
652 Trebino, C. E. *et al.* Impaired inflammatory and pain responses in mice lacking an inducible prostaglandin E synthase. *Proceedings of the National Academy of Sciences* **100**, 9044-9049 (2003).
653 Samuelsson, B., Morgenstern, R. & Jakobsson, P.-J. Membrane prostaglandin E synthase-1: a novel therapeutic target. *Pharmacological reviews* **59**, 207-224 (2007).
654 Xu, D. *et al.* MF63 [2-(6-chloro-1H-phenanthro [9, 10-d] imidazol-2-yl)-isophthalonitrile], a selective microsomal prostaglandin E synthase-1 inhibitor, relieves pyresis and pain in preclinical models of inflammation. *Journal of Pharmacology and Experimental Therapeutics* **326**, 754-763 (2008).
655 Wang, M., Song, W. L., Cheng, Y. & Fitzgerald, G. Microsomal prostaglandin E synthase-1 inhibition in cardiovascular inflammatory disease. *Journal of internal medicine* **263**, 500-505 (2008).
656 Scholich, K. & Geisslinger, G. Is mPGES-1 a promising target for pain therapy? *Trends in pharmacological sciences* **27**, 399-401 (2006).
657 Koeberle, A. & Werz, O. Perspective of microsomal prostaglandin E2 synthase-1 as drug target in inflammation-related disorders. *Biochemical pharmacology* **98**, 1-15 (2015).
658 Konya, V., Marsche, G., Schuligoi, R. & Heinemann, A. E-type prostanoid receptor 4 (EP4) in disease and therapy. *Pharmacology & therapeutics* **138**, 485-502 (2013).
659 Ganesh, T. Prostanoid Receptor EP2 as a Therapeutic Target: Miniperspective. *Journal of medicinal chemistry* **57**, 4454-4465 (2013).
660 Cicero, A. F., Derosa, G. & Gaddi, A. Combined Lipoxygenase/Cyclo-oxygenase Inhibition in the Elderly. *Drugs & aging* **22**, 393-403 (2005).
661 Elliott, J. A. & Smith, H. S. *Handbook of acute pain management*. (CRC Press, 2016).
662 Alvaro-Gracia, J. Licofelone—clinical update on a novel LOX/COX inhibitor for the treatment of osteoarthritis. *Rheumatology* **43**, i21-i25 (2004).
663 Playford, R. *et al.* Bovine colostrum is a health food supplement which prevents NSAID induced gut damage. *Gut* **44**, 653-658 (1999).

664 Playford, R. J. *et al.* Co-administration of the health food supplement, bovine colostrum, reduces the acute non-steroidal anti-inflammatory drug-induced increase in intestinal permeability. *Clinical Science* **100**, 627-633 (2001).

665 Mir, R. *et al.* The structural basis for the prevention of nonsteroidal antiinflammatory drug-induced gastrointestinal tract damage by the C-lobe of bovine colostrum lactoferrin. *Biophysical journal* **97**, 3178-3186 (2009).

666 Mir, R. *et al.* Structural and binding studies of C-terminal half (C-lobe) of lactoferrin protein with COX-2-specific non-steroidal anti-inflammatory drugs (NSAIDs). *Archives of biochemistry and biophysics* **500**, 196-202 (2010).